IVANE JAVAKHISHVILI TBILISI STATE UNIVERSITY
Mikheil Nodia Institute of Geophysics
Vakhushti Bagrationi Institute of Geography
GEORGIAN TECHNICAL UNIVERSITY
Institute of Hydrometeorology

INTERNATIONAL SCIENTIFIC CONFERENCE

Natural Disasters in the 21st Century:

Monitoring, Prevention, Mitigation

PROCEEDINGS

Tbilisi, December 20-22, 2021

IVANE JAVAKHISHVILI TBILISI STATE UNIVERSITY
MIKHEIL NODIA INSTITUTE OF GEOPHYSICS
VAKHUSHTI BAGRATIONI INSTITUTE OF GEOGRAPHY
GEORGIAN TECHNICAL UNIVERSITY
INSTITUTE OF HYDROMETEOROLOGY

INTERNATIONAL SCIENTIFIC CONFERENCE
Natural Disasters in the 21st Century: Monitoring, Prevention, Mitigation

Tbilisi, December 20-22, 2021

Proceedings

Tbilisi
2021

Conference Themes

- Earthquake and related events;
- Hydrometeorological disasters;
- Climate change and related disasters;
- Natural disaster hazard and risk modeling and forecasting;
- Stimulation of natural disasters as a result of anthropogenic impact;
- Environmental pollution;
- Geographic Information Sistem & Remote sensing;
- Terrestrial networks and point measurements;
- Forest fires;
- Heliocosmic disasters;
- Health disasters & Epidemics & Pandemics;
- Assessment of social and economic losses caused by natural disasters;
- Active and passive protection against natural disasters;
- Improvement of Emergency Response Services Activities for mitigating natural disasters results;

THE MOST TYPICAL FACTORS OF A DESTRUCTIVE EARTHQUAKE AFFECTING THE ENVIRONMENT (ON EXAMPLE OF THE 1988 SPITAK EARTHQUAKE)

Nazaretyan S.S.

Territorial survey for seismic protection, Ministry of Emergency situations of Armenia. 3115 V. Sargsyan str. 5a, Gyumri, Armenia
nazaretyan.siranush@mail.ru

Summary: *Destructive earthquakes can have a certain impact on the environment, conditioned by both the strength of the earthquake and local conditions, especially at the level of urbanization and seismic risk and the organization of disaster zone recovery. Based on the investigation data of the 1988 Spitak earthquake (intensity 9-10 points by EMS-98, M=7.0) these impacts can be divided into two groups based on the destruction of buildings and structures, activation of geological processes, and earthquake zone recovery period. The first group includes the collapse of buildings, activation of landslides, rock falls, soil liquefaction and subsidence's, and activation of other geological processes that lead to changes in the environment. Larger scale earthquakes may have significant impact on the environment. For example, more than 50% of destruction of urban areas (especially buildings), major landslides (millions of tons of mass), collapse of reservoir dams resulting in floods, damages to lifelines (especially the main water supply and sewerage system), etc. The second group includes human activities during the earthquake recovery operations: selection of places to accumulate rubble, creation of temporary residential areas for the homeless and new settlements and districts, construction of new structures and infrastructure (transport, industrial, agricultural, etc.) especially in non-urban areas, destruction of green areas, cutting of trees, use of new areas for keeping domestic animals or setting up households, etc.*

Key Words: *Destructive earthquake, environment, consequences, recovery of earthquake zone.*

Introduction. A strong earthquake, especially occurring in a high seismic risk zone, has a significant impact on the environment. These impacts are conditioned by the earthquake strength, local conditions, especially urbanization and seismic risk levels, disaster management processes, from the good organization of the work to the pace of remediation.[2, 4-8].It is clear that these three possible conditions are different in different seismic regions, and therefore the effect of the earthquake on the environment is different. It is more practical to consider the specifics and factors of earthquake impact on the environment on the example of a particular strong earthquake The example of such an earthquake in this work is the 1988 Spitak earthquake (M = 7.0, the intensity at the epicenter 9-10 point by EMS-98, the average depth of the hypocenter -10 km). Here are some important facts about earthquakes and their aftermath. The Spitak earthquake covered an area of about 10,000 km^2 with one million inhabitants. The area of the destruction zone (8 point intensity and more) was 3000 km^2. The quake affected 21 towns and 342 villages, completely destroyed 11 towns and 58 villages. Number of homeless people was 514,000. A total of 25,000 people died, of which 17,000 in Gyumri alone. The total lost residential area was 9 million m^2 (18% of the RA housing stock), of which 4.3 million m^2 were public sector buildings. Direct material losses are estimated at $ 15-20 billion. The Spitak city was entirely destroyed- 100%, Gyumri 60% and Vanadzor 30%. From Gyumri alone the ruins of 600,000 m^3 of 147 apartment buildings were taken out. Agro-industrial losses in 58 villages: destroyed houses - 21 000, schools - 84, kindergartens - 90, food and trade objects - 2260; 300 collective and state farms, 32 production and 52 construction companies were affected, a 600 km long irrigation line was out of order, 90,000 hectares of land were deprived of water. Damaged lifelines: 40 km railway section, highways in some places, settlements in the epicenter zone deprived of drinking water supply [4, 6].

Environmental changes. These changes are numerous, not mentioning the fact that everything in the devastating earthquake zone changes: from the subsoil to various changes in the earth's surface and in the atmosphere [2-4]. However, these changes occur at different scales and areas. This article will look at the

most significant and large-scale changes, mainly having a negative impact on the environment. These include changes in the earth's surface (relief, engineering-geological conditions, urban areas, including the man-made environment by economy, industry, enterprises, engineering structures), atmosphere (spread of hazardous and toxic substances), aquatic environmental soils, etc and other changes that also affect semi-diversity.

The paper [1-3] cites only damage to natural landscapes and vegetation, and possible massive flooding from dam destruction and waste disposal sites as factors of earthquake impact on the environment. Secondary impacts include consequences of temporarily displaced persons and damage to infrastructure and fuel leakage from storage facilities.

Main factors of a strong earthquake affecting the environment. We have conventionally divided the environmental factors of the 1988 Spitak earthquake into 5 groups. Below we present these groups and the most essential factors.

1. Geological factors and associated effects (factors directly affecting):
   • Landslides activation;
   • Rock falls, rock collapses,
   • Large seismic-gravitational phenomena,
   • Changes in riverbeds, formation of ponds due to collapse, etc.

2. In connection with the demolition of buildings and structures, cleaning and relocation of rubble (factors directly affecting):
   • Choosing the right place to collect rubbles and preservation of rubbles,
   • Impacts due to damage to water line,
   • Impact of damage to transport lines, especially highways, railways,
   • Factors related to damage to buildings of chemical and other hazardous objects and emissions of toxic substances,
   • Consequences of collapse of reservoir dams,
   • Impact of large dust retreats on biodiversity.

3. Factors arising from rescue operations and earthquake recover processes:
   • Impacts of settlement infrastructure damage during rescue operations,
   • Impact of temporary accumulation of building debris in the settlement,
   • Destruction of green areas,
   • Changes in the living conditions of animals (rodents, birds, etc.),
   • Exposure to large amounts of dust during rescue work.

4. Factors related to incomplete reconstruction of the earthquake zone or its delay, creation of new urbanized areas:
   • Tree felling, especially for winter heating,
   • Occupation of green and other free areas by buildings, residential districts, new settlements with their infrastructure,
   • Keeping domestic animals,
   • Creation of land plots (vegetable garden, garden) in settlements,
   • Changes in wildlife due to the creation of new settlements, districts and temporary districts,
   • Increasing groundwater levels and decreasing seismic resistance of buildings due to damage to sewer and water lines,
   • Groundwater level rise for the same reason and swamping of areas,
   • Factors arising from the construction of new buildings and structures or the restoration and strengthening of their damaged parts.

5. Other:
   • Semi-diversity changes due to non-use of agricultural lands,
   • Due to environmental changes in abandoned settlements and districts due to population emigration.

Of course, there may be other environmental factors that have little impact on the environment or will not necessarily be the case with all strong earthquakes. For example, changes in semi-diversity due to non-use of agricultural lands or non-functioning of the irrigation system, etc.

Results and discussion. The most important factors arising from the devastating earthquake, especially in the settlements, which may have some impact on the environment, have been eliminated. By origin, they are divided into 5 groups, most of which are typical of any devastating earthquake. The scale of most of the factors, the background and their impact on the environment are due to the intensity of the earthquake, local features, especially urbanization and seismic risk levels, and the processes of earthquake recovery. This data can be used in environmental impact assessment for an area that still needs special study. It will help prevent or minimize the impact of a devastating earthquake on the environment, human health, economic and social development.

<div align="center">

References

</div>

1. Directory by grade, murder and need after Emergency situations. // Environment. Interdisciplinary sector, vol. B, 2010, 36 p. (in Russian). https://www.recoveryplatform.org/assets/publication/PDNA/PDNA_VolumeB/Russian/ru-Environment.pdf
2. Handbook for assessment of socio-economic and ecological consequences of natural disasters. Injury to natural landscapes and vegetation. // CLACK and the American Bank for Development, Washington, DC, 2003.
3. Michael Allaby. Basics of Environmental Science. 2nd edition. // Routledge. London, N.Y. 2001. 340 p. ISBN 0-415-21175-1.
4. Nazaretyan S.N. Seismic hazard and risk of the city's of zone 1988 Spitak earthquake. // Publishing House "Gitutyun-Scienes" National academy of sciences RA. Yerevan, 2013, 212 p. (in Russian).
5. Nazaretyan Sergey, Nazaretyan Siranuish. The Public and Liquidation of Consequences of Seismic Catastrophe. Engaging the Public to Fight the Consequences of Terrorism and Disasters. // IOS Press, NATO Science for Peace and Security Series. Vol. 120. Netherlands, 2015. pp. 250-256 https://www.nato.int/cps/en/natohq/topics_140726.htm?
6. Nazaretyan S.N., Nazaretyan S.S. Assessment of the need for rescue forces during destructive earthquakes (a case study of Armenia). // Seismic Instruments. Vol. 57, N 2, 2021, pp. 150-162. Doi.org/10.3103/S0747923921020298
7. Nazaretyan S.N. Main features of the new methodology for seismic risk assessment of Armenian cities. // Seismic Instruments, 56, 2020, pp. 317-331. DOI:10.3103/S0747923920030093
8. Nazaretyan S.N., Nazaretyan S.S., Mirzoyan L.B. Some Baseline data for a effective response of Emergency servicis in a seismic disasters in Soutern Caucasus. // Proceedings of Inter. Scientific Conference „Natural Disasters in Georgia: Monitoring, Prevention, Mitigation". Publishing house of Tbilisi state university, 2020, pp. 36-39. DOI:10.13140/RG.2.2.11733.78565

LARGE ANCIENT LANDSLIDES OF ARMENIA FORMED DURING STRONG EARTHQUAKES, AND THEIR MANIFESTATION IN THE RELIEF

Boynagryan V.R.

Yerevan State University, Yerevan, Armenia
vboynagryan@ysu.am

Summary: *The territory of the Republic of Armenia is located within the Mediterranean-transasian seismic belt and at the present stage of its development is characterized by high seismicity. This circumstance provokes the formation of landslides. At the same time, large landslides-blocks and landslides-flows up to 5-8 km long, up to 1-2 km wide and up to 100-170 m or more can form during strong earthquakes. On the slopes, such landslides associated with strong earthquakes of the past are distinguished by a characteristic relief, a relatively small amount of vertical displacement (100-200m, rarely up to 300m). At the same time, the amplitude of their horizontal movement in places reaches 0.5-1 km. This is due to the excessive horizontal acceleration obtained by a landslide during an earthquake. The report will consider examples of such landslides and their distinctive features.*

Key Words: Earthquakes, landslides, vertical displacement, horizontal acceleration.

Introduction. The territory of Armenia, together with the entire Armenian Highlands, is located within the Mediterranean–Trans-Asian seismic belt and at the present stage of its development is characterized by high seismicity. Strong earthquakes cause the shaking of the slopes of mountain structures and their loose-block thickness, as well as rocks. At the same time, the stability of rocks is lost, existing landslides are activated and new landslides appear. For example, during the 1988 Spitak earthquake, 19 new landslides appeared in the northern part of Armenia alone and many old landslides intensified [1]. There is information about the descent of large landslides during the Vayots Dzor (735), Dvin (893.), Garni (1679.), Tsakhkadzor (1827.), Zangezur (1931 and 1968) and other earthquakes [2]. Earthquakes of magnitude from 8 to 9 are possible on the territory of Armenia. Naturally, such high seismic activity could have contributed to the formation of large landslides in the past. The latter, indeed, exist on the territory of Armenia and are distinguished by their characteristic features.

Methods. Large ancient landslides of seismogenic origin in Armenia were identified by us back in the late seventies of the twentieth century during field studies in the Aghstev river basin. In the course of the research, topographic maps of the scale of 1:25,000 and 1:100,000 and aerial photographs of the scale of 1:25,000 were analyzed and areas resembling landslide bodies were identified according to the characteristic relief. After that, these areas were examined in the field and their belonging to landslides was clarified. The accuracy of the results of the cameral interpretation of topographic maps and aerial photographs was almost 100%.

Results and discussion. Our research has shown that all the areas previously identified by us as supposed seismogenic landslides really differ from other landslides in their features. First of all, they are large landslides-blocks and landslides-streams with a bumpy surface with swampy depressions, shallow suffusion lakes, separate well-preserved blocks of bedrock that seem to "float" in crushed-loamy formations (the product of fragmentation and grinding of bedrock during earthquakes and landslide movements). The thickness of the rocks disturbed by landslide deformations in the basin of the Aghstev river (drilling data) ranges from several tens of meters to 100-170 m or more (Hovk - 110-160m, Achajur - 170m). The linear dimensions of seismogenic landslides are also impressive: the length is up to 6 km or more (the village of Hovk is 5-5.5 km, the village of Martuni is 6.5-7 km), the width is 1-2 km or more [3, 4]. Interestingly, large landslides-streams have a significant amplitude of horizontal displacement (up to 0.5-1.0 km) and in their "tongue" part the riverbeds are strongly deflected in the opposite direction (see Fig. 1).
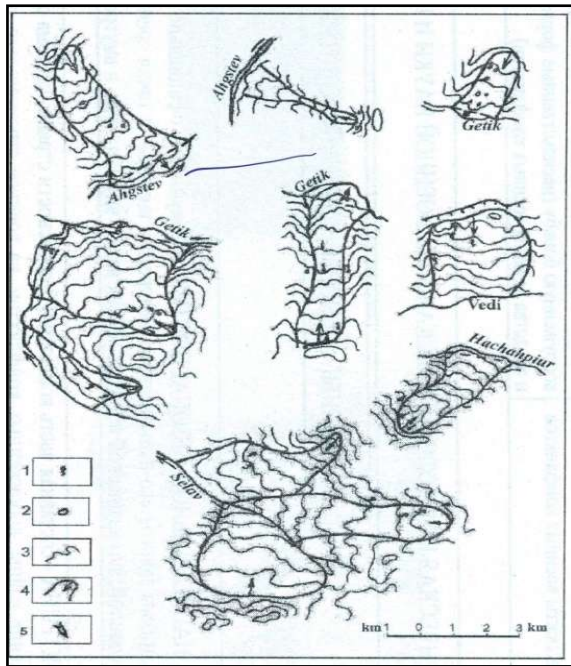
Fig. 1. Characteristic seismogenic landslides:
1 – springs, 2 – lakes, 3 - horizontals,
4 - contours of landslides, 5 – direction
of landslide displacement.

These large ancient (presumably Pliocene-Lower Quaternary age) landslide bodies are called by us tectonic-seismogravitational formations (or seismogenic landslides). One of these landslides (Hovk), due to its complex structure, was attributed to the olistostromes (*accumulation, or piling up,* of landslides) [5]. A large amount of horizontal displacement of the landslide body is characteristic of those of their varieties, in the formation of which a large role belongs to strong earthquakes [6]. It is strong earthquakes that give landslides excessive horizontal acceleration [7]. And the vertical displacements are relatively small.

A cluster of large seismogenic landslides is present in the zone of the Vayots Dzor active fault. These landslides cause significant damage to the villages of Ugedzor, Artavan, Saravan. A landslide formed on the slope of Amulsar Mountain is very active here. The only highway connecting Yerevan with the Syunik region is constantly being destroyed due to its progress.

There are also seismogenic landslides in the zone of the Garni seismically active fault (the villages of Vokhchaberd, Garni, Atsavan, Gehadir). At the same time, all these landslides are quite active, which is manifested by the destruction of buildings, deformations of the highway, etc. The most studied of the seismogenic landslides of the republic is the Hovk landslide-stream (length 5-5.5km, width 1.5-2 km), located on the southeastern slope of the Ijevan ridge (see Fig. 2).

It covers an area of with Hovk and its "tongue" part reaches the floodplain of the Aghstev river. In the northern part of the village, two active landslides of the second order stand out on the body of this large landslide: the northern (1.6 km long) and southern (1.9-2 km long) streams, both about 150-200m wide. In the upper part of the main landslide, another active landslide of the second order with a length of about 1 km and moving almost due south is isolated. The Hovk landslide-stream was first investigated by G.D.Sahakyan and K.A.Gulakyan back in 1958. In the future, many Armenian specialists took part in the study of this landslide. Since 1978. this landslide was investigated by employees of the Dilijan expedition of the IGS of the National Academy of Sciences of the Republic of Armenia and specialists from other organizations cooperating with them (the author took an active part in the work of this expedition).

Based on many years of research, the overall picture of the Hovk landslide-flow is presented as follows [8]. The landslide began to form back in the Upper Pliocene-Lower Quaternary, when differentiated movements of blocks of the Earth's crust intensified in the Lesser Caucasus. At this time, the collapse of the raised blocks and the formation of a giant collapse occurred. At the second stage, in the middle-Upper Quaternary, a giant sliding landslide formed on the body of an ancient stabilized landslide-collapse. In the Holocene (the third stage), a current landslide formed, which is still active at the present time. Small active landslides with numerous stretching cracks are currently forming on the body of this active landslide (the fourth stage) (see Fig. 3).

7

The total thickness of the displaced masses in Hovk is 110-160m (drilling data). In the upper part they are represented by fatty and carbonated sandy loams, loams and clays with inclusions of crushed stone and limestone blocks. The upper landslide mass is characterized by dustiness, increased $CaCO_3$ content (up to 32-44%), the number of soil plasticity is 12-26. This thickness has shifted along fatty and plastic clays of low density, lying at depths of 40-50m. Young landslide formations are underlain by limestone blocks that have shifted along the surface of dacitic porphyrites modified to a clay state [4].

a) b)

c)

Fig. 2. Hovk landslide [1]: a) - a general view of the landslide site,
b) - the active part of the landslide on the territory of the village of the same name,
c) - a karst funnel contributing to the concentration and infiltration
of precipitation moistening the landslide.

Fig. 3. A young active landslide formed on the body of an ancient landslide
(photo by V. Boynagryan). It periodically blocks the highway and
enters the flood-plain of the Aghstev river.

A typical ancient seismogenic landslide stream is the Martuni landslide on the left slope of the Getik River valley (right tributary of the Aghstev river). Its length is 6.5-7 km, width - 1.3-1.5 km. The head of the landslide is located at an altitude of 2600 m, the edge of the "tongue" of the landslide is at an altitude of 1700 m (the height difference is 900 m). The landslide deflected the riverbed 1 km to the right). Viscous and fatty clays, loams, sandy loams and gravel-crushed soils shifted here on the surface of hydrothermally altered porphyrites. Not only earthquakes played a significant role in the formation of this seismogenic landslide stream, but also numerous springs coming out at the foot of the slopes, as well as heavily moistened clay soils of the zone of faults passing here.

Currently, only the "tongue" part of the landslide is active. This activation of the ancient stabilized landslide is associated with the erosion of the "tongue" of the landslide by the waters of the Getik River, as well as

with water leaks from water pipes, the construction on the landslide of various structures. The "slide mirror" of the landslide passes at a depth of 19 to 38 m.

On the left bank of the Getik River, near the village of Dprabak, there is a large (length about 4 km, width up to 3.5 km) seismogenic landslide-block. The surface of the landslide has a bumpy-hilly, sometimes stepped relief. Numerous wetlands and small lakes stand out on it. The displacement here involves a thickness of quaternary formations with a thickness of 21-73 m, represented by moist, viscous, lumpy, greasy, dusty clays (less often loams and sandy loams) of light to dark brown and yellowish-gray color with inclusions of gravel, crushed stone and fragments of volcanic rocks (stone material is 25-40%). This stratum creeps along the surface of slightly altered, weathered porphyrites, tuff-breccia and quartz porphyrites. This landslide block is characterized by active displacement with speeds from 16 to 28 cm per year.

On the right bank of the Getik River there is a well-known Aigut landslide-a stream that is very clearly distinguished on topographic maps and aerial photographs, as well as on the terrain by the bumpy relief of the surface, the presence of suffusion depressions and small lakes on the body of the landslide. The body of the landslide with the NW and SE is limited by faults. Here clays, loams and crushed-gravel strata with fragments and blocks of porphyrites crawl along the surface of hydrothermally altered porphyrites of dark gray and black color. The power of the displaced mass is 25-51.6m. The landslide is quite active, periodically blocks the highway and goes to the riverbed.

Another active seismogenic landslide is located within the village of Vokhchaberd. Here, a block measuring 2.5 x 1.3 km^2 and with an average thickness of 70-80m fell off the steep slope of the Vokhchaberd ridge and shifted along the fault line of an overfault nature. In this area, Paleogene deposits are thrown up on Neogene ones. The southeastern wing of the fault is raised. The amplitude of the vertical displacement of the block, according to our measurements, is approximately 200-225m with a significant (up to 1 km) horizontal removal of the landslide body. This ratio of horizontal and vertical components confirms the seismogenic nature of the formation of this landslide [6]. The landslide has a stepped profile, the steepness of the landslide slope is 20-250; the Vokhchaberd and Hrazdan formations, as well as a whitish rock mass are crawling. The landslide is currently quite active. Near the village of Vokhchaberd, the roadbed is constantly deformed, there is an intensive destruction of residential and utility buildings. The activity of the landslide increased after the 1988 Spitak earthquake.

Conclusion. Ancient stabilized seismogenic landslides need to be identified and mapped, as they can represent a certain danger in the event of a violation of their equilibrium state in the case of engineering works. In the forested areas of northern Armenia, during field research, the author repeatedly encountered large deformations of the relief, resembling landslides-streams and landslides-blocks that changed the appearance of the terrain with the deviation of riverbeds in the opposite direction. The breakdown wall is not always clearly visible, but it can still be distinguished. Their external signs are not always clearly manifested, therefore, in order to identify them, it is necessary to use, along with field work, a preliminary analysis of aerial photographs and high-resolution satellite images. To identify and map large ancient seismogenic landslides, it is necessary to use a wide range of modern surveys in the visible, thermal infrared, radio wave, and other spectral zones. Good results in identifying traces of ancient seismogenic landslides can be obtained using radar technologies. At the stage of preliminary studies of the terrain, unmanned aerial vehicles can be used.

References

1. Landslides of Armenia. // Yerevan: ASOGIK, 2009, 308s.
2. Boynagryan V.R. Geomorphology of the Armenian Highlands. // Yerevan: ASOGIK, 2016, 650 p.
3. Boynagryan V.R. Landslide (block) violations of the slopes of the Aghstev river basin (Armenian SSR) and some issues of their study // News of the Academy of Sciences of the Armenian SSR. Earth Sciences, XI (1), 1988, pp. 30-37.
4. Boynagryan V.R. Slopes and slope processes of the Armenian Highlands. // Yerevan: Publishing House of YSU, 2007, 279 p.
5. Aslanyan A.T. Large olistostromes of Pliopleistocene age in the valley of the Aghstev river (ArmSSR) // Izvestiya AN ArmSSR. Earth Sciences, 1, 1979, pp. 24-32.
6. Tazieff H. Interpretation des glissements de terrain accompagnant legrand séisme du Chili. // Bull. Soc. Belge de Geologie, 69 (3), 1960.
7. Emelyanova E.P. Basic patterns of landslide processes. // M.: Nedra, 1972, 310 p.
8. Sahakyan G.D. The stages of development of the Vurgun landslide massif (the basin of the Aghstev river of the Armenian SSR). // Izvestia of the Academy of Sciences of the Armenian SSR, Earth sciences, 1, 1989, pp. 62-66.

ONI WATER REACTION ON EARTHQUAKE IN 2021

*Kobzev G., *Melikadze G., *Jimsheladze T., **Karel R., *Tchankvetadze A.

*Mikheil Nodia Institute of Geophysics of Ivane Javakhishvili Tbilisi State University, Tbilisi, Georgia
kobzev47@gmail.com
**GeoCosmo Research Centre in the United Kingdom

Summary: *It is known that variations of water level represent itself an integrated response of aquifer to different periodic as well as non periodic influences, including earthquake related strain generation in the earth crust. The article deals about detected anomalies at the Oni borehole, during preparation of strong earthquake, with long epicentral distance. For this purpose, were developed the data of water level for Oni borehole. Were registered the hidrodeformation anomalies caused by the earthquake preparation processes. As a result, have been identified precursory anomalies and has been confirmed high sensitivity to the geodynamic processes.*

Key Words: *hydrodynamic anomalies, seismic precursors.*

Introduction

Our earlier studies on the relationship of water level anomalies in wells with earthquakes are presented in [1-7]. The article contain information about several hydrodynamic anomalies were observed during earthquake in Oni borehole.

Well coordinate: 42.573° N 43.437° E, Georgia, Caucasus.

Well parameters: Length 255 m, screen 70-250 m. Confined sub-artesian aquifer; fractured shale and basalts. Well's resonance period: P=23.5 sec.

The water level in Oni borehole was recorded every 1 minute. Device XR5-SE-M and program LogXR used.

Seven earthquakes are depicting on fig.1. The moment of the earthquake announced as the starting (zero) time. Graph time (x-axis) is in format HH:MM (Hours: Minutes). Y-axis is in cm.

Below is water reaction in Oni borehole on remote earthquakes in 2021.

Sensitivity of well

Station Oni reacted on earthquake with maximal distance 16123 km, Mag=8.1, Kermadec Islands, New Zealand.

Comparison of earthquakes Q1 and Q5 showed, that water reaction on quake with shorter distance (7866 km, H=60 km) may be later, than on quake with longer distance (8919 km, H=43 km).

Quakes Q3 and Q6 with equal magnitude M=8.1 and distance (16123 km, 12890 km) have reaction (5.76 cm, 3.63 cm) for depths (25 km, 60 km), so smaller depth gives more reaction.

It is possible to compare quakes Q1 and Q6 with the same depth (60 km).

Quakes Q2 and Q3 was almost at the same place (16084 km, 16123 km), Kermadec Islands, on different depths (49 km, 25 km) and magnitudes (7.4, 8.1). Water reaction here: 0.95 and 5.6 cm.

For quakes Q4 and Q7 with the same depth, 10 km, and double distances (4771 km, 10666 km) water reacted trice stronger (5.05 cm and 1.42 cm) on M=7.4, 7.2.
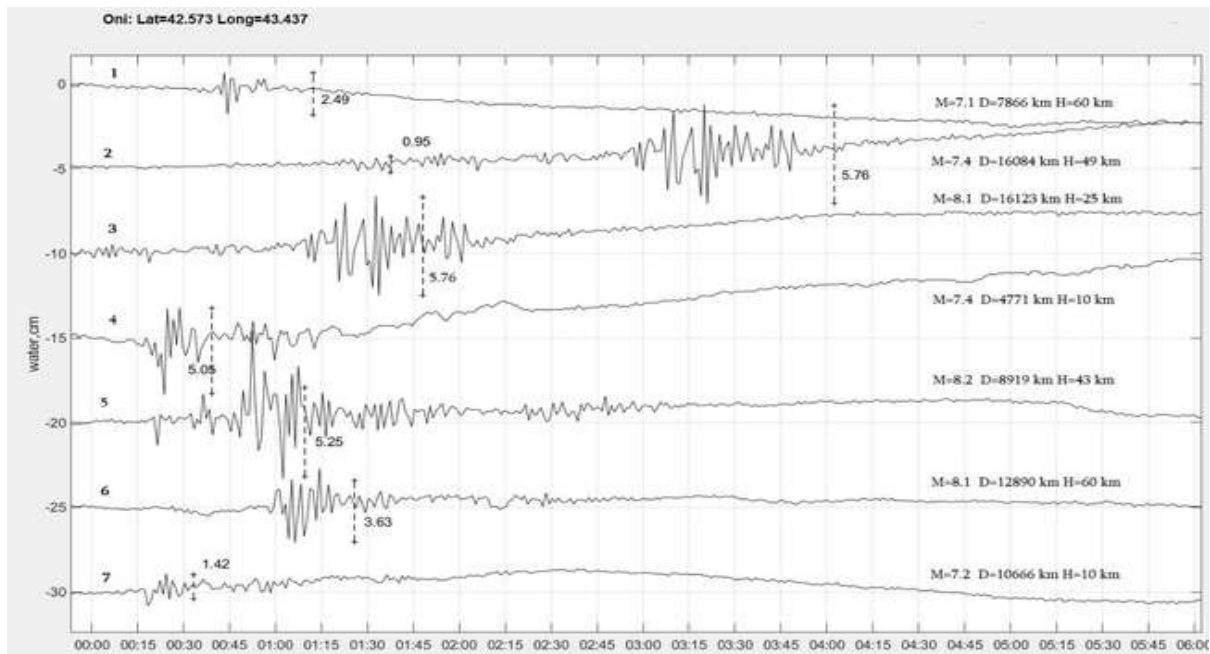
Fig.1. Oni, water reaction on the earthquakes in 2021. Earthquakes started at HH:MM=00:00

Table 1. Oni water reaction 2021

	Date	Magnitude	Distance, km	Depth, km	Azimuth	Earthquake's place	Water reaction, in cm
1	13/02/2021 14:07	7.1	7866	60	93.7	Near East Coast of Honshu, Japan	2.49
2	04/03/2021 17:41	7.4	16084	49	119.4	Kermadec Islands, New Zealand	0.95
3	04/03/2021 19:28	8.1	16123	25	119.3	Kermadec Islands, New Zealand	5.76
4	21/05/2021 18:04	7.4	4771	10	100.6	Southern Qinghai, China	5.05
5	29/07/2021 06:15	8.2	8919	43	82.8	Alaska, Peninsula	5.25
6	12/08/2021 18:35	8.1	12890	60	209.9	Southern Sandwich Islands Region	3.63
7	14/08/2021 12:29	7.2	10666	10	256.3	Haiti Region	1.42

Conclusion

Located in Georgia, Caucasus, the Oni well demonstrates high sensitivity to the distant earthquake of 2021.

Examples of earthquakes indicate an essential role of the depth of an earthquake: an earthquake depth of 60 km leads to a significant decrease in the amplitude of the reaction of water in the well, what is fixed as visual manifestation. For the first time, a strong earthquake was recorded for this well what was occurred in the Southern Hemisphere.

References

1. Melikadze G., Kobzev I., Kapanadze N., Machaidze Z., Jimsheladze T. Analyze of underground water regime factors for determine tectonic component. // LEPT Institute of Hydrogeology and Engineering Geology. Collection articles, vol. XYI. Proceeding of Conference Dedicate to the 100-th Anniversary of Professor Josef Buachidze, Tbilisi, 2007.
2. Kobzev G., Melikadze G. Methods of hydrodynamic analysis for revealing earthquakes precursors. // Workshop materials "Exploration and exploitation of groundwater and thermal water systems in Georgia, Tbilisi, Georgia, 2010, p. 60-6a9.
3. Chelidze T., Shengelia I., Zhukova N., Matcharashvili T., Melikadze G., GeKobzev G. Coupling of Multiple Rayleigh Waves and Water Level Signals during 2011 Great Tohoku Earthquake Observed in Georgia, Caucasus. // Bulletin of the Georgian National Academy of Sciences, vol. 8, no. 2, 2014.
4. Melikadze G., Jimsheladze T., Kobzev G., Tshankvetadze A., Devidze M., Kapanadze N. Methodologically detection of distribution in geodynamic field of the Earth during preparation the earthquakes. // Journal of Georgian Geophysical Society, Issue (A), Physics of Solid Earth, v.18a, 2015, pp. 3-12.
5. Melikadze G., Jimsheladze T., Kobzev G., Tchankvetadze A., Devidze M. Hydrodynamic and geomagnetic anomalies related with preparation of earthquakes in Caucasus. // Journal of Georgian Geophysical Society, Issue (A), Physics of Solid Earth, v.19a, 2016, pp. 79-96
6. Chelidze T., Melikadze G., Kobzev G., Shengelia I., Jorjiashvili N., Mepharidze N. Hydrodynamic and seismic response to teleseismic waves of strong remote earthquakes in Caucasus. // Acta Geophysica, AGPH-D-18-00617
7. Chelidze T., Melikadze G., Kiria T., Jimsheladze T., Kobzev G. Statistical and Non-linear Dynamics Methods of Earthquake Forecast: Application in the Caucasus. // Frontiers in Earth Science published: 29 June 2020 doi: 10.3389/feart.2020.00194,

ECOLOGICAL CONCEQUENCES OF NATURAL DISASTERS

*,**Berdzenishvili N., *Davitashvili M.

*Iakob Gogebashvili Telavi State University, 1, Kartuli Universiteti str., Telavi, 2200, Georgia
**Georgian Academy of Ecological Sciences
nanaka.berdzenishvili@yahoo.com

Summary: Earthquakes and Tsunamis are probably the scariest among the natural disasters that teach us about the forces of nature and their unpredictability. Knowing that there is nothing we can do to prevent the occurrence of an earthquake, we are forced to learn from our own experience. The environment at the place of occurrence of an earthquake is important for the survival of victims and also defines the particular medical and public health needs arising from its specificity. Understandably, the ecological consequences of landslides can be divided into social, As a natural or anthropogenic-natural factor. In each of these groups, we can draw direct and indirect conclusions.

Keywords: earthquake; environmental impacts; public health impacts, tsunamis, landslide.

Introduction

Earth is a dynamic planet, whose surface is continuously re-shaped by extreme, sudden events, such as fires, floods, storms, volcanic eruptions, earthquakes, and tsunamis. These phenomena are considered "natural disasters" from the human perspective, because they injure people and produce economic damages. From the ecosystem's perspective, they are forms of disturbance, defined as any discrete event in time and space that disrupts ecosystem, community, or population structure, and changes resources, substrate availability, or the physical environment. As severe phenomena of disturbance, natural disasters may affect biodiversity by increasing mortality and altering habitat quality. Understanding the impacts of earthquakes on groundwater communities is crucial to assess the resilience and sustainability of subterranean ecosystems and hence to perform conservation actions, such as a strict regulation of water extraction [1-6].

Results and discussion

Earthquakes are natural disasters that can occur at any time, regardless of the location. Their frequency is higher in the Circum-Pacific and Mediterranean/Trans-Asian seismic belt. A number of sophisticated methods define their magnitude using the Richter scale and intensity using the Mercani-Cancani-Sieberg scale. Recorded data show a number of devastating earthquakes that have killed many people and changed the environment dramatically. The consequences of an earthquake depend mostly on the population density and seismic resistance of buildings in the affected area. Environmental consequences often include air, water, and soil pollution. Direct impacts will be felt immediately and will cause damage on structures, buildings and land, including ground failure, landslides, and seiches. The damage is influenced by the particularities of the affected area: coastal areas could expect tsunami followed by enormous floods; earthquakes caused or followed by volcano eruption can bring tons of ashes and fires. Direct impacts include big changes in land morphology as well (disappearance of existing lakes or formation of new ones, for example). Indirect impacts are those that are mostly unforeseen but can cause long time problems in the environment.Hazardous material spills introduce sewage, medical, radioactive and poisonous

material into the air, water and earth. Land without trees can be subjected to huge soil erosion problems. In the Japan earthquake (March 11, 2011; Fukushima) the subsequent tsunami destroyed a part of a nuclear plant and population was exposed to radiation.

This consequence has both a direct and an indirect impact on population: radionuclides will persist in this environment for a very long time, causing health issues. Lost vegetation or/and animal species will define(undermine) the progress of affected population once they are back. Environmental impacts are, thus, very important to be assessed while their strength and type will define expected medical and public health consequences in populated areas. An imaginary estimate of the aftermath of an earthquake is incomplete, with a view to the far-reaching consequences, which This part is also unknown to us.

There are more known geological features than others that can be used for the day. Let us present the quantitative properties according to the strength of the earthquake.

The epicenter of the magnitude of the earthquakes of various magnitudes is given in Table 1.

Table 1.

Magnituda	Kerry length, km	Kerry width, km
5,0	11	6
6,5	25	18
7,0	50	30
7,5	100	35
8,0	200	50

It is clear that such a wide landscape change can not lead to ecological Changes to the terms of this and subsequent territories. More free and easy to explore than just a green space. , With liquidation of animal habitats (sometimes humans), habitual Violation of natural resources by violating natural resources and land migration rules.

Medical impacts will be mostly defined by the environment in which the earthquake happened: dense population, a lot of structures, non-seismic resistance buildings, affected elderly and/or children. Medical impacts characteristic of earthquakes are: direct impact of trauma (fractures, musculoskeletal injuries, hemotorax, bleeding), burns, poisoning and related respiratory problems, neurological and cardiovascular symptoms, drowning (if tsunami followsearthquake).

Past experience has shown that several types of landslides take place in conjunction with earthquakes. The most abundant types of earthquake induced landslides are rock falls and slides of rock fragments that form on steep slopes. Shallow debris slides forming on steep slopes and soil and rock slumps and block slides forming on moderate to steep slopes also take place, but they are less abundant. Reactivation of dormant slumps or block slides by earthquakes is rare. Large earthquake-induced rock avalanches, soil avalanches, and underwater landslides can be very destructive. Rock avalanches originate on over-steepened slopes in weak rocks. One of the most spectacular examples occurred during the 1970 Peruvian earthquake when a single rock avalanche killed more than 18,000 people; a similar, but less spectacular, failure in the 1959 Hebgen Lake, Montana, earthquake resulted in 26 deaths. Soil avalanches occur in some weakly cemented fine-grained materials, such as loess, that form steep stable slopes under non-seismic conditions. Many loess slopes failed during the New Madrid, Missouri, earthquakes of 1811-12. Underwater landslides commonly involve the margins of deltas where many port facilities are located. The failures at Seward, Alaska, during the 1964 earthquake are an example.

Tsunamis are water waves that are caused by sudden vertical movement of a large area of the sea floor during an undersea earthquake. Tsunamis are often called tidal waves, but this term is a misnomer. Unlike regular ocean tides, tsunamis are not caused by the tidal action of the Moon and Sun. The height of a tsunami

in the deep ocean is typically about 1 foot, but the distance between wave crests can be very long, more than 60 miles. The speed at which the tsunami travels decreases as water depth decreases. In the mid-Pacific, where the water depths reach 3 miles, tsunami speeds can be more than 430 miles per hour. As tsunamis reach shallow water around islands or on a continental shelf; the height of the waves increases many times, sometimes reaching as much as 80 feet. The great distance between wave crests prevents tsunamis from dissipating energy as a breaking surf; instead, tsunamis cause water levels to rise rapidly along coast lines.

Conclusion

Thus, Tsunamis and earthquake ground shaking differ in their destructive characteristics. Ground shaking causes destruction mainly in the vicinity of the causative fault, but tsunamis cause destruction both locally and at very distant locations from the area of tsunami generation. Earthquakes cause fear, panic, diseases, deaths and changed environment, leaving people in discomfort with their own vulnerability. Living in an earthquake prone area doesn't make us more vulnerable. It is our ignorance of how to react that makes us vulnerable and lost.   The most important thing is to bring people back to their homes once the disaster threat is over, to rehabilitate areas as soon as possible. As with all disasters, earthquakes function circularly, thusit is very important to learn from previous events and improve existing protocols based on experience.

References

1.Bird WA, Grossman E. Chemical Aftermath: Contamination and Cleanup Following the Tohoku Earthquake and Tsunami. // Environ Health Perspect. 2011;119(7): 290-301.
2. Boulder Weekly. Environmental impacts of the Haiti earthquake. // [Accessed October 25, 2017] Available from: http://www.boulderweekly.com/ legacy/earthtalk/environmental-impacts-of-the-haiti-earthquake/
3. Adeishvili T., Gabeshia A., Berodze M., Geophysics I. Earth's Physics.// Kutaisi, 2019
4. Adeishvili T., Berdzenishvili N. Geophysics III, Hydrosphere Physics. // Kutaisi, 2019
5. Chmyrev V.M. et al. A theory of small plasma density inhomogeneties and ULF/ELF magnetic field oscillation effected in the ionosphere prior to earthquakes. // Ed. M. Hayakawa. Tokyo. TERRA – PUB., 1999.
6. Уломов В.И. Сейсмическая опасность и «Синдром» землетрясений. // Медицина Катастроф. ЖВЦМК/Защита/, №1, 1996.

AVALANCHE HAZARDS IN THE MOUNTAINOUS REGIONS OF GEORGIA

Salukvadze M.

Institute of Hydrometeorology of the Georgian Technical University, Tbilisi, Georgia
Salukvadze.manana@yahoo.com

Summary: *56% of the Georgian territory is avalanche hazard, and 1882 avalanches poses serious risks to the settlements and infrastructure of the mountainous regions. The article presents the map indicating all avalanche-hazard and potentially hazard settlements. Based on the degree of the danger, article suggests grouping the settlements into 4 categories and provides methodology for determining the level of disaster risk. In addition, the article offers the mitigation measures and relevant recommendations.*

Key Words: *avalanche hazard, Georgia, mountainous regions*

Introduction

One of the natural disasters, snow avalanche, is widespread and every year, in winter or early spring, it significantly damages the mountainous regions of Georgia, causing destruction, damage, endangering human life, impeding traffic. The foundation of avalanche-populated areas, roads and various communications was based on long-standing (more than 40 years research. Of particular importance was the field material obtained after the massive arrival of the catastrophic avalanches of February 1971, January 1976 and January 1987, as avalanches came from almost all avalanche collectors during the extreme winters of those years. We also used data from the archives of the Hydrometeorological Department, literary sources, newspaper publications of various years, reports on the arrival of avalanches in the annual volumes of the "Caucasus Calendar" and the damage caused by them in the XIX and early XX centuries.

56% of the mountainous regions of Georgia are covered with avalanche-dangerous slopes. Avalanches occur in 20% of the area every year, and 36% have sporadic (rare recurrence) avalanches that may recur every 2-3 years or several decades, but their sudden arrival is marked by great devastating force and human casualties.

By processing all the above-mentioned sources or materials, it has been established that avalanches are dangerous for the roads that connect the mountainous populated areas of Eastern and Western Georgia. In high mountainous areas, high voltage towers, recreational or other facilities are located in the avalanche danger zone. Between 1846 and 2021, about 700 people were killed, hundreds of homes were destroyed and damaged by avalanches.

Methods

Avalanche danger in the mountainous regions of Georgia depends on the terrain (orography, hypsometry and slope inclination), climate (air temperature, precipitation and snow cover) and vegetation. The analysis of the above mentioned elements allows us to determine the origin of avalanches, their mode of arrival and the peculiarities of their spread, and the method of determining the quantitative characteristics of avalanche danger obtained by us: Avalanche activity of the area (active area in terms of avalanche formation), frequency of avalanches (number of avalanches per unit area), frequency of avalanches (number of avalanches from avalanches per winter) and number of avalanches per day (number of avalanches per day) [1,2].

To minimize the negative consequences caused by the sudden arrival of avalanches, it is important to assess the risk and plan for avalanche mitigation measures.

In Switzerland, for example, according to the average time of avalanche impact and the arrival of avalanches, since 1993, European countries, including the Russian Federation, have been exposed to 5 levels of risk: low, limited, medium, high and very strong. Snow stability is accepted as a criterion.

The level of avalanche risk in Georgia, especially for strong, strong, medium and weak avalanche-prone areas, is determined by the avalanche catchment area (ha), avalanche impact strength (t / m2) and the expected result (Table 1), [3].

Table 1. Level of disaster risk by avalanche impact strength (Pt / m2), avalanche catchment area (F, ha) and expected outcome in Georgia

N	Risk level	P t / m2),	F, ha	The result of the arrival of the avalanche
1	Weak	<20	<0,5	Human casualties, minor damage to buildings, as well as light wooden structures and other damage, traffic disruption, damage to forests and orchards, killing of small cattle.
2	Medium	21-40	0,5-1,0	Human casualties, demolition of wooden buildings and ancillary buildings, removal from transport, damage to buildings and pipelines, destruction of plantations and small areas of forest.
3	Strong	41-60	1,1-10	Human casualties, demolition of all types of buildings (trees, bricks, limestone), obstruction of movement, damage of vehicles, roads, bridges, destruction of cattle and small cattle, perennial plants and forests.
4	Very Strong	>60	>10	Human casualties, demolition of all types of buildings (including reinforced concrete), damage to railways and roads, traffic jams, destruction of cattle and small cattle, plants and forests.

Results and discussion

Using many years of fieldwork and theoretical methods, we have established that 1882 valleys, 338 settlements, passages and highways in the mountainous regions of Georgia are threatened by avalanches. 63% of the total number of such settlements are located in western Georgia, and 37% in eastern Georgia.

Zemo Svaneti (61 settlements and 314 avalanches), highland Adjara (92 settlements and 161 avalanches), Dusheti municipality (45 settlements and 83 avalanches), Shida Kartli (50 settlements and 66 avalanches), Mtskheta-Gudauri-Larsi road and Stepantsminda (13 settlements and 165 avalanches), Etc. For each of these avalanches, the morphometric and dynamic characteristics of the avalanches are calculated (Fig. 1) [3-6].

Conclusion. As we have mentioned in the methodology, the degree of avalanche danger in the territory of Georgia was assessed according to the four quantitative characteristics of avalanche danger in terms of avalanche formation with an active territory: The number of avalanches per unit area in winter; The number of avalanches per unit area; And the duration of an avalanche period. Particularly strong (3% of the total area of Georgia), strong (8%), medium (33%), weak (12%) and non-hazardous (44%) areas were distinguished [1,2].
In the regions of Georgia where winter tourism is developed, despite the work of the Georgian Rescue Service, safety norms are still being ignored, which often ends in fatal consequences. For example, in 2014-2021, 21 people died and 13 were injured due to neglect of avalanche danger and falling into unpaved snow. Fortunately, 47 people survived with the help of rescuers. Among the dead are both foreign and Georgian citizens [6].
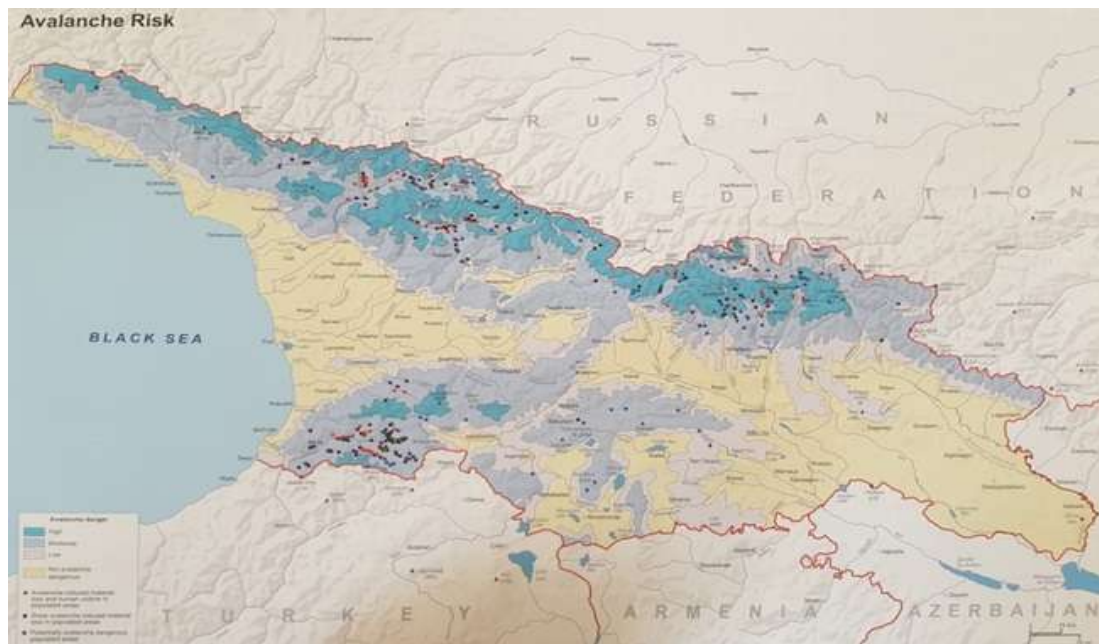
Fig. 1. Avalanche-hazardous and potentially avalanche-populated areas in Georgia

The following measures should be taken to mitigate the avalanche danger: It is necessary to assess the avalanche danger of the area as soon as the avalanche period occurs. The defense system should be activated as soon as the avalanche danger forecast is issued. In exceptional cases, for safety reasons, residents should be evacuated from the avalanche danger zone. It is also necessary to put up warning signs on the roads, mobilize the road cleaning equipment, in order to eliminate the expected damages, the energy specialists must ensure the readiness of the technical staff. When moving in mountainous areas, both locals and tourist groups should be aware of the impending avalanche danger, should know how to protect themselves in the event of an avalanche, as compliance with the rules of movement is one of the measures against avalanches. Rescue work requires great speed, because a person in an avalanche has a 50% chance of survival, and three hours after being in an avalanche this chance is 10%, sometimes even less [7].

References
1. Salukvadze M. Avalanche hazard regions in Georgia. // Proceedings of the Al. Javakhishvili Geographical Society. New Series I (XIX), 2018 pp. 117-128.
2. Kaldani L, Salukvadze M. Snow avalanches in Georgia. // Institute of Hydrometeorology of the Georgian Technical University, 2015, p. 169.
3. Salukvadze M. Snow Avalanche Cadastr of Georgia. // Monograph, Georgian Technical University, Institute of Hydrometeorology, 2018, p. 264.
4. Salukvadze M. Avalanche danger in the mountainous areas of Adjara. // Institute of Hydrometeorology of the Georgian Technical University, 2020, p. 104.
5. Saluqvadze M. Avalanche Risk; Annual Averago Snow Cover Heigt. // National Atlas of Georgia, Franz Steiner verlag.Stuttgart, 2018 , p. 42.
6. Salukvadze, M., Kobakhidze N. Georgian ski resorts and rules of movement in the avalanche dangerzone. // Proceedings of the HMI of the Georgian Technical University, vol. 127, 2019, pp. 7-11.
7. Salukvadze, M., Kobakhidze N., Jincharadze G. Anti-avalanche measures and the possiblity of their implementation in Georg. // Proceedings of the HMI of the GTU, vol. 120, 2014, pp. 57-60.

STRONG WIND ON THE TERRITORY OF GEORGIA IN 2014-2018

Beglarashvili N., **Chikhladze V., **,Janelidze I., *,**Pipia M., *Tsintsadze T.**

*Institute of Hydrometeorology of Technical University of Georgia, Tbilisi, Georgia
**Mikheil Nodia Institute of Geophysics of Ivane Javakhishvili Tbilisi State University, Tbilisi, Georgia
*** Georgian Technical University, Tbilisi, Georgia
m.pipia@gtu.ge

Summary: *2014-2018 data on strong wind cases (V≥15 m/s) are considered. The climatic characteristics of strong winds, such as the number of days, wind speed, and direction, are studied for a five-year study period. Also, strong wind distribution areas are defined according to the municipalities. Some cases of damage caused by strong winds in 2014-2018 are described.*
Based on the available data a geoinformation map of the distribution of strong winds in the regions of Georgia are compiled.

Key Words: Strong winds, dangerous weather phenomena, climatic characteristics, geoinformation map.

Introduction

Strong wind is one of the most dangerous weather phenomena. The damage caused by him is significant for the country's economy. Strong winds (V≥15 m/s) damage infrastructure, pull out trees, carry dust over long distances, interrupt and damage power lines, disrupt air traffic and cause blizzards. It also causes great damage to agriculture, carries fires over large areas, posing a threat to the country's ecological environment. Therefore, the study of the characteristics of strong winds on the territory of Georgia is of great importance.

The peculiarity of the relief that characterizes the territory of Georgia contributes significantly to the development of strong winds. Several works are devoted to its study, in which wind-hazardous regions of Georgia are highlighted [1-4]. Such territories include, for example, the valley of the Rioni River within the Kolkheti lowland, where the maximum wind speed is 66 m/s. on the territory of Kutaisi; The gorge of the Mtkvari river within the Shida Kartli lowland, the maximum speed of 65 m/s is observed at the Tbilisi airport. Mount Sabueti also has a maximum wind speed [2].

Methods and Materials

According to data for 2014-2018, and 2017-2019 in 2019-2021 we have carried out work on other hazardous weather phenomena (hail, rainfall, floods, wind etc.), and conducted an overview of the entire territory of Georgia, as well as individual regions [5-10].

The article examines the cases of strong winds on the territory of Georgia in 2014-2018. The processing of this data, to some extent, makes it possible to identify regions and municipalities where the threat of strong winds has recently been observed. The study also analyzes the dynamics of the strong winds and trends over the study period.

Strong wind data provided by the National Environment Agency. The work was carried out using the methods of probability theory and mathematical statistics [11-12].

Results

Table 1 below, compiled as a result of processing data on strong winds in 2014-2018. The table shows data on the number, speed, direction and areas of distribution of days with strong winds in the regions of Georgia.

Table 1. Strong wind incidents in the regions of Georgia in 2014-2018

Region	Distribution Area (Municipality)	Number of days	Wind speed (m/s)	Wind direction
Adjara	Batumi, Kobuleti, Keda, Khelvachauri	22	16-28	West, North-west, South-west, East
Kakheti	Telavi, Kvareli, Gurjaani, Lagodekhi, Sagarejo, Dedoplistskaro, Signagi, Akhmeta	22	20-30	West, North-west, East
Shida Kartli	Gori, Khashuri, Kaspi	8	15-25	West, North-west
Kvemo Kartli	Tsalka, Bolnisi, Tetri Tskaro, Marneuli, Rustavi, Gardabani	10	24-31	West, North-west
Imereti	Kutaisi, Chiatura	13	20-30	East, West, South-west
Guria	Ozurgeti, Chokhatauri	12	-	West
Samegrelo - Zemo Svaneti	Poti, Zugdidi, Tsalenjikha, Chkhorotsku, Senaki	16	15-30	East, West, North-west
Samtskhe-Javakheti	Akhalkalaki, Borjomi	3	18	West
Raja-Lechkhumi and Kvemo Svaneti	Oni, Ambrolauri	3	22	West
Mtskheta-Mtianeti	Dusheti, Mtskheta, Kazbegi	9	18-31	West, North-west, South-west, East
Tbilisi	Tbilisi, (Digomi, Airport)	22	18-33	North-west, West

As can be seen from Table 1, during the five-year study period (2014-2018), strong winds are observed throughout Georgia. If we consider the regions, then by the high number of days the regions of Adjara, Kakheti, and Tbilisi stand out, wherein 2014-2018, 22 days were observed in each of them when the wind speed exceeded 15 m/s (V ≥15 m/s). The smallest number of days is observed at a wind speed of V≥15 m/s in the regions of Samtskhe-Javakheti and Racha-Lechkhumi Kvemo Svaneti (3-3 days).

As for the wind speed, the maximum was recorded at the Tbilisi airport and amounted to 33 m / s. In addition, high wind speeds (30-31 m / s), as shown in Table 1., are observed in several regions of the country (Kakheti, Kvemo Kartli, Imereti, Samegrelo-Zemo Svaneti, Mtskheta-Mtianeti).

The region of Kakheti is distinguished, where the zone of distribution of strong winds during the five years of research covers the entire territory of the region and is observed in all municipalities.

As for the direction of the wind, the winds of the western direction prevail throughout the territory of Georgia. Northwest winds are also frequent. Eastern winds are also often observed in western Georgia.
Based on Table 1, a geoinformation map of the distribution of strong winds has been compiled, which shows the strong wind situation in the regions of Georgia in 2014-2018 by the number of days.

Fig. 1 shows the wind hazardous areas identified in 2014-2018. The number of days with strong winds over the five-year study period is distributed from 3 to 22 days across regions.

As mentioned in the introduction, strong winds can cause significant damage. This is evidenced by the cases of damage from strong winds described in the data for 2014-2018. For example:

On March 17, 2014, in Gurjaani (Kakheti region), high-voltage power lines and roofs of houses were damaged by strong winds. In Kakheti, 3,000 subscribers were disconnected from electricity;

On March 29, 2015, in Zugdidi (Samegrelo-Zemo Svaneti region), a strong wind damaged the roofs of 100 houses, knocked down trees, and damaged 10 cars. Due to damage to power lines, electricity was cut off to 20,000 consumers. 6 villages of Chkhorotsku suffered significant damage. 3 public schools in Zugdidi were damaged.
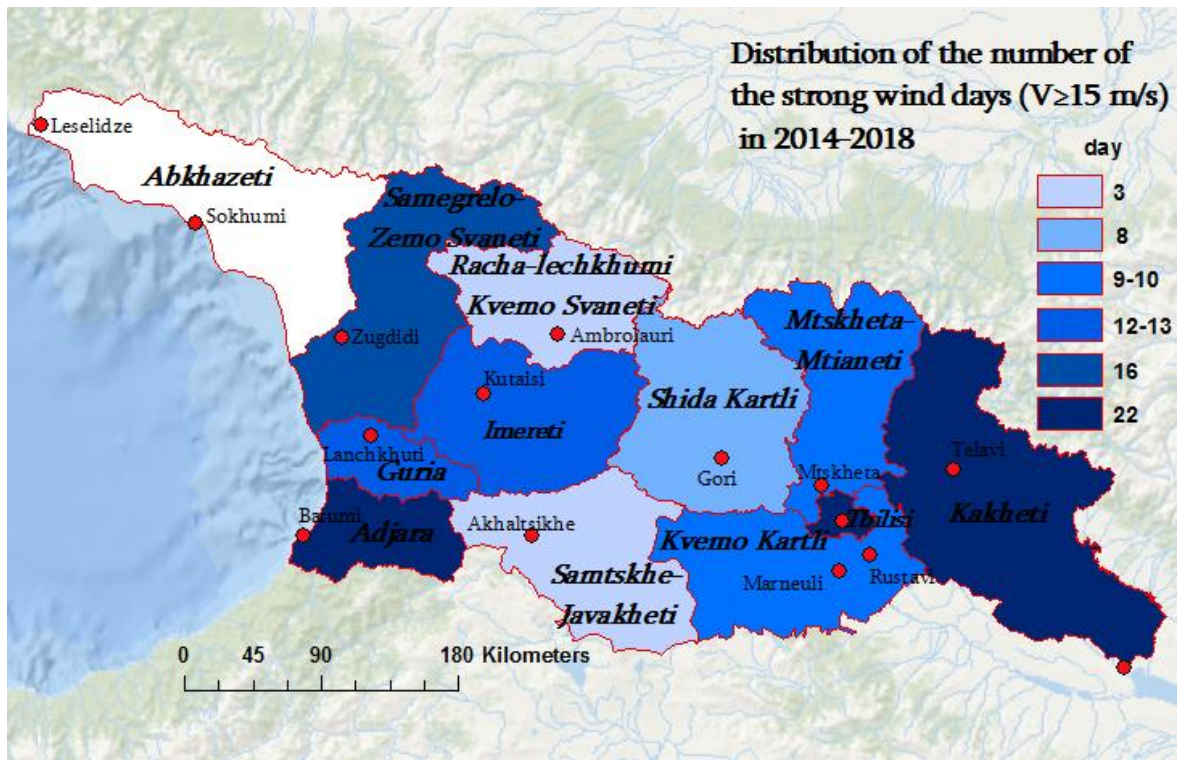

Fig.1. Distribution of the number of days with strong winds (V≥15 m / s) in 2014-2018, by regions of Georgia

On April 21, 2016, due to strong winds at Tbilisi International Airport, 8 flights were canceled, as a result of strong winds in the area of the Delisi metro station and on December 5 street in Tbilisi, cars and power lines were damaged. Strong winds created problems in Rustavi, uprooted perennial trees, damaged power lines and roofs.

On October 16, 2017, a magnolia tree fell in Batumi Park (Adjara region), a strong wind blew off the roof of Batumi State University.

On November 30, 2018, in Kutaisi (Imereti region), flights were delayed due to strong winds, roofs of about 150 houses were damaged, and trees were uprooted.

Several examples given show that strong winds can cause significant damage to a country, so it is important to study its climatic conditions and characteristics in terms of taking preventive measures.

Conclusion.

As a result of a study based on data from 2014-2018. Three regions of Georgia (Adjara, Kakheti and Tbilisi) were identified, where, in comparison with other regions, cases of strong wind are especially frequent.

On the whole territory of Georgia, according to the five-year study period, westerly and north-westerly winds prevail.

References

1. Elizbarashvili E. Climate of Georgia. // Institute of Hydrometeorology of the Georgian Technical University, Tbilisi, 2017, (in Georgian)

2. Kapanadze N., Khvedelidze Z., Zotikishvili N. The Statistical Distribution of Strong Wind in the Imereti Region and its Role in the Evolution of Ecological Processes. // International Scientific Conference „Modern Problems of Ecology" Proceedings, ISSN 1512-1976, v. 6, 2018, pp. 139-143, (in Georgian)

3. Elizbarashvili E. Elizbarashvili M. Extreme Weather Events Over the Territory of Georgia. // Institute of Hydrometeorology of the Georgian Technical University, Tbilisi, 2012, (in Russian).

4. Varazanashvili O., Tsereteli N., Amiranashvili A., Tsereteli E., Elizbarashvili E., Dolidze J., Qaldani L., Saluqvadze M., Adamia Sh., Arevadze N., Gventcadze A. - Vulnerability, Hazards and Multiple Risk Assessment for Georgia. // Natural Hazards, Vol. 64, Number 3, 2012, pp. 2021-2056, DOI: 10.1007/s11069-012-0374-3, http://www.springerlink.com/content/9311p18582143662/fulltext.pdf.

5. Janelidze I., Pipia M. Hail Storms in Georgia in 2016-2018. // International Scientific Conference „Natural Disasters in Georgia: Monitoring, Prevention, Mitigation", Proceedings, 2019, pp.114-116.

6. Beglarashvili N., Janelidze I., Pipia M., Varamashvil N. Hail Storms in Kakheti (Georgia) in 2014-2018. // International Scientific Conference „Modern Problems of Ecology" Proceedings, ISSN 1512-1976, v. 7, 2020, pp. 176-179.

7. Beglarashvili N., Janelidze I., Pipia M., Varamashvil N. Heavy Rainfall, Floods and Floodings in Kakheti (Georgia) in 2014-2018. // International Scientific Conference „Modern Problems of Ecology" Proceedings, ISSN 1512-1976, v. 7, 2020, pp. 180-184.

8. Amiranashvili A.G., Chikhladze V.A., Gvasalia G.D., Loladze D.A. Statistical Characteristics of the Daily Max of Wind Speed in Kakheti in 2017-2019. // Journal of the Georgian Geophysical Society, ISSN: 1512-1127, Physics of Solid Earth, Atmosphere, Ocean and Space Plasma, v. 23(1), 2020, pp. 73-86.

9. Amiranashvili A., Chikhladze V., Gvasalia G., Loladze D. Statistical Characteristics of the Daily Max of Wind Speed in Kakheti in the Days with and without Hail Processes in 2017-2019. // Int. Sc. Conf. „Modern Problems of Ecology", Proc., ISSN 1512-1976, v. 7, Tbilisi-Telavi, Georgia, 26-28 September, 2020, pp. 197-201.

10. Pipia M., Beglarashvili N., Jincharadze G. Hail and Damage Caused by it on the Territory of Georgia in 2014-2018. // Scientific Reviewed Proceedings of the IHM, GTU, vol.131, 2021, pp.40-43, (in Georgian)

11. KobishevaN.V., Narovlyansky. Climatological processing of meteorological information. // L., Gidrometeoizdat, 1989, (in Russian)

12. Agekyan T.A. Fundamentals of the theory of errors. // Moscow, Science, 1972, (in Russian).

TORNADOES IN GEORGIA

Chikhladze V., Jamrishvili N., Tavidashvili Kh.

Mikheil Nodia Institute of Geophysics of Ivane Javakhishvili Tbilisi State University, Tbilisi, Georgia
vicachikh@gmail.com

Summary: *The concept of tornado, conditions and causes of occurrence, types of tornadoes are given. Fujita scale introduced. A tornado in Kobuleti is described, illustrations are shown. The question of a more detailed study of tornadoes in Georgia is being discussed.*

Key Words: *Natural disasters, tornado.*

A tornado is an atmospheric vortex that occurs in a cumulonimbus (thunderstorm) cloud and spreads down, often to the very surface of the earth, in the form of a cloud sleeve or trunk tens and hundreds of meters in diameter. Usually, the transverse diameter of a tornado funnel in the lower section is 300-400 m, although if the tornado touches the water surface, this value can be only 20-30 m, and when the funnel passes over the land, it can reach 1.5-3 km.

It is believed that the speed of the vortex inside exceeds 18 m/s and can, according to some indirect estimates, reach 1300 km/h. The tornado itself moves along with the cloud that generates it. This movement can give speeds of tens of km/h, usually 20-60 km/h. Tornadoes arise in the following way. From the central part of a powerful thundercloud, the lower base of which takes the form of an overturned funnel, a gigantic dark trunk descends, which extends towards the surface of the Earth or the sea. Here, a wide funnel of dust or water rises to meet him, into the open bowl of which the trunk, as it were, plunges its end. A solid column is formed, moving at a speed of 20-40 km/h. The narrowest part of this pillar falls approximately in the middle, its height reaches 800-1500 m. Several tornado funnels can descend from a thundercloud [1–3].

A tornado is a Benard vortex in which the magnitude of the centripetal force is greater than the magnitude of the centrifugal force. This property of the vortex leads to the fact that its trunk constantly throws out part of the mass outward, and does not transfer it to the periphery of the vortex. With the ejected mass, energy also leaves, which reduces the value of the energy of the vortex itself. Therefore, like any other single Benard vortex, a tornado cannot exist without energy from the outside entering it.

As you know, tornadoes arise from powerful thunderclouds with sufficient moisture reserves. The cloud itself does not pose any danger: the moisture of the cloud must still be condensed to the size of drops. This is what the trunk of the Benard vortex, which appears in the cloud, is engaged. The Benard vortex occurs when there is a temperature gradient along the height. As a rule, thunderclouds appear at the border of a warm and cold fronts. Therefore, after the emergence of clouds, their bottom should be heated from the surface of the earth. And only after the appearance of a temperature gradient, a Benard vortex can appear in the cloud.

The vortex has appeared, but in order to transform it into a tornado, it must increase its energy. Energy can only come from moisture condensation. The rotation of the humid environment in the trunk condenses moisture, while releasing energy. And the more moisture is contained in a cloud, the more energy is released during moisture condensation [4, 5].

The cause of classic tornadoes is the strongest, prolonged thunderstorms, which exist due to the oblique and constantly rotating ascending air stream. The width of this stream reaches 16 -18 km in diameter and 15 -16 km in height. It takes 20 to 60 minutes for a tornado to form. If this rotation begins to appear on the screen of the Doppler weather radar, then it is called a mesocyclone. Tornadoes are an extremely small part of this large-scale circulation. The most powerful tornadoes are caused by severe thunderstorms.

Three conditions must be met for the formation of a funnel:

- the mesocyclone should be formed from cold dry air masses, which provides a particularly large temperature gradient along the height;

- the mesocyclone should go to an area where a lot of moisture has accumulated in the surface layer 1-2 km thick at a high air temperature of 25-35 ˚C, which allows the mesocyclone to suck in moisture from large spaces and throw it to a height of 10-15 km.

- ejection of masses of rain and hail. Fulfillment of this condition leads to a decrease in the flow diameter from the initial value of 5-10 km to 1-2 km and an increase in velocity from 30-40 m / s in the upper part of the mesocyclone to 100-120 m / s in the lower part.

The temperature inside the meso cyclone increases abruptly along the entire height due to the heat brought in by moisture, accumulated not only by saturated vapor, but also by water droplets.

What kind of tornado are there - the most common type of tornado is whip-like, in which the length of the funnel usually significantly exceeds its radius. Usually seen over the sea. Above the land, the so-called blurry - shaggy, rotating clouds reaching the ground are more often observed. Usually the diameter of such a tornado even exceeds its height. They are very powerful and capable of causing tremendous damage due to their high speed inside the vortex and their large size, more than 500 meters in diameter. Often so-called composite tornadoes can be observed both over the sea and over land. when one or several other tornadoes appear around the main central one. Such tornadoes can be of any power, but they are usually very powerful, with great destructive power. And finally, fire tornadoes that arise as a result of powerful fires or volcanic eruptions. A vivid example is the fiery tornado that arose in Dresden after the massive bombing at the end of World War II and practically wiped it off the face of the Earth.

The strength of a tornado is determined according to the so-called Fujita scale [1]:

Fujita scale F	Wind speed (km/ h)	Impact on the average (e.g. brick) European home
F0	64 - 116	(Almost) no damage
F1	117 - 180	Slight to moderate damage to the roof
F2	181–253	Significant damage to the roof / roof is missing
F3	254–332	The roof has disappeared / some walls have collapsed
F4	333–418	Most of the walls have collapsed
F5	419–512	Blown up and possibly blown in the wind

Fig. 1. Tornado in Kobuleti [8].

Fig. 2. Tornado in Poti [11].

Tornadoes are mainly observed in the temperate zone of both hemispheres, from approximately 60th parallel to 45th parallel in Europe and 30th parallel in the United States. Likewise in the southern hemisphere. Here, tornadoes are often observed in Argentina, South Africa, Australia, etc. The largest number of tornadoes is observed in the United States - more than 1200 per year; in Europe it is less, on average about 300 per year [6]. Tornadoes are also observed in the Black Sea waters, occasionally coming ashore. One of such cases was observed recently, at the beginning of September, in Kobuleti, accompanied by a heavy rain, the Smerch came ashore from the sea, blew off roofs from several houses, uprooted several trees, one of which fell on a car (fig. 1). The gas pipeline was also damaged [8].

Earlier, several cases of tornadoes ashore were noticed in the Poti area, for example, on November 24, 2017. In 2021, tornadoes were also seen in Poti and Khobi municipalities (fig. 2). The tornado tore off the roofs of more than a dozen residential buildings in Western Georgia. The element lasted for about a minute and a half. A gusty wind blew off windows and roofs. During the tornado, trees were felled, farmland was damaged, and dozens of families were left without electricity. In two villages of the Khobi municipality - Patara Poti and Uchagari, 13 houses were left without roofs. In the Black Sea town of Poti, three families were affected. In addition, several shipping containers at the port were damaged [9].

It should be noted that the tornado in Georgia was observed not only on the coast. So, on June 12, 2007, a tornado raged in the Telavi region. Here, within a few minutes, a tornado uprooted trees, demolished roofs from houses, tore power lines and destroyed crops. According to an eyewitness, a sudden wind blew the roofs from the houses, destroyed the walls, pulled out the trees and lifted them into the air [10].
Judging by the consequences, tornadoes observed on the Black Sea coast, according to the Fujita scale, are no higher than F2 in strength, moreover, they usually occur no more than once or twice a year, or even less often. As for the tornado in Telavi, its strength corresponds to the F3 category, but after 2007 it did not appear on the territory of Georgia anymore. The question arises - how often there is a tornado in Georgia, how dangerous is it, is there an opportunity and sense to fight it? Catastrophic tornadoes are rare, so it is difficult to use statistics to predict them. It is generally believed that tornadoes can occur where they have

25

already been. The development and improvement of the network of meteorological radars in Georgia will make it possible, as information accumulates, to make appropriate early forecasts [12-14].

References

1. Арсеньев С. Смерчи и торнадо. // http://www.krugosvet.ru/.
2. http://geography.kz/slovar/smerch/.
3. Герштейн М. Л Смерчи. // М. Л. Герштейн, // НЛО. - 2000. - N40. - С. 17-23
4. https://zen.yandex.ru/media/id/5d612125fe289100adb4ad8d/unichtojit-tornado-net-problem-5ef098b720cc4c3337e85195
5. https://rostec.ru/news/dozhdi-po-zakazu-kak-rabotaet-piropatron-dlya-vyzova-osadkov/?sphrase_id=184853.
6. https://ec.europa.eu/research-and-innovation/en/horizon-magazine/300-tornadoes-hit-europe-every-year
7. https://www.myvideo.ge/v/606163.
8. https://ajaratv.ge/article/825414
9. https://www.apsny.ge/2021/other/1632679962.php
10. https://www.radiotavisupleba.ge/a/1552970.html
11. http://newsday.ge/new/index.php/ka/component/k2/item/10877-%E1%83%A5%E1%83%90%E1%83%A0%E1%83%91%E1%83%9D%E1%83%A0%E1%83%91%E1%83%90%E1%83%9A%E1%83%90-%E1%83%A4%E1%83%9D%E1%83%97%E1%83%A8%E1%83%98
12. Avlokhashvili Kh., Banetashvili V., Gelovani G., Javakhishvili N., Kaishauri M., Mitin M., Samkharadze I., Tskhvediashvili G., Chargazia Kh., Khurtsidze G. Products of Meteorological Radar «METEOR 735CDP10». // Trans. of Mikheil Nodia Institute of Geophysics, ISSN 1512-1135, vol. 66, Tb., 2016, pp. 60-65, (in Russian).
13. Amiranashvili A., Chikhladze V., Dzodzuashvili U., Ghlonti N., Sauri I., Telia Sh., Tsintsadze T. Weather Modification in Georgia: Past, Present, Prospects for Development. // International Scientific Conference „Natural Disasters in Georgia: Monitoring, Prevention, Mitigation", Proceedings, Tbilisi, Georgia, December 12-14, 2019, pp. 213-219.
14. Gvasalia G., Loladze D. Modern Meteorological Radar "WRM200" In Kutaisi (Georgia). // International Scientific Conference „Natural Disasters in the 21st Century: Monitoring, Prevention, Mitigation".Proceedings, Tbilisi, Georgia, December 20-22, 2021.

COMPARATIVE ANALYSIS OF THE VARIABILITY OF MONTHLY AND SEASONAL AIR TEMPERATURE IN TBILISI AND KISLOVODSK IN 1931-2020

*Amiranashvili A., **Povolotskaya N., ***Senik I.

*Mikheil Nodia Institute of Geophysics of Ivane Javakhishvili Tbilisi State University, Tbilisi, Georgia
avtandilamiranashvili@gmail.com
**Pyatigorsk Research Institute of Resort Study of the Federal Medico-Biological Agency, Russia
***A.M. Obukhov Institute of Atmospheric Physics of Russian Academy of Sciences

Summary: *A statistical analysis of data on monthly and seasonal values of air temperature in Tbilisi and Kislovodsk from 1931 to 2020 was carried out. Comparison of monthly and seasonal mean values of air temperature in three thirty years of time (1931-1960, 1961-1990 and 1991-2020) was carried out. In particular, it was found that in Tbilisi, the effect of climate warming is more pronounced than in Kislovodsk.*

Key Words: Climate change, air temperature.

Introduction

In recent decades the problem of observed and expected climate change on our planet acquired special urgency [1]. This problem is of great importance for Georgia and Russia due to the diversity of climatic regions on their territory [2, 3]. In our recent studies, using various statistical methods, we studied the variability of air temperature and its expected changes in the coming decades for some regions of Georgia (including Tbilisi), as well as St. Petersburg [4-10].

This paper presents the results of a comparative analysis of the variability of monthly and seasonal air temperature in Tbilisi (large city with a population of over a million people) and Kislovodsk (resort town with a population around 130 thousand people) in 1931-2020.

Material and methods

Data of the Hydrometeorological department of Georgia and [http://www.pogodaiklimat.ru/history/37123.htm] about monthly mean air temperature in Tbilisi and Kislvodsk in the period from 1931 to 2020 are used.

The standard statistical methods are used. The following designations will be used below: Mean – average values; Min – minimal values; Max - maximal values; T - air temperature, ˚C; Cold – cold season from October to March; Warm – warm season from April to September .

Missing observational data using standard methods were recovered. Comparison of mean values of air temperature in three thirty years of time (I - 1931÷1960, II - 1961÷1990 and III - 1991÷2020) was produced with the use of Student's criterion with the level of significance α not worse than 0.15.

Results and discussion

Results in table 1, 2 and Fig. 1-4 are presented.

In table 1 and 2 statistical characteristics of monthly mean and seasonal values of air temperature in Tbilisi and Kislovodsk are presented.

As follows from table 1 monthly mean values of air temperature in Tbilisi in 1931-2020 changes from 1.9 °C (January) to 24.8 °C (July). Range of changeability of (Max – Min) monthly values of air temperature

composes 32.3 °C (-3.5 °C in January and 28.8 °C in August). The same data for three thirty-year time periods are as follows.

Table 1. Statistical characteristics of monthly and seasonal values of air temperature in Tbilisi in 1931-2020.

Month	Jan	Feb	Mar	Apr	May	Jun	Jul	Aug	Sep	Oct	Nov	Dec	Year	Cold	Warm
Year	1931-2020 (Full period)														
Max	6.3	7.3	11.9	16.8	20.3	25.5	28.1	28.8	23.5	17.1	10.9	9.2	15.3	9.1	21.9
Min	-3.5	-2.1	2.8	9.4	15.0	18.8	21.9	22.1	15.4	10.1	0.4	-1.1	11.8	4.1	18.5
Mean	1.9	3.2	7.0	12.6	17.6	21.7	24.8	24.5	19.9	13.9	7.9	3.5	13.2	6.3	20.2
Year	1931-1960 (I period)														
Max	5.2	6.8	10.5	15.2	19.6	23.1	26.4	27.0	22.9	17.0	9.7	5.8	14.1	7.3	21.5
Min	-3.0	0.5	2.8	9.7	15.1	18.8	22.6	22.3	17.0	10.1	4.2	0.2	11.8	4.6	19.0
Mean	1.3	3.1	6.0	12.1	17.5	21.5	24.6	24.4	19.8	13.7	7.8	2.9	12.9	5.8	20.0
Year	1961-1990 (II period)														
Max	6.3	7.3	9.9	16.3	20.0	23.6	26.7	25.9	22.3	16.0	10.4	6.2	14.8	9.1	21.4
Min	-3.5	-2.1	4.4	9.4	15.0	19.1	21.9	22.1	17.5	10.3	5.4	1.0	11.9	4.1	18.5
Mean	1.8	2.8	6.9	12.8	17.4	21.2	24.4	23.7	19.6	13.4	8.1	3.8	13.0	6.2	19.9
Year	1991-2020 (III period)														
Max	5.6	7.0	11.9	16.8	20.3	25.5	28.1	28.8	23.5	17.1	10.9	9.2	15.3	8.6	21.9
Min	-1.5	0.1	2.9	9.5	15.6	20.0	22.3	23.1	15.4	12.6	0.4	-1.1	11.9	4.6	18.7
Mean	2.8	3.8	7.9	12.9	17.8	22.4	25.2	25.5	20.4	14.7	7.7	3.8	13.7	6.8	20.7

- 1931-1960: T mean changes from 1.3 °C (January) to 24.6 °C (July), range of changeability of T is 30.0 °C (-3.0 °C in January and 27.0 °C in August).
- 1961-1990: T mean changes from 1.8 °C (January) to 24.4 °C (July), range of changeability of T is 30.2 °C (-3.5 °C in January and 26.7 °C in July).
- 1991-2020: T mean changes from 2.8 °C (January) to 25.5 °C (August), range of changeability of T is 30.3 °C (-1.5 °C in January and 28.8 °C in August).

Table 2. Statistical characteristics of monthly and seasonal values of air temperature in Kislovodsk in 1931-2020.

Month	Jan	Feb	Mar	Apr	May	Jun	Jul	Aug	Sep	Oct	Nov	Dec	Year	Cold	Warm
Year	1931-2020 (Full period)														
Max	2.0	3.6	7.0	12.7	15.8	19.4	21.5	22.7	18.0	13.1	8.7	5.5	10.3	4.8	16.8
Min	-9.8	-8.7	-3.5	4.4	10.1	13.7	15.4	14.9	10.4	3.5	-4.7	-7.0	6.3	-0.7	13.0
Mean	-2.6	-1.9	1.6	8.0	13.0	16.3	18.8	18.4	14.0	8.6	3.2	-0.7	8.1	1.4	14.8
Year	1931-1960 (I period)														
Max	1.9	3.6	7.0	12.7	15.3	18.4	21.5	21.1	17.8	12.6	6.3	4.1	9.1	3.3	16.8
Min	-9.8	-8.7	-3.5	4.8	10.4	14.6	16.9	15.6	10.6	3.5	-3.6	-5.1	6.6	-0.6	13.8
Mean	-2.9	-2.2	0.8	7.8	13.2	16.6	19.2	18.8	14.0	8.7	2.7	-1.2	8.0	1.0	15.0
Year	1961-1990 (II period)														
Max	2.0	3.2	6.3	12.7	15.0	18.1	20.2	21.0	16.4	13.1	7.1	3.5	9.9	4.8	16.3
Min	-9.8	-7.6	-1.7	4.4	10.2	13.7	15.4	14.9	11.0	4.4	-0.2	-5.4	6.5	-0.6	13.0
Mean	-2.9	-2.2	1.5	8.2	12.7	15.8	18.2	17.6	13.6	8.0	3.7	-0.4	7.8	1.3	14.4
Year	1991-2020 (III period)														
Max	0.7	3.6	7.0	12.0	15.8	19.4	21.4	22.7	18.0	12.9	8.7	5.5	10.3	3.9	16.7
Min	-6.5	-6.5	-1.3	4.9	10.1	14.3	16.6	16.0	10.4	6.4	-4.7	-7.0	6.3	-0.7	13.1
Mean	-2.2	-1.4	2.6	7.9	12.9	16.6	19.1	18.9	14.5	9.3	3.2	-0.6	8.4	1.8	15.0

As follows from table 2 monthly mean values of air temperature in Kislovodsk in 1931-2020 changes from -2.6 °C (January) to 18.8 °C (July). Range of changeability (Max – Min) of monthly values of air temperature composes 32.5 °C (-9.8 °C in January and 22.7 °C in August). The same data for three thirty-year time periods are as follows.

- 1931-1960: T mean changes from -2.9 °C (January) to 19.2 °C (July), range of changeability of T is 31.3 °C (-9.8 °C in January and 21.5 °C in July).
- 1961-1990: T mean changes from -2.9 °C (January) to 18.2 °C (July), range of changeability of T is 30.8 °C (-9.8 °C in January and 21.0 °C in July).
- 1991-2020: T mean changes from -2.2 °C (January) to 19.1 °C (July), range of changeability of T is 29.2 °C (-6.5 °C in January and 22.7 °C in August).

In fig. 1 data about difference between air temperature ΔT in Tbilisi and Kislovodsk in 1991-2020 and 1931-1960, 1991-2020 and 1961-1990, 1961-1990 and 1931-1960 are presented.

	Jan	Feb	Mar	Apr	May	Jun	Jul	Aug	Sep	Oct	Nov	Dec	Year	Cold	Warm
■ Tb (III-I)	1.5	0.7	1.9	0.7	0	0.9	0.6	1.1	0	1.0	0	0.9	0.8	1.0	0.7
■ Kisl (III-I)	0	0	1.8	0	0	0	0	0	0	0	0	0	0.5	0.8	0
□ Tb (III-II)	1.0	1.0	1.0	0	0	1.1	0.8	1.8	0.7	1.2	0	0	0.7	0.6	0.8
■ Kisl (III-II)	0	0	1.1	0	0	0.8	0.9	1.3	0.9	1.3	0	0	0.6	0.5	0.6
■ Tb (II-I)	0	0	0.9	0.7	0	0	0	-0.7	0	0	0	0.8	0	0.3	0
■ Kisl (II-I)	0	0	0	0	-0.5	-0.8	-1.0	-1.1	0	0	1.0	0	0	0	-0.6
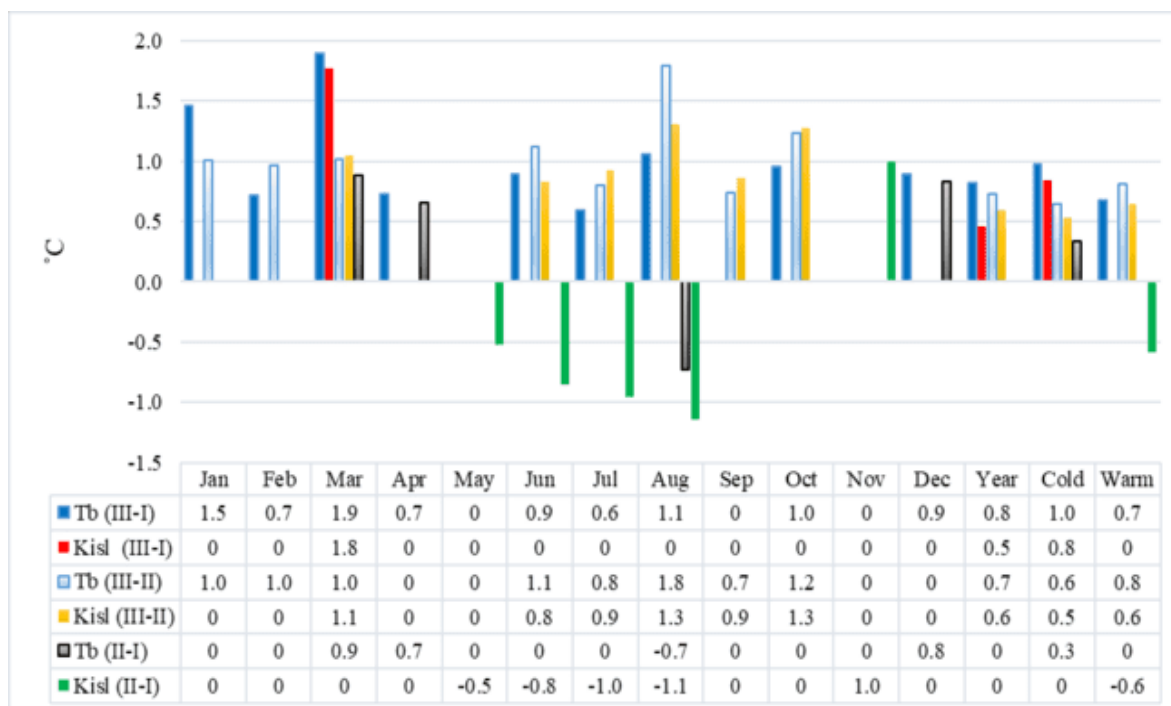
Fig. 1. Difference between mean monthly and seasonal values of air temperature in Tbilisi and Kislovodsk in 1991-2020 and 1931-1960, 1991-2020 and 1961-1990, 1961-1990 and 1931-1960.

In the indicated periods of time a significance changes of air temperature for indicated towns are as follows.

ΔT(III-I): Tbilisi - increase of the air temperature in third thirty-year period of time in comparison with the first period is observed during all months and seasons, excluding May, September and November. The greatest increase of the ΔT in March is observed (+1.9 °C). Kislovodsk - increase of the ΔT only in March (+1.8 °C), year and cold period is observed.

ΔT(III-II): Tbilisi - increase of the air temperature in third thirty-year period of time in comparison with the second period is observed during all months and seasons, excluding April, November and December. The greatest increase of the ΔT in August is observed (+1.8 °C). Kislovodsk - increase of the ΔT in March, from June to October and all seasons is observed. The greatest increase of the ΔT in Kislovodsk in August and October is observed (+1.3 °C).

ΔT(II-II): Tbilisi - increase of the air temperature in second thirty-year period of time in comparison with the first period is observed only in March (Max ΔT = +0.9 °C), April, December and cold season. In August decrease of ΔT is observed (-0.7 °C). Kislovodsk - increase of the ΔT only in November is observed (+1.0 °C). From May to August and warm season decrease of ΔT is observed. The greatest decrease of the ΔT in Kislovodsk in August is observed (-1.1 °C).

So in Tbilisi, the effect of climate warming is more pronounced than in Kislovodsk.

Conclusion

In the near future, it is planned to analyze these data using statistical methods for non-stationary observation series, as well as to carry out a comparative assessment of the expected changes of air temperature in Tbilisi and Kislovodsk for several decades.

References

1. Masson-Delmotte V., Zhai P., Pirani A., Connors S. L., Péan C., Berger S., Caud N., Chen Y., Goldfarb L., Gomis M.I., Huang M., Leitzell K., Lonnoy E., Matthews J.B.R., Maycock T. K., Waterfield T., Yelekçi O., Yu R., Zhou B. (eds.). IPCC, 2021: Summary for Policymakers. // In: Climate Change 2021: The Physical Science Basis. Contribution of Working Group I to the Sixth Assessment Report of the Intergovernmental Panel on Climate Change, 2021, 41 p.
2. Tavartkiladze K., Begalishvili N., Kharchilava J., Mumladze D., Amiranashvili A., Vachnadze J., Shengelia I., Amiranashvili V. // Contemporary Climate Change in Georgia. Regime of Some Climate Parameters and their Variability. // Monograph, ISBN 99928-885-4-7, Tbilisi, 2006, 177 p., (in Georgian).
3. Bardin M.Y., Platova T.V. Changes in Seasonal Air Temperature Extremes in Moscow and the Central Regions of European Russia. // Russ. Meteorol. Hydrol. 45, 2020, pp. 466–477. https://doi.org/10.3103/S106837392007002X
4. Tavartkiladze K.A., Amiranashvili A.G. Expected Changes of the Air Temperature in Tbilisi City. // Trans. of the Institute of Hydrometeorology, vol. 115, ISSN 1512-0902, Tb., 2008, pp. 57–65, (in Russian).
5. Amiranashvili A., Matcharashvili T., Chelidze T. Climate Change in Georgia: Statistical and Nonlinear Dynamics Predictions. // Journal of Georgian Geophysical Soc., Iss. (A), Physics of Solid Earth, vol.15a, Tbilisi, 2011-2012, pp. 67-87.
6. Amiranashvili A., Kartvelisjvili L., Khurodze T. Application of Some Statistic Methods for the Prognostication of Long-Term Air Temperature Changes (Tbilisi Case). // Trans. of the International Scientific Conference Dedicated to the 90th Anniversary of Georgian Technical University "Basic Paradigms in Science and Technology Development for the 21th Century", Tbilisi, Georgia, September 19-21, 2012, Part 2, ISBN 978-9941-20-098-4, Publishing House "Technical University", 2012, pp. 331-338, (in Russian).
7. Amiranashvili A. Changeability of Air Temperature and Atmospheric Precipitations in Tbilisi for 175 Years. // International Scientific Conference "Natural Disasters in Georgia: Monitoring, Prevention, Mitigation". Proceedings, ISBN 978-9941-13-899-7, Publish House of Iv. Javakhishvili Tbilisi State University, December 12-14, Tbilisi, 2019, pp. 86-90.
8. Amiranashvili A.G., Kartvelishvili L.G., Trofimenko L.T., Khurodze T.V. The Statistical Evaluation of the Expected Changes of Air Temperature in Tbilisi and St.-Petersburg up to 2056 Years. //Trans. of the Institute of Hydrometeorology, Georgian Technical University, ISSN 1512-0902, 2013, vol. 119, pp.58-622, (in Russian).
9. Amiranashvili A., Kartvelishvili L., Trofimenko L., Khurodze T. Statistical Structure of Mean Annual Air Temperature in Tbilisi and St.-Petersburg in 1850-2012. // Proc. of Int. Conf. "Modern Problems of Geography", Dedicated to the 80th Anniversary Since the Foundation of Vakhushti Bagrationi Institute of Geography, Collected Papers New Series, N 5(84), ISSN 2233-3347, Tbilisi, 2013, pp. 160-163, (in Russian).
10. Amiranashvili A., Chargazia Kh., Trofimenko L. Dynamics of the thirty-year moving average values of the air temperature in Tbilisi and St.-Petersburg with 1851 to 2010 and their extrapolation to 2051-2080. // International Conference "Applied Ecology: Problems, Innovations", ICAE-2015. Proceedings, Tbilisi-Batumi, Georgia, ISBN 978-9941-0-7644-2, 7-10 May, 2015, Tbilisi, 2015, pp. 12-16, http://icae-2015.tsu.ge/

CHANGEABILITY OF THE TOTAL CLOUDINESS IN TBILISI IN 1956-2015

[*]Bliadze T., [**]Kartvelishvili L. , [*]Kirkitadze D.

[*]*Mikheil Nodia Institute of Geophysics of Ivane Javakhishvili Tbilisi State University, Tbilisi, Georgia*
teimuraz.bliadze@gmail.com
[**]*National Environmental Agency of Georgia*

Summary: *The results of a statistical analysis of the monthly, semiannual and annual values of total cloudiness G in Tbilisi in 1956-2015 are represented. In particular, it was found that in the period from 1986 to 2015 compared to the period 1956-1985 in Tbilisi for all months and periods of the year (with the exception of August and December - no change of G values, and October - increase of cloudiness), there is a decrease of the values of total cloudiness. The linear trends of total cloudiness were studied for the period from 1956 to 2015. It is shown that the largest decrease of G values in 2015 compared to 1956 relative to the average value of total cloud cover in 1956-2015 was observed in June: -20.3%, the smallest - in April: -6.4%.*

Key Words: *Total cloudiness, climate change.*

Introduction

In Georgia, as in the rest of the world, in recent decades, special attention has been paid to the study of modern climate change [1,2]. Cloudiness is one of the important climate forming factors [1-3]. In particular, a number of studies have been carried out in Georgia to study long-term variations in total and lower cloudiness [4], the influence of cloudiness on the solar radiation regime [5,6], the effect of cosmic radiation on cloudiness [7,8], bioclimatic characteristics of cloudiness [9-11], etc.

In this work, which presents the continuation of the foregoing studies, some results of the changeability of the monthly, semiannual and annual values of total cloudiness in Tbilisi in 1956-2015 are represented.

Material and methods

Data of the National Environmental Agency of Georgia about mean monthly values of total cloudiness (G) in Tbilisi in 1956-2015 are used. The standard statistical methods are used. The following designations will be used below: Mean – average value of G for 1956-2015; Min – minimal values; Max - maximal values; St Dev -standard deviation; σm - standard error, (68% - confidence interval of mean values); Cv - coefficient of variation, (%), R^2 - coefficient of determination, R – coefficient of correlation; α(R) - the level of significance α of R; a and b – linear trend regression equation coefficients; 95%(+/-) - 95% of the lower and upper levels of the confidence interval of the average values; Year – mean annual values of G; Cold - mean values of G from October to March; Warm – mean values of G from April to September; (I) – average value of G for 1956-1985 (first period of time); (II) - average value of G for 1986-2015 (second period of time). Missing observational data using standard methods were recovered. Comparison of mean values of precipitations in two periods of time was produced with the use of Student's criterion with the level of significance not worse than 0.2. The unit of measurement of cloud cover is one tenth of the sky, it is omitted below.

Results and discussion

Results in tables 1-2 and fig. 1-2 are presented.

Table 1. Statistical characteristics of monthly, annual and semiannual values of total cloudiness in Tbilisi in 1956-2015.

Parameter	Mean	Min	Max	St Dev	σ_m	Cv (%)	95%(+/-)
Jan	6.4	4.0	9.0	1.12	0.15	17.5	0.29
Feb	6.6	3.8	8.3	1.06	0.14	15.9	0.27
Mar	6.9	4.1	9.0	1.00	0.13	14.7	0.26
Apr	6.8	5.0	8.2	0.80	0.10	11.7	0.20
May	6.5	4.8	8.7	0.79	0.10	12.3	0.20
Jun	5.6	4.0	8.0	0.83	0.11	14.9	0.21
Jul	5.3	3.0	7.1	0.79	0.10	15.0	0.20
Aug	5.1	2.0	7.2	1.00	0.13	19.8	0.26
Sep	5.3	3.0	7.0	0.94	0.12	17.6	0.24
Oct	5.8	3.0	9.0	1.10	0.14	19.0	0.28
Nov	6.3	3.1	9.0	1.17	0.15	18.6	0.30
Dec	6.2	3.5	8.2	1.05	0.14	17.0	0.27
Year	6.1	5.2	6.9	0.39	0.05	6.5	0.10
Cold	6.4	4.9	7.4	0.56	0.07	8.8	0.14
Warm	5.8	4.7	6.8	0.44	0.06	7.6	0.11

In table 1 the statistical characteristics of monthly, annual and semiannual values of total cloudiness in Tbilisi in 1956-2015 is presented. In particular, as follows from this table the monthly values of G changes from 2.0 (August) to 9.0 (January, March, October and November). The greatest variations in the values of G are observed during August (C_v = 19.8 %), smallest - in April (C_v = 11.7 %). The mean values of G changes from 5.1 (August) to 6.9 (March).

Table 2. Characteristics of changeability of total cloudiness in Tbilisi in 1956-2015.

Parameter	(II) – (I)	R	α(R)	a	b	{G(2015)-G(1956)}/Mean, %
Jan	-0.4	-0.15	0.25	-0.0095	25.246	-8.9
Feb	-0.5	-0.15	0.25	-0.0090	24.422	-8.1
Mar	-0.7	-0.35	0.01	-0.0199	46.386	-17.4
Apr	-0.4	-0.16	0.22	-0.0073	21.274	-6.4
May	-0.7	-0.41	<0.005	-0.0186	43.464	-17.3
Jun	-0.6	-0.40	<0.005	-0.0189	43.197	-20.3
Jul	-0.4	-0.23	0.08	-0.0105	26.113	-11.9
Aug	No	-0.12	0.36	-0.0067	18.482	-7.9
Sep	-0.4	-0.13	0.32	-0.0069	19.085	-7.8
Oct	0.4	0.20	0.13	0.0124	-18.894	12.8
Nov	-0.4	-0.19	0.15	-0.0126	31.348	-12.0
Dec	No	-0.22	0.09	-0.0134	32.704	-13.1
Year	-0.4	-0.45	<0.005	-0.0101	26.069	-10.0
Cold	-0.3	-0.27	0.04	-0.0087	23.535	-8.2
Warm	-0.4	-0.46	<0.005	-0.0115	28.602	-12.0
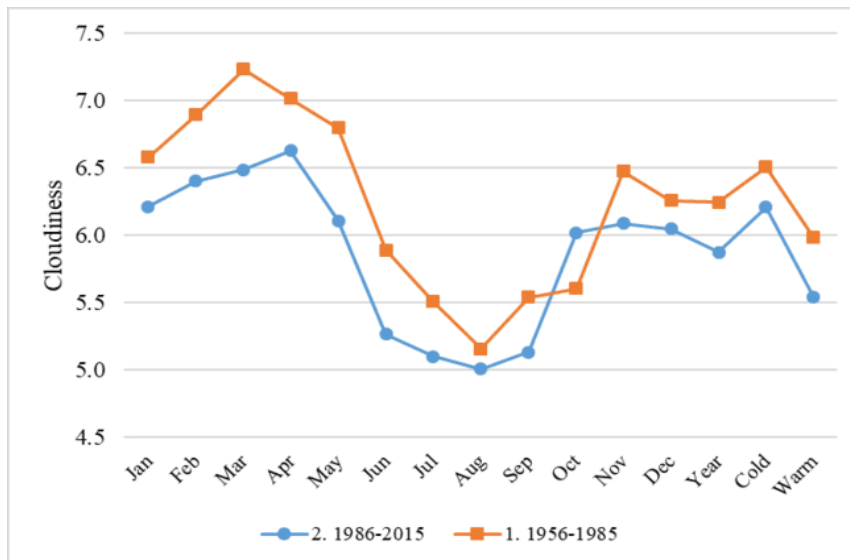
Fig. 1. The intraannual diatributions of mean monthly and seasonal values of total cloudiness in Tbilisi in 1956-1985 and 1986-2015.

In table 2 and fig. 1 the characteristics of changeability of monthly, annual and semiannual values of total cloudiness in Tbilisi in 1956-2015 is presented. Table 2 also presents data on the values of the coefficients of the linear regression equation a and b of the cloudiness trend in 1956-2015. In particular, as it follows from table 2 and fig. 1 in the period from 1986 to 2015 compared to the period 1956-1985 in Tbilisi for all months and periods of the year (with the exception of August and December - no change of G values, and October - increase of cloudiness), there is a decrease of the values of total cloudiness. The largest decrease of G values in 2015 compared to 1956 relative to the average value of total cloud cover in 1956-2015 was observed in June: -20.3%, the smallest - in April: -6.4%.
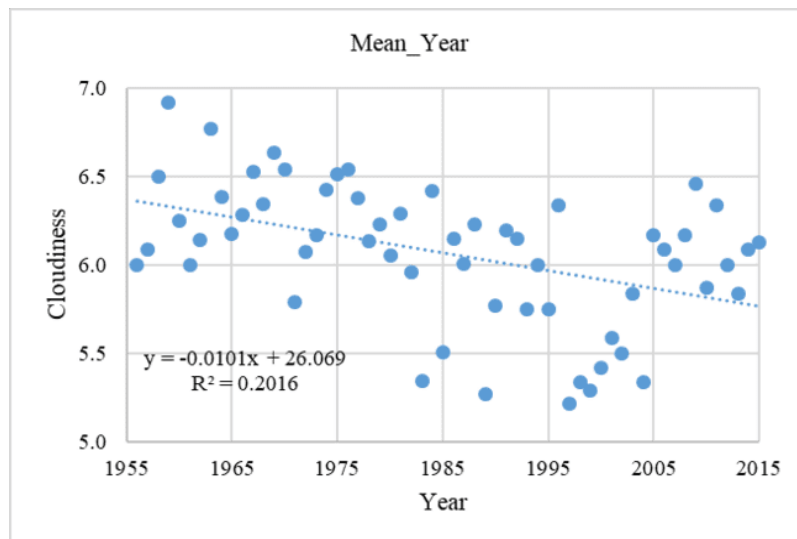
Fig. 2. Trend of the mean annual values of total cloudiness in Tbilisi in 1956-2015.

In fig. 2 example of lbnear trend of the mean annual values of total cloudiness in Tbilisi in 1956-2015 is presented.

33

Conclusion

In the future, similar studies will be carried out for other locations in Georgia.

References

1. Amiranashvili A.G., Amiranashvili V.A., Gzirishvili T.G., Kharchilava J.F., Tavartkiladze K.A. Modern Climate Change in Georgia. Radiatively Active Small Atmospheric Admixtures. // Institute of Geophysics,Monograph, Trans. of M. Nodia Institute of Geophysics of Georgian Acad. of Sc., ISSN 1512-1135, v. LIX, 2005, 128 p.
2. Tavartkiladze K., Begalishvili N., Kharchilava J., Mumladze D., Amiranashvili A., Vachnadze J., Shengelia I., Amiranashvili V. Contemporary Climate Change in Georgia. Regime of some Climate Parameters and their Variability. // Monograph, ISBN 99928-885-4-7, Tb., 2006, 177 p., (in Georgian).
3. Amiranashvili A., Bliadze T., Chikhladze V. Photochemical Smog in Tbilisi. // Monograph, Trans. of Mikheil Nodia institute of Geophysics, ISSN 1512-1135, v. 63, Tb., 2012, 160 p., (in Georgian).
4. Amiranashvili A., Amiranashvili V., Gzirishvili T., Kolesnikov Yu., Tavartkiladze K. Spatial-Temporary Variations of Total and Lower Layer Cloudiness Over the Georgian Territory. // Proc.13th Int.Conf. on Clouds and Precipitation, Reno, Nevada, USA, August, 14-18, vol. 2, 2000, 1159-1162.
5. Amiranashvili A., Amiranashvili V., Tavartkiladze K. Influence of Cloudiness Trends on the Total Solar Radiation in Tbilisi. // Proc.13th Int. Conf. on Clouds and Precipitation, Reno, Nevada, USA, August 14-18, vol. 2, 2000, 876-877.
6. Amiranashvili A.G., Amiranashvili V.A., Tavartkiladze K.A. Influence of Cloudiness and Aerosol Pollution Trends on the Total Solar Radiation in Some Non Industrial Regions of Georgia. // Proc. 14th International Conference on Clouds and Precipitation, Bologna, Italy,18-23 July 2004,3_1_217.1-3_1_217.2.
7. Amiranashvili A.G., Bakradze T.S., Ghlonti N.Ya., Khurodze T.V., Tuskia I.I. On the Connection Between Annual Variations of the Intensity of Galactic Cosmic Rays and the Changeability of Cloudiness and Air Temperature in Tbilisi. // Journal of the Georgian Geophysical Society, Issue B. Physics of Atmosphere, Ocean and Space Plasma, v.19B, Tbilisi, 2016, pp. 128-134.
8. Amiranashvili A., Bakradze T., Erkomaishvili T., Ghlonti N., Tuskia I. On the Relationship of Annual Variations of the Intensity of Galactic Cosmic Rays with the Variability of Total Cloudiness, Atmospheric Precipitation and Air Temperature in Tbilisi in 1966-2015. // Journal of the Georgian Geophysical Society, ISSN: 1512-1127, Physics of Solid Earth, Atmosphere, Ocean and Space Plasma, v. 23(2), 2020, pp. 64 – 71.
9. Amiranashvili A., Kartvelishvili L., Matzarakis A. Comparison of the Holiday Climate Index (HCI) and the Tourism Climate Index (TCI) in Tbilisi. // Int. Sc. Conf. „Modern Problems of Ecology", Proc., ISSN 1512-1976, v. 7, Tbilisi-Telavi, Georgia, 26-28 September, 2020, pp. 424-427.
10. Amiranashvili A.G., Kartvelishvili L.G. Holiday Climate Index in Kakheti (Georgia). // Journal of the Georgian Geophysical Society, e-ISSN: 2667-9973, p-ISSN: 1512-1127, Physics of Solid Earth, Atmosphere, Ocean and Space Plasma, v. 24(1), 2021, pp. 44-62.
11. Amiranashvili A.G., Revishvili A.A., Khazaradze K.R., Japaridze N.D. Connection of Holiday Climate Index with Public Health (on Example of Tbilisi and Kakheti Region, Georgia). // Journal of the Georgian Geophysical Society, e-ISSN: 2667-9973, p-ISSN: 1512-1127, Physics of Solid Earth, Atmosphere, Ocean and Space Plasma, v. 24(1), 2021, pp. 63-76.

THE IMPACT OF CLIMATE CHANGE ON SLOPE GEOLOGICAL PROCESSES (WITH THE EXAMPLE OF HOVK COMMUNITY LANDSLIDE)

Igityan H., Grigoryan E., Arakelyan S., Gevorgyan M., Nazaretyan S., Gabrielyan A.

Institute of Geological Sciences of NAS, RA
Igityanhayk@gmail.com

Summary: *Climate change in mountainous areas increases the likelihood of activation of slope geological processes. Due to climate change, the total amount of precipitation in the South Caucasus has decreased by 10-15%. At the same time, the intensity of precipitation increases, as a result of which surface and groundwater flows increase. Increased intensity of surface erosion and the rise of groundwater level, especially in steep slopes, contribute to activation of landslides or their reactivation. For sustainable and safe development of communities, it is very important to study the risks and hazards of climate change, to assess them, and to plan the measures to mitigate the effects.*

Key Words: *Climate change, landslide, risks and hazards*

Introduction.

The area of the Republic of Armenia is characterized by intense and wide-scale development of landslide processes. More than 3,500 landslides have been mapped in the entire area of Armenia. These landslides and zones exposed to their likely impacts cover about 4% of the area of Armenia, and more than 10% of all populated areas are located within landslide-prone areas or adjacent to them. Landslides exist in any region with steep and high-elevation mountain slopes [1]. During the last 20 years, the Ministry of Emergency Situations of the RA recorded 166 cases of landslide activation, of which 25% occurred in Tavush region. To understand the reasons for the activation of landslides in the Tavush region, let us consider the landslide of Hovq community. The settlement of Hovq is situated in Tavush region, on the Yerevan-Ijevan inter-state M4 Highway, on the left-bank slope of the Aghstev River valley. Active slope effects that are observed in the eastern part of the Hovq settlement manifest themselves as landslides. The landslide develops in an area south of the watershed of the Ijevan mountain range, delimited by the Aghstev River. Two landslide toes rest upon the left bank of the Aghstev River. Landslide dimensions encompass almost the entire area of the settlement (Figure 1). The landslide has developed on a natural slope with an angle of 35-50°. The annual intensity of precipitation in the Hovq settlement corresponds to 800-900 mm. The Hovq landslide has been activated several times, and, as a consequence, 70 houses in the settlement turned extremely dangerous to live in, about 350 m long site within the 117 km[th] section of the Yerevan-Ijevan Highway was completely closed, and the channel of the Aghstev River was partially dammed; as a result people, vehicles, etc were damaged [2].

Study.

The Hovq landslide represents a slide displaying very slow (creep-like) dynamics, characterized by motion dynamics at the rate of 0.3 m during up to 5 years. Landslides of this type do not pose hazard generally, and are not risky for the communities. Abundance of deformations and cracks (joints) are characteristic for creep-type landslides (Figure 2).
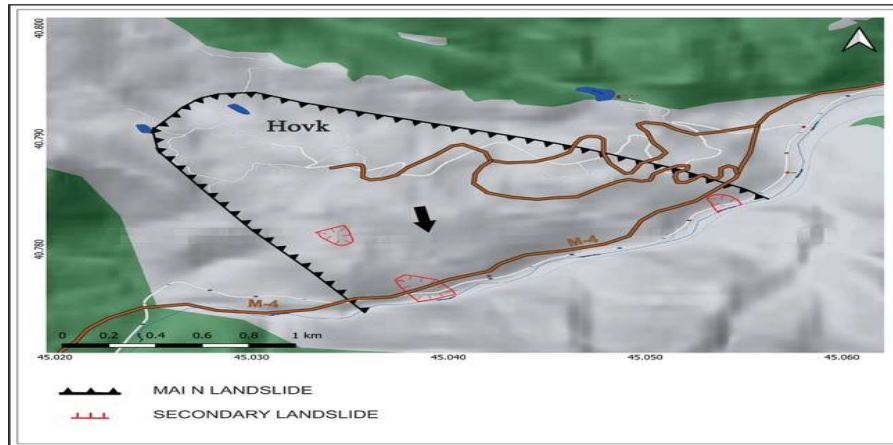
Fig. 1. Structure of the Hovq Community landslide, black lines outline the general area of the landslide (main landslide body), and red lines contour the secondary landslides that have developed this year

Water flows generated during rapid snow melting or long-term precipitation periods infiltrate also through these cracks inside the landslide body, and lead to the rise of groundwater level and over-saturation of the soils with water (Figure 3). The over-moistening leads to changes of the physical parameters of soils such as cohesion coefficient, internal friction angle, and other indicators. Therefore, it is not by coincidence that landslides found in critical equilibrium state can become active under the impact of weather anomaly manifestations resulting from climate change. In 2010, intense atmospheric precipitation preceded landslide body activation recorded at the settlement of Hovq [4]. The over-moistening leads to changes of the physical parameters of soils such as cohesion coefficient, internal friction angle, and other indicators. Therefore, it is not by coincidence that landslides found in critical equilibrium state can become active under the impact of weather anomaly manifestations resulting from climate change.

Fig. 2. Cracks (joints) observed in the landslide site of the Hovq settlement

In 2010, intense atmospheric precipitation preceded landslide body activation recorded at the settlement of Hovq [4]. The landslide became active also in February 2021, which led to the damage of houses, generation of two new landslides, and more features of soil deformation and cracks developing in the settlement area. As per accounts of the villagers, intense precipitation preceded the landslide activation. The amounts of precipitation in the month of February recorded in the community over the last 30 years were analyzed to clarify if the last landslide activation at the Hovq settlement could have been related with climate change.
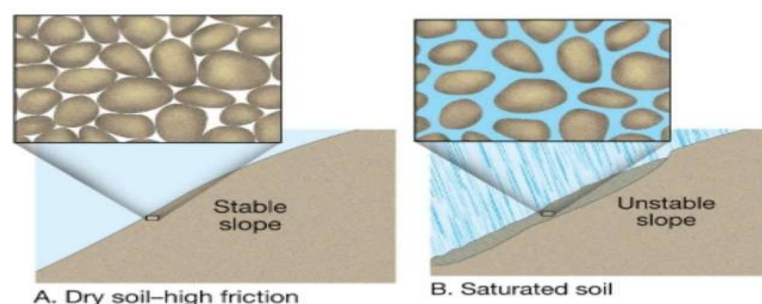
Fig. 3. Schematic layout illustrating the impact on the soils caused by water infiltrating into the landslide body in case of intense precipitation – stable slope, unstable slope, dry soil, water-saturated soil [3].

The analysis makes it clear that the daily precipitation rate in February of this year exceeds the average precipitation rate for the month of February recorded during 30 years [5]. Hence, it is possible to suggest that among other factors, weather changes determined by climate change, and the growing intensity of precipitation and snow melting, in particular, also influence re-activation of the landslides.

Conclusion.

In mountainous countries, climate change produces new hazards and risks. Studies have demonstrated that among other circumstances, growing intensity of precipitation and weather anomaly manifestations determined by climate change contribute to landslide re-activation and increase the rate of vulnerability of settlements located in landslide-prone areas. Climate forecast scenarios attest that in spite of general reduction of the total rate of precipitation, its intensity is growing. Therefore, sustainable development of landslide-prone communities requires assessment of the hazard and risks, followed by elaboration of mitigation measures. To achieve this goal, it is extremely important to undertake capacity-building actions at the vulnerable communities, elucidate and familiarize the population with natural hazards specific for community settlements, develop skills that help both to recognize effects facilitating activation of natural hazards and precursory signs of such activation, and to work with the toolkit of simple techniques to cope with, mitigate and monitor such effects. This knowledge will contribute to the sustainable community development, reasonable land use of areas exposed to landslide hazard, and reduction of risks posed by natural hazards. Moreover, better awareness might preclude or reduce intense irrigation of landslide-prone areas, realization of earth works in sloping sections, and deforestation, and help to build a system of ditches in upper sections of the slopes to protect against intense precipitation, and other. Hence, communities can develop local capacities, elaborate climate change adaptation plans independently and reduce natural hazards and risks.

References

1. Matossian A.O., Baghdasaryan H., Avagyan A., Igityan H., Gevorgyan M., Havenith H-B. A New Landslide Inventory for the Armenian Lesser Caucasus: Slope Failure Morphologies and Seismotectonic Influences on Large Landslides.// Geosciences, 10(3), 2020, 111.URL: https://doi.org/10.3390/geo-sciences10030111
2. About nature-related emergency situations that occurred in the area of the RA, damages they caused and actions taken to eliminate the consequences. // Reference Document; Republic of Armenia, Ministry of Emergency Situations, Yerevan, 2020.
3. Allegheny County Landslide Portal; Possible Causes of Landslides. // URL: https://landslide-portal-alcogis.opendata.arcgis.com/pages/types-and-effects
4. Republic of Armenia, Ministry of Emergency Situations, "About nature-related emergency situations that occurred in the area of the RA, damages they caused and actions taken to eliminate the consequences". // Reference Document; Yerevan, 2021.
5. Republic of Armenia, Ministry of Emergency Situations, "State Hydro-Meteorology and Monitoring Survey of Armenia". // SNCO, Yerevan, 2021.

IMPACT OF CLIMATE CHANGE ON AGRO-CLIMATIC CHARACTERISTICS AND ZONES OF MTSKHETA-MTIANETI REGION

Meladze M., Meladze G.

Institute of Hydrometeorology at the Georgian Technical University, Tbilisi, Georgia
m.meladze@gtu.ge

Summary: *The temporal change tendency of agro-climatic characteristics for the vegetation period in the Mtskheta-Mtianeti region has been revealed taking into account climate change; In particular, the vegetation period prolongation in the arid subtropical, mountainous and highland zones of the region and the increase of the active temperature sum (>10°C), and the decrease dynamics of atmospheric precipitation (mm) and hydrothermal coefficient (HTC). According to the current (basic) and future scenarios (2020-2049), agro-climatic zones are allocated taking into account the temperature increase by 2°C, with recommendations for the spread of appropriate perspective crops by the height above the sea level. The forecast equation for the potato crop is drawn according to the temperature of the latter scenario. It is established that according to the future scenario (2020-2049), the increase of the projected temperature by 2°C will not have a negative impact on agricultural crops.*

Key Words: climate change, active temperature, agroclimatic zone

Introduction. The impact of climate change on the environment is far-reaching and is reflected on the ecological equilibrium established during centuries and on the macro-climate of the Earth's air wholly. Its action can lead to the melting of eternal glaciers, floods, storms, hurricanes, droughts and other natural disasters (catastrophes). Many sectors of the Worlds economics, including agriculture, damage significantly. Modern climate change has also affected the territory of Georgia, especially the eastern part of Georgia, where there is a tendency of higher temperatures compared to the western part of Georgia. This is indicated by the statistical analysis of multi-year meteorological observation data. Temperature increase was observed from the western humid subtropics of Georgia to the highland area of the Kakheti region in the east of Georgia (0.2-0.5°C), respectively [1, 2]. The given temperatures have to be taken into account, because if the process of global warming is prolonged, the temperature may rise further and reach 2°C and above in three to four decades. Therefore, it is necessary to know in advance what impact it will have on the sectors of the country's economy, especially the agrarian sector. The temperature increases by 3-4°C and above can have a negative impact on existing, adapted plants, especially in lowland areas up to 300-600m above the sea level, because, even more heat will be accumulated in such places. Therefore, the normal productivity of vulnerable crops such as cereals, fruits, vegetables and other crops will be in danger.

Methods. Our aim was to identify agroclimatic zones for distribution of crops according the baseline (current) and future scenario (2ºC temperature increase) in Mtskheta-Mtianeti region. In order to solve the given issues we used and processed baseline (current) meteorological observation. The data of the many-year (1948-2017) meteorological observations of the National Environment Agency of Georgia - average air temperatures and atmospheric precipitation sums (mm) are used and processed. The data of agrometeorological observations were treated by using the method of mathematical statistics. Also, the data of the future scenario are processed, temperature increase by 2°C (2020-2049), which were obtained by regional climatic model RegCM-4 and social-economic development scenario A1. This was used for the Framework Convention on Climate Change in the scope of the Third National Frame Communication of Georgia [1]. In the above-mentioned region, the date of transition of air temperature above >10°C to below <10°C was determined by the following equations: y=-2.4x+79 (in spring), y=3.2x-33 (in autumn). In the equations - y is the dates of the spring and autumn temperatures above >10°C and below <10°C; x - the sum

of the average temperatures of two months or each month in spring and autumn. Also, the method of harvesting agrometeorological forecasting is used.

Results and discussion. The agriculture of Mtskheta-Mtianeti region is economically important, which is reflected in ensuring the social and economic level of the population. Despite the rather difficult mountainous terrain and, consequently, the different types of climatic conditions created here, it is possible to develop cereals, fruits, vines, vegetables, beekeeping, livestock and other fields of agriculture and get high quality crop [3]. In the context of recognized global climate change, there is no relevant scientifically sound experience as to whether the agro-climatic characteristics of normal development and productivity of these crops in the territory of a given region will change. Therefore, it is advisable to identify their changes in order to develop appropriate mitigation measures and recommendations for the negative impact on the agro-climatic characteristics.

In this regard, the agro-climatic characteristics of the arid subtropical, mountainous and highland zones of the Mtskheta-Mtianeti region with the future scenario (2020-2049), taking into account global warming when the air temperature rises by 2°C (Tab. 1).

Tab. 1 Agroclimatic characteristics according to the scenario, with the temperature rises by 2°C

Region/ Zone	Meteo-station, Altitude (mm) a.s.l.	Data of transition air temperature t>10°C	Data of transition air temperature t<10°C	Duration of the vegetation period	Sums of active temp. >10°C (IV-X)
Mtskheta-Mtianeti, arid subtropical	Mtskheta, 460	31.III	7.XI	221	3986
Mtskheta-Mtianeti, Mountainous	Dusheti, 922	9.IV	31.X	205	3581
Mtskheta-Mtianeti, Highland	Kazbegi, 1744	12.V	1.X	142	2088

According to the future scenario (2020-2049) the temperature increase by 2°C in the given zones, the increase of active temperature sums (> 10°C) and the prolongation of vegetation periods will not negatively affect the normal growth and development of crops and full fruit ripening if soil moisture remains in adequate conditions. The growth temperature will be especially positive for the normal development-productivity of crops that have limited heat supply. Based on the meteorological observations, the active temperature sums (>10°C) and atmospheric precipitation (mm) in the warm period (IV-X and V-IX) are also analyzed, processed and calculated for dry subtropical, mountainous and highland areas of Mtskheta-Mtianeti, also the hydrothermal coefficients during the period of active vegetation (VI-VIII). The dynamics of their course were depicted by trends, for example in the arid subtropical zone Mtskheta is presented (Fig. 1).
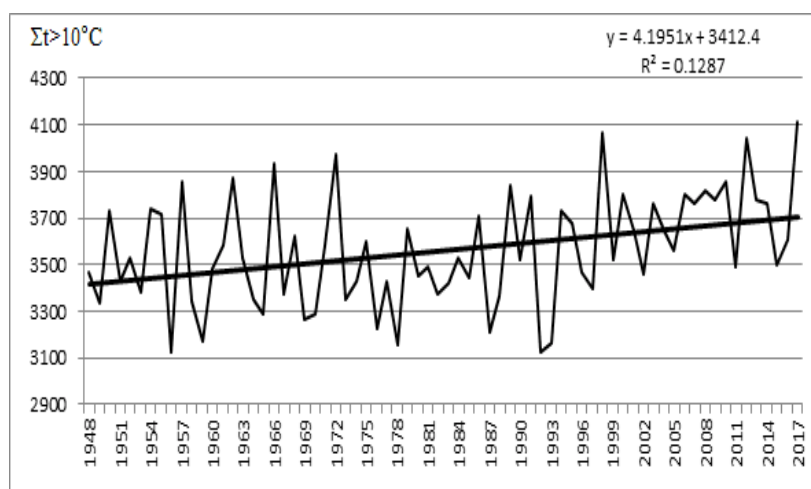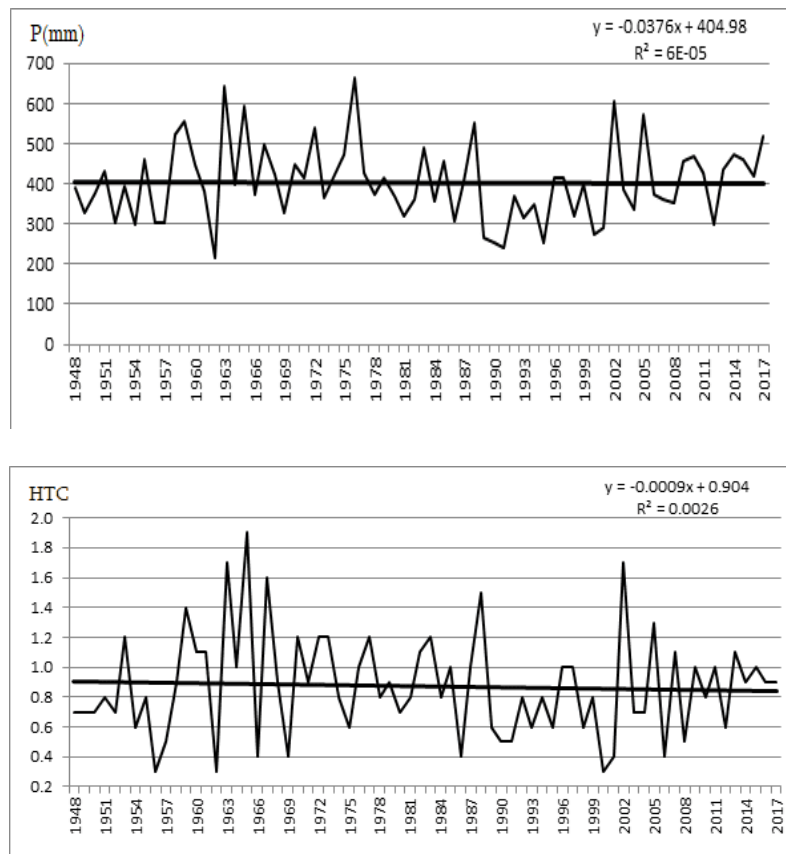
Fig. 1. Dynamics of sums active temperatures (> 10°C) and atmospheric precipitation (mm) and HTC (arid subtropical zone, Mtskheta)

According to the zones trends, the tendencies of increasing the active temperature sums and decreasing tendencies of atmospheric precipitation and hydrothermal coefficients are revealed. According to the agro-climatic characteristics calculated from the trend equations, the active temperature sums in the arid subtropical zone in 1948-2017 is 289°C, in the mountains and in the highlands - 216°C, 286°C, respectively. The atmospheric precipitation sum is reduced by 3 mm in the arid subtropical zone, and by 19 and 113 mm in the mountainous and highland areas, respectively. If the active temperature sums trend increasing continues in the future, after 4-5 decades the temperature sums in the arid subtropical zone may reach 3900-4000°C and slightly higher, in the mountainous zone - 3400-3500°C and slightly higher, and in the highlands - 1900-2000°C and slightly more. However, it will not be a nuisance for mountainous and highland areas, as for normal development and more productivity the agricultural crops are less heat-supplied. Conversely, it may even be beneficial in conditions of adequate soil moisture. Based on the above, the atmospheric precipitation decrease tendency will be observed in the given zones. Therefore, during the active vegetation period (VI-VIII) in the arid subtropical zone it will be necessary to carry out watering measures 2-3 times for annual crops and 1-2 times for perennials.

The 5 agro-climatic zones were allocated in the territory of Mtskheta-Mtianeti region with vertical zoning in order to spread the relevant agricultural crops.

Zone I includes the arid subtropical area of the region, located at the 600 m above the sea level. The active temperature sum above 10°C is 3651°C (basic), and by the future scenario (2020-2049) when the temperature rises by 2°C - 4211°C. In the conditions of the mentioned zone it is possible to expand the distribution area and produce of dry subtropical fruit crops, cereals, early and late grape varieties. The given zone is less provided with atmospheric precipitation during the active vegetation period (VI-VIII). Therefore, for the unimpeded development of the specified crops, it is necessary to provide the soil with adequate moisture.

The II - Zone extends up to 1000 m above the sea level. The active temperature sums (> 10°C) is 2917°C (base) and when the temperature rises by 2°C - 3362°C. The given temperatures are favorable for the propagation-production of early (1300-1400 m elevation) and late (1100-1200 m altitude) vine varieties, widespread propagation-production of wheat, corn, vegetables, fruits and other crops. The atmospheric

precipitation sum during the active vegetation period (VI-VIII) is 180 mm, which is not enough for the normal development and productivity of plants. Therefore, water should be provided to the plants root system (soil irrigation-cultivation).

The III - Zone includes mountainous areas and extends from 1000 m to 1500 m above the sea level. The sum of active temperature sum (> 10°C) averages 2184°C, and by the scenario, when the temperature rises by 2°C - 2512°C. Due to the thermal characteristics of this zone, it is possible to propagate autumn and spring wheat, barley, potato, corn and vegetable crops up to 1200-1300 m, and early vine varieties up to 1300-1400 m. During the active vegetation period (VI-VIII) the atmospheric precipitation sum is 215 mm, which is sufficient for the development-productivity of the indicated crops.

The IV - Zone extends from 1500 to 2000 m above the sea level and includes highland areas. The sum of active temperature sum (> 10°C) is slightly reduced and amounts to 1451°C (basic), by the scenario, when the temperature rises by 2°C - 1663°C. The atmospheric precipitation sums during the period of active vegetation (VI-VIII) averages to 355 mm. It is possible to grow autumn and spring wheat up to 1600-1800 m and more, to grow the early fruit, berries and livestock feed in the zone.

The V - Zone extends from 2000 to 2500m above the sea level. It almost covers the upper border of the subalpine zone. The sum of active temperature sum (> 10°C) at 2500 m altitude in this zone is significantly reduced (717°C, basic). According to the scenario, it reaches 814°C. Under such temperature, the development and productivity of barley, oats, potatoes, vegetables, berries, and livestock root crops are limited and unprofitable. According to the future scenario, the active temperature sum (> 10°C) at the altitude of 2300 m if temperature increases by 2°C is 1153°C, which creates relatively favorable conditions for the development of these crops. The atmospheric precipitation amount in the zone is sufficient, it is almost identical to zone IV.

Given the above, whilst promising crops propagation indicated in agro-climatic zones, it is important to take into account their forecasted yield [4]. Crop formation during the development of different phenological phases depends on the need for environmental factors. For example, the period from the emergence of flower cockles to the flowering phase is of great importance for the potato crop, between which the tubers are formed in June-July. It is this period that is remarkable for how it will be provided with precipitation and more than >10 mm rainfall days. The height (cm) of the potato crop should also be considered, as the height is closely related to the crop with atmospheric precipitation. In the absence of plant height biometric observation data, the following equation is used: $U = 0.3565 \cdot x + 5.918$. In the equation x - is the atmospheric precipitation sum (mm) in June-July; Here is the prediction equation of potato crop yield:

$$U = 1.5866 \cdot x + 2.7075 \cdot y - 4.5406 \cdot z + 16.60$$

In the equation: U - is the forecasted crop, t/ ha; x - atmospheric precipitation sum (mm) in June-July; y - ≥10 mm number of rainy days in the same period; z - average height (cm) of potato plant at the end of July from $1m^2$. The total multiple correlation coefficient is R=0.92, the equation allowable error is Su ± 1.5 t/ha. The forecast is made in the first pentad of August; the expectancy is up to 2.5 months.

Conclusion. Climate change in the Mtskheta-Mtianeti region leads to the changes of agro-climatic characteristics, in particular, increase of active temperatures, prolongation of the vegetation period, reduction of atmospheric precipitation and hydrothermal coefficients during the vegetation period. As a result of the influence of these characteristics, the agro-climatic zones of plant distribution is changed. Nevertheless, according to the future scenario (2020-2049), the projected temperature increase by 2°C will not have the negative impact on the development of agricultural crops if it does not exceed this temperature increase.

References

1. The Third National Communication Climate Change of Georgia. // UNDP, 2015, p. 288.
2. Tavartkiladze K., Begalishvili N., Tsintsadze T., Kikava A. Influence of global warming on the near surface air temperature field in Georgia. // Bulletin of The Georgian National Academy of Sciences, vol.6, №3, 2012, pp. 55-60
3. Meladze G., Meladze M. Estimation of agroclimatic potential of Mtsheta-Mtianeti region // Transactions of the Institute of Hydrometeorology, Georgian Technical University, vol.119, 2013, pp. 87-90
4. Meladze G., Meladze M. Climate Change: Agroclimatic Challenges and Prospects in Easter Georgia // Tbilisi, Publ. house „Universal", 2020, p. 200.

ON CLIMATE CHANGE MITIGATION MEASURES IN FERROUS AND NON-FERROUS METALLURGY (GENERAL ANALYSIS)

* Jandieri G., **Janelidze I.

*Metallurgical Engineering and Consulting Ltd, Tbilisi, Georgia
**Georgian Technical University, Tbilisi, Georgia
ingajanelidze9@gmail.com

Summary: *The role of metallurgical carbothermal production processes in the problem of global emission and accumulation of greenhouse gases is analyzed and highlighted. Hence, one of the effective measures to mitigate climate change are identified the need to reduce the risk of carbon sequestration of reactive raw materials (coke, coal, anthracite) to atmospheric oxygen, - reducing of its premature burnout, - reducing of carbon mono- and dioxide emissions, and increasing the degree of carbon beneficial use. The main ways and methods of this problem solving are described. A rational way of solving it are suggested to temporarily passivate the surface of carbonaceous raw materials using such fine-grained metallurgical wastes as industrial oxide-containing dust or sludge.*

Key Words: *Greenhouse gases, Emission, Metallurgy, Coke, Carbothermia, Temporary passivation.*

Introduction.

The modern world community is one of the most progressive ways to mitigate the threats posed by global climate change is considering a policy of transition to a green, energy-saving, low-carbon economy, where the problem of minimizing greenhouse gas emissions is dominant [1].

According to various sources [2-4], the global emission rate of greenhouse gases was increasing by 60% in the period 1990-2019, from 22.7 up to 36.4 billion tons, calculated in terms of carbon dioxide equivalent. It is noteworthy that in the given period, only the EU is distinguished by the tendency of decreasing greenhouse gas emissions. The total emissions of the EU countries decreased from 3.87 to 2.92 billion t. Emissions from China increased up to 400%, from 2.42 up to 10.17 billion tons, in the case of India, the emission growth rat exceeded 500%, from 0.58 up to 2.62 billion tons. Emissions in the US are relatively stable, with a slight increase of $5.13 \rightarrow 5.28$ billion. According to recent data, a further 5% increase in world greenhouse gas emissions is expected in 2021-2022 [5].

According to the key policy documents on climate change mitigation, by 2030 Georgia will make an unconditional commitment to reduce total greenhouse gas emissions by 35% compared to 1990 levels (2030 greenhouse gas emissions target - 29.655 million ton $CO_{2eq.}$); At the same time, Georgia is committed to reducing its total greenhouse gases emissions up to 50-57% by 2030 compared to 1990 levels if it receives international support. A 50% reduction will be needed if the world community decides to reduce or decrease the average global temperature up to +2°C, and with a policy of +1.5°C increasing the temperature, it will be necessary to reduce greenhouse gas emissions by 57% [6].

Contribution of metallurgical industry in greenhouse gas emissions.

The highest carbon demand sector in the world economy is considered to be thermal power generation that is mainly built near large-scale industrial facilities and centers and serves their proper functioning. ≈25% of the generated energy comes from the metallurgy of ferrous and non-ferrous metals that is accompanied by carbon dioxide emitted by its own production. The share of ferrous and non-ferrous

metallurgy in the world greenhouse gas emissions according to various sources is 9-13% [4, 7], due it this sector is considered to be the undisputed leader in greenhouse gas emissions.

It is known that from 2023 in the EU the so-called a carbon tax is planned to be introduced [8] that envisages the imposition of an additional duty on the amount of carbon dioxide emitted into the atmosphere in the production of any kind of commodity. This measure will place a particularly heavy burden on industrial enterprises with particularly high consumption of carbon using outdated technologies, including one of the most painful blows that the metallurgy sector will receive. According to the official Geostat data on Georgia's foreign trade [9], the sector of extraction and processing of ferrous and non-ferrous metals (manganese, copper) occupies one of the leading positions in the Georgian economy. Therefore, their impact on the economic development and sustainability of Georgia is crucial. The decision to regulate greenhouse gas emissions will put the future of this field at a high risk.

Carbon is an essential component for the recovery and removal of metals from ores. It is supplied in a burden for carbothermic processing in the form of solid metallurgical coke. Carbon in coke is represented by allotropic modification of graphite, the content of that fluctuates in the range of 82-88% (ISO 18894: 2018). Its flow rate for the production of per ton of ferroalloy makes in average up to 350-450 kg. Solid carbon is also one of the main components for the production of high-capacity graphite or Soderbergh self-annealing electrodes for the delivery of high-capacity electricity to electric furnace furnaces [10]. Carbon, under the conditions of high-temperature, electrothermal processing (softening and melting) of a pre-prepared reaction compound, joins oxygen atoms from the metal oxides present in the ore, thus reducing them to the metal phase, oxidizing itself into carbon monoxide and carbon dioxide and passing through the dust collecting bag filters, is almost unchecked released in the atmosphere [11].

According to our data, the metallurgical sector of Georgia emits an average of 0.5-0.6 mln. ton carbon-containing gas with a greenhouse effect. The total amount of greenhouse gases emitted, including ancillary enterprises and logistics services, is approaching up to 1 million tons of carbon dioxide equivalent.

Analysis of the possibility of reducing greenhouse gas emissions.

In the electrometallurgy of ferrous and non-ferrous metals, electrocarbonothermal production of ferroalloys is characterized by a particularly low rate of carbon useful use. Here, the coefficient of target uptake of carbon does not exceed 0.80-0.85, the rest of it burns in vain with atmospheric oxygen, on the surface of the shaft top of the smelting furnace, which is irretrievable losses of economically valuable and ecologically harmful carbon. Thus, in order to exclude carbon deficiency, coke dosing is always carried out in excess of the stoichiometric amount of carbon required for recovery processes by 15-20%. This technical solution is an ecologically and economically harmful, but technologically necessary measure. The problem is exacerbated in the cast iron industry. World average production of ferrous cast iron (1,200 million tonnes) averages 50 times that of ferroalloys. The electrometallurgy of primary copper and aluminum is also a significant problem in terms of solid carbon consumption and greenhouse gas emissions. The issue of the high "carbon capacity" of the metallurgical industry is somehow already in the world's attention, and a number of well-founded studies and reports on the need to address it have been published [12, 13, 14], although studies on mitigation and prevention measures are still in their infancy.

Thus, from the all of above mentioned, solving the problem of coke reaction surface insulation from atmospheric oxygen, eliminating its waste combustion and increasing the target carbon utilization rate should be considered as one of the key issues with the potential to mitigate the harmful effects on the environment by the metallurgical industry.

Effective measures to reduce greenhouse gas emissions.

Based on the main principles of energy saving recommended by the concept 3R [15] "Reduce, Reuse, Recycle", the rational way to solve this problem is to pre-cover (temporarily passivate) the coke porous surface (passivation) emits in the ferroalloys production process by thin dusts or slime (1-3 mm) layer. This measure involves closing the pores opened at the surfaces of the coke granules by pre-annealing them with light dust by pelletizing them or extruding them into briquettes [16]. As a result of this measure, the solid coke supplied with the raw material in the furnace is protected from contact and reaction with atmospheric oxygen that will significantly reduce its in vain combustion. On the other hand, the close contact of coke and metal oxide dust will maximize the kinetics of the recovery-removal process of metal elements from this rear end, thereby increasing the rate of useful use of processed ore and recyclable metal-bearing secondary resources. In addition to reducing of vain combustion and thus mitigating the effects of adverse environmental impacts, this measure will significantly increase charge's electrical resistance, thus reducing the intensity of short circuits and power overloads, which in turn will significantly reduce electricity consumption per ton of products produced. It is noteworthy that the reduction of the volume of exhaust gases from the furnace also reduces the heat losses of the furnace, which will further improve the technical-economic and ecological characteristics of the melting process.

Accumulation of carbon dioxide (CO) emitted from the reaction zone and return to reverse for initiating the effect of plasma according to the scheme presented in the study [17] is also a rational solution in terms of reducing the intensity of greenhouse gas emissions. In terms of minimizing heat loss, a rational approach would also be to set up and operate special two-chamber duplex furnaces [18]. Technically just as rational, but economically relatively high-cost approach is the replacement of AC furnaces with hermetically sealed DC furnaces of the new generation [19]. There is no doubt that for enterprises with large-capacity production of widely demanded metallurgical products (silicon and manganese ferroalloys, pig iron, copper, and aluminum), our proposed approach of coke passivation is the most optimal.

Conclusion.

Thus, from the stated above brief analysis, it would be concluded that one of the rational and techno-economically justified ways to reduce the contribution of ferrous and non-ferrous metal metallurgy to global greenhouse gas emissions is to isolation/safeguarding a solid carbon contained in the used in cabothermal recovery processes reactive raw materials, from atmospheric oxygen. The process by which we ensure this operation is called as temporary carbon passivation.

Temporary passivation of carbonaceous raw materials is also an effective technical solution for improving the technical-economic index of recovery-extraction of target metals from ores and for the secondary use of physical-chemical energy of gases and dust released from the crucible of furnace.

References

1. Paris Agreement. United Nations, 2015. https://unfccc.int/sites/default/files/english_paris_agreement.pdf
2. Center for Sustainable Systems, University of Michigan. 2020. "Climate Change: Policy and Mitigation Factsheet." Pub. No. CSS05-20
3. Fekete H., Kuramochi T., Roelfsema M., Elzen M.D., Forsell N., Höhne N., Luna L., Hans F., Sterl S., Olivier J., Soest H.V., Frank S., Gusti M. A review of successful climate change mitigation policies in major emitting economies and the potential of global replication. // Renewable and Sustainable Energy Reviews, № 137, 2021, pp. 1364-0321. https://doi.org/10.1016/j.rser.2020.110602

4. Ritchie H., Roser M. CO₂ and Greenhouse Gas Emissions. (2020) Published online at OurWorldInData.org. Retrieved from: https://ourworldindata.org/co2-and-other-greenhouse-gas-emissions [Online Resource]

5. IEA, Global Energy Review 2021. //IEA, Paris. https://www.iea.org/reports/global-energy-review-2021 (Accessed 07.09.2021)

6. Samkharadze I., Chitanava M., Janashia N., Vardosanidze K. Impact of Climate Change Mitigation Policy on the Labor Market: Context, Possible Future Development Scenarios and Recommendations: The Example of Georgia. // Short research paper, Tbilisi, 2021, 70 p. (in Georgian)

7. Muller S., Lai F., Beylot A., Boitier B., Villeneuve J. No mining activities, no environmental impacts? Assessing the carbon footprint of metal requirements induced by the consumption of a country with almost no mines. // Sustainable Production and Consumption, Elsevier, 2020, https://doi.org/10.1016/j.spc.2020.02.002ff.

8. State and Trends of Carbon Pricing 2021. International Bank for Reconstruction and Development / The World Bank. https://openknowledge.worldbank.org/handle/10986/35620

9. External Trade of Georgia 2020. // Statistical Publication, Tbilisi 2021, 44 p. https://www.geostat.ge/media/39340/External-Merchandise-Trade-2020_publication-2021.pdf

10. White J.F., Rigas K., Peter Andersson S. et al. Thermal Properties of Söderberg Electrode Materials. // Metall Mater Trans B 51, 2020, pp. 1928-1932. https://doi.org/10.1007/s11663-020-01890-0

11. Jandieri G., Sakhvade G. Smelting of Alumosilicomanganese from Technogenic and Secondary Resources Mining-Metallurgical Industry of Georgia. // X International Congress Machines, Technologies, Materials 2013 (September 18-20 2013) Varna, Bulgaria. pp. 107-110 http://mtmcongress.com/winter/1-2013.html

12. Simonyan L.M. Analysis of the methodology for determining CO₂ emissions on the territory of the Russian federation in respect to the ferrous metallurgy. // Izvestiya VUZov. Chernaya Metallurgiya = Izvestiya. Ferrous Metallurgy, Vol. 61. No. 9,2018, pp. 721-730. https://doi.org/10.17073/0368-0797-2018-9-721-730 (in Russian)

13. Gates B. How to Avoid a Climate Disaster. // Penguin, Allen Lane, 2021, 272 p.

14. Together, Let's Speed up the Energy Transition to Create a Carbon-Neutral Society by 2050. // Corporate Communications, TOTAL SE, 2020, 60 p.

15. Srinivas H. The 3R Concept and Waste Minimization. GDRC Research Output - Concept Note Series E-093, 2015. Kobe, Japan: Global Development Research Center. Retrieved from https://www.gdrc.org/uem/waste/3r-minimization.html

16. Jandieri G., Jishkariani G., Sakhvadze D., Tavadze G. Technologies of Rendering Harmless and Regenerating Solid and Liquid Inorganic Industrial Wastes. // The Jubilee Conference on Modern Technologies and Methods of Inorganic Materials Science. Dedicated to the 100 Anniversary of Acad. Ferdinand Tavadze. Tbilisi, 2012, pp. 304-318

17. Janelidze I., Jandieri G., Tsertsvadze T. Thermodynamic analysis of interaction of components in the SIO_2-C system: improvement of technical silicon production technological process. // Physics and Chemistry of Solid State. 22, 2, Jun. 2021, pp. 345-352. https://doi.org/10.15330/pcss.22.2.345-352

18. Jandieri G., Sakhvadze D. Duplex-Furnace for Processing Manganese-containing Technogenic Waste with the Possibility of Obtaining Low-Phosphorus Manganese Ferroalloys. // International Conference: Key Aspects of the Development of the Metallurgical Industry, At: Kyiv, Ukraine, 2014, pp. 41-44 (in Russian)

19. DC Submerged ARC Furnace (SAF). Tenova Pyromet. Electronic resource, access mode (09.08.2021): https://www.tenova.com/product/ac-submerged-arc-furnace-%28saf%29/

MUTUAL INFLUENCE OF THE ATMOSPHERE AND THE OCEAN UNDER WAVE PROCESSES

Kirtskhalia V.

*Vekua Sokhumi Institute of Physics and Technology, Sokhumi State University,
v.kirtskhalia@gmail.com*

Summary: *In the report the problem of surface gravitational waves using the theory of tangential discontinuity between media: air-water is considered. Using the improved equation of mass continuity and taking into account the atmosphere inhomogeneity in the gravitational field of the Earth, it is shown that during wave processes, these two media mutually influence each other, which explains the reason for the formation of a stormy condition over the ocean and the drop in atmospheric pressure before the storm. The mechanism of the formation of the "killer wave" has been established and thus the "greatest mystery of nature" has been solved. The scale of wind and tsunami wavelengths has been established.*

Key Words: *Atmosphere, Ocean, Gravitational Waves, Waves of Wind, Tsunami Waves, Killer Wave.*

Introduction. Surface gravity waves are the most common natural phenomena. These waves are divided into two types - wind waves and tsunami waves, however, there is no clear criterion that distinguishes the lengths of these waves. These waves are generated and propagated at the interface between water and air and, therefore, studying them is a typical task of tangential discontinuity. In modern theory, these waves are investigated using the equations of hydrodynamics. relating only to water, which excludes the possibility of establishing the influence of the atmosphere on the problem under study. In addition, it is assumed that water is incompressible and its motion is potential, which leads to many contradictions in the problems of hydrodynamics and thus is not true [1,2] .

We obtain the dispersive equations of gravitational waves for an inhomogeneous atmosphere and water using the improved Euler and mass continuity equations and then, in accordance with the theory of tangential discontinuity, we stitch their solutions at the interface using the correct boundary conditions. This approach makes it possible to reveal the mutual influence of the ocean and the atmosphere during wave processes, to establish the causes of origin of the storm and "killer wave" and also to establish the scale of the wavelengths of the wind and tsunami.

Methods. The system of improved equations of hydrodynamics has the form [3]

$$
\begin{cases}
\rho \dfrac{\partial \vec{V}}{\partial t} = -\nabla P + \rho \vec{g} \\
\dfrac{\partial \rho}{\partial t} + (\vec{V}\nabla)\rho = -\rho \nabla \vec{V} - \dfrac{\vec{V}\nabla P}{C_p^2}
\end{cases}, \qquad (1)
$$

Where C_p − isobaric speed of sound, which determines the degree of inhomogeneity of the medium, In a homogeneous medium $C_p = \infty$ [4]. Linearizing system (1) with using the equation of state of the medium $\rho' = P'/C^2$ and the equilibrium condition in the gravitational field of the Earth $\nabla P_0 = \vec{g}\rho_0$, where P_0, ρ_0 and P', ρ' stationary and perturbed values of pressure and density and also representing all perturbed quantities in the form of a plane wave $f'(x,z,t) = f_a(z)\exp i(kx - \omega t)$, where $k = 2\pi/\lambda$ is the

wavenumber, λ is the wavelength and ω is its frequency, we obtain the equation of a gravitational wave with respect to the amplitude of perturbed pressure in the form:

$$\frac{d^2 P_a(z)}{dz^2} + \frac{g}{C_s^2(z)}\frac{dP_a(z)}{dz} - \left(k^2 + \Omega(z) - \frac{\omega^2}{C^2(z)}\right)P_a(z) = 0 \quad , \tag{2}$$

Here C is the true value of the speed of sound in atmosphere, which is related to the adiabatic C_s and isobaric C_p speeds of sound by the ratio $C^2 = C_s^2 C_p^2 / (C_s^2 + C_p^2)$. $\Omega(z)$ is a value that depends on C, C_s, C_p and their derivatives along the vertical coordinate z. The atmosphere is an inhomogeneous medium due to the influence of the Earth's gravitational field on it, and water is a homogeneous medium, since the gravitational force is negligible in comparison with intermolecular forces. Therefore, equation (2) for air is a second order differential equation with variable coefficients, the analytical solution of which is impossible. Based on this, we average these coefficients in the troposphere in the height interval from $z = 0$ to $z = 10^4 m$, where their dependences on z are known

$$\overline{C}_{s1} = 320 m/\sec, \overline{C}_{p1} = 590 m/\sec, \overline{C}_1 = 280 m/\sec, \overline{\Omega}_1 = -8.19 \times 10^{-9} m^{-2} \tag{3}$$

For water, these coefficients do not depend on z and therefore

$$C_{p2} = \infty, C_{s2} = C_2 = \overline{C}_2 = 1480 m/sek \text{ и } \Omega_2 = \overline{\Omega}_2 = 0 \tag{4}$$

We will seek a solution to equation (2) for air in the form $P_{a1}(z) = A\exp(\gamma z)$ and for water $P_{a2}(z) = B\exp(\delta z)$, after which they will have the form:

$$P_{a1}(z) = A_1 \exp(\gamma_1 z) + A_2 \exp(\gamma_2 z) \quad , \qquad P_{a2}(z) = B_1 \exp(\delta_1 z) + B_2 \exp(\delta_2 z) \quad ,$$
(5)

where A_1, A_2, B_1, B_2 are constants and

$$\gamma_1 = -\frac{k}{\theta_{s1}}\left[1 + \sqrt{1 + \theta_{s1}^2\left(1 + \frac{\overline{\Omega}_1}{k^2} - x^2\right)}\right], \quad \gamma_2 = -\frac{k}{\theta_{s1}}\left[1 - \sqrt{1 + \theta_{s1}^2\left(1 + \frac{\overline{\Omega}_{1`}}{k^2} - x^2\right)}\right] \tag{6}$$

$$\delta_1 = -\frac{k}{\theta_{s2}}\left[1 + \sqrt{1 + \theta_{s2}^2\left(1 - \frac{C_1^2}{C_2^2}x^2\right)}\right] < 0, \quad \delta_2 = -\frac{k}{\theta_{s2}}\left[1 - \sqrt{1 + \theta_{s2}^2\left(1 - \frac{C_1^2}{C_2^2}x^2\right)}\right] > 0 \tag{7}$$

$$\theta_{s1} = \frac{2k\overline{C}_{s1}^2}{g}, \quad \theta_{s2} = \frac{2kC_2^2}{g}, \quad x = \frac{U_p}{C_1}, \quad U_p = \frac{\omega}{k} .\text{- phase velocity of wave.} \tag{8}$$

Since the wave is surface and the atmosphere is not bounded from above, the condition $P_{a1}(z) \to 0$ at $z \to \infty$ must be fulfilled. It is seen from (6) that if fulfilled the condition

$$1 + \theta_{s1}^2\left(1 + \frac{\overline{\Omega}_1}{k^2} - x^2\right) > 1$$

(9) $\qquad\qquad\qquad\qquad\qquad\qquad\qquad\qquad \gamma_1 < 0$ and $\gamma_2 > 0$ and then only the first term remains in the expression for $P_{a1}(z)$. If

$$0 \le 1 + \theta_{s1}^2\left(1 + \frac{\overline{\Omega}_1}{k^2} - x^2\right) < 1 \tag{10}$$

$\gamma_1 < 0, \gamma_2 < 0$ and both terms are present in. Substituting the value $\overline{\Omega}_1$ and parameter values from (3), solutions (9) and (10) respectively, will be:

$$k > 9{,}05 \times 10^{-5}/\sqrt{1 - x^2}\, m^{-1} \Rightarrow \lambda < 6.94 \times 10^4 \sqrt{1 - x^2}\, m \tag{11}$$

$$k < 9{,}05 \times 10^{-5}/\sqrt{1-x^2}\, m^{-1} \Rightarrow \lambda > 6{,}94 \times 10^4 \sqrt{1-x^2}\, m \qquad (12)$$

Waves whose lengths satisfy condition (11) will be called wind waves, and condition (12) - tsunami waves. The boundary conditions used by solving the problem are as follows:

$$P_2\big|_{z=0} = P_1\big|_{z=0} + \rho_{02}\, g\varsigma(x,t), \quad V_{z1}\big|_{z=0} = V_{z2}\big|_{z=0} = \frac{\partial \xi}{\partial t}, \quad V_{z2}\big|_{z=-H} = 0, \qquad (13)$$

where $\xi(x,t) = a\exp\left[i(kx - \omega t)\right]$ is the vertical displacement of the surface of the tangential discontinuity and H — the depth of the ocean. These conditions give the following dispersion equations for waves of wind and tsunami respectively:

$$\left\{ \frac{2}{\theta_{p1}} + \frac{1}{\vartheta_{s1}} \left[1 - \sqrt{1 + \theta_{s1}^2\left(1 + \frac{\overline{\Omega}_1}{k^2} - x\right)} \right] \right\} \times \left[\frac{kg}{\omega^2}\tanh(kH) - 1 \right] = 0$$

(14)

$$\left\{ \frac{2}{\theta_{p1}} + \frac{1}{\vartheta_{s1}} \left[1 + \sqrt{1 + \theta_{s1}^2(1-x)} \right] \right\} \times \left[\left(\frac{kg}{\omega^2} + \frac{1}{\theta_{s2}} \right)\tanh(kH) - 1 \right] = 0$$

(15)

Results and discussion. Equation (14) splits into two equations:

$$\frac{2}{\theta_{p1}} + \frac{1}{\theta_{s1}} \left[1 - \sqrt{1 + \theta_{s1}^2\left(1 + \frac{\overline{\Omega}_1}{k^2} - x^2\right)} \right] = 0 \qquad (16)$$

$$\frac{kg}{\omega^2}\tanh(kH) - 1 = 0 \qquad (17)$$

Equation (16) describes longitudinal waves in the air excited by perturbationson the surface of water and propagating along this surface. Substituting the values of the parameters from (3), its solution will be:

$$|x| = \sqrt{1 - \frac{1{,}17\times 10^{-8}}{k^2}} \Rightarrow \left|U_p\right| = \sqrt{1 - \frac{1{,}17\times 10^{-8}}{k^2}}\,\overline{C}_1 = \sqrt{1 - \frac{1{,}17\times 10^{-8}\,\lambda^2}{4\pi^2}}\,\overline{C}_1 \qquad (18)$$

From (18) we find

$$k = \frac{1{,}08\times 10^{-4}}{\sqrt{1-x^2}} \qquad (19)$$

which is consistent with the condition (11) and therefore the roots (18) are not extraneous for any valid values k. We see that for $k > 10^{-3}\,m^{-1} \Rightarrow \lambda < 6{,}3\times 10^3\,m$, the phase velocity of the wave in the air is constant and equal to $U_p = \overline{C}_1 \cong 280\,m/\sec$, and then, witha decrease of k, it falls and at $k = 1.08\times 10^{-4}\,m^{-1} \Rightarrow \lambda = 5.81\times 10^4\,m$ we have $x = 0$ i.e. , the wave stops. This means that at this wavelength, two regions of about 30 km long, with high and low pressures are formed in the atmosphere above water. In the area of low atmospheric pressure, the amplitude of the surface wave will increase and the pressure difference between the two areas will lead to the appearance of wind. When is further reduced k to its minimum value, which is defined from (11) $k_{min} \cong 9\times 10^{-5}\,m^{-1} \Rightarrow \lambda_{max} \cong 7\times 10^4\,m$, the roots of equation (18) and the corresponding frequencies of standing waves in the atmosphere become imaginary, which leads to a sharp increase in the pressure difference and, consequently, the amplitude of the surface

wave and the wind force. This result clearly explains the reason for the drop in atmospheric pressure over the sea and ocean before the storm, as well as the reason for its strengthening..

The solution to equation (17), which describes surface gravitational waves on water, is:

$$|U_p| = \sqrt{\frac{g}{k}\tanh(kH)} = \sqrt{\frac{g\lambda}{2\pi}\tanh\left(\frac{2\pi H}{\lambda}\right)}$$

(20)

which coincides with the well-known expression for the phase velocities of wind and tsunami waves.

The phase velocity of a wave in the atmosphere does not depend on the depth of the ocean and decreases from the speed of sound to zero with increasing wavelength. In the ocean, on the contrary, the phase velocity increases from zero with increasing wavelength and depth. It is evident, that at certain wavelengths, which will depend on the depth of the ocean, these speeds will coincide and resonance of the frequencies will occur of waves in the atmosphere and the ocean. This fact is shown in Fig. 1.
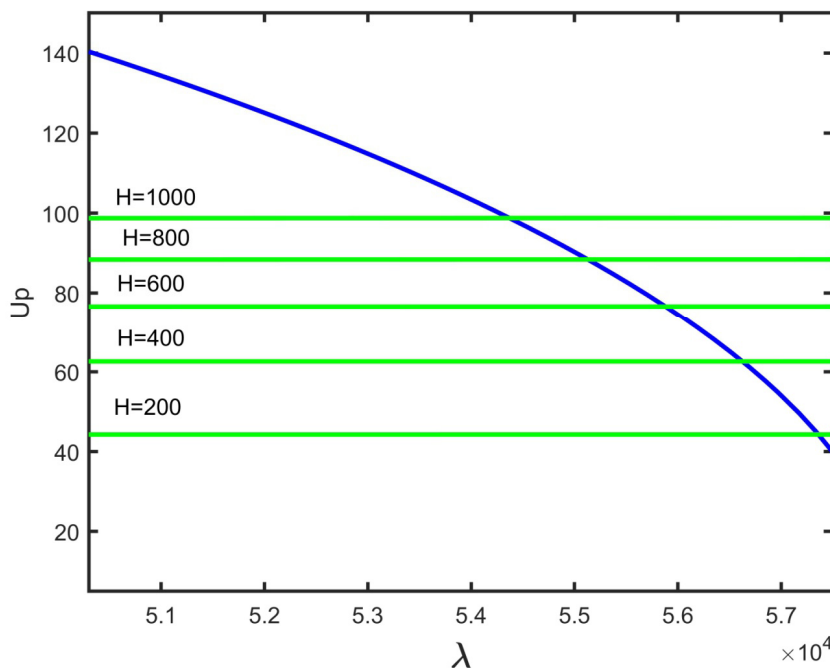
Fig. 1. Plots of dependences of the phase velocities of longitudinal waves on the air
(18) (blue curve) and on the water surface (20) (green curves) for different depths.

We can assume that this resonance is the cause of origin of the "killer wave", especially since there is no other explanation yet. It should be noted, that the resonance alone is not enough for the appearance of a "killer wave"—it is essential that the oscillations in the air and in the water are occurring in antiphase.

Equation (15) for tsunami waves also splits into two equations, the first of which has no solution based on the condition (10), which means that tsunami waves do not affect the atmosphere. The solution to the second equation coincides with (20).

Conclusion. This report does not claim to be highly accurate or to be the ultimate truth. The upper boundary of the troposphere changes depending on geographic parameters, and this concludes, that the average values of the problem parameters calculated here and, therefore, all the numerical data given in him are rather conditional. However, undoubtedly the proposed method for solving the problem is new and makes it possible to trace the correlation between the ocean and the atmosphere during wave processes. In particular,

it became clear why the atmospheric pressure in the ocean drops before the storm, as well as differentiating between the wavelengths of wind and tsunami became possible. Its apparent advantage is also that at the level of a highly plausible hypothesis, it reveals the greatest mystery of nature called the "Killer Wave". Now it is clear. why this wave is solitary. This is due to the fact that the flat relief of the ocean floor is disturbed at the distances of the order of the wavelengths that we calculated. It is also clear why a cavity, is formed before the wave. This is attributed to the fact that there is a region in front of the wave, where the pressure in the water sharply drops and in the atmosphere sharply increases.

References

1. Kirtskhalia V.G. Correct Definition of Sound Speed and its Consequences in the Tasks of Hydrodynamics. // Journal of Fluids, Volume 2016, 9 pages, http://dx.doi.org/10.1155/2016/4519201
2. Kirtskhalia V.G. The New Determination of the Criteria of Compressibility and Incompressibility of Medium . // Journal of Modern Physics, V.4, No. 8, 2013, pp. 1075-1079, doi.org/10.4236/jmp.2013.48144
3. Kirtskhalia V.G. The Linearity of the Euler Equation as a Result of the Compressibility of a Fluid. // Journal of Modern Physics, V. 10, No. 4, 2019, , pp.452-458, doi.org/10.4236/ jmp. 2019.104030
4. Kirtskhalia V.G. Speed of sound in atmosphere of the Earth. // Open Journal of Acoustics, V.2, N 2, 2012, pp. 80-85, doi.org/10.4236/oja.2012.22009

ON THE WATER QUANTUM PROPERTIES IN METEOROLOGY

Tatishvili M.

Institute of Hydrometeorology of Georgian Technical University, Tbilisi, Georgia
m.tatishvili@gtu.ge

Summary: *The interaction of light (photon) and cloud particles according main quantum assumption that system internal energy is composed by bound microparticles (cluster) under certain conditions can obtain allowed discrete significances has been discussed in the article. The objective is to calculate the transition probability from one state into another caused by inner forces or any internal processes. The cluster may be presented as multipole system. The some peculiarities of microstructure of cloud formations have been discussed using quantum disperse forces or Van-Der-Vaals forces that are typical for water particles. To obtain the expression for interaction potential the wave functions of basic and exited states of clusters and dispersion matrix have been introduced describing by virtual photon. It has been turned out that virtual photon interaction causes potential holes and barriers that are decreased by height and width. The isolated long wave quant may be the radiation that is generated throughout observed microphysical processes.*

Key Words: *Quantum transportation, interaction potential, cloud medium, dispersion matrix, microphysical processes.*

Introduction. Water is a compound and polar molecule, which is liquid at standard temperature and pressure. It has the chemical formula H_2O, meaning that one molecule of water is composed of two hydrogen atoms and one oxygen atom. Water is found almost everywhere on earth and is required by all known life. About 70% of the Earth's surface is covered by water. The important feature of the water molecule is its polar nature. The water molecule forms an angle with hydrogen atoms at the tips and oxygen at the vertex. Since oxygen has a higher electronegativity than hydrogen, the side of the molecule with the oxygen atom has a partial negative charge. Usually the molecule with such charge difference is called a dipole. The charge differences cause water molecules to be attracted to each other and to other polar molecules. This attraction is known as hydrogen bonding. This bonding gives water unusual properties. Many studies and experiments with HT equipments are made to understand water properties [1].

The interaction of light (photon) and cloud particles according main quantum assumption that system internal energy is composed by bound microparticles (cluster) under certain conditions can obtain allowed discrete significances has been discussed in the article. The objective is to calculate the transition probability from one state into another caused by inner forces or any internal processes. The cluster may be presented as multipole system. The multipole is the system composed by couple opposite charges that have definite symmetry type. The simplest is the dipole. If the transition is forbidden in dipole approach it may happen in higher approaches – quadrupole (electric) or magnetic dipole. Their probability is approximately 10^6 times less than dipole. To search out transition probability of cluster from basic state into exciting or virtual one interacting with electromagnetic field the identification of Einstein factors have to be needed [2,3].

The some peculiarities of microstructure of cloud formations have been discussed using quantum disperse forces or Van-Der-Vaals forces that are typical for water particles. To obtain the expression for interaction potential the wave functions of basic and exited states of clusters and dispersion matrix have been introduced describing by virtual photon. It has been turned out that virtual photon interaction causes potential holes and barriers that are decreased by height and width. The isolated long wave quant may be the radiation that is generated throughout observed microphysical processes.

Methods. The water H_2O is the molecule everybody knows and life is impossible without it. But for all its familiarity and import for life, aspects of water's behavior have been hard to understand, including its transformation in cloud medium.

Meteorology is an extraordinarily interdisciplinary subject, with quantitative links to many of the applied sciences and now in presented paper cloud medium is discussed using quantum theory.

Microparticles are described using wave function in quantum mechanics. The quantum system state is considered defined if its wave function (Schrödinger) or ket-vector (Dirac) is given.

The system energy change comes with quantum transportation from one energetic level into another. If $E_1 > E_2$ than system emits energy equal to $E_1 - E_2$ and if $E_1 > E_2$ then absorbs. Such transportations happen while interaction with electromagnetic radiation. Emitted or absorbed photon energy is defined by Bohr frequency law:

$$\hbar w_{12} = |E_2 - E_1| \qquad (1)$$

Molecules full energy may be presented by the kinetic energy sum connected with mass center and by internal energy sum. Molecules energy may be considered as compound from three parts:

1. Electron energy connected with their rotation around nuclei
2. E_{os} – oscillation energy connected with nuclear vibration towards mass center
3. E_{rot} –rotation energy connected with molecules rotation towards mass center

Diatomic molecule rotates around mass center located on symmetry axis of molecule. Rotation energy is defined as:

$$E_{rot} = \hbar^2 \frac{K(K+1)}{2I} = BK(K+1) \qquad (2)$$

where $I = MR_o^2$ inertial moment;
B- rotation constant;
K=0, 1, 2, 3 rotation quantum number
$|M_{rot}| = \sqrt{K(K+1)}\hbar$ - impulse momentum of rotation

Vibration energy may be defined as following

$$E_{os} = \hbar w_0 (q + \tfrac{1}{2}) - \hbar w_0 \kappa (q + \tfrac{1}{2})^2 \qquad (3)$$

where $\kappa = \frac{\hbar w_0}{4D} \ll 1$ –is nonharmonic constant.

Characterization of electric terms doesn't differ from diatomic molecule terms. In molecule nucleus electic field have no central symmetry thus the full orbital moment haven't been kept. In diatomic molecule the electric field has axial symmetry and in this case the component on the axis passing through the nucleus of orbital momentum has been kept. It is called molecule orbital quantum number and gets discrete values 0,1,2,...

Molecule state is also chracterized by full electron spin S and it has internal quantum number
$\Omega = \Lambda + S$

The light is considerd as the combination of photons with ka state and $-\hbar w$, $\hbar k$ impulses. Photon or molecular system interaction happens by forming or disappearance of light quants. During this process energy and impulse are keeping. Quantum trasformation is system trasportation from one energetic state into another. The task is to identify transformation probability from one energetic state into another. Clusters may be presented as multipole systems. Multipole is the system compound from couple of opposite charges, obtaining definite symmetry. The simpliest is dipole. If transpostation is prohebitated in dipole approach it may happen in higher approach – quadropole (electric) or magnetic dipolic.

Their probability is 10^6 time less than dipole. To identify transportation probability the Einstein members have to be defined according clusters properties. Spontaneous and forced motion members may be identifies.

Quantum transition combination is characterized by D_{mn} numbers two dimensional unity and is infinite matrix:

$$\left\| \begin{matrix} D_{11,}D_{12},.....D_{1n}.... \\ D_{21},D_{22},...D_{2n}.... \\ .... \\ D_{n1},D_{n2},...D_{nn}... \\ .... \end{matrix} \right\|$$

where $D_{mn}^0 = e\int\limits_{v} \psi_m^* \vec{r}\, \psi_n dv$

is dipole transition matrix element

The nondiagonal matrix elements are time functions and corresponds light absorption or emitting by those frequencies defined from Bohr frequency selection low.

And Einstein members can be defined as for spontaneous and forced transition probabilities:

$$A_{mn} = \frac{w_{mn}^3}{3q_0 \pi \hbar c^3}\left(D_{mn}\right)^2$$ - spontaneous transition probability

$$B_{mn} = \frac{\pi}{12 q_0 \hbar^2}\left(D_{mn}\right)^2$$ -forced transition probability

Amn is approximately 10^8 sec $^{-1}$

If some matrix element equals 0 it is called prohibited then this transition doesn't happens in dipole approach and happens in magnetic. If transitions are prohibited or banned for clusters higher energetic level the lower energetic level is called metastable and clusters life duration is 10^{-3} sec. or more.

If transition is allowed in dipole approach then system life duration is of spontaneous transition probability order. If transition is banned in dipole approach or $D_{mn}=0$ it doesn't mean that it haven't happen generally as cluster has electric quadruple or magnetic dipole moment. If transition is banned for clusters high energetic level than lower level in electric dipole interactions is called as metastable level. In this clusters life duration is 10^{-3} sec or more. In first quantum transition approach there acts Bohr prohibition principle. If such transition still happens it would be on the second or higher approach order and probability will be also less. Such are light scattering in viscous medium, mist, aerosols and etc.

This process on molecular level happens as follows: if outer emitting frequency differs from absorption frequency energy quant is anyway transmitted to the cluster which transforms into virtual state with short life period and will be defined from the uncertainty principle. Then it emits same frequency photon and returns at initial state. I definite conditions cluster may transform into final state from virtual. I simple case the falling wave is flat and emitted spherical. Energy and impulse are kept as usual except virtual state, when energy isn't keeping. For those transitions it is necessary that the electron-photon interaction matrix element have to be differs from 0.

In definite conditions cluster may transform from virtual into final state that will be differ from initial. Also emitted photon has different polarization and frequency.

In second approach it is possible the existence of two photon absorption process. After absorbing photon system transits into virtual state where it absorbs another photon and then transports into stationary state

On Earth the dimpliest and common is water molecule that has essential significance in existence of organ and nonorganic life. The most of its properties are preconditioned by the fact that three component atoms aren't placed on one line. Negative charge prevailed on oxygen atoms part and positive on hydrogen. Thus water molecule is electrically polarized. The cloud properties and their stability may be explain from water molecules properties and characterizing forces that reach maximum for 1micro-meter particles and are separated from each other on 50km distance

Among atoms and molecules acts force that always has attractive character. It is intermolecular dispersive or Van-Deer-Vaalse force. It is only one of the expressions of electromagnetic force. It acts among electrically neutral systems such as dipole or quadruple. In dipoles force reduces by r^4 inverse proportional and in quadrupole by r^{-6}. It is not temperature dependent and it s nature is quantum. By increasing dipole number their interaction increases. But its interaction is limited by the matter that light speed is finite

For cluster stable and exiting states wave function $\Psi = \Psi(x, y, z, t)$ have been used. Its physical essence is that it is particle detection probability in d_v volume for t time moment.

Probability is defined as

$$W = |\Psi(x, y, z, t)|^2 = \Psi^* \Psi \qquad (4)$$

Ψ^* is complex conjugated quantity of Ψ.

$\int_v |\Psi(x, y, z, t)|^2 dv = 1$ - is rationing condition and Ψ function that assure this condition standardized.

Generally it is expressed as:

$$\Psi(x, y, z, t) = \iiint \varphi(P_x, P_y, P_z, t) \exp(i \tfrac{px + py + pz}{h}) \frac{dp_x dp_y dp_z}{(2\Pi\hbar)^{3/2}}, \qquad (5)$$

Suppose φ_1, φ_2 are clusters basic and exited states wave functions. Their interaction in lower approach is described by so called scattering matrix

$$\varphi(x, t) = \widehat{S}(t, t_0) \varphi(x, t_0), \qquad (6)$$

where
$$\widehat{S}(t, t_0) = \exp(-\tfrac{i}{h} \widehat{H}(t - t_0)).$$

$\widehat{H}$ is system Hamiltonian. The matrix elements of scattering operator define transition probability from initial quantum state into another.

$$S_{if} = -i \int d\vec{r}_1 d\vec{r}_2 dt \, \varphi_1^* \varphi_2^* U(r) \varphi_2 \varphi_1 \exp(-i(E_{1i} + E_{2i} - E_{1f} - E_{2f})t),$$

where $E_i E_f$ is clusters basic and final states kinetic energies.

The interaction potential may be connected with averaged scattering matrix that is described by one-photon resonant exchange Hamiltonian

$$H = -\vec{d}_1 \vec{E}_1(r) - \vec{d}_2 \vec{E}_2(r)$$

where $\vec{d}, \vec{E}$ are dipole moment and field tension operators. Then for potential the following is obatained:

$$U(\vec{r}) = \tfrac{i}{4\Pi} \int_{-\infty}^{\infty} d\omega \omega^2 \alpha_{ik}(\omega) D_{ik}(\omega, \vec{r}),$$

$$\qquad (7)$$

Where D_{ik} is photon Green function and

$$\alpha_{ik} = \tfrac{1}{3} \delta_{ik} \sum_n |d_n|^2 \left[(\omega_n - \omega - i\Gamma_n)^{-1} + (\omega_n + \omega - i\Gamma_n)^{-1} \right], \qquad (8)$$

is the polarization tensor.

After integration (7) considering (8) the following expression is obtained for potential

$$U(r) = -\frac{2}{3c^2} \sum_n r_n^{-1} |d_n|^2 \omega_n^2 \exp(\frac{\Gamma_n r}{c}) \cos\frac{\omega_n r}{c}. \tag{9}$$

In equation summarization occurs for all levels.

Conclusion

Thus one photon resonance exchange creates decreasing potential holes by height and depth. From this expression may be obtaied solution for isolated long-wave radiation potentials. isolated long-wave quants may be the radiation which happens when on cluster surface or cristallyne lattice additional molecule enters or in drop while molecule difussion [5,6].

During cristalization and condensation the some portion of latent heat may be trasformed in characterized radiation. The transformation energy is distributed between existed and new energetic levels. They are called as phase radiation and is depended on medium optical properties. The cloud medium may be imagined as unity of clusters that are on different energetic levels, interacting through energy emition-absorbtion. According to this Earth surrounding environment is one of possible renewable energy source [8], the use of which gives chanse on transition into new energy transportation means.

References

1. Yang J., Dettori R., Nunes J.P.F., List N.H., etc. Direct observation of ultrafast hydrogen bond strengthening in liquid water. // Nature, 2021, DOI: 10.1038/s41586-021-03793-9
2. Landau L.D., Lifshic E.M. Quantum Mechanics, v. 3, 1989
3. Perelman M.E., Badinov I.Ia. Model of cloud formations. // Bulletin of Georgian Acedemy of Sciences. v. 131, N 2, 1988
4. Hasted D. Physics of atomic collisions, 1965/.
5. Tatishvili M. Some peculiarities of mathematical simulation of cloud microstructure. // Transactions of the Institute of Hydrometeorology, v.114, 2009, (in Georgian).
6. Tatishvili M. Energy transformation in clouds according quantum principles. // International Scientific Journal, Journal of Environmental Science, vol. 3, 2014, pp. 7-9.
7. Developing Weather Forecasting System in Georgia. // Ecology & Environmental Sciences, 2(7), 2017, DOI:10.15406/mojes.2017.02.00046
8. Tatishvili M.R., Palavandishvili A.M. Impact of Short-Term Geomagnetic Activity on Weather and Climate Formation in Georgian Region. // Journal of the Georgian Geophysical Society, Physics of Solid Earth, Atmosphere, Ocean and Space Plasma, ISSN: 1512-1127, v. 23(2), 2020.
9. Tatishvili M.R., Khvedelidze Z.V., Demetrashvili D.I. On some weather forecasting models in Georgia. // Journal of the Georgian Geophysical Society, Physics of Solid Earth, Atmosphere, Ocean and Space Plasma, ISSN: 1512-1127, v. 23(2), 2020.

ON THE MODELING OF THERMAL MECHANISM OF VORTEX GENERATION IN THE LOWER ATMOSPHERE

*Chkhitunidze M., *Khvedelidze I., **Zhonzholadze N.

*Mikheil Nodia Institute of Geophysics of Ivane Javakhishvili Tbilisi State University, Tbilisi, Georgia
**I. Gogebashvili Telavi State University
marina_chxitunidze@yahoo.com
khvedelidze.i@gmail.com

Summary: *Energy dissipation in the atmosphere layer near the Earth surface is associated with diffusive and convective processes, which are determined by differential equations of the second order. Self-consistency in hydrodynamic equations systems is a particularly difficult mathematical problem. Therefore, there is a method of using simplifying assumptions in order to receive an image of atmospheric mass motion. Namely, during any laminar motion in the sea or atmosphere there may generate a vortex that will cause a local perturbance.*

***Key words**: vortex, model, inversion, valley.*

Introduction.

The painful experience of 13.06.2015 makes it obvious that the flood problem in the Vere Gorge are actual in the future as well. This problem can be solved only by means of relevant forecasting model regarding emergency situations. For its construction we used the classical hydrodynamic theory of liquid flow in pipes, theory of ideal liquid jets and bifurcation theory.

However, there is also the problem of narrow mountain canyons bordering fairly high slopes which is identical to the problem of the Vere Valley problem in terms of microclimate. In particular, such valleys are on the southern slope of the Caucasus, as well as on the Gombori ridge.

In these valleys there is a systematic disturbance of the lower layers of the atmosphere under the influence of the sun, which spreads in the form of hurricanes of different sizes in the environment.

Formally, we may consider the existence of vortex as stability violation in the environment, i.e., generation of a turbulent supplement in a laminar flow. To fully describe such a process may appear quite difficult. Therefore, the problem is often reduced to approximate modeling of the image of perturbance distribution in the medium, which adequately describes the real motion. In some cases such goal is quite effectively reached by means of some kinematic model of hydrodynamic velocity, which must satisfy certain criteria, i.e., the conditions of dynamic potential of motion [1,2], for example, below, the cylindrical coordinate system shows a plane analytical model of velocities, which fulfills Euler equation of noncompressible ideal liquid motion and gives so called solenoid solution

$$V_r = \frac{1}{2} u_0 \left(\frac{r}{R_0}\right)(\cos\varphi + \sin\varphi), \qquad V_\varphi = u_0 \left(\frac{r}{R_0}\right)(\cos\varphi - \sin\varphi), \qquad (1)$$

where R_0 radius is a linear scale of the problem, u_0 is velocity characteristic of the vortex perturbance distribution.

In case if we consider the medium viscosity as a substantial factor, the motion of which must lead us to the formation of a boundary layer, we can construct a model

$$V_\varphi = u_0 \frac{R_0 - r}{R_0}(\cos\varphi - \sin\varphi), \quad V_r = \frac{u_0}{2}\frac{R_0 - r}{R_0}(\cos\varphi + \sin\varphi), \qquad (2)$$

which unlike Model (1), does not fulfill the plane equation of medium infiniteness. It means there must be a motion towards Z axis. Such limitation decreases the value of the kinematic model, which more or less corresponds to the vortex motion, though only in certain conditions. Despite that, the kinematic model (2) appeared quite useful in regard to quantitative assessment of viscosity effect.

Inversion of wind direction in canyons and generation of small-scale atmospheric vortex. Generally, narrow valleys with similar morphologic parameters are characterized with almost the same local climatic-meteorological regimes. Naturally, there are many such canyons in Georgia, among which are, for example: The Vere, the upper height of which is 1672 m above sea level and the lower height is 390 m above sea level, i.e., the difference between heights is 1282 m, whereas the length of the river is 42.5 km. The river generates at the south-eastern ending of the Trialeti Ridge (the highest peak of the ridge is Shaviklde with height of 2850 m, the heights of other summits vary between 2300-2800 m). It reaches its characteristic width of 400-450 m at the lower section of the valley (about 7 kilometers before joining the river Mtkvari). (fig.1.)
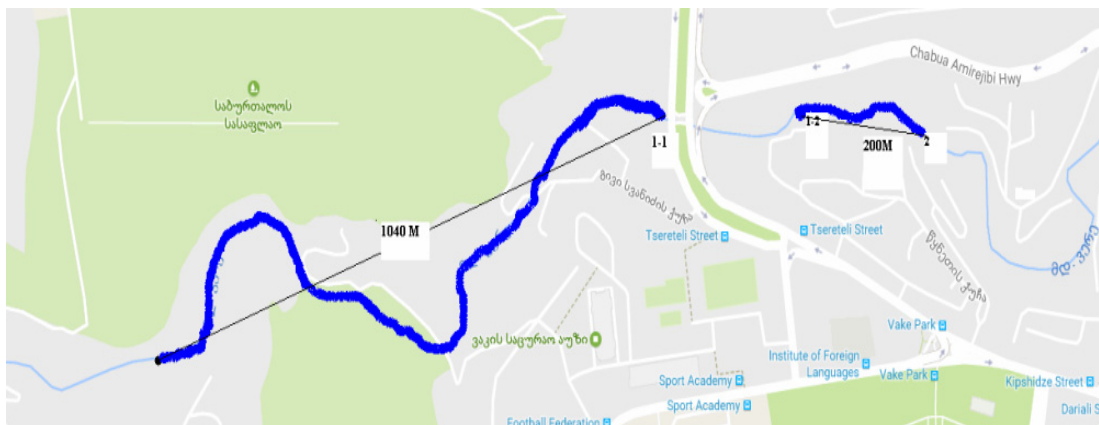
Fig.1. Topology of the river Vere

In the region of Kakheti: the Kisiskhevi has the upper height of 1755m and the lower height is 64 m above sea level, i.e., the difference between the heights is 1691 m. The length of the river is 37km.

Batsara river, Batsara gorge, length about 15 km, borderon the right by Tsinagora rodge, on the left by Kekhuriskhevi ridge, its headwaters are located at 2000 m above sea level. Attached to the river Alazani (Sea level 700m).
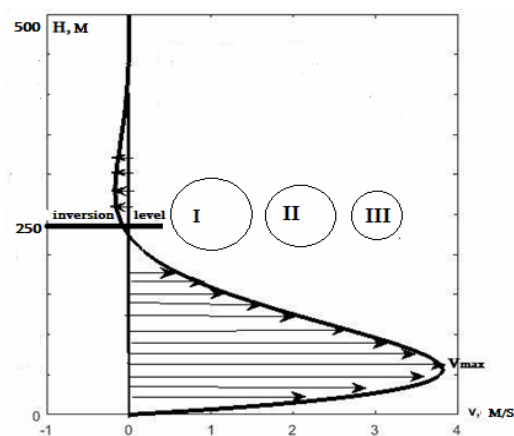
Fig.2. Profile velocity from Kanion level;V_{max}=3.8m/s

We can consider these valleys as an analogy of the channel of liquid motion curve, where the moving liquid is bounded by rather high walls. In the canyon, together with the height, the parameters of the surface atmosphere layer parameters also change. Motion of air masses generated due to pressure gradient in

the narrow valley permanently undergoes perturbance due to interaction with the valley slopes. Namely, it is known that at certain heights (200-250 m) of canyons, on so called "inversion" surface the wind velocity direction changes oppositely. This effect is caused by the inhomogeneity of the temperature field of the lower atmosphere that is associated with the main orographic property of the canyon, the ridges bordering the valley. The daily variation of the mountain slopes surface temperature in natural conditions takes place in a quite large diapason, whereas the hydrodynamic model of the process of the air mass motion associated with it, belongs to L. Prandtl, author of the boundary layer theory. The effect, which is qualitatively observed identically practically in all valleys, quantitatively may be expressed variously. Generally, it is known that the "inversion" height during the increase in atmospheric instability grows as well as the wind velocity. In normal (calm), less cloudy natural conditions, wind flow on the mountain slope, approximately half an hour after the sun set, moves downwards the valley. In warm conditions, after the sun rise, the wind blows in the same direction approximately during an hour. Further, the direction of the wind changes from downwards to upwards. In calm conditions the characteristic velocity of the wind is (1-3) m/s [3] (Fig.2).

Conclusion. Thus, the variation of the wind direction in the canyon is a precondition for the generation of the local instability that most probably ends with the generation of atmospheric vortex having certain linear scale. Obviously, such votex will undergo bifurcation in a short time, i.e., it will be broken down into smaller size vortices. Consequently, the mechanical energy of the turbulent vortex formation will be dissipated, which may be used for the change of the local thermosdynamical characteristics. The vortex breakdown effect can be imagined as development of balance states that are unsteady but short-term in time. Models (1) and (2) are convenient exactly for description of such a chain of events. The models are given in Figures (3) and (4).
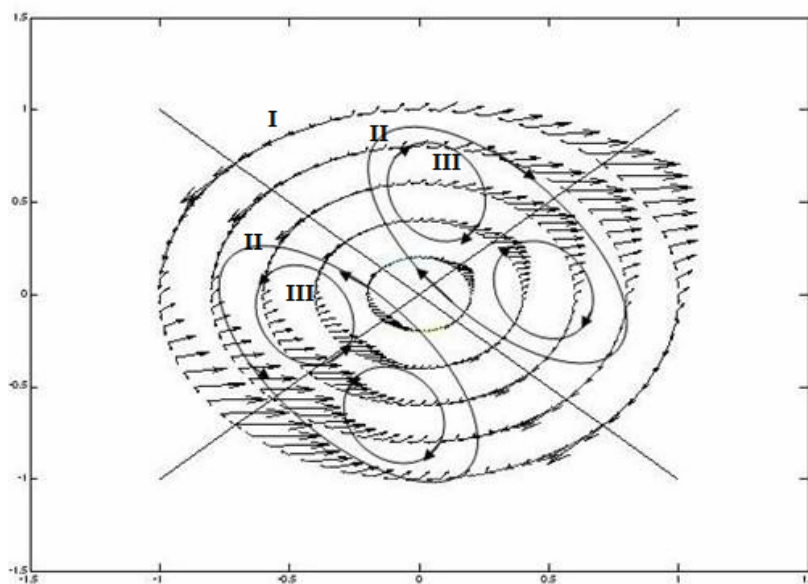
Fig. 3. Breakdown of the vortex. Model (1) is normalized on U_0

These figures, which have symmetric sectoral structures, are quite useful in regard to their development in time. Mainly, it is obvious that the evolution of the vortex chain must occur in the direction of the couple formation. Thus, we may consider the atmospheric vortex chain as the result of hydrodynamical instability development.
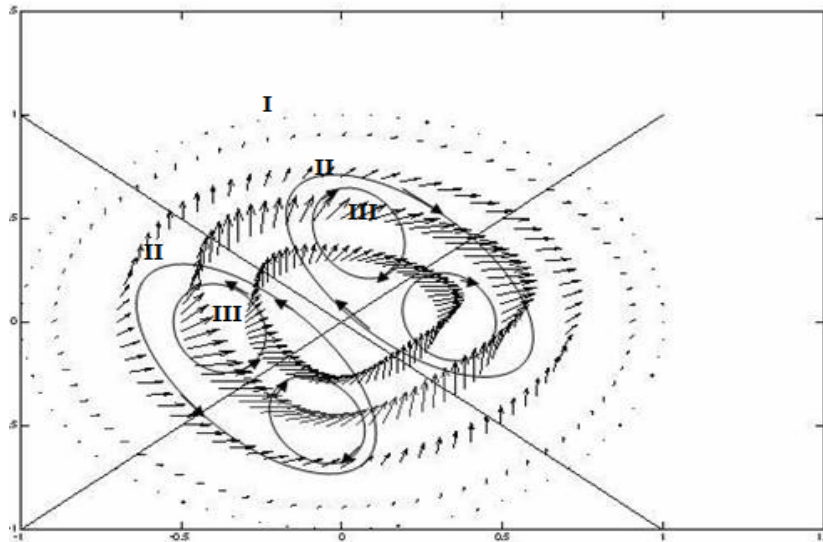
Fig. 4. Breakdown of the vortex. Model (2), I,II,III- vortices

These figures, which have symmetric sectoral structures, are quite useful in regard to their development in time. Mainly, it is obvious that the evolution of the vortex chain must occur in the direction of the couple formation. Thus, we may consider the atmospheric vortex chain as the result of hydrodynamical instability development.

References

1. Kirtskalia V., Kereselidze Z., Dzonzoladze N., Chkhitunidze M. An Analytical Model of an Asymmetrical Temperature Field in the Polar and Auroral Ionosphere. Georgian International. // Journal Of Science and Technology, Volume 3, Issue 4, 2012, pp. 381-390. https://www.novapublishers.com/catalog/product_info.php?products_id=32804
2. Khvedelidze I., Chkhitunidze M., Zhonzholadze N. The Model of the Local Atmospheric Purturbance in the Lower Part of the River Vere. // Trans. of M. Nodia Institute of Geophysics, ISSN 1512-1135, vol. LXX, 2019.
3. Khrgyan A. Physics of Atmosphere, vol 2. // Leningrad, Hydrometizdat, 1978, p. 237.

HYDRODYNAMIC PROBLEM OF CLOSED CHANNEL IN THE GORGE OF THE RIVER VERE

Khvedelidze I., Kereselidze Z.

Mikheil Nodia Institute of Geophysics of Ivane Javakhishvili Tbilisi State University, Tbilisi, Georgia
khvedelidze.i@gmail.com

Summary: *It is obvious that the project of the section of the high-speed highway in the gorge of the river Vere could not contain an analysis of probable negative consequences of this construction. It was miscount assumed that the closed channel, in addition to the transport problem, could also solve the flood problem in the lower part of the Vere gorge. It seems that mistakes were made during the design process, the reason of which is disregard of the factor of the hydraulic resistance in the tunnels having corrugated inner surfaces. As a result, the closed riverbed turned into an even greater danger than the historically known river Vere. Proceeding from such a vision of the reason for the development of the events, we cannot agree with the widely spread opinion that the devastating flood on 13.06.2015 was caused by anomalously heavy precipitation.*

Key Words:*. Vere river, floods, Stagnant zones, tunnels.*

Introduction.

The typical mountain river Vere is considered as one of the most dangerous in East Georgia due to frequent recurrent floods characterized by two orders of magnitude greater water flow than the average yearly value $Q | 1m \square^3 s^{-1}$.   Usually, floods used to occur in the lower part of the Vere gorge near the boundary of Tbilisi city. In the case of intense precipitations the lower, part of the Vere gorge turns into a fairly large catchment basin.. After constructing the part of the high-speed highway in 2010 in the lower part of the gorge, the river Vere appeared partially contained in the artificial closed bed consisting of several tunnels joined by open sectors. The new closed bed of the river Vere, instead of two, has seven tunnels with general length of 2100 m. The two tunnels, which had been constructed earlier, were partially elongated and as a result, nowadays the first tunnel is l 360 m and the other is l 1200 m long. Therefore, the geometrical properties of the natural bed corresponding the orography of the gorge, was significantly changed. In the Soviet period the flood zone was the area between the two tunnels (underground tubes) constructed in the first half of the last century. The first tube, which is nowadays situated under the Tamarashvili Highway, was 108 m long. The other tube was significantly longer, l 700 m. It occupied the natural bed of the river Vere before the junction with the river Mtkvari. Before 13.06.2015 night, for a long time, the flood taking place on 04.07.1960 was considered as the heaviest one. According to various assessments the flood was caused by the h 100 mm precipitations, which fell during two and half an hour. According to approximate assessments, during this time period, According to our assessments the water flow in the closed bed of the river Vere during the night of 13.06.2015 was probably was not more the one of the 04.07.1960 flood, when the maximum water flow in the Vere bed could be $Q | 260$ m$\square^3$ s^{-1} [1].   However, the result of the last flood appeared much disastrous due to human life losses and enormous material damage.

The security problem of the closed channel.

The structure of the closed and sufficiently long arched tunnels of the river Vere was made of corrugated steel sheets. In particular, the total length of the tunnels of the closed channel was 46% of the original length of the natural river bed between the Tamarashvili highway and the river Mtkvari.The theory of the construction of water supply canals states that arched tunnels and bridges constructed from corrugated steel have a sufficiently high seismic stability. Therefore, according to their technical and economic characteristics, they are almost as stable as structures made of stone, reinforced concrete or metal. Moreover, large water pipes made of corrugated steel have some advantages over concrete ones due to technological simplicity and less labour-intensiveness for construction and installation works. It is known that one of the advantages of arched tunnels and bridges made of corrugated steel is their ability to gradually fracture, i.e. soft bedding in case of considerably strong and prolonged tremors. However, they should not be used for hydrotechnical objects in regard to mountain rivers with fairly long closed riverbed. Therefore, when designing a closed channel in the Vere gorge, it was necessary to a priori consider the dangers that could arise in case of severe weather conditions. Due to the constant threat of flooding, it was obviously not reasonable to use such constructions that could reduce the capacity of the closed channel. It would be quite likely that there would be retrospective data on the 04.07.1960 flood in order to assess the degree of danger potentially threatening the urbanized gorge of the river Vere. There were also valuable data on series of floods that occurred in the subsequent period of time. First of all, it was quite possible to estimate how much the capacity of the new tunnels of the closed channel corresponded to the full load of the modernized first tunnel. As it is shown below, most likely the damming occurred not only before the first tunnel, but also in front of other tunnels. An important proof in favour of such an assertion is the fact that the water from the dam formed on Svanidze Street did not flow over the Tamarashvili highway. Consequently, this highway was a watershed, dividing the gorge into two parts. Therefore, we can assume that the flooding beyond the watershed began independently from the reason of damming of the first tunnel. For this, e. g, it was sufficient that water flow in any of the tunnels was reduced due to the increase in hydraulic resistance, and also because of the drain of urban storm water in the lower part of the gorge. As it is known, on 04.07.1960, flooding occurred in front of both tunnels, where had formed the stagnation zones. It should be assumed that in emergency situations floods in a closed channel in the future can be caused not only by factors of roughness and curvature, but also other negative mechanisms. Obviously, roughness, under harsh conditions, in all sufficiently long tunnels of the closed channel will always contribute to the intensification of the turbulence and initiation of return flows. Therefore, we assume that the increase in hydraulic resistance to the critical level in the tunnels of the closed channel was one of the reasons that led to the disaster on 13.07. 2015. In particular, at the initial stage the flood zone formed in front of the first tunnel, the reason of which, in addition to the hydraulic resistance, was also partial overlapping of the inlet of the tunnel by various household objects and trees brought by the water flow. As a result, the flood zone gradually expanded and, according to oure estimates, a reservoir of volume /3.1-4.4/10^5 m^3 rapidly formed and was kept long enough along the entire length of Svanidze Street. Such a factor of mechanical damping, but to a lesser extent than before the first tunnel, was observed for a certain time also in front of the second tunnel. However, in our opinion, it is necessary to pay special attention to the fact that the section of the gorge between the first and second tunnel was dammed while the water flow in the first tunnel was diminishing.

Hydraulic resistance in the tunnels of the closed channel.

It seems that during the design process of the sector of the high-speed highway in the Vere gorge, increase in the hydraulic resistance of tunnels of the closed channel under severe conditions was underestimated. According to the prevailing opinion, the cause of the devastating flood was precipitation of exceptional intensity, as well as trees, brought by the water flow and accumulated in front of the inlet of the first tunnel. However, it seems that such an explanation is insufficiently substantiated. Undoubtedly, the inlet of the first tunnel for some time was actually partially blocked that contributed to the flooding in Svanidze Street. However, it is especially noteworthy that from here the water did not flow over the Tamarashvili Highway, which turned out to be a watershed. After some time, the inlet of the first tunnel was released. Therefore, the previously partially blocked tunnel could not operate at its maximum throughput. Besides, there was a flood also in the area between the outlet of the first tunnel and the inlet of the last one. In design calculations the maximum value of the water flow in a closed channel was $Q \mid 260$ m^3 s^{-1} (according our

estimations |200 m□³ s⁻¹), which fully corresponds to emergency situations. However, we need additional facts for proving our opinion. Thus, below is a brief qualitative analysis, the basis of which is the hydrodynamic theory of turbulent water flow in rough pipes.

As far as the first tunnel was partially blocked, this could hardly have been caused only by the additional flow of water from urban drains and precipitation in the area of this part of the Vere gorge. Indeed, according to rough estimates, an additional volume of water in the area beetwin first two tunnels, beyond the watershed, could be V≈ 2.5*10^{5}м^3. Such an amount could accumulated during 2.5-3 hours. This corresponds approximately to the flow rate of water $Q\approx$ 25-30 m^3 s^{-1}, which is about (8-10)% of the estimated throughput of the first tunnel. However, the first tunnel was partially blocked for some time, and consequently its capacity was lower than the design one. Therefore, in spite of the additional volume of water received from the gutter, in the case of sufficiently effective operation of other tunnels (especially the last one), floods in the lower part of the gorge were unlikely to have occurred.

Modelling of the closed tunnels.

It is well known that the coefficient of hydraulic resistance in a circular pipe depends on the characteristic value of the Reynolds number and also on the curvature and roughness of the inner surface of the pipe. There must be a similar dependence for all natural and artificial channels, including tunnel water pipelines. Therefore, using the hydrodynamic similarity method, it is possible to correctly model the hydraulic resistance of a water channel of any shape. Consequently, it is possible to accurately determine the characteristic value of the coefficient of hydraulic resistance of the tunnels of the closed bed of the river Vere. To do this, it is necessary to approximate the closed channel (i.e., any of the tunnels) with a circular cross-section curved rough pipe. Obviously, such an analogy, both for a separate tunnel and for a closed channel as a whole, is physically fully justified. The analogy between a tunnel with a corrugated inner surface and a rough pipe is also evident. It enables to determine the coefficient of hydraulic resistance, the key parameter on which the flow of water in any water pipe depends. The main determinant of the degree of

turbulence in the water flowing in the pipe is the dimensionless parameter, the Reynolds number $R_e = \dfrac{\bar{u}D}{\nu}$,

where $\bar{u}$ is average water flow velocity, D is the pipe diameter, ν is kinematic viscosity of water. Therefore, for the closed channel of the Vere, the linear characteristics of which is the constant hydraulic radius of the tunnels, the speed of the river flow determines the characteristic value of the Reynolds number. It is known that for different hydrotechnical objects the permissible relative roughness can vary within the limits of 0.2%-7% [2].This parameter is the relation of the characteristic height of roughness to the radius of a pipe, or to the characteristic linear dimension of the cross-section of a water channel of any other shape. The longer the roughened tube, the lower the upper limit of the interval of subcritical values of the relative roughness. However, in case the throughput of a smooth analogue of a pipe approximating the water supply considerably exceeds the volume of incoming water, the upper limit of the permissible relative roughness of the inner surface of the water pipe can be increased to 7% and more. According our model estimates, the characteristic value of the coefficient of total hydraulic resistance of the closed channel of the river Vere was equal to|0.14 Consequently, the relative roughness of the inner surface of the river Vere closed channel

actually amounted to 4% [3]. We assume that the increase in hydraulic resistance to the critical level in the tunnels of the closed channel was one of the reasons that led to the disaster on 13.07. 2015. Another reason maybe problems associated with the formation of stagnant zones or, zones of liquid stagnation, which are well known in the hydrodynamic theory [4]. In particular, at the initial stage the flood zone formed in front of the first tunnel, the reason of which, in addition to the hydraulic resistance, was also partial overlapping of the inlet of the tunnel by various household objects and trees brought by the water flow. As a result, the flood zone gradually expanded and, according to oure estimates, a reservoir of volume /3.1-4.4/10^5 m^3 rapidly formed and was kept long enough along the entire length of Svanidze Street. Such a factor of mechanical damping, but to a lesser extent than before the first tunnel, was observed for a certain time also in front of the second tunnel. However, in our opinion, it is necessary to pay special attention to the fact that the section of the gorge between the first and second tunnel was dammed while the water flow in the first tunnel was

diminishing. Thus, it becomes obvious that the initial flood in the lower part of the Vere gorge occurred before inlet of the first tunnel. Then, regardless of the rapidly formed reservoir along the Svanidze Street, the areas in front of other tunnels were apparently also flooding. For example, after the first tunnel such a place could be the inlet of the second tunnel, or the inlet of the longest, the last tunnel connecting the Vere to the main river Mtkvari. Probably, it was the joint action of all local flood zones that resulted in heavy flooding. However, regarding the probability of possible repetition of severe meteorological conditions in the future, it seems that the discussion of the technical causes of the devastating 13.06.2015 flood should be supplemented with the fact that the river Vere has a sharp bend in front of the second tunnel. Therefore, it can be assumed that together with the negative effect of the hydraulic resistance of the tunnel, this place inevitably became one of the initial flood areas during the devastating flood. Thus, it becomes obvious that the initial flood in the lower part of the Vere gorge occurred before inlet of the first tunnel. Then, regardless of the rapidly formed reservoir along the Svanidze Street, the areas in front of other tunnels were apparently also flooding. For example, after the first tunnel such a place could be the inlet of the second tunnel, or the inlet of the longest, the last tunnel connecting the Vere to the main river Mtkvari. Probably, it was the joint action of all local flood zones that resulted in heavy flooding. However, regarding the probability of possible repetition of severe meteorological conditions in the future, it seems that the discussion of the technical causes of the devastating 13.06.2015 flood should be supplemented with the fact that the river Vere has a sharp bend in front of the second tunnel.

Conclusion.

1. The reason for the devastating flood on 13.07.2015 in the gorge of the river Vere was both natural and artificial causes. It seems that an anomalous natural phenomenon was added to a technical factor associated with structural deficiencies in a closed river channel, which is an integral part of the project of a high-speed highway section in the lower part of the Vere gorge. Therefore, in conditions of frequently repeated intense precipitation, the gorge remains a real threat for Tbilisi city in the future.

2. The analysis of the possible technical reasons that contributed to the disastrous results of the flood on the river Vere on 13.06.2015 may become the basis for preventive actions in case of a repeat of such a phenomenon in the future. For this purpose, simultaneous observation of the water level at critical locations of the closed channel, in particular, before the first and second tunnels, is quite effective. In these places, so-called stagnant zones, which serve as an indicator of the formation of recurrent currents, may appear. Stagnant zones can form even in case of medium intensity precipitation. As to the factor of hydraulic resistance, it will fully manifest itself in the case of extremely intense precipitation, i.e. under the condition of the maximum load of the tunnels of the closed channel. Consequently, until a certain moment, the zone of stagnation will not cause the decrease in the flow of water in the tunnels. Moreover, local water stagnation in front of the first and second tunnels can reduce, or simply prevent flooding in the area between the second and the following tunnels.

References

1. Kereselidze D., Alaverdashvili, Kiknadze D., Tsintsadze N., Kokaia N. Devastating Floods on the River Vere and the Methods for their Estimations. // TSU Transaction, series GEOGRAPHY, № 8-9, 2011, (in Georgian).
2. Schlichting G. The Theory of the Boundary Layer. // Moscow, Publishing House NAUKA, 1974, 711 p., (in Russian).
3. Kereselidze Z., Shergilashvili G. Overflow of the Vere River on13 June and Hydrodynamic Problem of Closed Channel. // Proceed. Of Institute of Geophysics, v. 67, 2016, pp. 199-221, (in Georgian).
4. Gurevich M. Theory of Ideal Incompressible Jets of Liquid. // Moscow, Nauka, 1979, 536 p. (in Russian).

PREDICTION OF HYDROPHYSICAL FIELDS IN THE GEORGIAN SECTOR OF THE BLACK SEA AND THE WAYS OF ITS IMPROVEMENT

*Kukhalashvili V., *,**Demetrashvili D., *,**Surmava A.

*Mikheil Nodia Institute of Geophysics of Ivane Javakhishvili Tbilisi State University, Tbilisi, Georgia
** Institute of Hydrometeorology of Georgian Technical University, Tbilisi, Georgia
Demetr_48@yahoo.com

Summary: *Since 2010, a short-term regional marine forecasting system of hydrophysical fields – the current, temperature and salinity operates for the Georgian sector of the Black Sea and adjacent water area. This system, which is developed at M. Nodia Institute of Geophysics of Iv. Javakhishvili Tbilisi State University, is one of the parts of the Black Sea basin-scale Nowcasting/Forecasting System. The forecasting system is based on the regional model of Black Sea dynamics of M. Nodia Institute of Geophysics (RM-IG), which is nested in the basin-scale model of Black Sea dynamics of Marine Hydrophysical Institute (Sevastopol). 2D and 3D impurities dispersion models are coupled with RM-IG. Further development and improvement of the regional forecasting system is associated with the development of a very high-resolution forecasting subsystem for the coastal zone of Adjara-Poti-Anaklia (with a horizontal grid step 200-250 m) with the inclusion of a model of wind-induced surface waves in the subsystem.*

Key Words: *forecasting system, numerical modeling, regional circulation, system of equations.*

Introduction. At present, under conditions of intense anthropogenic load of the world ocean (including the Black Sea), a marine forecasting system is becoming more relevant, providing forecasting of the state of the Black Sea in near operational mode.

At the beginning of the XXI century, a new phase in Black Sea oceanography began, characterized by the development of the basin-scale Black Sea Nowcasting/ Forecasting system. This System is developed under the framework of EU International scientific-technical projects ARENA, ASCABOS and ECOOP [1-3]. One of the parts of this system is the regional forecasting system developed at M. Nodia Institute of Iv. Javakhishvili Tbilisi State University, which operates for the Georgian sector of the Black Sea and adjacent water area since 2010. The forecasting system is based on the regional model of Black Sea dynamics of M. Nodia Institute of Geophysics (RM-IG), which is nested in the basin-scale model of Black Sea dynamics of Marine Hydrophysical Institute (Sevastopol). Within the framework of the Shota Rustaveli National Science Foundation Grant (2013-2015), the regional forecasting system was improved by inclusion of 2D and 3D numerical models of impurity distribution in the forecasting system. These numerical models are coupled with the RM-IG. The regional forecasting system provides 3-days forecast of hydrophysical fields – the current, temperature and salinity with 1 km spatial resolution [4-7]. In accidental situation, the regional system also makes it possible to predict pollution zones and concentrations of oil and other polluting substances. The regional forecast outputs are regularly posted at the Web-addresses: www.ig-geophysics.ge and www.oceandna.ge.

The most important part of the Georgian Black Sea sector is the Adjara-Poti-Anaklia nearshore, where human economic activity is growing significantly (if we do not take into account the 2020-2021 COVID-19 pandemic). There are the ports of Batumi and Poti in this zone, through which important port operations and sea transportation are carried out. This water area has a complex seabed topography, characterized by underwater canyons near the mouths of some rivers. Therefore, adequate modeling and forecasting of hydrophysical fields in this zone requires a higher spatial resolution of the models.

The goal of the present paper is briefly describe the method of short-term forecasting of the state of the sea with illustration of calculation of predicted fields and to discuss the ways of further improvement of the marine forecasts for the Batumi-Anaklia nearshore.

Methods. The RM-IG is received by adapting the basin-scale model of the Black Sea dynamics [8] to the easternmost part of the sea and increasing the spatial resolution from 5 km to 1 km. The RM-IG is based on a full system of ocean hydrothermodynamics equations in hydrostatic and non-compressible fluid approximation in z coordinates. Atmospheric forcing is taken into account through the upper boundary conditions by given of wind stress components, heat flux, atmospheric precipitation and evaporation from the sea surface, which is considered as a rigid surface. This model with 1 km spatial resolution is nested in the basin-scale model of the Black Sea dynamics of the Marine Hydrophysical Institute (MHI, Sevastopol) with 5 km resolution. The RM-IG covers the Georgian sector of the Black Sea and the adjacent water area having along the meridian a maximum length of 346 km and along the parallel – a maximum length of 215 km. The study area is limited from the west by the liquid boundary coinciding with the meridian 39.08^0E passing near the city of Tuapse (Russian Federation).

All the data needed for the calculation of short-range marine forecast are available from MHI via the Internet, providing the RM-IG with initial and boundary conditions. These data are as follows: 1. 3D initial fields of flow, temperature and salinity; 2. The flow, temperature and salinity values at the western liquid boundary; 3. Predicted meteorological fields at the sea surface – wind stress, heat fluxes, atmospheric precipitation and evaporation from the sea surface.

For modeling and forecast of oil products and other impurities in the sea environment there is considered advection-diffusion approach based on numerical solution of 2D and 3D nonstationary advection-diffusion equations.

The solution of the equations of the numerical models included in the forecasting system is based on the two-cycle splitting method with respect to physical processes and spatial coordinates. The splitting method is one of the most effective means of solving a wide range of problems in ocean and atmospheric dynamics, which is based on the representation of the main task operator as a sum of simpler operators and substantially simplifies the implementation of complex non-stationary mathematical models of geophysical hydrodynamics [9].

The modeling area is covered by a spatial grid, whose parameters are: in the RM-IG 30 calculated levels on a vertical with non-uniform vertical steps with a minimum step of 2 m at the sea surface and a maximum step of 100 m at the seabottom. The number of grid points on each horizon is 216 x 347 with the spatial horizontal resolution 1 km. The time step is 0.5 h.

Results and discussion. With the purpose of validating the RM-IG, forecast outputs were compared with the real data [5, 6]. Comparison of the computed sea surface temperature and surface flow fields with satellite observational data showed the ability of the model to really reflect the hydrophysical processes occurring in the easternmost part of the Black Sea.
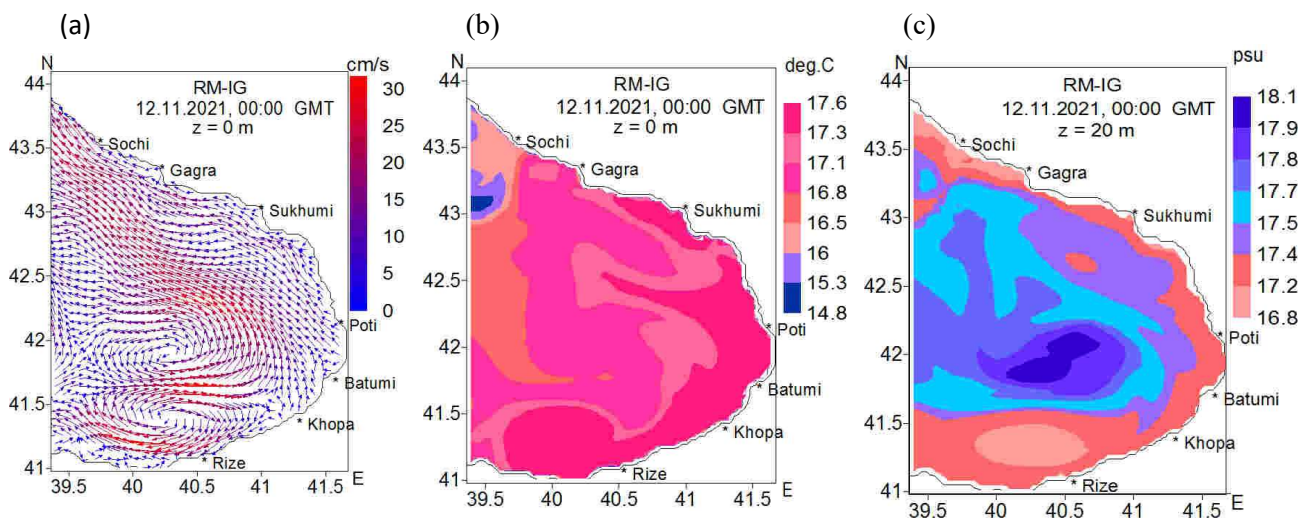
Fig.1. Predicted fields of sea surface circulation (a), sea surface temperature (b) and salinity on z = 20m (c) at t = 72 h (00:00 GMT, 12 November 2021). Forecasting interval is 9-12 November 2021.

The computations of marine forecasts, carried out regularly since 2010, have shown that the hydrophysical processes in the eastern waters of the Black Sea Basin are characterized by a significant variety and specific features of the spatial-temporal distribution of dynamic fields, accompanied by the permanent formation of mesoscale and submesoscale eddies during the year. The nonstationary atmospheric processes over the sea, having direct effect on the formation of the Black Sea hydrological structure under Earth's rotation, play an important role in the seasonal and interannual variability of sea dynamic processes, but specificity of this variability is largely determined by the sea bottom relief and the configuration of the coastline, baroclinicity, turbulent diffusion.

As an example, in Fig.1 prognostic fields of the sea surface current, the surface temperature and salinity on the depth of 20 m are shown at t = 72 h (after the start of the forecast) corresponding to 00:00 GMT, November 12, 2021. From the Fig.1a is visible, that the sea current is generally directed to the north-west in the considered regional area, but on this background, in the south-west part of the considered area formation of the dipole structure consisting of mesoscale cyclonic and anticyclonic eddies is observed. maximum flow speed of 30 cm / s is observed. The flow regime has a significant effect on the salinity field. In the area of cyclonic rotation more salinity waters with 17.9 – 18.1 psu and in the area of anticyclonic rotation less salinity waters with 16.8-17.2 psu are observed (Fig.1c). The sea surface temperature field is characterized more high temperature with 17.3-17.6 C^0 at Georgian and Turkish nearshore for the considered time moment. With distance from the coast, the waters gradually become cold (Fig.1b).

Further improvement of the existing regional forecasting system is connected to the development of a very high resolution coastal forecasting subsystem (with 200-250 m horizontal grid step) for the Adjara-Poti-Anaklia coastal zone, which will be included in the existing regional system as a subsystem. The purpose of this subsystem is to specify and make more detailed the forecast of dynamic and other fields in this nearshore water area. Operation of the subsystem will be able jointly with the existing regional forecasting system using nested modeling. At the same time the sea surface wave model will be included in the coastal subsystem. This subsystem will provide not only forecast of dynamic fields and spread of polluting substances, but also the height and direction of surface waves for the Adjara-Poti-Anaklia coastal zone. The wind surface wave model will be based on the spectral wave energy balance equation. It should be noted that the same equation is base of a well-known SWAN (Simulating Waves Nearshore) model, which quite fully describes the formation and transformation of wave motion in coastal zones and is widely used to calculate wind wave parameters in a number of coastal zones [10].

With use of the one-way nesting modeling method a joint realization of the regional model of the sea dynamics (with 1 km resolution) and very high-resolution coastal model of the sea dynamics (with 200-250 m resolution) will be carried out. The regional model outputs will be used on the liquid boundary for the high-resolution coastal model.

Thus, a new advanced version of the regional forecasting system will provide not only forecast of hydrological fields and spreading of impurities in the Georgian sector of the Black Sea with 1 km spacing, also will provide very detailed 3 days' forecast of dynamical fields and spreading of polluting substances in very important water area of the Georgian coastal zone – Adjara-Poti-Anaklia nearshore.

Conclusion. Since 2010, a short-term regional maritime forecasting system of hydrophysical fields – the current, temperature and salinity developed at M. Nodia Institute of Geophysics of Iv. Javakhishvili Tbilisi State University operates for the Georgian sector of the Black Sea and adjacent water area. This system, which is one of the parts of the Black Sea basin-scale Nowcasting/Forecasting System, consists of the RM-IG and coupled with its 2D and 3D impurities dispersion models. The regional forecasting system provides a three-day forecast of main hydrophysical fields with a spatial resolution of 1 km, and in emergency situations – a forecast of the spread of oil and other impurities in the sea.

Further development and improvement of the regional forecasting system is associated with the development of a very high-resolution forecasting subsystem for Adjara-Poti-Anaklia coastal zone (with horizontal grid step 200-250 m) and with inclusion of a model of wind-induced surface waves in the subsystem. Thus, a new improved version of the regional forecasting system will combine the forecasting system for the Georgian coastal zone with 1 km resolution and the coastal forecasting subsystem with a higher spatial resolution for the Adjara-Anaklia-Poti nearshore.

References

1. Korotaev G. K., Oguz T., Dorofeyev V. L., Demyshev S. G., Kubryakov A. I., Ratner Yu. B. Development of the Black Sea nowcasting and forecasting system. // Ocean Science, 7, 2011, pp. 629-649. DOI:10.5194/os-7-629-2011/.
2. Kubryakov A. I., Korotaev G. K., Dorofeev V. L., Ratner Y. B., Palazov A., Valchev N., Malciu V., Matescu R., Oguz T. Black Sea coastal forecasting system. // Ocean Science, 8, 2012, pp.183-196.
3. Marchuk G. I., Paton B. E., Korotaev G. K., Zalesny V. B. Data-computing technologies: a new stage in the development of operational oceanography. // Izvestiya, Atmospheric and Oceanic Physics, 49 (6) 2013, pp. 579-591.
4. Kordzadze A.,Demetrashvili D. Operational forecasting for the eastern Black Sea. // Proceed. of the 13th International MEDCOAST Congress on Coastal and Marine Sciences, Engineering, Management and Conservation, MEDCOAST 2017, 30 October – 4 November, 2017, Mellieha, Malta, t.2, 2017, pp.1215-1224.
5. Kordzadze A.,Demetrashvili D. Black Sea oceanography in the past and at current stage. // I. Javakhishvili Tbilisi State University Press. 2017, 187 p.
6. Demetrashvili D., Kukhalashvili V. High-resolving modeling and forecast of regional dynamic and transport processes in the easternmost Black Sea basin. // Proceed. of the International Conference on Geosciences (GEOLINKS 2019), 26-29 March 2019, Athens, Greece, Book 3, vol.1, 2019, pp.99-107.
7. Demetrashvili D., Kukhalashvili V., Surmava A., Kvaratskhelia D. Modeling of variability of the regional dynamic processes, developed during 2017-2019 in the easternmost part of the Black See. // Proceed. of the International Conference GEOLONKS 2020, Plovdiv, Bulgaria, ISSN 2603-5472, ISBN 978-619-7495-09-6, Book 2, V.2, 2020, pp. 111-120. DOI 10.32008/GEOLINKS2020/B2/V2 .
8. Demetrashvili D., Kvaratskhelia D., Gvelesiani A. On the vortical motions in the Black Sea by the 3-D hydrothermodinamical numerical model. // Advances in Geosciences, 14, 2007, pp. 295-299, www.adv-geosci.net/14/295/2008/
9. Marchuk G. I. Numerical solution of problems of atmospheric and oceanic dynamics. // Gidrometeoizdat, Leningrad. 1974, 303 p., (in Russian).
10. Akpınar A., Gerbrant Ph.van Vledder, Komurcu M. I., Ozger M. Evaluation of the numerical wave model (SWAN) for wave simulation in the Black Sea. // Continental Shelf Research, 50–51, 2012, pp. 80–99.

NUMERICAL MODELING OF PM2.5 PROPAGATION IN TBILISI ATMOSPHERE IN WINTER.
I. A CASE OF BACKGROUND NORTH LIGHT WIND

*,**Surmava A., **Kukhalashvili V., *Intskirveli L., *Gigauri N. , *Mdivani S.

*Institute of Hydrometeorology at the Georgian Technical University,Tbilisi, Georgia,
**Mikheil Nodia Institute of Geophysics of Ivane Javakhishvili Tbilisi State University, Tbilisi, Georgia
aasurmava@yahoo.com

Summary: *PM2.5 propagation at Tbilisi territory in winter period in case of background north light wind is numerically modeled and analyzed through combined integration of 3D regional model of atmospheric processes evolution and equation of admixtures transfer-diffusion. Motor transport moving at city streets and trunk lines is a main source of atmosphere pollution. There are investigated the main peculiarities, which characterize the process of microaerosols spatial distribution under rugged terrain conditions. PM2.5 high concentration zones are established at the territory of city, time intervals, when high air pollution forms or air self-purification takes place, are determined. Temporal and spatial variations of PM2.5 concentration in the lower part of atmospheric boundary layer are studied. It is established that 25 mkg/m³ and higher concentration is obtained from 11AM to 1PM and from 7PM to 10PM in the surroundings of Ponichala situated in the eastern part of the city.*

***Key Words*:** PM2.5 concentration, atmosphere pollution, numerical modeling.

Introduction

Atmospheric air pollution may be one of the contributing factors of COVID-19 pandemic [1]. PM2.5 and PM10 microparticles present in the air are especially dangerous from this viewpoint. They have double negative effect ability. On one side, they easily penetrate into human body and cause pulmonary and cardiovascular diseases [2-4]. On the other, as virus carriers they promote COVID-19 virus penetration into organism and complication of current cardiologic, pneumonic, urological and other diseases that is highly dangerous during pandemic. Studies carried out in 70 cities of China showed that there is a direct link between number of COVID-19 diseases and time variation of PM2.5 concentration level [5, 7]. That is why, under current conditions, study of large cities atmosphere pollution with PM2.5, and temporal and spatial variation of its concentration is a very topical problem, which is urgent for Tbilisi, as well, where an acute pandemic situation exists for the second straight year.

Brief statement of the problem

There are no large industrial facilities in Tbilisi. However, thousands of vehicles move up and down in its narrow streets and trunk roads of a rugged terrain. That is why, an assumption is made in this work that the main source of atmosphere pollution with PM2.5 is represented by microaerosols getting on air resulting from motor transport traffic. Spatial distribution of pollution source and city orography are shown in Fig. 1.

In Fig. 2 there is shown a time variation of PM2.5 emission rate at 0,5 m height from the earth surface in 1 m³ volume in case of 3000 veh/h traffic intensity at trunk road. It is obtained through experimental measurements, analysis of National Environment Agency data obtained from observation points and results of carried-out numerical experiments. At that, it is assumed that time variation of PM2.5 atmospheric emission rate at other trunk roads is similar to those shown in Fig. 2 and is proportional to motor transport traffic intensity.
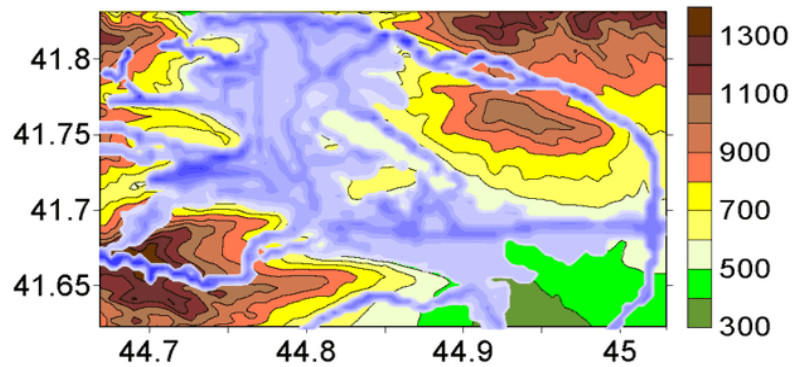
Fig. 1. Tbilisi city orography (m) and spatial distribution of pollution sources (dark blue areas).
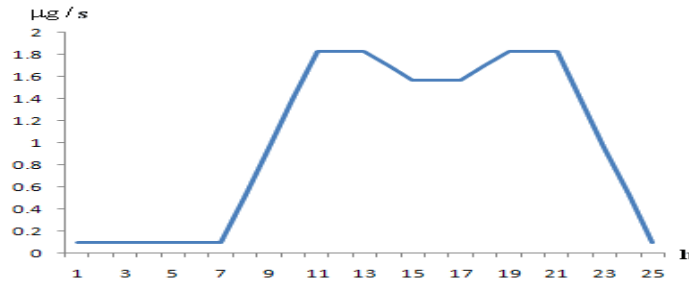

Fig. 2. Temporal variation of PM2.5 emission rate in 1 m^3 volume area at road with maximum traffic intensity (3000 veh/h)

Numerical model of development of meso-scale atmospheric processes in Caucasus and polluting ingredients propagation is used for study of time variation of PM2.5 concentration and its spatial distribution [8, 9]. Equation used during modeling, which describes the process of atmospheric propagation of passive admixtures at territories with a rugged terrain, can be written as follows:

$$\frac{\partial C}{\partial t} + u\frac{\partial C}{\partial x} + v\frac{\partial C}{\partial y} + (\tilde{w} - \frac{w_0}{h})\frac{\partial C}{\partial \zeta} = \frac{\partial}{\partial x}\mu\frac{\partial}{\partial x} + \frac{\partial}{\partial y}\mu\frac{\partial}{\partial y} + \frac{1}{h^2}\frac{\partial}{\partial \zeta}v\frac{\partial C}{\partial \zeta} + F$$

1

where t is time, x and y – coordinates plotted along parallel and meridian, $\zeta = i$ – dimensionless vertical coordinate, $\delta(x, y)$ – terrain height above sea level; $h = H - \delta$ – troposphere thickness, $H(t, x, y)$ – tropopause height, C – ingredients concentration; u, v, w and $\overline{w}$ – wind velocity components along x, y, z and ζ axes; w_o – dust precipitation rate; $F(t, x, y, \zeta)$ – dust discharge into atmosphere by a source; μ and v – factors (coefficients) of horizontal and vertical turbulence. Wind velocity components and turbulence factors can be calculated through numerical integration of equations given in [7, 8] and formulas determining turbulence factors.

Dust propagation in free atmosphere and surface layer of the atmosphere is modeled via numerical integration of equation (1), using the corresponding initial and boundary conditions. Numerical grid steps along x and y axes are equal to 300 and 400 m, and vertical dimensionless step in free atmosphere is 1/31 that roughly corresponds to 300 m. Vertical step in 100 m thick surface layer of the atmosphere varies from 0,5 to 15 m. Time step is 1 sec. Calculations are made for 3 day-and-night periods. Cases of background north light wind (BNLW) and background eastern light wind (BELW) under dry weather conditions of January are considered. Wind velocity varies from 1 m/sec (at 100 m from earth surface) to 20 m/sec (in tropopause at 9 km altitude). Relative atmospheric humidity is 50%.

Analysis of modeling results

In Fig. 3 there are shown the fields of wind velocity (m/sec) and PM2.5 concentration (mkg/m^3) obtained through numerical integration in the surface layer of the atmosphere – at 2, 100 m and boundary layer – at 600 m altitude, when t = 3 h and 6 h in case of background south light wind with 1 m/sec value. It is seen from Fig. 3 that terrain effect in surface and boundary layers of the atmosphere causes wavelike

disturbance of wind velocity directed from the north to the south, a main stream of which follows the course of Mtkvari valley. Wind velocity value varies within limits of 1-6 m/sec.

Wind field promotes taking out of PM2.5 particles available in the city from urban territories towards south-eastern direction and reduces surface wind pollution. In the course of the first 6 hours of a day, at 2 m height from a ground spatial distribution of concentration is qualitatively uniform: concentration in the outskirts of the city is 0,01-0,1 mgk/m^3, at urbanized territories and in the eastern part of the city concentration values are mainly within limits of 0,1-1 mgk/m^3. Concentration value 5-10 mgk/m^3 is obtained in two parts of the city only – westward, in the surroundings of avenues situated in Vake-Saburtalo districts and in the eastern part – along the Kakheti highway.

Concentration values at 100 m height from a ground at 3 and 6 in the morning differ from each other. While at 3 in the morning concentration over the city is mainly within 0,1-1 mgk/m^3, by 6AM a pollution zone forms over the eastern part of the city, where PM2.5 concentration reaches 25 mgk/m^3. In atmospheric boundary layer (600m) PM2,5 concentration is less than 0.1 mgk/m^3 in the major part of the city, and varies within limits of 0.1-1 mgk/m^3 in the eastern part of the city.
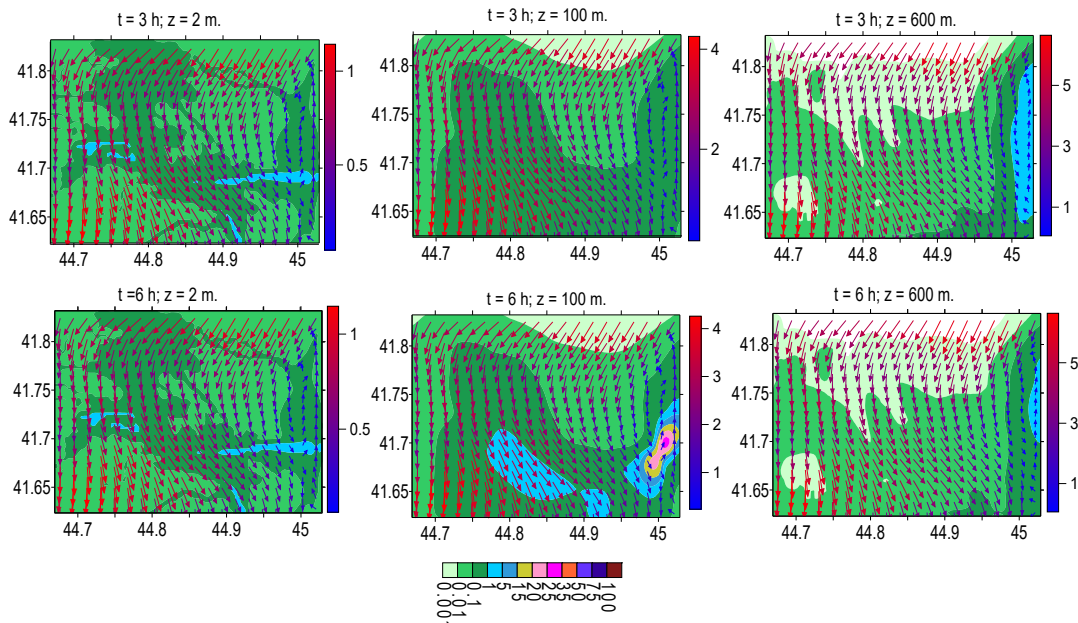
Fig. 3. Wind velocity (m/sec) and PM2.5 concentration fields (mkg/m^3) in surface and boundary layers of the atmosphere, when t = 3 and 6 h

In time period of a day, when t = 9-15h, microaerosols concentration increase takes place almost in all modeling areas (Fig. 4 and 5) along with increase of motor transport traffic intensity and related growth of PM2.5 emission rate (Fig. 2). Remarkable increase is obtained at 9AM, when a rate of aerosols discharge into atmosphere becomes maximal. At this point PM2.5 concentration in the eastern part of Kakheti Highway at 2 m height from the ground becomes maximal and reaches 25-30 mkg/m^3. In some areas of TEMKA, Vake, Saburtalo and Ponichala, at relatively small territories, concentration is within limits of 15-20 mkg/m^3. At that, formation of low pollution zones (0.1-1 mkg/m^3) in the central and peripheral parts of the city should be mentioned.

From 9AM to 3PM, despite the fact that a maximum amount of microaerosols is emiited into atmopsphere, PM2,5 concentration little by little reduces at almost entire territory of the city. In this time range, maximum concentration values are within limits of 5-15 mkg/m^3 at 2 m height. Relatively high pollution level is obtained at upper boundary of surface layer of the atmosphere (100 m). At this altitude, in the major part of a space, concentration varies within a limit of 1-5 mkg/m^3, while in the south-eastern part, at quite large area concentration is within a range of 5-15 mkg/m^3, when t = 12h. At 100 m height air pollution level increases from t = 9 to 12 h and drops when t=12-15h.
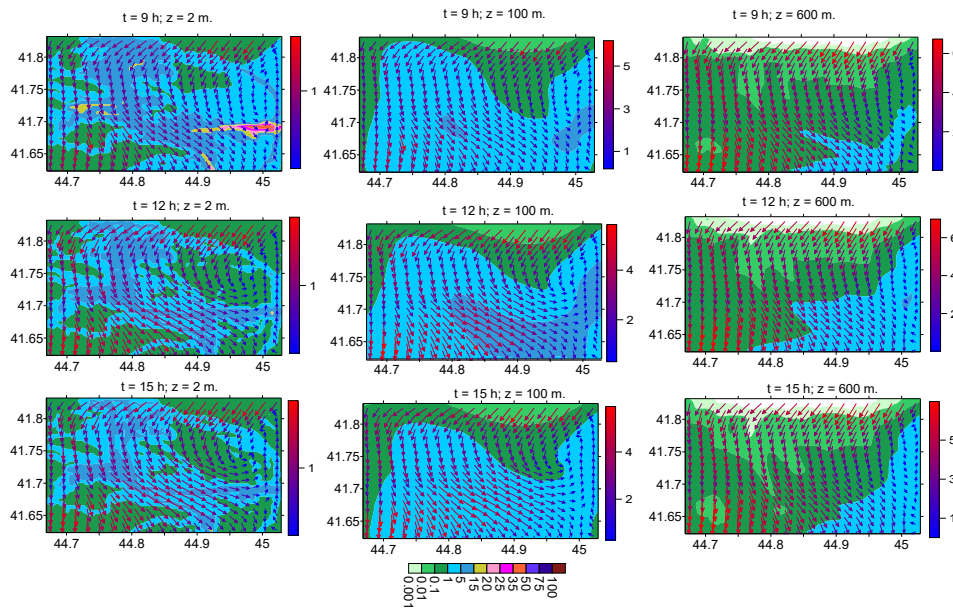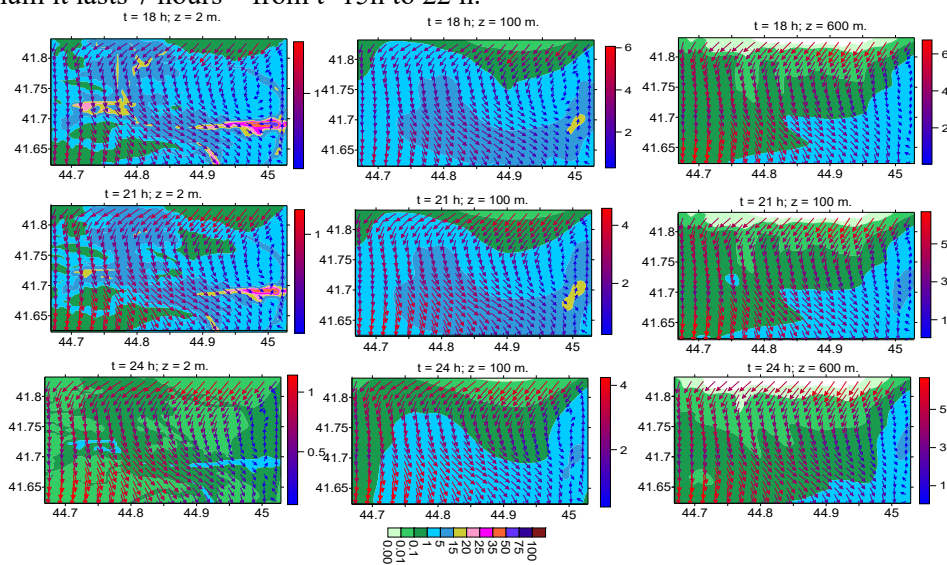
Fig. 4. Wind velocity (m/sec) and PM2.5 concentration fields (mkg/m³) in surface and boundary layers of the atmosphere, when t = 9, 12 and 15 h

It is obtained via calculations that along with onset of the second "rush hour" of motor transport traffic, atmospheric pollution with PM2,5 increases in the central districts of the city at 2 m height from the ground. When t = 18h, concentration is especially high in the eastern part of Kakheti Highway and northern part of Vazha-Pshavela Avenue. Concentration values reach 20 mkg/m³ in these places, while at quite large area concentration is within 5-15 mkg/m³ range.

In time period from t=18 h to 21 h, a ground-level concentration in Vake, Saburtalo, Gldani districts drops by 10 mkg/m³, while along Kakheti Highway the decrease is relatively small. In the vicinity of the upper boundary of surface layer of the atmosphere, aerosols concentration in time period from t = 18h to 24 h first increases a little, and then reduces. Studies conducted after 24 hours showed that in case of constant background wind the process of atmosphere pollution is of quasi-stationary nature.

Temporal variation of concentration in 4 points of densely populated city areas and 2 points in the outskirts of town is shown in Fig. 6. It is seen from Fig. 6 that time variation of concentration has 2 maximums. One maximum is reaches round t = 11h and another near t = 21 h. The process of concentration growth corresponding to the first maximum runs during 4 hours – from t = 7h to 11 h, while in case of the second maximum it lasts 7 hours – from t=15h to 22 h.

Fig. 5. Wind velocity (m/sec) and PM2.5 concentration fields (mkg/m³) in surface and boundary layers of the atmosphere, when t = 18, 21 and 24 h

Vertical distribution of PM2,5 for different points of time is shown in Fig. 7, where the concentration isolines of 3 cross-sections drawn along the parallel in the surface layer of the atmosphere are shown. It is seen from Fig. 7 that in time period from 3AM to 6AM a vertical distribution of PM2.5 concentration in the lower part of surface layer of the atmosphere is uniform. The latter is caused by coincidence of vertical turbulent and convective transfers in the field of formed local anticyclone. After t = 6h, an uniform structure of aerosols vertical distribution is damaged with increase of motor transport traffic intensity. Vertical turbulent diffusive flows of aerosol are formed, which promote territory ventilation and taking out of pollution from territory of the city. The only exceptions are two zones in the surroundings of Vake and Ponichala. In these zones, a high pollution zone is formed from t = 9h to 21 h in 50 m thick lower part of the atmosphere on leeward side of orographic resistance.
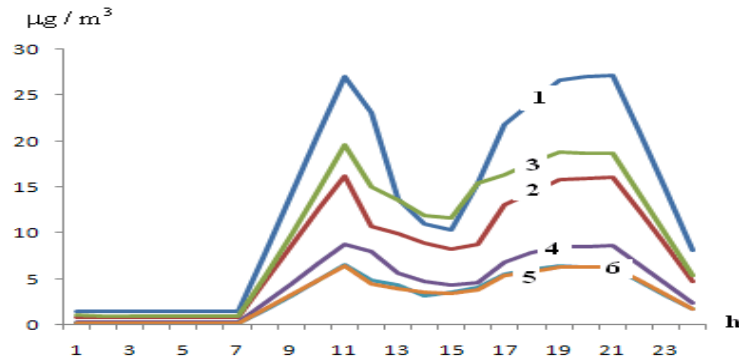
Fig. 6. Temporal variation of PM2.5 concentration in 6 points of modeling area: 1 – Ponichala; 2 – Vazha-Pshavela Ave., 3 – Akhmeteli Theater; 4 – Freedom Square; 5 – Tskhneti; 6 – Digomi
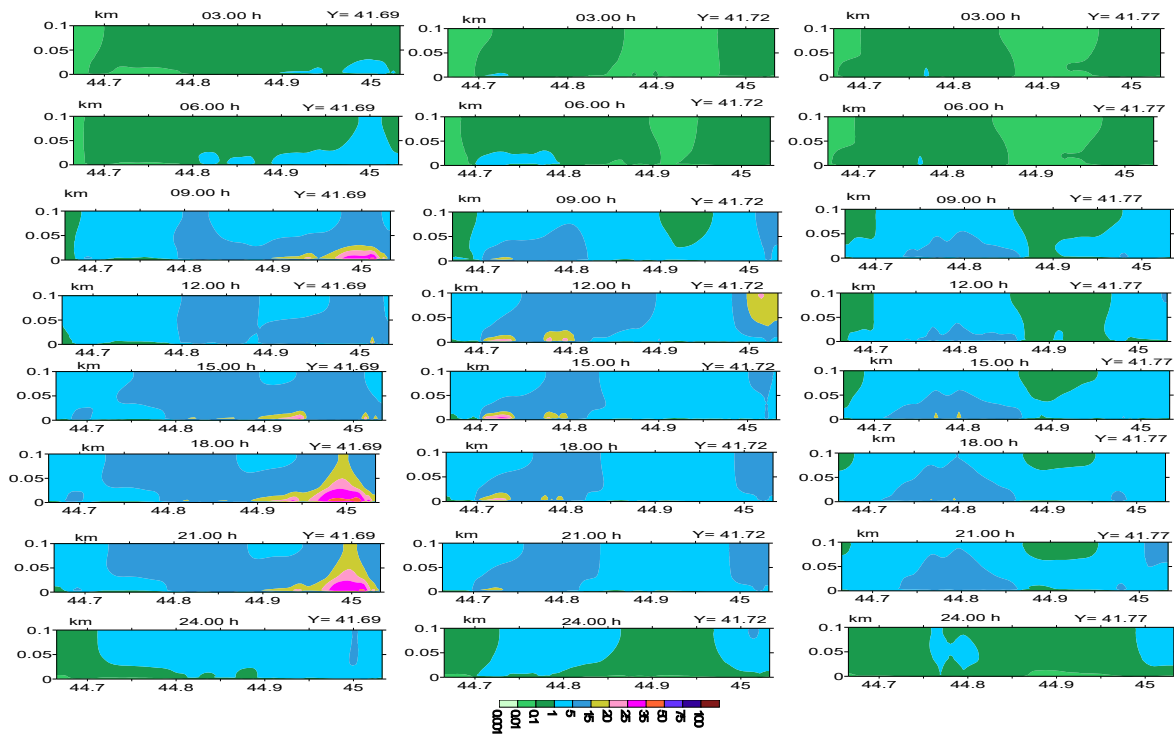
Fig. 7. PM2.5 concentration isolines in three vertical cross-sections drawn along the parallel in 100 m thick lower layer of the atmosphere

Conclusion

Carried-out calculations showed that in case of background north light wind a city orography promotes city ventilation and Tbilisi atmosphere pollution with PM2.5 is not high at all. The only exceptions are two zones – Vake and Ponichala districts, where concentrations round t = 11 and 21 h reach and even exceed 25 mkg/m^3. In time period from midday to 6PM the concentration values obtained via calculation are significantly less than measurement data [10]. In other points of time the observation data are also higher than those obtained through calculations. The mentioned fact is presumably related to the circumstance, that a background level of pollution, which is not established for Tbilisi atmospheric air, is not taken into account in the model.

Acknowledgement

References

1. Bourdrel T., Annesi-Maesano I., Alahmad B., et al. The impact of outdoor air pollution on COVID-19: a review of evidence from in vitro, animal, and human studies. // Eur Respir Rev 2021; 30:200242 [https://doi.org/10.1183/16000617.0242-2020].
2. Yixing Du, Xiaohan Xu, Ming Chu, Yan Guo, Junhong Wang. Air particulate matter and cardiovascular disease: the epidemiological, biomedical and clinical evidence. // J Thorac Dis. 2016 Jan; 8(1): E8–E19. Doi: 10.3978/j.issn.2072-1439.2015.11.37
3. Adaji E. E., Ekezie W., Clifford M., Phalkey R. Understanding the effect of indoor air pollution on pneumonia in children under 5 in low- and middle-income countries: a systematic review of evidence. // Environmental Science and Pollution Research. https://doi.org/10.1007/s11356-018-3769-1
4. Gonzalez-Barcala F.J., Pertega S., Garnelo L., Castro T.P. , Sampedro M., Lastres J.S., San M.A., Jose Gonzalez, Bamonde L., Valdes L., Carreira J.-M., Silvarrey A.L. Truck traffic related air pollution associated with asthma symptoms in young boys: a cross-sectional study. // Public Health, 127, 2013., 10.1016/j.puhe.2012.12.028.
5. Wang B., Liu J., Fu S., et al. An effect assessment of airborne particulate matter pollution on COVID-19: a multi-city Study in China. //medRxiv 2020; preprint [https://doi.org/10.1101/2020.04.09.20060137].
6. Zhu Y., Xie J., Huang F., et al. Association between short-term exposure to air pollution and COVID-19 infection: evidence from China. // Sci Total Environ 2020; 727: 138704.
7. Copat C., Cristaldi A., Fiore M., Grasso A., Zuccarello P., Signorelli S. S., Conti G. O., Ferrante M. The role of air pollution (PM and NO$_2$) in COVID-19 spread and lethality: A systematic review. // Environmental Research. Volume 191, December 2020, 110-129 https://doi.org/10.1016/j.envres
8. Surmava A., Intskirveli L., Kukhalashvili V., Gigauri N. Numerical Investigation of Meso - and Microscale Diffusion of Tbilisi Dust. // Annals of Agrarian Science, v. 18, No. 3, 2020, pp. 295-302.
9. Surmava A., Kukhalashvili V., Gigauri N., Intskirveli L., Kordzakhia G. Numerical Modelling of Dust Propagation in the Atmosphere of a City with Complex Terrain. The Case of Background Eastern Light Air. // Journal of Applied Mathematics and Physics, v. 8, No.7, 2020, pp. 1222-1228. https://doi.org/10.4236/jamp.2020.87092.
10. Gigauri N., Kukhalashvili V., Surmava A., Intskirveli L., Pipia M. Spatial distribution of PM10 and PM2.5 concentrations in the atmosphere of Tbilisi according to regular observations and experimental measurements. // Scientific Reviewed Proceedings of the IHM, GTU, vol. 131, 2021, pp. 44-50, (in Georgian).

NUMERICAL MODELING OF PM2.5 PROPAGATION IN TBILISI ATMOSPHERE IN WINTER.
I. A CASE OF BACKGROUND SOUTH LIGHT WIND

Gigauri N.,,**Surmava A.,*Intskirveli L.,*,**Demetrashvili D.,***Gverdtsiteli L.,*,**Pipia M.

*Institute of Hydrometeorology at the Georgian Technical University,Tbilisi, Georgia,
**Mikheil Nodia Institute of Geophysics of Ivane Javakhishvili Tbilisi State University, Tbilisi, Georgia
***Georgian Technical University, Tbilisi, Georgia
natiagigauri18@yahoo.com

Summary: *Temporal and spatial variations of PM2.5 distribution originated resulting from motor transport traffic during background south light wind are studied via numerical modeling. PM2.5 high concentration zones at the territory of the city are established, and time intervals, where air high pollution forms or air self-purification process occurs, are determined. There is established a difference, which exists between PM2.5 spatial distributions in case of background south and north winds.*

Key words: *PM2.5 concentration, atmosphere pollution, numerical modeling.*

Introduction

Since the beginning of the XXI century a special attention is given to the study of microaerosol pollution of atmospheric air of industrial regions and large administrative centers. The problem became particularly topical in the course of last 2-3 years, since the transfer and diffusion processes of viruses getting on PM2.5 and PM10 can be considered as one of the main reasons of COVID-19 pandemic throughout a world [1].
The presented article is an extension of studies started in [2] the goal of which is to theoretically study Tbilisi city atmospheric pollution with PM2.5 in case of background south light wind using numerical model [3, 4]. At that, an assumption is made that the pollution source is a motor transport, and related PM2.5 emission rate in the atmosphere is calculated empirically [2].

Analysis of modeling results

In Fig. 1 there are shown the fields of wind velocity and PM2.5 concentration at 2, 100 and 600 m height from the Earth surface in winter season at 3AM and 6AM during background south light wind, which are obtained through numerical integration. Calculations showed that in case of time-constant background south light wind, due to terrain effect, at the major part of territory of the city a quasi-stationary south wind is formed, which velocity varies from 0 to 15 m/sec in 600 m thick lower layer of the atmosphere. Vertical change of wind velocity is especially large (from 0 to 12 m/sec) in 100 m thick surface layer of the atmosphere. Rugged terrain influence on wind velocity is mainly manifested in the northern and north-western parts of the city, where roughly 8 km diameter local, ground cyclonic vortexes are formed.

PM2.5 spatial distribution is not uniform in the atmosphere at t = 0h. Its concentration at 2 m height from the ground is within limits of 0.001-0.01 mkg/m^3 at the major part of the city. In the city center, at territories of Vake, Saburtalo districts, Tsereteli Avenue, in the vicinity of Kakheti Highway and trunk road connecting Tbilisi and Rustavi cities, PM2.5 concentrations vary from 1 to 5 mkg/m^3. In time interval from t = 3h to 6h a concentration change is virtually insignificant. At altitudes higher than 100 m a concentration decrease takes place and its value doesn't exceed 1 mkg/m^3 at 600 m height.
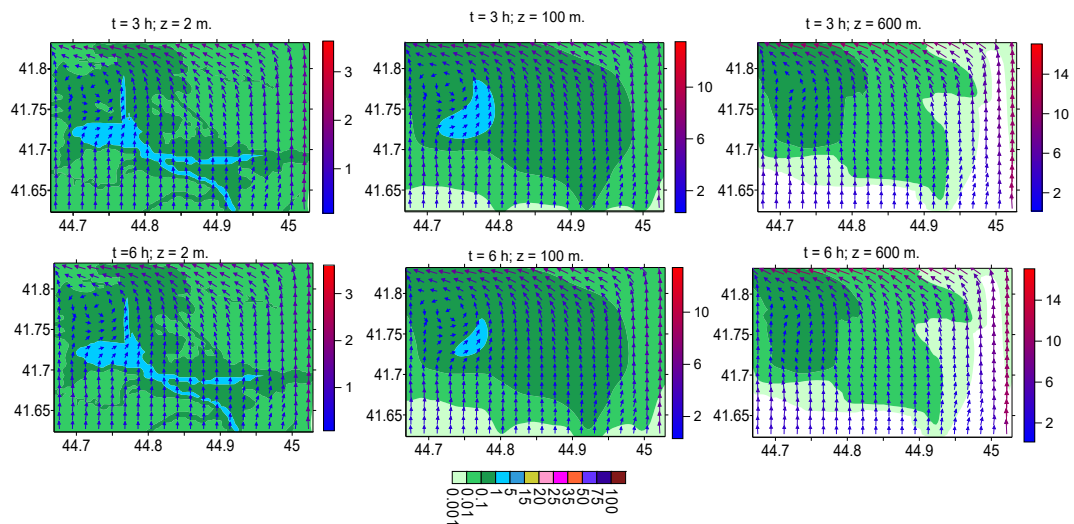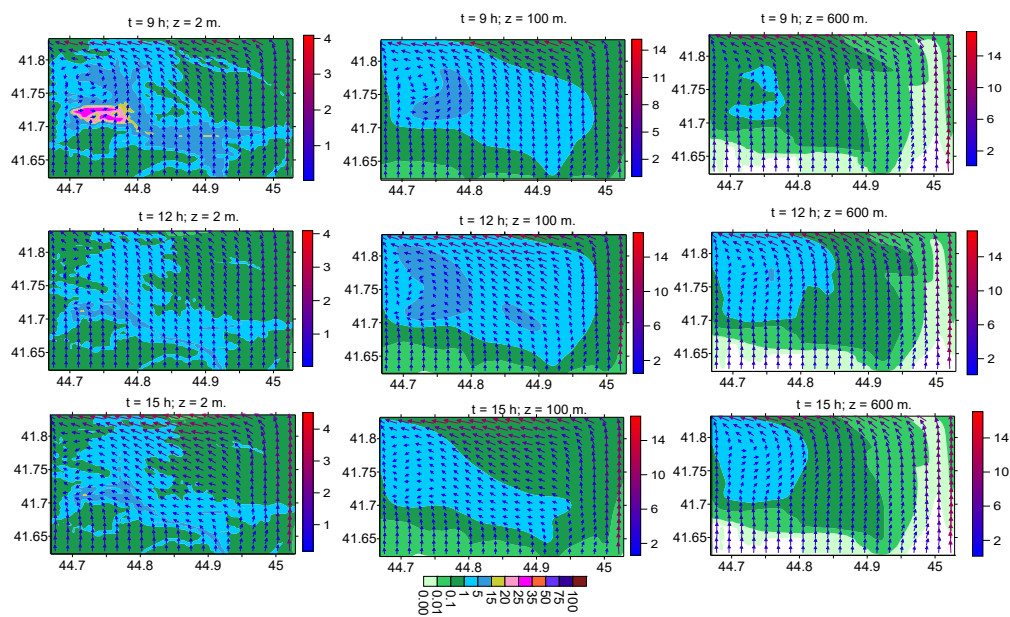
Fig. 1. Wind velocity (m/sec) and PM2.5 concentration (mkg/m³) fields in surface and boundary layers of the atmosphere, when t = 3h and 6h

After 6 in the morning, PM2,5 concentration increases throughout the territory of the city along with motor transport traffic growth. Concentration increase is not uniform (Fig. 2). It is especially high in the city center, Vake and Saburtalo districts. At this territory, by 9 in the morning concentration value changes within limits of 25-35 mkg/m³ at 2 m height. In contradistinction from concentration field formed during background north light wind there is no PM2.5 concentration increase in the surroundings of Kakheti Highway.

After 9 in the morning concentration is dropped in the main pollution areas and a quasi-stationary distribution of microaerosols is established. The obtained distribution is characterized by slight positive vertical gradient in 100 m thick surface layer and by slight negative gradient at altitude above 100 m.
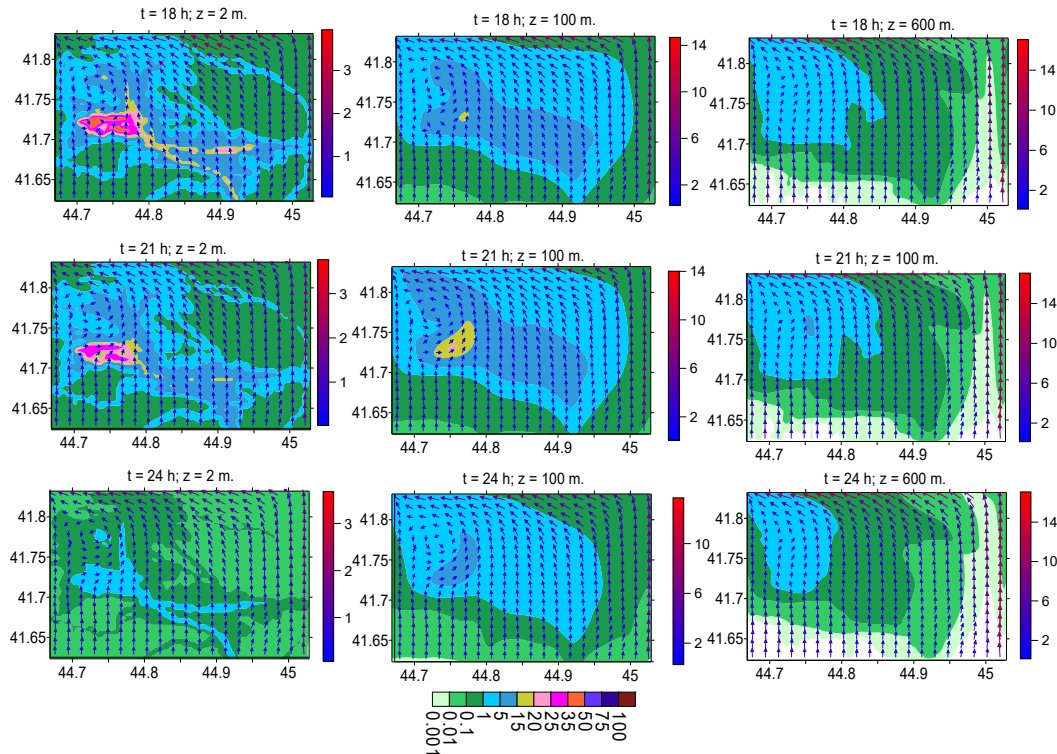

Fig. 2. Wind velocity (m/sec) and PM2.5 concentration (mkg/m³) fields in surface and boundary layers of the atmosphere, when t = 9, 12 and 15 h

In the period from t=15h to 21h there takes place PM2.5 concentration increase, which is related to the second "rush hour" of motor transport traffic (Fig. 3). A sharp increase of concentration at 2 m height from the ground is obtained in Vake and Saburtalo districts, when t=18h. Concentration varies within limits of 25-35 mkg/m³ at these territories. Concentration growth is relatively smaller in some small-size areas of Rustaveli and Gorgasali Avenues, Kakheti and Rustavi Highways, and Ortachala and Ponichala. From t=18h to 21h PM2.5 concentration is dropped in the areas of relatively high pollution. Vertical turbulent and

convective diffusion takes place with increase of ground-level concentration and therefore PM2.5 content increases at 100 and 600 m altitudes. Maximum concentration values at these levels become equal to 20 and 15 mkg/m^3 by t = 18h. After t = 18h at 2 m height a slow reduction of concentration begins, while at 100 m height its growth continues. This process lasts until t = 24 h. By t = 24h such vertical distribution of microaerosols is established, when PM2.5 concentration at 100 m height is more than concentrations obtained at 2 and 600 m altitude. As for time variation of pollution, after 24 h the process repeats on a quasi-periodical basis.

Fig. 3. Wind velocity (m/sec) and PM2.5 concentration (mkg/m^3) fields in surface and boundary layers of the atmosphere, when t = 18, 21 and 24 h

In Fig. 4 there are shown diagrams of PM2.5 concentration time variation in the surface layer at 2 m height. It seen from Fig. 4 that time evolution of concentration in case of background south light wind is qualitatively similar to temporal variation obtained for background north light wind (Fig. 8[2]) – there are obtained two periods of maximum and minimum pollution with corresponding time intervals.
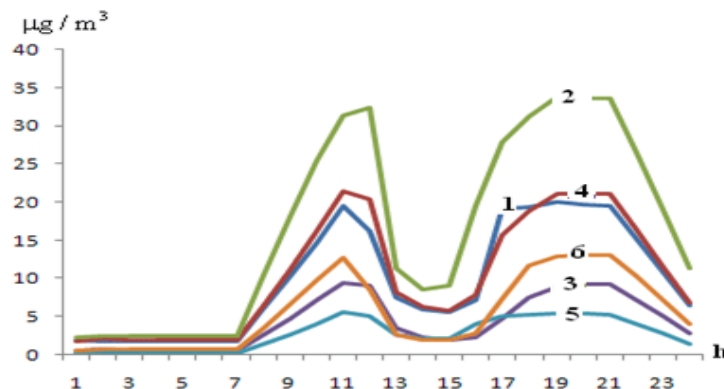
Fig. 4. Temporal variation of PM2.5 concentration in 6 points of modeling area: 1 – Ponichala, 2 – Vazha Pshavela Ave., 3 – Akhmeteli Theater, 4 – Freedom Square, 5 – Tskhneti, 6 – Digomi

76

Despite the fact that aerosols are emitted according to one and the same regularities in different pollution areas (points), temporal variation of formed concentrations is different, namely: the moments of reaching a maximum concentration, time variation gradients, concentration values in points located in the central and peripheral parts of the city etc.

In Fig. 5 there is shown a diurnal variation of concentration differences obtained via calculations in 6 modeling points at 2 m height in case of background south and north light winds. It is seen from Fig. 3 that in Ponichala, in the surroundings of Freedom Square and Digomi, in case of background south wind, during rush hours, concentration values are 1-20 mkg/m^3 higher than those obtained for north wind cases. On the contrary, at Vazha-Pshavela Avenue and in the vicinity of Akhmeteli Theater – in case of background north wind concentration is approx. 3-10 mkg/m^3 higher than concentrations obtained for south wind cases. As for concentrations in points located outside the town, the differences between them are small.
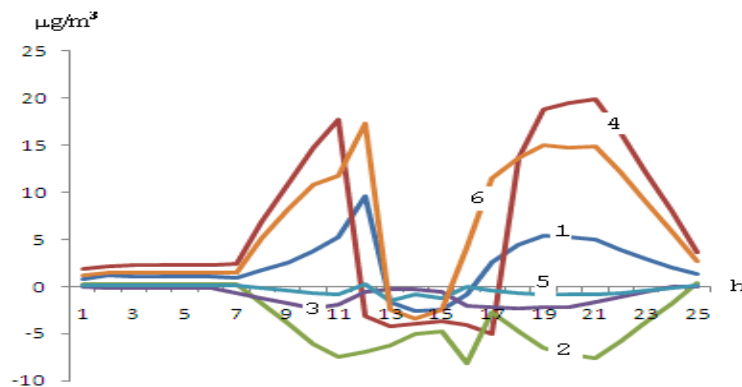
Fig. 5. Temporal variation of PM2.5 concentration differences in cases of background south and north light winds in 6 points of modeling area:
1 – Ponichala, 2 – Vazha-Pshavela Ave., 3 – Akhmeteli Theater, 4 – Freedom Square, 5 – Tskhneti, 6 – Digomi

A vertical distribution of PM2.5 concentration in three vertical sections drawn along the parallel to the surface layer of the atmosphere is shown in Fig. 5, from where is seen that in the period from t = 3h to 6 h, PM2.5 concentration in surface layer of the atmosphere is ≤ 5 mkg/m^3 and is characterized by a slight reduction trend. After t = 6 h, aerosols concentration in the surface layer increases along with motor transport traffic intensity and by t=9h the zones of average and high pollution are formed. They are of quite large vertical and horizontal sizes and cover almost the entire surface layer. In the period from t=9h to 15h, despite a constant quantity of aerosols getting on atmosphere (t = 9-12h) and its small reduction (t = 12-15h) (Fig. 2) a significant drop of concentration and air quality improvement take place. A sharp increase of ground-level concentration is obtained in the time interval from t=16h to 21h. In this time period a maximum concentration value reaches 50 mkg/m^3 at small area near the earth surface. If we analyse PM2.5 concentration vertical distribution in different points of time, we can come to conclusion that in case of background light wind the prevailing mechanisms of aerosols propagation are represented by vertical and horizontal turbulent diffusion in the surface layer of the atmosphere. Turbulent flows transfer aerosols from surface layer to boundary layer, where an advective transfer causes pollution dissipation at large areas and air self-purification.
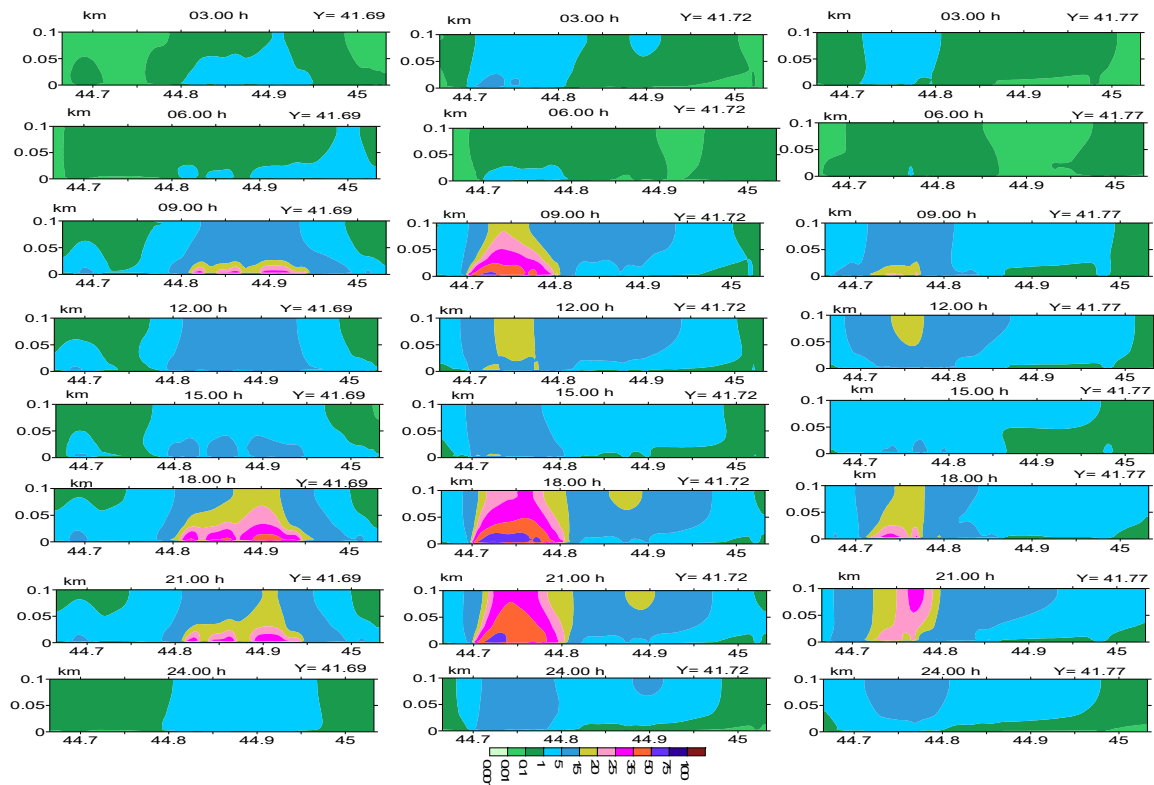
Fig. 6. PM2.5 concentration isolines in 100 m thick lower atmospheric layer in three vertical sections drawn along the parallels

Conclusion. Carried-out experiments showed that in case of background south light wind the city orography doesn't assist city aeration, so Tbilisi atmosphere pollution with PM2.5 is relatively high. In the vicinity of Freedom Square, Ponichala, Digomi maximum concentrations of PM2,5 are approx. 10-20 mkg/m^3 higher than those obtained during north wind. Ground-level concentrations from t=18h to 21h are high at the territories of Vake, Saburtalo, Ortachala and in the surroundings of Freedom Square. From midday to 6PM time period the concentration values obtained through calculation don't exceed 5 mkg/m^3.

References

1. Copat C., Cristaldi A., Fiore M., Grasso A., Zuccarello P., Signorelli S.S., Conti G.O., Ferrante M.. The role of air pollution (PM and NO$_2$) in COVID-19 spread and lethality: A systematic review. // Environmental Research. Vol., 191, December 2020, pp. 110-129 https://doi.org/10.1016/j.envres.
2. Surmava A., Kukhalashvili V., Intskirveli L., Gigauri N., Mdivani S. .Numerical modeling of PM2.5 propagation in Tbilisi atmosphere in winter. 1.A case of background north light wind. // The International Scientific Conference on the theme „Natural Disasters in the 21st Century: Monitoring, Prevention, Mitigation", December 20-22, 2021, Tbilisi, Georgia.
3. Surmava A., Kukhalashvili V., Gigauri N., Intskirveli L., Kordzakhia G. Numerical Modeling of Dust Propagation in the Atmosphere of a City with Complex Terrain. The Case of Background Eastern Light Air. // Journal of Applied Mathematics and Physics, v. 8, No.7, 2020, pp. 1222-1228. https://doi.org/10.4236/jamp.2020.87092
4. Surmava A., Intskirveli L., Kukhalashvili V., Gigauri G. Numerical Investigation of Meso-and Microscale Diffusion of Tbilisi Dust. // Annals of Agrarian Science, v. 18, No 3, 2020, pp. 295-302.

ON THE REPRESENTATIVENESS OF DATA FROM METEOROLOGICAL STATIONS IN GEORGIA FOR ANNUAL AND SEMI-ANNUAL SUM OF ATMOSPHERIC PRECIPITATION AROUND OF THESE STATIONS

[*]**Amiranashvili A.,** [*]**Chelidze T.,** [*]**Svanadze D.,** [*,**]**Tsamalashvili T.,** [*,***]**Tvauri G.**

[*]*M. Nodia Institute of Geophysics of Iv. Javakhishvili Tbilisi State University*
avtandilamiranashvili@gmail.com
[**]*A. Janelidze Geological Institute of Iv. Javakhishvili Tbilisi State University*
[***]*E. Andronikashvili Institute of Physics of Iv. Javakhishvili Tbilisi State University*

Summary: *Results of study of the representativeness of data from 39 meteorological stations in Georgia for annual and semi-annual sum of atmospheric precipitation around of these stations are presented. Period of observation – from 1936 to 2015. In particular, it was found that in general for the year data of meteorological stations on precipitations are representative around these stations on distance from 19 km (Mta-Sabueti, Kobuleti) to 46 km (Gori); in cold period of year - from 13 km (Mta-Sabueti) to 49 km (Zugdidi); in warm period of year - from 20 km (Chokhatauri) to 43 km (Pasanauri).*

Key words: *Atmospheric precipitations, correlation and regression analysis, natural catastrophe, landslides.*

Introduction

Atmospheric precipitation is one of the most important components of the climate [1,2], bioclimate [3], the state of ecosystems [4]. Atmospheric precipitation often has an extremely negative impact on the human environment. Their deficiency leads to droughts, an excess can provoke floods, flooding, mudflows, landslides and other dangerous natural phenomena [4-9]. In particular, the time scale of the effect of atmospheric precipitation on provoking of different natural catastrophe (including landslides) has a wide range - from several tens of minutes to several days, months, and years (climatic time scale) [5-9]. Since the number of meteorological stations is usually limited, in order to study the impact of precipitation on the environment, it is necessary to have data on the representativeness of these stations depending on the distance from them.

Results of study of the representativeness of data from 39 meteorological stations in Georgia for annual and semi-annual sum of atmospheric precipitation around of these stations are presented below.

Study area, material and methods

Study area – territory of Georgia.

The data of Georgian National Environmental Agency about the annual and semi-annual sum of atmospheric precipitations for 39 meteorological stations are used. Period of observation: 1936-2015 (80 years). The locations of meteorological stations and their names are shown below (in fig. 1, 3 and table 1).

In the proposed work the analysis of data is carried out with the use of the standard statistical analysis methods.

The following designations will be used below: R^2 – coefficient of determination; R – coefficient of linear correlation; α - the level of significance; Year – period from January to December; Cold – period from October to March; Warm – period from April to September; a – coefficient of regression equation; L – distance around meteorological station, km.

The degree of correlation was determined in accordance with [10]: very high correlation ($0.9 \leq R \leq 1.0$); high correlation ($0.7 \leq R < 0.9$); moderate correlation ($0.5 \leq R < 0.7$); low correlation ($0.3 \leq R < 0.5$); negligible correlation ($0 \leq R < 0.3$).

Determination of the representativeness of data meteorological stations for sum of atmospheric precipitation around of these stations was carried out in two stages.

1. The linear correlation coefficient R of each meteorological station with all other stations on the sum of atmospheric precipitation was calculated.
2. The dependence of this correlation coefficient on distance L between meteorological station from all other stations was determined. This dependence for each station has the form: $L = (1-R)/a \cdot R$, $\alpha(R^2) < 0.01$. A representative value of L was considered when R values were not less than 0.7 (high correlation).

Results and discussion

Results clearly shown from fig. 1-3 and table 1.
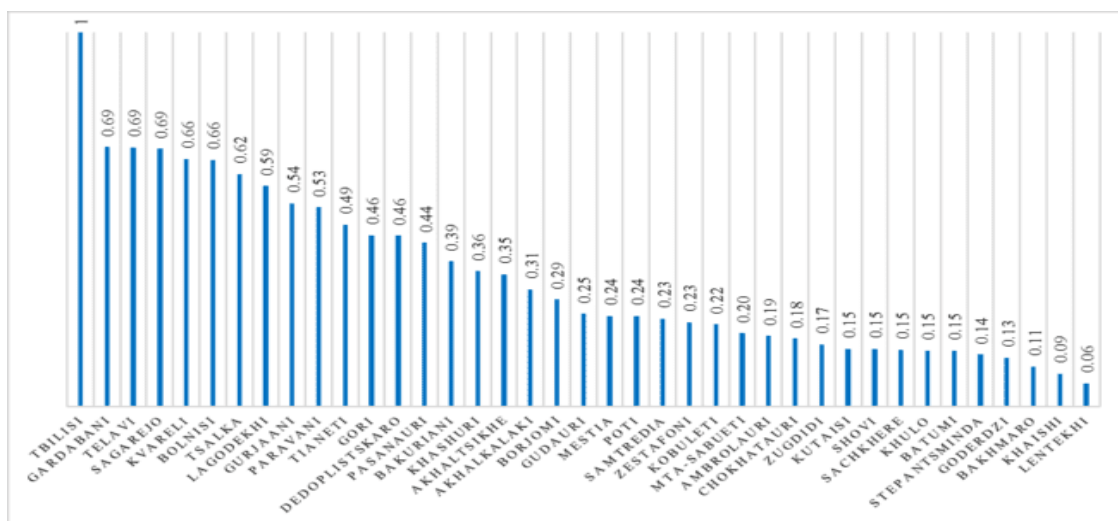
Fig.1. Example of linear correlation between annual sum of atmospheric precipitations in Tbilisi with annual sum of atmospheric precipitations on each meteorological stations in Georgia.
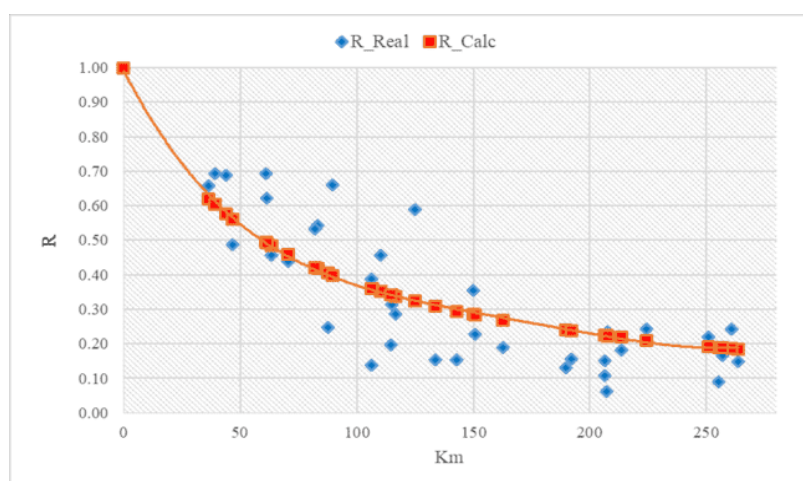

Fig.2. Dependency example of coefficient of linear correlation between annual sum of atmospheric precipitations in Tbilisi and annual sum of atmospheric precipitations on each of meteorological stations with distance for these stations.

Table 1. The values of the coefficients of the regression equation a between the linear correlation coefficient and the distance between an individual meteorological station with all the others. The radius of the circle L, within which the data of meteorological stations on the annual and semiannual precipitation amounts are applicable with a high level of representativeness. L = (1-R)/a·R, α(R²)<0.01.

| Season	Year		Cold		Warm		Year	Cold	Warm
Parameters	a	R²	a	R²	a	R²	L, km		
Akhalkalaki	0.018193	0.45	0.018464	0.17	0.013727	0.66	24	23	31
Akhaltsikhe	0.010752	0.62	0.010053	0.51	0.011932	0.66	40	43	36
Ambrolauri	0.012694	0.78	0.010341	0.67	0.012614	0.81	34	41	34
Bakhmaro	0.018383	0.72	0.014404	0.74	0.018085	0.71	23	30	24
Bakuriani	0.012598	0.56	0.011032	0.41	0.012604	0.58	34	39	34
Batumi	0.017508	0.78	0.010375	0.76	0.02003	0.79	24	41	21
Bolnisi	0.017659	0.66	0.017376	0.55	0.014228	0.74	24	25	30
Borjomi	0.011612	0.72	0.012024	0.58	0.013012	0.74	37	36	33
Chokhatauri	0.017225	0.72	0.011347	0.71	0.021237	0.75	25	38	20
Dedoplistskar	0.018893	0.82	0.01299	0.75	0.015518	0.8	23	33	28
Gardabani	0.015331	0.87	0.019399	0.71	0.011177	0.85	28	22	38
Goderdzi	0.020563	0.78	0.016303	0.69	0.01747	0.83	21	26	25
Gori	0.009388	0.57	0.009232	0.2	0.012206	0.74	46	46	35
Gudauri	0.016302	0.65	0.012512	0.77	0.01653	0.76	26	34	26
Gurjaani	0.018205	0.77	0.012512	0.77	0.014824	0.77	24	34	29
Khaishi	0.011683	0.52	0.008834	0.54	0.019672	0.61	37	49	22
Khashuri	0.010981	0.71	0.012398	0.48	0.0136	0.79	39	35	32
Khulo	0.016729	0.53	0.015553	0.61	0.01491	0.77	26	28	29
Kobuleti	0.022229	0.72	0.013826	0.76	0.018158	0.72	19	31	24
Kutaisi	0.013413	0.79	0.010558	0.72	0.016546	0.86	32	41	26
Kvareli	0.012935	0.79	0.011184	0.73	0.010735	0.8	33	38	40
Lagodekhi	0.017227	0.64	0.01953	0.73	0.012371	0.72	25	22	35
Lentekhi	0.014129	0.68	0.011749	0.68	0.015871	0.74	30	36	27
Mestia	0.013416	0.67	0.011397	0.67	0.018976	0.46	32	38	23
Mta-sabueti	0.022931	0.57	0.033486	0.39	0.015417	0.67	19	13	28
Paravani	0.012469	0.35	0.012838	0.25	0.010318	0.57	34	33	42
Pasanauri	0.010785	0.55	0.010541	0.45	0.00986	0.65	40	41	43
Poti	0.017946	0.52	0.01207	0.7	0.015214	0.56	24	36	28
Sachkhere	0.012828	0.69	0.009654	0.61	0.014984	0.75	33	44	29
Sagarejo	0.015512	0.78	0.017009	0.71	0.011933	0.85	28	25	36
Samtredia	0.010364	0.79	0.009046	0.78	0.012541	0.79	41	47	34
Shovi	0.011859	0.63	0.009992	0.58	0.012529	0.67	36	43	34
Stepantsminda	0.017628	0.59	0.013294	0.48	0.017922	0.61	24	32	24
Tbilisi	0.016781	0.74	0.01491	0.65	0.01471	0.74	26	29	29
Telavi	0.013321	0.81	0.011367	0.77	0.010096	0.81	32	38	42
Tianeti	0.014262	0.61	0.0105	0.63	0.014458	0.71	30	41	30
Tsalka	0.014415	0.59	0.01519	0.48	0.012837	0.64	30	28	33
Zestafoni	0.015892	0.74	0.013046	0.64	0.019988	0.81	27	33	21
Zugdidi	0.010878	0.64	0.008682	0.62	0.012191	0.57	39	49	35
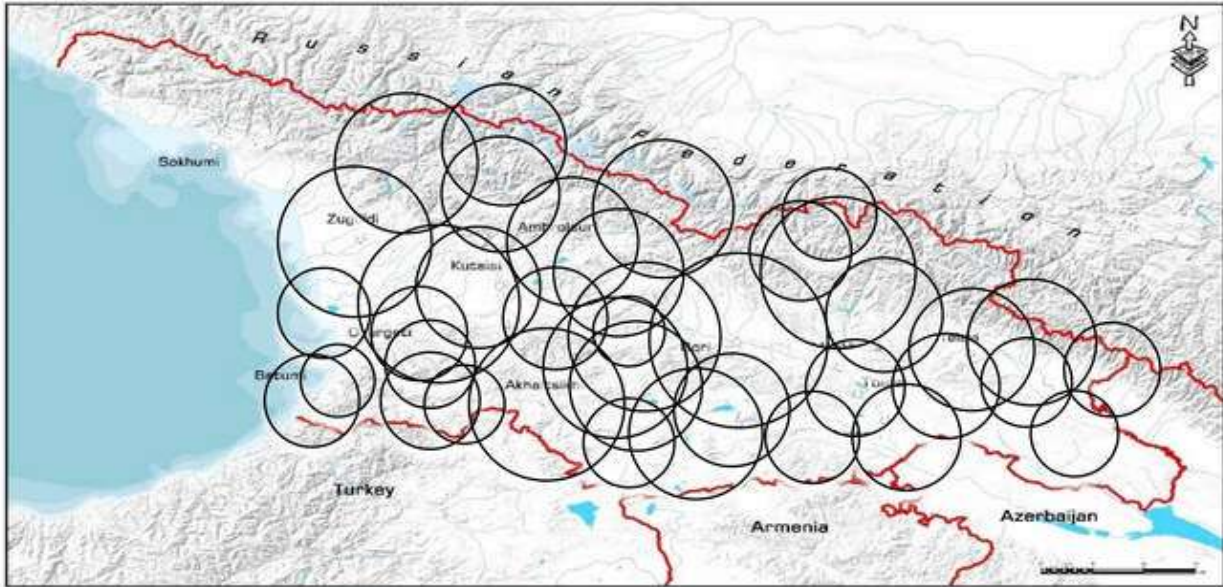
Fig. 3. Example of the areas of circles around meteorological stations within which the data of these stations on the annual sum of atmospheric precipitation with a high level of representativeness can be used.

In fig.1 the example of linear correlation between annual sum of atmospheric precipitations in Tbilisi with annual sum of atmospheric precipitations on each meteorological stations in Georgia is presented. As follows from this fig. coefficient of correlation for this case changes from 0.06 to 0.69.

In fig.2 the dependency example of coefficient of linear correlation between annual sum of atmospheric precipitations in Tbilisi and annual sum of atmospheric precipitations on each of meteorological stations with distance for these stations is presented. The distance L can be determined from the regression curve and in this case it is equal to 26 km.

Table 1 presents information for all 39 meteorological stations on the values of a and L in three periods of the year. In particular, in general for the year data of meteorological stations on precipitations are representative around these stations on distance from 19 km (Mta-Sabueti, Kobuleti) to 46 km (Gori); in cold period of year - from 13 km (Mta-Sabueti) to 49 km (Zugdidi); in warm period of year - from 20 km (Chokhatauri) to 43 km (Pasanauri).

Finally, for clarity in fig. 3 the example of the areas of circles around meteorological stations within which the data of these stations on the annual sum of atmospheric precipitation with a high level of representativeness can be used is presented.

Conclusion

In the future, these studies will be continued for monthly and daily data of atmospheric precipitation.

Acknowledgement

References

1. Tavartkiladze K., Begalishvili N., Kharchilava J., Mumladze D., Amiranashvili A., Vachnadze J., Shengelia I., Amiranashvili V. // Contemporary Climate Change in Georgia. Regime of Some Climate Parameters and their Variability. // Monograph, ISBN 99928-885-4-7, Tbilisi, 2006, 177 p., (in Georgian).

2. Amiranashvili A. Changeability of Air Temperature and Atmospheric Precipitations in Tbilisi for 175 Years. // International Scientific Conference "Natural Disasters in Georgia: Monitoring, Prevention, Mitigation". Proceedings, ISBN 978-9941-13-899-7, Publish House of Iv. Javakhishvili Tbilisi State University, December 12-14, Tbilisi, 2019, pp. 86-90.

3. Amiranashvili A.G., Revishvili A.A., Khazaradze K.R., Japaridze N.D. Connection of Holiday Climate Index with Public Health (on Example of Tbilisi and Kakheti Region, Georgia). // Journal of the Georgian Geophysical Society, e-ISSN: 2667-9973, p-ISSN: 1512-1127, Physics of Solid Earth, Atmosphere, Ocean and Space Plasma, v. 24(1), 2021, pp. 63-76.

4. Varazanashvili O., Tsereteli N., Amiranashvili A., Tsereteli E., Elizbarashvili E., Dolidze J., Qaldani L., Saluqvadze M., Adamia Sh., Arevadze N., Gventcadze A. Vulnerability, Hazards and Multiple Risk Assessment for Georgia. // Natural Hazards, Vol. 64, Number 3, 2012, pp. 2021-2056. DOI: 10.1007/s11069-012-0374-3, http://www.springerlink.com/content/9311p18582143662/fulltext.pdf.

5. Erener A., Düzgün H.B.S. A regional scale quantitative risk assessment for landslides: case of Kumluca watershed in Bartin, Turkey. // Landslides, 10.1, 2013, pp. 55-73, DOI 10.1007/s10346-012-0317-9

6. Segoni S., Piciullo L., Gariano S.L. A review of the recent literature on rainfall thresholds for landslide occurrence. // Landslides, 15, 2018, pp. 1483–1501, DOI 10.1007/s10346-018-0966-4.

7. Kirschbaum D., Stanley T. Satellite-Based Assessment of Rainfall-Triggered Landslide Hazard for Situational Awareness. // Earth's Future, 6, 2018, pp.505-523, https:// doi.org/10.1002/, 2017EF000715

8. Amiranashvili A., Chelidze T., Dalakishvili L., Svanadze D., Tsamalashvili T., Tvauri G. Preliminary Results of a Study of the Relationship Between the Monthly Mean Sum of Atmospheric Precipitation and Landslide Cases in Georgia. // Journal of the Georgian Geophysical Society, ISSN: 1512-1127, Physics of Solid Earth, Atmosphere, Ocean and Space Plasma, v. 23(2), 2020, pp. 37 – 41.

9. Amiranashvili A., Chelidze T., Dalakishvili L., Svanadze D., Tsamalashvili T., Tvauri G. Preliminary Results of a Study of the Relationship Between the Variability of the Mean Annual Sum of Atmospheric Precipitation and Landslide Processes in Georgia. // Int. Sc. Conf. „Modern Problems of Ecology", Proc., ISSN 1512-1976, v. 7, Tbilisi-Telavi, Georgia, 26-28 September, 2020, pp. 202-206.

10. Hinkle D. E., Wiersma W., Jurs S. G. Applied Statistics for the Behavioral Sciences. // Boston, MA, Houghton Mifflin Company, 2003.

DISTRIBUTION OF HAIL BY MEAN MAX SIZE ON THE TERRITORIES OF MUNICIPALITIES OF THE KAKHETI REGION OF GEORGIA

*Amiranashvili A., **Bolashvili N., **Gulashvili Z., *Jamrishvili N., **Suknidze N., *Tavidashvili Kh.

*M. Nodia Institute of Geophysics of Iv. Javakhishvili Tbilisi State University, 1 M Alexsidze Str 0160, Tbilisi, Georgia
avtandilamiranashvili@gmail.com
**Vakhushti Bagrationi Institute of Geography of Iv. Javakhishvili Tbilisi State University, Tbilisi, Georgia

Summary: *Results of modeling of the distribution of hailstones by mean max diameter (D) on the territories of municipalities of the Kakheti region of Georgia using data of the freezing level in the atmosphere and radar measurements of hail max sizes in clouds are presented. Data about D on the territories of municipalities of the Kakheti region for individual months, from April to September, are presented. The vertical distribution of D on the indicated territories was studied.*
Key words: *Hail, hail distribution by size.*

Introduction

The problem of hail in Georgia is devoted to numerous works covering a wide range of studies, such as climatology of hail [1-3], theoretical and experimental studies of the mechanisms of hail formation [4, 5], radar observation on hail processes [6, 7], methods of impact on hail processes [8], analysis of impact results [9, 10], etc.

To solve various problems of scientific or applied significance detailed information on the spatial-temporary characteristics of hail distributions and its sizes on different locations is necessary. The results of such studies for Georgia, in particular, are presented in works [1-3, 6, 7, 11].

To construct of spatial-temporary maps of the distribution of hail processes, data from radar observations of convective clouds are also used [6, 7, 11]. In particular, in the paper [11] results of modeling of the distribution of hailstones by mean max diameter (D) on the territory of Kakheti (Georgia) using data of the freezing level in the atmosphere and radar measurements of hail max sizes in clouds are presented. Maps of the distribution of hail by the average maximum diameter in the territory of Kakheti for individual months, from April to September, have been built. The vertical distribution of D on the indicated territory in the range of heights from 0.11 to 3.84 km was studied.

This work is a continuation of the study [11]. Results of modeling of the distribution of hailstones by mean max diameter (D) on the territories of municipalities of the Kakheti region of Georgia using data of the freezing level in the atmosphere and radar measurements of hail max sizes in clouds are presented below.

Study area, material and methods

Study area – eight municipalities of Kakheti region of Georgia (Akhmeta, Dedoplistskaro, Gurjaani, Kvareli, Lagodekhi, Sagarejo, Signagi, Telavi). Data of meteorological radar "METEOR 735 CDP 10 - Doppler Weather Radar" of Anti-hail service of Georgia about the max diameter of hailstones in the clouds (cm) - radar products HAILSZ (Size) [7, 8] - are used. Period of observation: April-September, 2016-2019.

The expected diameter of hailstones falling out to the earth's surface according to the Zimenkov-Ivanov model of hail melting in the atmosphere [11, 12] by taking into account the radar data about their max diameter in the clouds and freezing level in atmosphere was calculated [11].

To calculate the mean max diameter of hailstones (D) on the surface of the earth, the territory of Kakheti was divided into 465 squares, the range of heights ΔH was $0.11 \div 3.84$ km (Akhmeta: 95 squares, $\Delta H = 0.43 \div 3.84$ km; Dedoplistskaro: 102 squares, $\Delta H = 0.11 \div 0.87$ km; Gurjaani: 35 squares, $\Delta H = 0.23 \div 1.10$ km; Kvareli: 36 squares, $\Delta H = 0.26 \div 2.61$ km; Lagodekhi: 37 squares, $\Delta H = 0.21 \div 2.84$ km; Sagarejo: 66 squares, $\Delta H = 0.43 \div 1.63$ km; Signagi: 51 squares, $\Delta H = 0.19 \div 0.97$ km; Telavi: 43 squares, $\Delta H = 0.36 \div 2.94$ km). The monthly average values of the max sizes of hailstones and their 99% values of the lower and upper levels of the average were calculated.

For the data analysis the standard statistical methods are used. The following designations of statistical information are used below: Mean – average values; 99% _Low and 99%_Upp – 99% of lower and upper levels of the mean accordingly.

Results. Results in fig. 1 and 2 are presented.

	Low Apr	Mean Apr	Upp Apr	Low May	Mean May	Upp May	Low Jun	Mean Jun	Upp Jun	Low Jul	Mean Jul	Upp Jul	Low Aug	Mean Aug	Upp Aug	Low Sep	Mean Sep	Upp Sep
Akh	0.64	0.98	1.27	1.24	1.42	1.59	1.38	1.60	1.82	1.15	1.47	1.77	0.00	0.43	1.31	1.08	1.44	1.78
Ded	0.10	0.64	1.00	0.92	1.13	1.33	1.06	1.32	1.56	0.74	1.14	1.49	0.00	0.00	0.94	0.68	1.14	1.53
Gur	0.18	0.69	1.04	0.96	1.17	1.36	1.10	1.35	1.59	0.79	1.18	1.52	0.00	0.00	0.98	0.73	1.18	1.56
Kvar	0.29	0.75	1.09	1.02	1.22	1.41	1.16	1.41	1.64	0.87	1.25	1.57	0.00	0.10	1.06	0.81	1.23	1.61
Lag	0.21	0.71	1.06	0.98	1.19	1.38	1.12	1.38	1.61	0.82	1.21	1.54	0.00	0.09	1.01	0.75	1.20	1.58
Sag	0.29	0.74	1.08	1.01	1.21	1.40	1.15	1.39	1.63	0.86	1.23	1.56	0.00	0.01	1.04	0.79	1.22	1.59
Sig	0.08	0.63	0.99	0.91	1.12	1.32	1.05	1.31	1.55	0.72	1.13	1.48	0.00	0.00	0.93	0.66	1.13	1.52
Tel	0.36	0.80	1.12	1.06	1.26	1.44	1.20	1.44	1.67	0.93	1.29	1.61	0.00	0.12	1.10	0.86	1.27	1.64

Fig. 1. Mean max diameter of hailstones and their 99% lower and upper levels in Kakheti munitipalities from April to September.

Fig. 1 demonstrated distribution of hailstones by mean max diameter and their 99% lower and upper levels on the territories of munitipalities of Kakheti from April to September. As follows from fig. 1 mean values of D change from 0 cm (August – Dedoplistskaro, Gurjaani and Signagi munitipalities) to 1.60 cm (June – Akhmeta munitipality). Values of 99% _Low of the D change from 0 cm (August – all munitipalities) to 1.38 cm (June, Akhmeta munitipality). Values of 99% _Upp of the D change from 0.93 cm (August – Signagi munitipality) to 1.82 cm (June, Akhmeta munitipality).
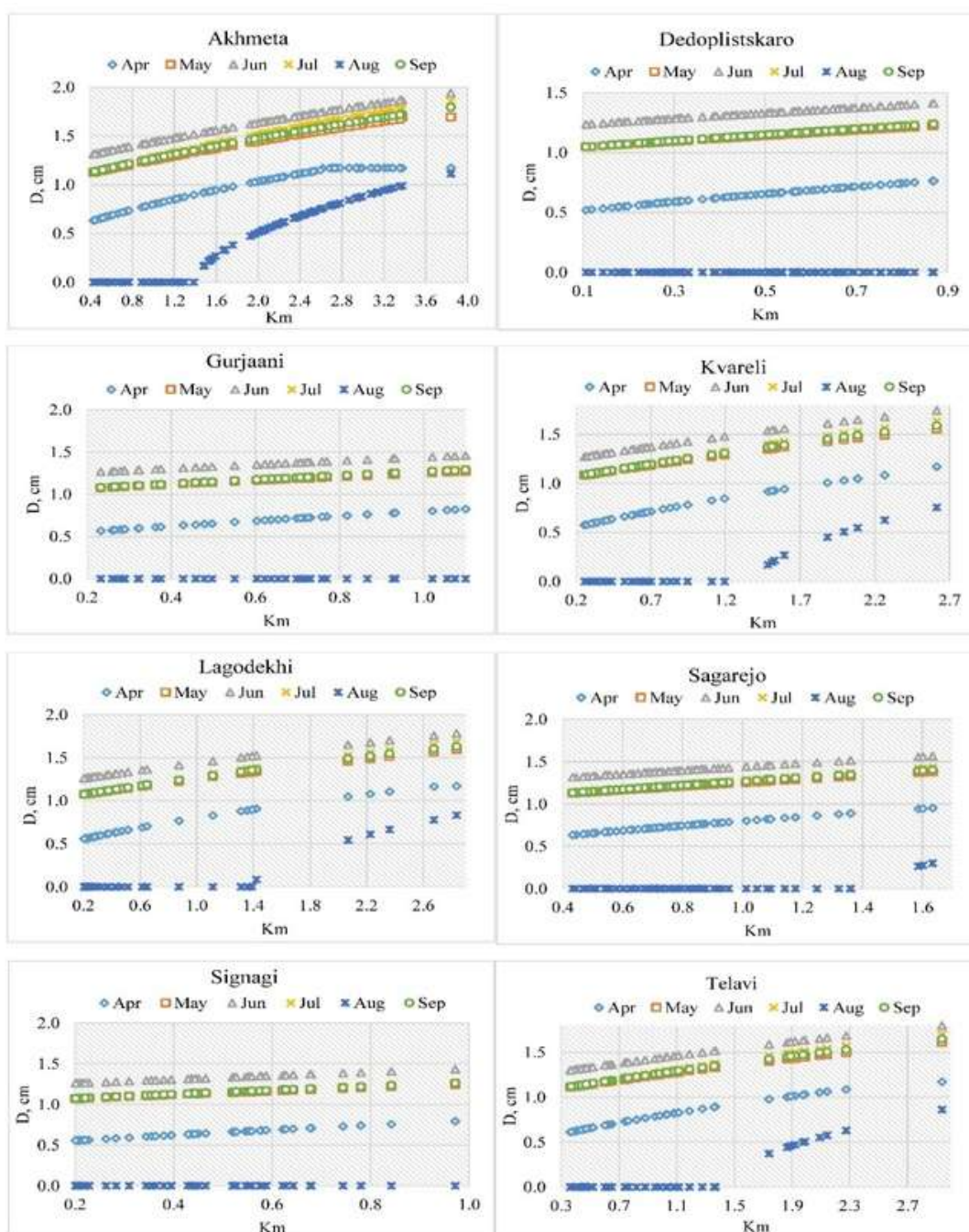
Fig. 2. Vertical distribution of mean max diameter of hailstones in different municipalities of Kakheti from April to September.

In fig. 2 vertical distribution of mean max diameter of hailstones in eight munitipalities of Kakheti from April to September are presented. In particilar, fig. 2 shows, that the variability of the mean maximum hail diameter on the territories of munitipalities of Kakheti in is as follows:

- Akhmeta. April: 0.63÷1.17 cm; May: 1.12÷1.69 cm; June: 1.31÷1.94 cm; July: 1.13÷1.86 cm; August: 0÷1.11 cm; September: 1.13÷1.79 cm; April-September: 1.32 cm.
- Dedoplistskaro April: 0.52÷0.76 cm; May: 1.05÷1.22 cm; June: 1.24÷1.41 cm; July: 1.04÷1.25 cm; August: 0÷0 cm; September: 1.05÷1.24 cm; April-September: 0.84 cm.
- Gurjaani. April: 0.57÷0.82 cm; May: 1.08÷1.27 cm; June: 1.27÷1.46 cm; July: 1.08÷1.31 cm; August: 0÷0 cm; September: 1.08÷1.29 cm; April-September: 0.88 cm.

- Kvareli. April: 0.57÷1.17 cm; May: 1.08÷1.55 cm; June: 1.27÷1.74 cm; July: 1.08÷1.63 cm; August: 0÷0.76 cm; September: 1.09÷1.59 cm; April-September: 0.98 cm.
- Lagodekhi. April: 0.56÷1.17 cm; May: 1.07÷1.59 cm; June: 1.26÷1.78 cm; July: 1.07÷1.68 cm; August: 0÷0.83 cm; September: 1.07÷1.63 cm; April-September: 0.93 cm.
- Sagarejo. April: 0.63÷0.95 cm; May: 1.13÷1.38 cm; June: 1.31÷1.57 cm; July: 1.13÷1.43 cm; August: 0÷0.30 cm; September: 1.13÷1.40 cm; April-September: 0.94 cm.
- Signagi. April: 0.55÷0.79 cm; May: 1.07÷1.25 cm; June: 1.26÷1.43 cm; July: 1.06÷1.28 cm; August: 0÷0 cm; September: 1.07÷1.26 cm; April-September: 0.82 cm.
- Telavi. April: 0.61÷1.17 cm; May: 1.11÷1.61 cm; June: 1.30÷1.80 cm; July: 1.11÷1.70 cm; August: 0÷0.86 cm; September: 1.11÷1.65 cm; April-September: 1.03 cm.

Conclusion. In the near future, we plan to modeling the damage from hail to vineyards, wheat and corn in the agricultural regions of Kakheti.

References

1. Gigineishvili V.M. Gradobitia v vostochnoi Gruzii. // Leninhrad, Gidrometeoizdat, 1960, 123 s.
2. Elizbarashvili E. Sh., Amiranashvili A. G., Varazanashvili O. Sh., Tsereteli N. S., Elizbarashvili M. E., Elizbarashvili Sh. E., Pipia M. G. Hailstorms in the Territory of Georgia. // European Geographical Studies, ISSN: 2312-0029, vol.2, № 2, 2014, pp. 55-69, DOI: 10.13187/egs.2014.2.55, www.ejournal9.com, (in Russian).
3. Varazanashvili O., Tsereteli N., Amiranashvili A., Tsereteli E., Elizbarashvili E., Dolidze J., Qaldani L., Saluqvadze M., Adamia Sh., Arevadze N., Gventcadze A. Vulnerability, Hazards and Multiple Risk Assessment for Georgia. // Natural Hazards, Vol. 64, Number 3 (2012), 2021-2056, DOI: 10.1007/s11069-012-0374-3, http://www.springerlink.com/content/9311p18582143662/fulltext.pdf
4. Amiranashvili A., Gzirishvili T. Aerosols and Ice Crystals in the Atmosphere. // Tbilisi, Metsniereba, 1991, 113 p., (in Russian).
5. Amiranashvili A., Bliadze T., Jamrishvili N., Kekenadze E., Tavidashvili Kh., Mitin M. Some Characteristics of Hail Process in Georgia and Azerbaijan on May 28, 2019. // Journal of the Georgian Geophysical Society, ISSN: 1512-1127, Physics of Solid Earth, Atmosphere, Ocean and Space Plasma, v. 22(2), 2019, pp. 40–54.
6. Amiranashvili A., Amiranashvili V., Doreuli R., Khurodze T., Kolesnikov Yu. Some Characteristics of Hail Processes in the Kakheti Region of Georgia. // Proc.13th Int. Conf. on Clouds and Precipitation, Reno, Nevada, USA, August 14-18, vol.2, 2000, 1085-1087.
7. Amiranashvili A., Chikhladze V., Kveselava N., Kvilitaia N., Sauri I., Shavlakadze Sh. Some Characteristics of Hail Processes in Kakheti (Georgia) According to Radar Observations into 2016-2019. // Journal of the Georgian Geophysical Society, ISSN: 1512-1127, Physics of Solid Earth, Atmosphere, Ocean and Space Plasma, v. 23(2), 2020, pp. 50 – 56.
8. Amiranashvili A., Chikhladze V., Dzodzuashvili U., Ghlonti N., Sauri I., Telia Sh., Tsintsadze T. Weather Modification in Georgia: Past, Present, Prospects for Development. // International Scientific Conference "Natural Disasters in Georgia: Monitoring, Prevention, Mitigation". Proceedings, ISBN 978-9941-13-899-7, Publish House of Iv. Javakhishvili Tbilisi State University, December 12-14, Tbilisi, 2019, pp. 216-222.
9. Amiranashvili A., Dzodzuashvili U., Lomtadze J., Sauri I., Chikhladze V. Some Characteristics of Hail Processes in Kakheti. // Trans. of Mikheil Nodia Institute of Geophysics, ISSN 1512-1135, vol. 65, Tb., 2015, pp. 77 – 100, (in Russian).
10. Amiranashvili A., Chikhladze V., Kveselava N., Sauri I. Some Results of Anti-Hail Works in Kakheti into 2016-2019. // Int. Sc. Conf. „Modern Problems of Ecology", Proc., ISSN 1512-1976, v. 7, Tbilisi-Telavi, Georgia, 26-28 September, 2020, pp. 153-156.
11. Amiranashvili A.G., Bolashvili N.R., Gulashvili Z.M., Jamrishvili N.K., Suknidze N.E., Tavidashvili Kh.Z. Modeling the Distribution of Hailstones by Mean Max Sizes on the Territory of Kakheti (Georgia) using Data of the Freezing Level in the Atmosphere and Radar Measurements. // Journal of the Georgian Geophysical Society, e-ISSN: 2667-9973, p-ISSN: 1512-1127, Physics of Solid Earth, Atmosphere, Ocean and Space Plasma, v. 24(1), 2021, pp. 25-36.
12. Zimenkov V.A., Ivanov V.V. Raschet tayaniya gradin v estestvennykh protsessakh. // Tr. VGI, 1966, vyp. 3(5).

THE MAIN CAUSES OF ACTIVATION TWO LARGE LANDSLIDES OF THE DEBED RIVER GORGE IN XXI CENTURY

[*]Atabekyan R.A., [*]Nazaretyan S.N., [**]Igityan H.A.

[*]*Territorial survey for seismic protection", Ministry of Emergency situations of Armenia. 3115 V.Sargsyan str. 5a, Gyumri, Armenia*
[**] *Institute of Geological sciences, National academy of sciences of Armenia, 0019 Bagrhamyan ave. 22, Yerevan, Armenia*
snaznssp@mail.ru

Summary: *Specialists have estimated about 3000-3500 active landslides in the territory of the Republic of Armenia, which occupy 8-10% of the territory and threaten 15% of the population of the Republic of Armenia. The average annual damage to them is about $10-30 million. There are two major landslides in the 21st century, located in the Devbed river gorge, threatening the only functioning railway connecting Armenia to Georgia, one of the main highways. One of them is the landslide-collapse of Ayrum, which suddenly became active in 2011 and took the lives of 5 people and caused huge material losses. A large part of the railway was destroyed and the highway became impassable. The second landslide, which became active in 2018 was near the town of Tumanyan. Here, a huge number of stones were moved, landslide tongue was approached to the transport infrastructure, which posed a serious threat to the republic. Our on-site studies have shown that the causes of both landslides are a result of anthropogenic impact. The article suggests specific measures to prevent landslides.*

Key Words: *Landslide, activation, lifelines, anthropogenic impact.*

Introduction

There are about 3000-3500 active landslides in the territory of the Republic of Armenia, which occupy 8-10% of the territory of the republic. In addition, 15% of the population of Armenia (about 470000 people) live in landslide-prone areas. The direct damage caused by landslides averages $ 10-30 million a year. Therefore, landslides are one of the major natural disasters in the country after the earthquake [1-2; 4].
In 02.10.2011 a landslide near Ayrum (Bagratashen) killed 5 people, targeted 35 cars, and closed the railway to Georgia for a long time. According to the expert opinion, the analysis of the aerial photographs of 1947, 1975 and 2006 shows that until 01.10. 2011 there was no sign of landslide activation. This landslide was not registered as active landslides in the territory of the Republic of Armenia in the database. The other, Tumanyan's landslide, which was known to experts because it was active several times in the twentieth century, moved sharply on January 12, 2018. He threatened to close the railway and the highway, due to which a very disturbing situation was created in the republic. Fortunately, it stabilized when the inflow of water to the landslide body was stopped.

The authors of this article have studied both of these landslides on the spot and submitted a conclusion to the RA Ministry of Emergency Situations on the reasons for their structure and activation.
Let us briefly present the structural features of these two landslides and the main reasons for their activation.

Ayrum (Bagratashen) landslide-collapses of 02.10.2011

This is a landslide-collapses, because there are elements that characterize both the landslide and the collapse. The landslide-collapses body is mainly represented by low-strength loess soils with a visible capacity of up to 30 m. There is also a small amount of coarse-grained soils. Prior to the landslide, most of the area was covered with basalts up to 7 m thick (Fig. 1). One of the main features of loess soils is the significant loss of strength when moisturizing and dynamic impacts. At present, any intervention on the landslide-body is fraught with a new movement of the masses.
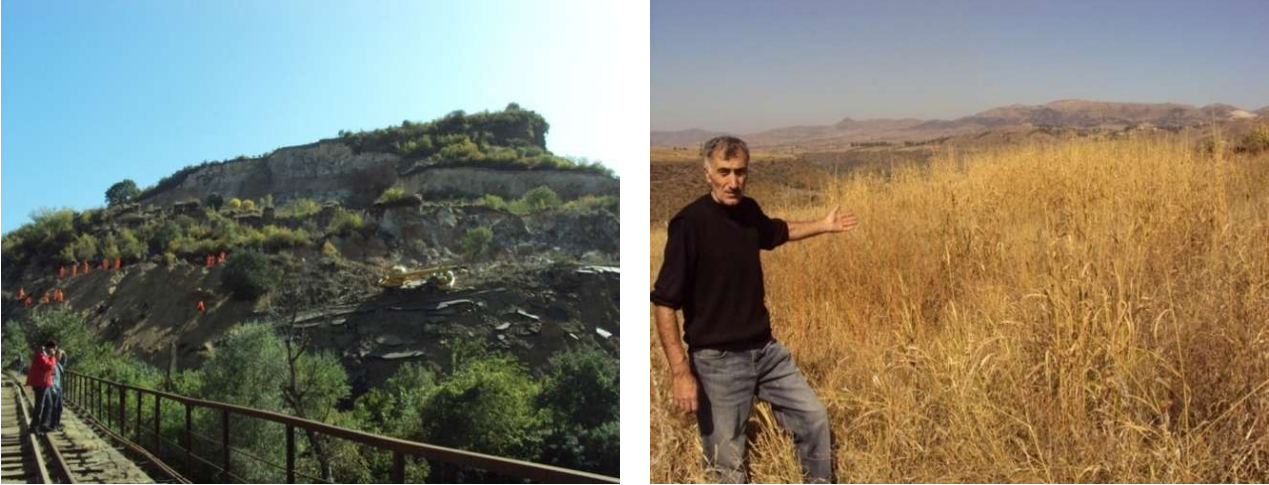
88

Fig. 1. Overview of Ayrum landslide-collapses area (the basalt cover is destroyed). On the site, above the collapse, the ground is water-saturated, wetlands.

The situation in the area adjacent to the landslide-collapse head. No noticeable cracks or other deformations were found in this area due to the presence of basalt cover. In the southern part of the landslide there is groundwater outlet, and above (on the platform) there are irrigated lands and swamps with an area of 500 m^2, including reeds. This indicates of the additional moisture of. The area above the landslide is unstable. Only large-scale collapses are possible here, due to basalt cover.

Possible causes of landslide-collapses. The slope was in the ultimate stress (stable) state before the landslide occurred. Any additional effects could lead to loss of stability. One of these additional effects, was the September 27 earthquake in Dmanisi (Georgia), with a intensity of 5-6 point by EMS-98 (M=4.4), which had a intensity of 3-4 in the study area. Were it not for the earthquake and heavy equipment on the highway, it would still be in the future landslide zone. In other words, the impact of the earthquake and heavy equipment could not be the cause of the landslide; they just contributed to its activation.

Conclusions: 1. Cause of landslide-collapse is the long-term wind blowing of the slope, ultimate stress state and additional moistening of loess soils. The impact of the earthquake and heavy equipment were factors contributing to the activation of landslide-collapse; 2. The landslide body is currently in a very unstable state, any intervention can lead to new movements of the masses; 3. Given the situation, the best decision is to build a new, landslide-bypassing highway. Unpredictable consequences are possible on the restored road due to the presence of weak loess soils.

Tumanyan landslide 12.01.2018

General brief description of the landslide. The landslide is located in against of Tumanyan community of Lori region, in the area directly adjacent to the railway on the left bank of the Devbet river. Man-made factors also take place here; these are mainly construction and operation of the water line serving the brick factory (especially the pool that extinguishes the water pressure). The outline of the landslide body is clearly visible in the satellite photos taken 10 years ago (Fig. 2).

Its activation in the past is evidenced by the deformations of the surface of the earth preserved in the area, the presence of reinforced concrete rappers previously installed to control movements, references by locals, etc. The landslide was particularly active in 1955, 1988-1989. The experts considered the reason for the two activations to be the outflow of water from the water pipe coming from the upper plateau, the feeding of the landslide body with that water.

Peculiarities of landslide structure. The landslide is located on the northern denudation slope of Lori deep gorge. Here various deluvial formations cover the radical volcanic basalts. Slope and landslide body soils are represented by loam with various debris content. Often the volume of fragments increases and the soils

according to the classification become large grains with the content of stones. Groundwater is practically non-existent, there is no fixed groundwater horizon. The landslide body stretches up to 320 m and has more than 3 hectares area (32500 m^2 area and about 35000 m^3 volume). Among the features of the landslide it is necessary to mention: a) almost the entire surface of the landslide body, except for the collapse site on the tongue, is represented by a thickness of 4 m, with solid or semi-solid ground crust; b) the basalt foundations of the landslide body have protrusions and grooves that cross the landslide slide surface (Fig.2; Fig.3); c) surface water has no significant effect: d) within the collapsed tongue of the landslide, rapid discharge of accumulated water is observed.
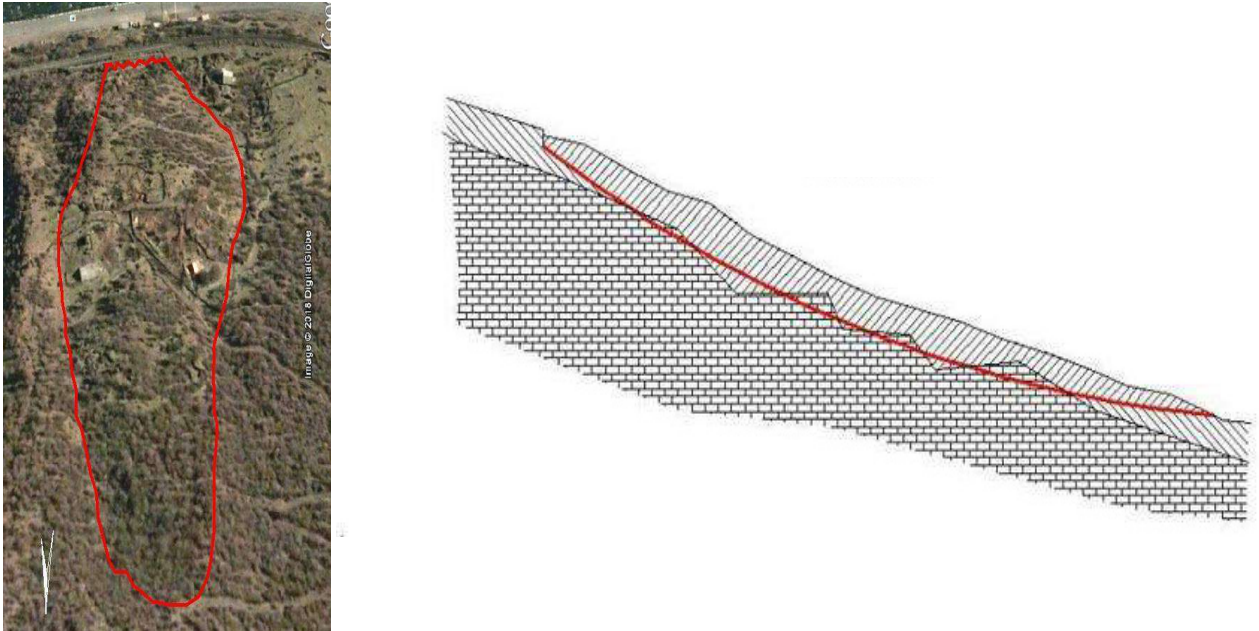
Fig. 2. General view Tumanyan landslide on satellite image and schematic section of the landslide area.

Fig. 3. The view of the Tumanyan landslide (the threat of a displaced mass on the rail) and the crack at the top, on which beacons are placed to record the movements.

The situation in the landslide zone. As of January 13, 2018, the landslide had stabilized as the flow of water through the pipeline was stopped. The possible proofs of this are: a) 1955 և 1988-1989 after activation, when the flow of water from the pipeline to the landslide body was eliminated, the movement of the landslide stopped; b) this time, when the operation of the water line was stopped, the landslide was stabilized; c) the volume of water flowing out of the landslide site near the railway has significantly decreased. In 2018 the displacements caused by the landslide were smaller than the previous ones. Thus, if the horizontal displacements due to the observed activation in the fracture cracks up to 3-4 m depth are 30-50 cm, then they have previously reached meters. The difference between the amplitudes of the old and new vertical displacements at the head of the landslide is obvious. Old, 1989 the vertical drop amplitude of the resulting fault is at least 1.5 m, and in the new fault 0.3-0.4 m.

Conclusions: The cause of all three landslide activations is man-made and was due to water pipe accidents and water penetration into the landslide body. Due to the large mass of the landslide body, the known methods of stabilizing it (construction of a retaining wall, installation of pile, etc.) are not effective. In this situation, the only correct approach to the landslide body is to stop the entry of water, which has already been done.

Landslide has stabilized and abrupt and large-scale activation is possible if strong earthquake with intensity 7 point by EMS-98 occur in this area [3, 5].

Results and discussion:

1. Activation of the two major landslides observed is the result of anthropogenic impact. They would not be activated if there was no water in the landslide bodies.
2. Based on the importance of the Vanadzor-Ayrum railway and highway for the republic, is necessary through specialized organizations, at least visually investigate the presence of landslides and rocky belts along the entire length of the mentioned lines and assess the probability of their activation, depending on man-made and seismic reasons.

<div align="center">

References

</div>

1. Boynagryan V.R., Stepanyan V.E., Khachatryan D.A., Yadoyan R.B., Arakelyan D.G., Gyurjyan Yu. G. Landslides in Armenia. // Published with the support of the OSCE. Publishing house "ASOGIK" LLC. Yerevan, 2009. 308 p. (in Russian).
2. Boynagryan V.R. Influence of landslide of Armenia on the transport communications and populated areas. // Scientific notes of Yerevan state university, Geology and Geography, N 3, 2009, pp. 22-30 (in Russian).
3. Havenith H., Torgoev A., Braun A. et al. A new classification of earthquake-induced landslide event sizes based on seismotectonic, topographic, climatic and geologic factors. // Geoenviromental Disasters 3, Article number 6. 2016.
4. Matossian A., Baghdasaryan H., Avagyan A., Igityan H., Gevorgyan M., Havenith H. New Landslide Inventory for the Armenian Lesser Caucasus: Slope Failure Morphologies and Seismotectonic Influences on Large Landslides. // Geosciences 2020, 10, 111.
5. Nazaretyan, S.N. Main features of the new methodology for seismic risk assessment of Armenian cities. // Seismic Instruments, 56, 2020, pp. 317-331.

FORMATION OF THE HAGHARTSIN LANDSLIDE (ARMENIA) AS A CONSEQUENCE OF THE VIOLATION OF THE EQUILIBRIUM STATE OF THE SLOPE DURING ENGINEERING

Boynagryan V.R.

Yerevan State University, Yerevan, Armenia
vboynagryan@ysu.am

Summary: *The Haghartsin landslide is located on the right bank of the Aghstev River, near the village of Haghartsin. It is an activated part of a large structural ancient landslide formed during a strong earthquake in the Pliocene-Upper Quaternary time. The first landslide phenomena began to be observed in this area in the 80s of the XX century, literally as soon as the pruning of the slope for the construction of roads and railways began. Significant movements first occurred in 1985 on the slope between the railway track and the highway, as well as on the slope above the railway track. In the 90s of the XX century, this section of the railway was completely destroyed, and already in 1996 a landslide body blocked the highway. Currently, landslide movements cover all new areas. The tongue of a landslide almost every year in May blocks the riverbed of the Aghstev River with the corresponding flooding of rural houses.*

Key Words: *Aghstev, Haghartsin, highway, landslide, railway.*

Introduction. The occurrence of landslide displacements of rocks is possible under certain conditions and the presence of a so-called "trigger" [1, 2] or "reason" – the main reason that triggered the landslide mechanism [3, 4]. Usually, the formation of landslides is influenced by a number of factors: geomorphological, geological and physico-geographical conditions, as well as anthropogenic impact. And one of the factors seems to "overflow the bowl", violates the limit of stability of rocks, causing displacement. Therefore "... it is rarely possible to explain a landslide by one specific cause, if at all possible" [5, p. 70].

Human economic activity has a great impact on the formation of new and activation of existing landslides. One of such landslides in Armenia is the Haghartsin, whose current activity is due to the pruning of the body of the seismogenic landslide of the same name for the laying of roads and railways. At the same time, protective measures were not carried out to strengthen the slope.

Methods. The ancient seismogenicHaghartsin landslide was identified by the author in the late 70s of the twentieth century when deciphering aerial photographs and a topographic map of 1:25,000 scale and confirmed as a result of field research. In 1986-1988, employees of the Moscow State University carried out a repeated phototheodolite survey of an active landslide site formed at the site of the slope trimming for engineering purposes. In subsequent years, observations of the landslide condition were carried out by employees of the Ministry of Emergency Situations of Armenia and the Dilijan expedition of the IGS of the National Academy of Sciences of the Republic of Armenia [6].

Results and discussion. The Haghartsin landslide is located within the Dilijan basin, on the right bank of the Aghstevriver, opposite the village of Haghartsin. The upper absolute mark of the landslide site is 1100m, the basis of erosion is at an altitude of 995m. It is an activated part of a large structural (tectonic-seismogravitational) ancient landslide (see Fig. 1).

 The first landslide phenomena began to be observed at this site in the eighties of the XX century, when the slope was cut for the construction of roads and railways without assessing its stability and the necessary engineering protection. Significant progress first occurred in 1985 on the slope between the railway track and the highway. At the same time, landslide processes began on the slope above the railway track, which contributed to the complete destruction of this section of the railway in the 90s, and already in 1996 a landslide body blocked the highway (see Fig. 2).

Fig. 1. General view of the Haghartsin landslide site.

a)

b)

c)

Fig. 2. The railway destroyed by a landslide - a); blocked by climb down masses
the railway track - b); the bypass road - c).

The Haghartsin landslide as a whole, according to the mechanism of manifestation, refers to a block shift landslide, and its eastern part (the eastern block) with its characteristic hydrogeological regime and obvious signs of suffusion phenomena refers to a viscoplastic landslide with suffusion removal. The landslide site covers an area of 82,000 m^2, its length is 270 m, width is 300 m, the volume of the landslide mass is 2,184,000 m^3. Within this landslide, three blocks are allocated with the following parameters (see Table and Fig. 3).

Table 1.The ratio of the parameters of the landslide blocks of the site "Haghartsin" [7]

Block name	Area		Volume		Depth of capture, m	Mechanism of manifestation
	m^2	%	m^3	%		
Eastern	37 000	45,2	102 600	46,9	23	Viscoplastic with suffusion removal
Central	28 000	34,1	638 000	29,3	22	Block shift
Western	17 000	20,7	520 000	23,8	30,5	Technical shift
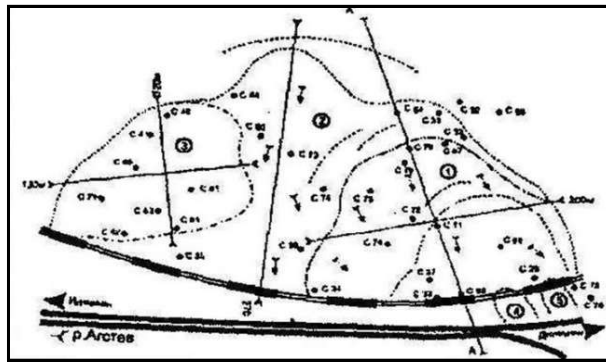
Fig. 3. Schematic plane of landslide Haghartsin [7].

The upper boundary of the landslide body is expressed by a wall of disruption with a length of 70-80m and a height of up to 12m. The western wall of the breakdown reaches a height of 17 m, the eastern wall is indistinct, but its location coincides with the fracture zone recorded in 1993.

The Haghartsin landslide developed on a slope composed of a volcanogenic-sedimentary complex of rocks of the Middle Eocene, covering mid-quaternary landslides and modern (proluvial, alluvial-proluvial, eluvial-deluvial and lacustrine) formations [7]. The Eastern block (block 1) is characterized by the greatest activity, in the body of which a number of local landslide stabs are distinguished. The active state of block 1 provoked the movement of neighboring blocks and the formation of a single landslide array with one breakaway point, as well as a change in vectors and displacement velocity. The landslide block 1 has a length of 190m, a width of 200m, an area of 37,000 m^2, the volume of the displaced mass is 1,026,000 m^3. The sliding plane passes at a depth of 15 to 23 m in deluvial-proluvial formations, sometimes captures hydrothermally altered bedrock. The structure of block 1 involves loose-block slope formations (deluvium, defluction), technogenic accumulations, deluvial-proluvial formations (lenses of bentonite clays, clay-loamy soils with layers of gravel and gravel), alluvial and alluvial-proluvial accumulations of terraces of the river Aghstev, as well as Middle Eocene andesites and andesite-dacites and their modified differences. In the period from 2000 to 2010, the entire landslide site was activated as a result of the termination of engineering protection works (the creation of a buttress and drainage system, unloading measures, partial unloading of the tongue part of the landslide zone along the railway track, as well as the construction of wall drainage and upland ditches to intercept atmospheric and man-made waters) due to lack of funding [6]. The consequence of this was a catastrophic displacement of the earth masses and the actual unification of all three landslide blocks into a single whole. The railway track was completely destroyed, the bypass road was put out of operation. In April 2001.the tongue of the landslide dammed 75% of the riverbed of the Aghstev river, which required large expenses for its cleaning from the debris of the soil (see Fig. 4).

Fig. 4. A bypass road blocked by a landslide - a); landslide masses that collapsed into the riverbed of the Aghstev river - b).

New landslide movements with riverbed closure occurred on May 27, 2005 and April 28, 2006. At the same time, the lower floors of more than 20 houses with their homesteads, a rural school (in its northern building, the height of the water level was 1.2 m) were flooded. After 2006, almost every year in the spring, landslide masses block the riverbed, creating a lot of problems not only for the villagers, but also for the

94

Ministry of Emergency Situations of the republic. The houses of the residents of the village of Haghartsin are destroyed as a result of constant flooding (see Fig. 5).

Fig. 5. Destroyed buildings on the left bank of the Aghstev river (05.07.2013).

Conclusion. To date, the situation at the landslide site "Haghartsin" is extremely critical. Landslide movements cover all new areas not only in breadth, but also up the slope and down the depth (see Fig. 6).

To stop a landslide, comprehensive protective measures are needed: drainage of watered rocks; piercing with piles buried in the underlying rocks below the sliding mirror; artificial improvement of the properties of sliding soils (cementation, the use of Uisit powder - developed by employees of the former Dilijan expedition of the IGS NAS RA together with geologists of Moscow State University, etc.). However, all this requires large financial investments, which the republic is currently unable to implement.

References

1. Emelyanova E.P. Basic patterns of landslide processes. // M.: Nedra, 1972, 310 p.
2. Sowers G.B., Sowers G.F. Introductory soil mechanics and foundations. // New York: Macmillan, 1970, 556 p.
3. Lomtadze V.D. Engineering Geology.Engineering geodynamics. // L.: Nedra, 1977, 479 p.
4. Maslov N.N. Conditions of stability of slopes and slopes in hydropower construction. // M.-L.: Gosenergoizdat, 1955, 468 p.
5. Varns D.D. Slope movements, types and processes Landslides. Research and strengthening. // Moscow: Mir, 1981, pp. 32-85.
6. Landslides of Armenia. // Yerevan: ASOGIK, 2009, 308 p.
7. Stepanyan V.E., Gurdjian Yu.G., Sereda M.N. Conceptual approaches to risk management processes from the   manifestation of dangerous natural landslide processes // Proceedings of the III Central Asian International Symposium, vol. 2, Dushanbe, 2005.

CHANGEABILITY OF MONTHLY MEAN VALUES OF SURFACE OZONE CONCENTRATION (SOC) IN THREE POINTS OF TBILISI FROM JANUARY 2017 TO OCTOBER 2021

Kharchilava J., Kekenadze E.

Mikheil Nodia Institute of Geophysics of Ivane Javakhishvili Tbilisi State University, Tbilisi, Georgia
kekenadze@gmail.com

Summary: *The statistical characteristics of the surface ozone concentration (SOC) in three points of Tbilisi city (A. Kazbegi av., A. Tsereteli av. and Varketili) from January 2017 to October 2021 are represented. The data of National Environmental Agency of Georgia about the mean monthly values of SOC are used. In particular, it is obtained that the greatest average values of SOC during entire period of observations in Varketili were observed (68.0 mcg/m³), smallest - on A. Tsereteli av. (43.9 mcg/m³). The value of the linear correlation coefficient between the mean monthly values of SOC on all points changes from 0.88 to 0.96. The influence of limitation on the movement of public transport in Georgia in different time periods from March 2020 to August 2021 in connection with the pandemic of coronavirus COVID-19 to the changeability of the level of SOC is studied.*

Key Words: *surface ozone concentration, ecology.*

Introduction

Atmospheric ozone is one of the most important species defining the quality of life [1-3]. Therefore, special attention in many countries of world, including in Georgia, is paid to studies of surface ozone concentration (SOC) [4-10].

The ozone concentration in the atmospheric surface layer, varies widely depending on photochemical processes, horizontal advection, intrusions of stratospheric air, vertical mixing, dry and humid deposition, etc. In particular limitation on the movement of public transport in Georgia in connection with the pandemic of coronavirus COVID-19 influenced the ozone content in the air in Tbilisi, causing it to some rise [11,12].

In recent years, the Environment Agency has been monitoring surface ozone concentrations in Georgia in accordance with international standards. This paper presents the results of a statistical analysis of monthly mean data of SOC values at three points in of Tbilisi from January 2017 to October 2021, including period with limitation on the movement of public transport in Georgia in different time periods from March 2020 to August 2021 in connection with the pandemic of coronavirus COVID-19.

Study area, material and methods

Study area – three locations of Tbilisi (A. Kazbegi av. – KZBG, A. Tsereteli av. – TSRT, Varketili – VRKT). Coordinates of this locations of air pollution measurements points in [10] are presented.

The data of Georgian National Environmental Agency about the surface ozone concentration (SOC) in three points of Tbilisi city are used [http://air.gov.ge/reports_page]. Period of observation: January 1, 2017- October 31, 2021.

The data analysis with the use of standard statistical methods was conducted. The following designations will be used below: Mean – average values; Min – minimal values; Max - maximal values; Range = Max-Min; St Dev – standard deviation; Cv = 100·St Dev/Mean, coefficient of variation (%); 99% Low and 99% Upp – 99% confidence interval of lower and upper calculated level accordingly; R – coefficient of linear correlation. Comparison of mean values of SOC in two periods of time was produced with the use of Student's criterion with the level of significance α not worse than 0.25.

Results and discussion

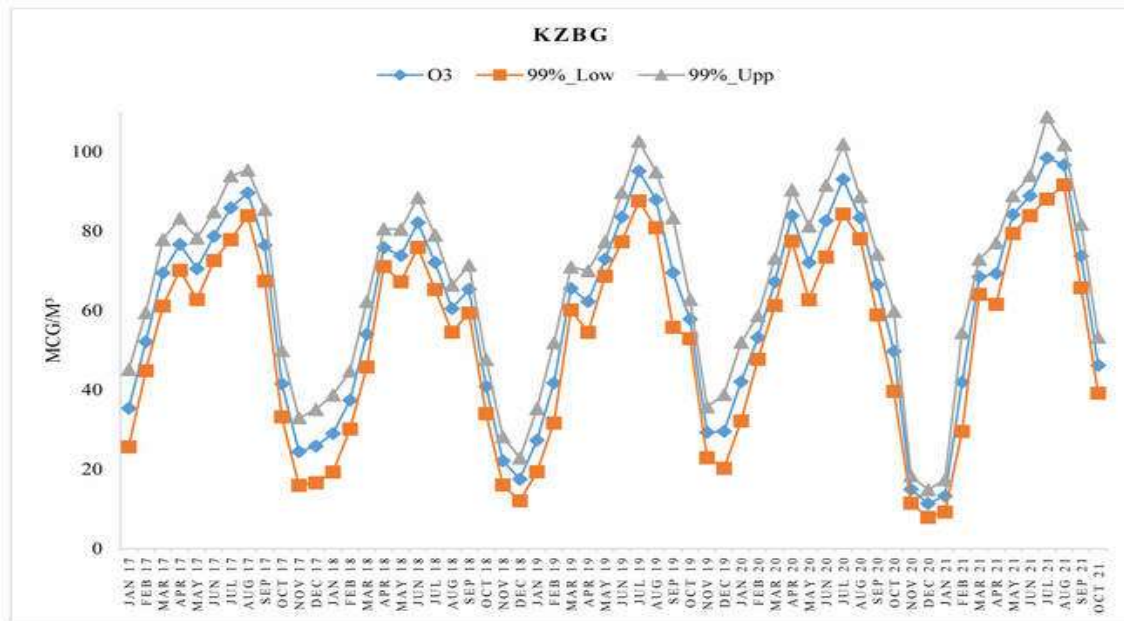Results in fig. 1-3 and tables 1-2 are presented.

Fig. 1. Monthly mean values of SOC and their 99% confidence intervals on the A. Kazbegi av. from January 2017 to October 2021.
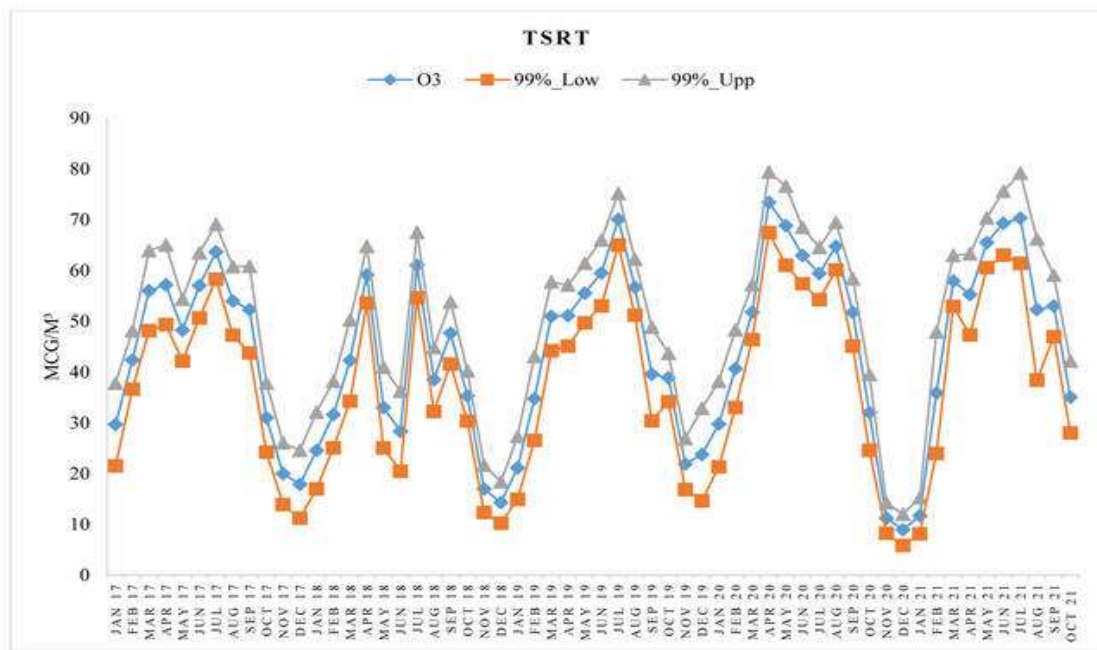

Fig. 2. Monthly mean values of SOC and their 99% confidence intervals on the A. Tsereteli av. from January 2017 to October 2021.
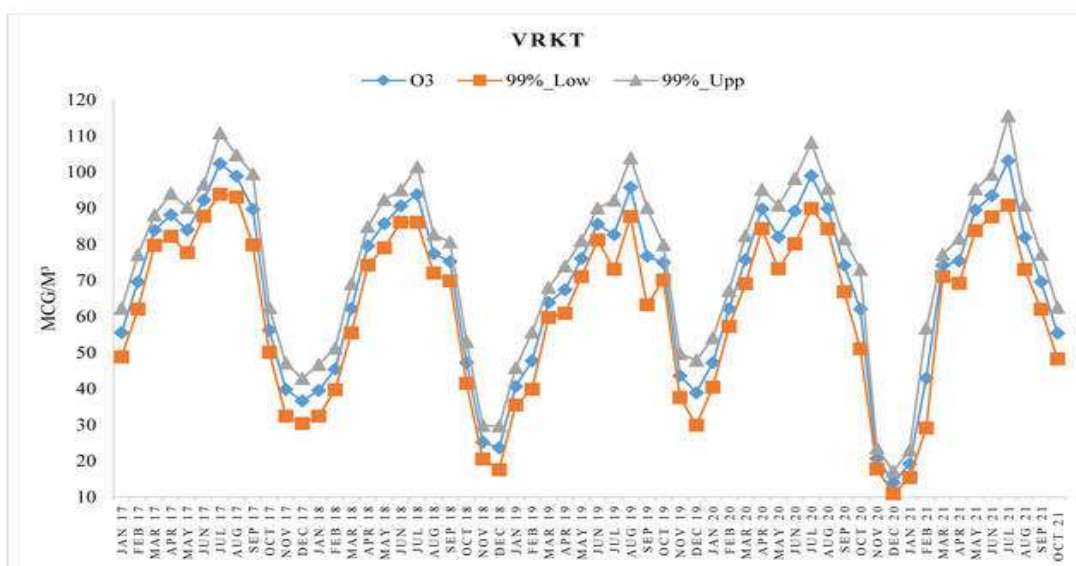
Fig. 3. Monthly mean values of SOC and their 99% confidence intervals in Varketili from January 2017 to October 2021.

In fig. 1-3 data about monthly mean values of SOC and their 99% confidence intervals on the three points of measurements in Tbilisi sity in the insestigation period are presented.

As follows from these figures, the intra-annual distribution of SOC in Tbilisi as is wave-like - an increase in the warm half-year, a decrease in the cold season of the year.

Table 3. Statistical characteristics of the monthly mean values of SOC at three points of Tbilisi from January 2017 to October 2021 (mcg/m³).

Parameter	KZBG	TSRT	VRKT
Max	98.4	73.4	103.1
Min	11.3	8.9	14.0
Range	87.1	64.5	89.1
Mean	60.0	43.9	68.0
St Dev	24.3	17.5	23.6
Cv, %	40.5	39.9	34.7
	Correlation Matrix (R)		
KZBG	1	0.91	0.96
TSRT	0.91	1	0.88
VRKT	0.96	0.88	1

The statistical characteristics of the monthly mean values of SOC for three points of Tbilisi from January 2017 to October 2021 in table 1 are presented. As it follows from this table and fig. 1-3 the monthly mean value of SOC changes from 8.9 mcg/m³ (TSRT) to 103.1 mcg/m³ (VRKT).

The greatest average values of SOC during entire period of observations in the Varketili were observed (68.0 mcg/m³), smallest - on A. Tsereteli av. (43.9 mcg/m³).

The values of the linear correlation coefficient between the mean monthly values of SOC on all points changes from 0.88 to 0.96 (table 1).

In connection with the pandemic of coronavirus COVID-19 in Georgia were introduced the limitations in the movement of different type of transport in different time periods from March 2020 to August 2021.

The preliminary studies of the influence of these limitations on the daily and monthly content of SOC in Tbilisi in spring 2020 are given to [11,12].

Data about influence of the various limitation on the movement of transport in Georgia from March 2020 to August 2021 in connection with the pandemic of coronavirus COVID-19 to the mean level of SOC in this period of time are presented below.

Table 2 presents the data about changeability of mean values of SOC at three points of Tbilisi city in three periods of time. I. March 2017-August 2018, first pre-pandemic period; II. March 2018 - August 2019, second pre-pandemic period; III. March 2020 - August 2021, period with pandemic.

Table 2. Changeability of mean values of SOC at three points of Tbilisi city in three periods of time, mcg/m³

Parameter	KZBG	TSRT	VRKT
I. Mean (Mar 2017-Aug 2018)	62.4	43.1	74.7
II. Mean (Mar 2018 - Aug 2019)	61.1	43.1	67.8
III. Mean (Mar 2020 - Aug 2021)	65.9	50.1	70.9
Differ. (II-I)	No sign		
Differ. (III-II)	No sign	7.0 ($\alpha \approx 0.25$)	No sign
Differ. (III-I)	No sign	7.1 ($\alpha \approx 0.25$)	No sign

In particular, as it follows from table 2, in the second period of time, as compared with the first, the average ozone content did not change at any of the measurement points. In the third time period (the period of the pandemic), as compared to the first and the second, an increase in the mean ozone content at Tsereteli measurement point (+7 mcg/m³) is noted. For the other two measurement points, stability is observed in the variability of SOC.

Conclusion

Over the long term is planned the more detailed study of variations of surface ozone concentration in Tbilisi and other cities of Georgia, identifying the links between SOC and other air pollutants, etc.

References

1. Kharchilava J. Some Results of Investigations of Atmospheric Ozone in Georgia. // Trans. of M. Nodia Institute of Geophysics, ISSN 1512-1135, vol. LXIX, 2018, pp. 211-219 (In Russian).
2. Amiranashvili A., Bliadze T., Chikhladze V. Photochemical smog in Tbilisi. // Monograph, Trans. of Mikheil Nodia institute of Geophysics, ISSN 1512-1135, vol. 63, Tbilisi, 2012, 160 p., (in Georgian).

3. WHO Air quality guidelines for particulate matter, ozone, nitrogen dioxide and sulfur dioxide. Global update 2005 Summary of risk assessment. // World Health Organization, 2006, 22 p., http://apps.who.int/iris/bitstream/handle/10665/69477/WHO_SDE_PHE_OEH_06.02_eng.pdf;jsessionid =48F380E7090ADBB4A166AC7A8610624A?sequence=1

4. Kharchilava J., Amiranashvili A. Studies of Atmospheric Ozone Variations in Soviet Georgia. // Results of Researches on the International Geophysical Projects, SGC, Moscow, 1998, 114 p. (in Russian).

5. Amiranashvili A., Amiranashvili V., Chikhladze V., Kharchilava J., Kartvelishvili L. The statistical analysis of average seasonal, semi-annual and annual values of surface ozone concentration in Tbilisi in 1984-2003. // Journal of the Georgian Geophysical Society, Issue B. Physics of Atmosphere, Ocean and Space Plasma, ISSN 1512-1127, vol. 12B, Tbilisi, 2008, pp. 45–48.

6. Stankevich A.S., Titarenko O.V., Amiranashvili A.G., Chargazia Kh. Z. Determination of Distribution of Ozone Content in Lower Troposphere and Atmospheric Aerosol Optical Thickness over Territory of Georgia Using Satellite Data and Ground Truth Measurements. // Journal of the Georgian Geophysical Society, Issue (B). Physics of Atmosphere, Ocean, and Space Plasma, v.17b, 2014, pp. 26-37.

7. Stankevich S., Titarenko O., Amiranashvili A., Chargazia Kh. Modeling of Ozone Content Distribution in Lower Troposphere over the Territory of Georgia Using the Data of Satellite and Ground Observations. // Bulletin of the Georgian National Academy of sciences, vol. 9, No. 2, 2015, pp. 54-58.

8. Kekenadze E., Kharchilava J., Chkhaidze G., Senik I. Comparative Analysis of the Surface Ozone Concentration in Tbilisi and at Kislovodsk High Mountain Station. // Int. Sc. Conf. "Natural Disasters in Georgia: Monitoring, Prevention, Mitigation". Proc., ISBN 978-9941-13-899-7, Publish House of Iv. Javakhishvili Tbilisi State University, December 12-14, Tbilisi, 2019, pp. 150-154

9.   Lagidze L., Matchavariani L., Svanadze D., Khomasuridze G. Influence of Meteorological Factors on Ecological Conditions of the Atmosphere in Tbilisi, Georgia. // J. Environ. Biol., 41, 2020, pp. 391-395.

10. Kekenadze E.N. Statistical Characteristics of Surface Ozone Concentration in Three Points of Tbilisi in 2017-2018. // Journal of the Georgian Geophysical Society, ISSN: 1512-1127, Physics of Solid Earth, Atmosphere, Ocean and Space Plasma, v. 22(2), 2019, pp. 63 - 67.

11. Amiranashvili A.G., Kirkitadze D.D., Kekenadze E.N. Pandemic of Coronavirus COVID-19 and Air Pollution in Tbilisi in Spring 2020. // Journal of the Georgian Geophysical Society, ISSN: 1512-1127, Physics of Solid Earth, Atmosphere, Ocean and Space Plasma, v. 23(1), 2020, pp. 57-72.

12. Kharchilava J., Kekenadze E. Variability of Monthly Mean Values of Surface Ozone Concentration (SOC) in Three Points of Tbilisi from January 2017 to May 2020. Pandemic of Coronavirus Covid-19 and SOC in Spring 2020 in Tbilisi. // International Scientific Conference „Modern Problems of Ecology", Proceedings, ISSN 1512-1976, v. 7, Tbilisi-Telavi, Georgia, 26-28 September, 2020, pp. 263-267.

CHANGEABILITY OF MONTHLY MEAN VALUES OF PM2.5 AND PM10 IN THREE POINTS OF TBILISI FROM JANUARY 2017 TO OCTOBER 2021. PANDEMIC OF CORONAVIRUS COVID-19 AND PM2.5/10 IN TBILISI FROM MARCH 2020 TO AUGUST 2021

Kirkitadze D.
Mikheil Nodia Institute of Geophysics of Ivane Javakhishvili Tbilisi State University, Tbilisi, Georgia
darejan.kirkitadze@gmail.com

Summary: *The statistical characteristics of the weight concentrations of aerosols (particulate matter PM2.5 and PM10) in three points of Tbilisi city (A. Kazbegi av., A. Tsereteli av. and Varketili) from January 2017 to October 2021 are represented. The data of National Environmental Agency of Georgia about the mean monthly values of PM2.5 and PM10 are used. In particular, it is obtained that the greatest average values of PM2.5 during entire period of observations on the A. Tsereteli av. were observed (20.1 mcg/m³), smallest - on A. Kazbegi av. (15.0 mcg/m³). The greatest average values of PM10 during entire period of observations also on. A. Tsereteli av. were observed (44.8 mcg/m³), smallest - in Varketili (34.0 mcg/m³).*
It is obtained, that the value of the linear correlation coefficient between the mean monthly values of PM2.5 and PM10 on all points changes from 0.70 to 0.96. The annual mean of PM2.5 and PM10 for all of measurements points are higher, that maximum permissible concentration according to the standards of the <u>*World Health Organization*</u>*.*
The influence of limitation on the movement of public transport in Georgia in different time periods from March 2020 to August 2021 in connection with the pandemic of coronavirus COVID-19 to the changeability of the level of aerosol pollution of atmosphere is studied.

Key words: *Atmospheric aerosols, particulate matter, PM2.5, PM10.*

Introduction

In Georgia for many decades has been conducting research on atmospheric aerosols (including radioactive ones) and their properties [1-7]. In recent years, in Georgia, the Environmental Agency, in accordance with international standards, began monitoring particulate matter with a diameter of ≤2.5 mcm (PM2.5) and ≤10 mcm (PM10). Some results of this monitoring in [8-11] are presented.

The PM2.5 and PM10 contents in atmosphere directly depends on industrial and transport emissions.

In particular limitation on the movement of public transport in Georgia in connection with the pandemic of coronavirus COVID-19 influenced on PM2.5 and PM10 contents in the air in Tbilisi, causing them to decrease [10,11].

This paper is a continuation of previous studies and in it the results of a statistical analysis of mean monthly data about PM2.5 and PM10 values at three points in the city of Tbilisi from January 2017 to October 2021, including period with limitation on the movement of public transport in Georgia in different time periods from March 2020 to August 2021 in connection with the pandemic of coronavirus COVID-19 is presented.

Study area, material and methods

Study area – three locations of Tbilisi (A. Kazbegi av. – KZBG, A. Tsereteli av. – TSRT, Varketili – VRKT). Coordinates of these locations of air pollution measurements points in [8] are presented.

The data of Georgian National Environmental Agency about the dust concentration (atmospheric particulate matter - PM2.5 and PM10) in three points of Tbilisi city are used [http://air.gov.ge/reports_page]. Period of observation: January 1, 2017 - October 31, 2021.

The data analysis with the use of standard statistical methods was conducted. The following designations will be used below: Mean – average values; Min – minimal values; Max - maximal values;

Range = Max-Min; St Dev – standard deviation; Cv = 100·St Dev/Mean, coefficient of variation (%); 99% Low and 99% Upp – 99% confidence interval of lower and upper calculated level accordingly; R – coefficient of linear correlation. Comparison of mean values of SOC in two periods of time was produced with the use of Student's criterion with the level of significance α not worse than 0.01.

In the correspondence with the standards of the World Health Organization maximum permissible concentration (MPC) composes: annual mean for PM2.5 - 10 mcg/m³ and for PM10 - 20 mcg/m³ [12].

Results and discussion
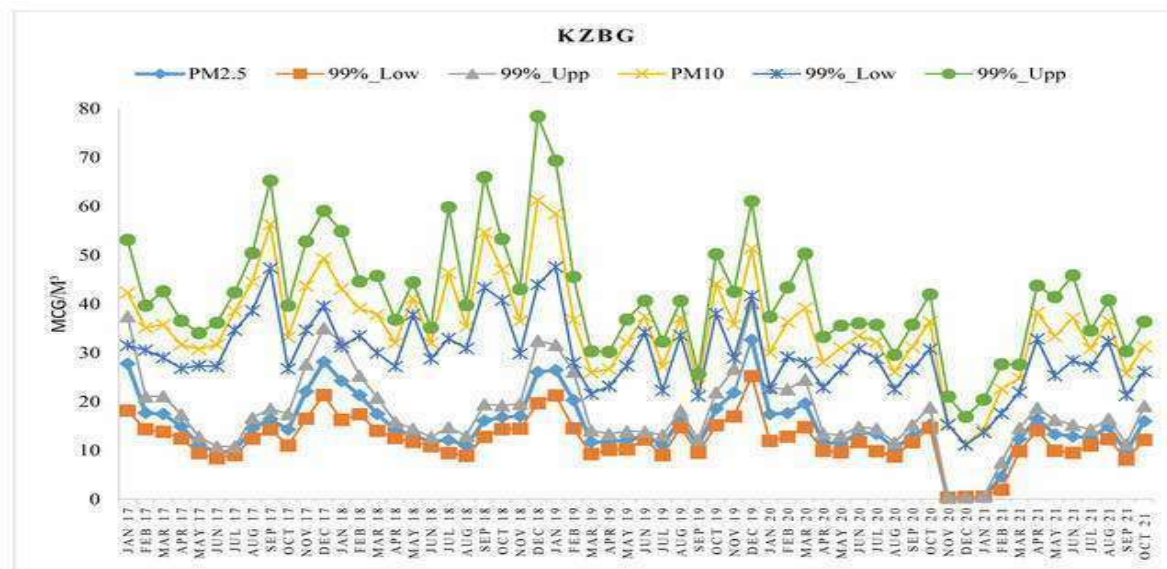
Results in fig. 1-3 and tables 1-2 are presented.

Fig. 1. Monthly mean values of PM2.5 and PM10 and their 99% confidence intervals on the A. Kazbegi av. from January 2017 to October 2021.

Fig. 2. Monthly mean values of PM2.5 and PM10 and their 99% confidence intervals on the A. Tsereteli av. from January 2017 to October 2021.
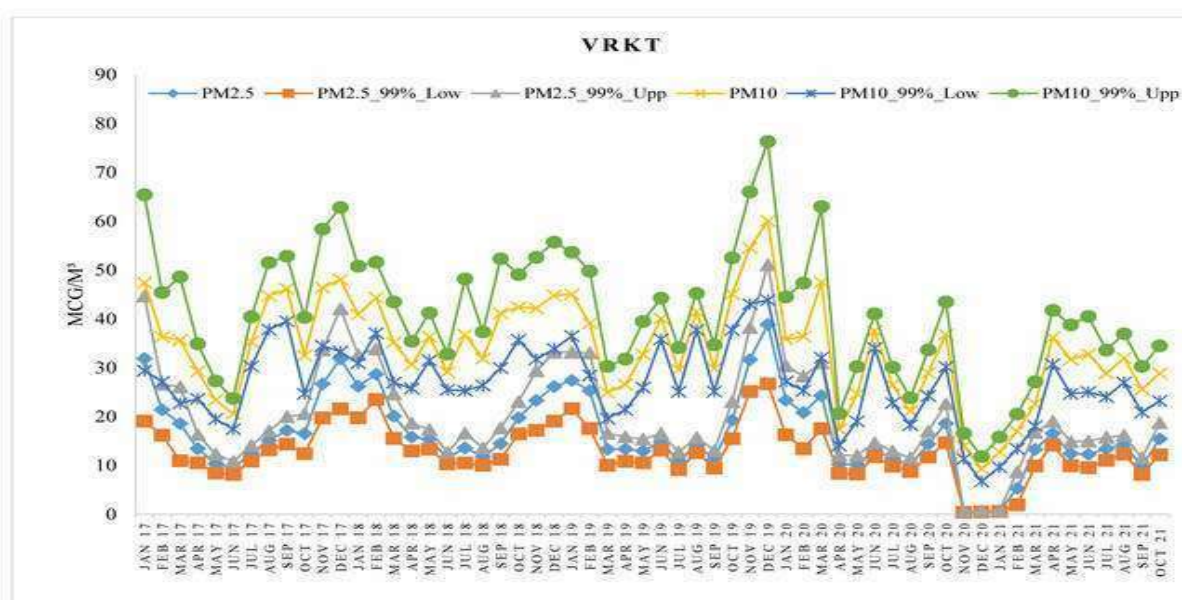
Fig. 3. Monthly mean values of PM2.5 and PM10 and their 99% confidence intervals
in Varketili from January 2017 to October 2021.

In fig. 1-3 data about monthly mean values of PM2.5 and PM10 and their 99% confidence intervals
on the three points of measurements in Tbilisi sity from January 2017 to October 2021 are presented.

As follows from these figures, the intra-annual distribution of aerosol pollution of the atmosphere in
Tbilisi as a whole is wave-like - an increase in the cold half-year, a decrease in the warm season of the year.

Table 1. Statistical characteristics of the monthly mean values of PM2.5 and PM10 at three points of Tbilisi
from January 2017 to October 2021 (mcg/m³).

Location	KZBG	KZBG	TSRT	TSRT	VRKT	VRKT
Parameter	PM2.5	PM10	PM2.5	PM10	PM2.5	PM10
Max	32.7	61.2	43.6	75.5	38.9	60.1
Min	0.3	11.3	0.8	5.4	0.5	9.3
Range	32.4	49.9	42.8	70.1	38.4	50.8
Mean	15.0	35.5	20.1	44.8	16.5	34.0
St Dev	6.3	10.0	8.7	15.0	7.8	10.4
Cv, %	42.1	28.1	43.3	33.4	47.6	30.5
	Correlation Matrix (R)					
KZBG, PM2.5	1	0.78	0.92	0.79	0.96	0.87
KZBG, PM10	0.78	1	0.73	0.77	0.70	0.83
TSRT, PM2.5	0.92	0.73	1	0.90	0.93	0.82
TSRT, PM10	0.79	0.77	0.90	1	0.76	0.79
VRKT, PM2.5	0.96	0.70	0.93	0.76	1	0.88
VRKT, PM10	0.87	0.83	0.82	0.79	0.88	1

The statistical characteristics of the monthly mean values of PM2.5 and PM10 for three points of
Tbilisi from January 2017 to October 2021 in table 1 are presented. As it follows from this table and fig. 1-3
the monthly mean values of PM2.5 changes from 0.3 mcg/m³ (KZBG) to 43.6 mcg/m³ (TSRT); the monthly
mean values of PM10 changes from 5.4 mcg/m³ (TSRT) to 75.5 mcg/m³ (TSRT).

The greatest average values of PM2.5 during entire period of observations on the A. Tsereteli av. were observed (20.1mcg/m³), smallest - on A. Kazbegi av. (15.0 mcg/m³). The greatest average values of PM10 during entire period of observations also on. A. Tsereteli av. were observed (44.8 mcg/m³), smallest - in Varketili (34.0mcg/m³).

The annual mean of PM2.5 and PM10 for all of measurements points are higher, that maximum permissible concentration according to the standards of the World Health Organization.

The values of the linear correlation coefficient between the mean monthly values of PM2.5 and PM10 on all points changes from 0.70 to 0.96 (table 1).

In connection with the pandemic of coronavirus COVID-19 in Georgia were introduced the limitations in the movement of different type of transport in different time periods from March 2020 to August 2021.

The preliminary studies of the influence of these limitations on the daily and monthly content of PM2.5 and PM10 in Tbilisi in the spring 2020 are given to [10,11].

Data about influence of the various limitation on the movement of transport in Georgia from March 2020 to August 2021 in connection with the pandemic of coronavirus COVID-19 to the mean values of PM2.5 and PM10 in this period of time are presented below.

Table 2 presents the data about changeability of mean values of PM2.5 and PM10 at three points of Tbilisi city in three periods of time. I. March 2017-August 2018, first pre-pandemic period; II. March 2018 - August 2019, second pre-pandemic period; III. March 2020 - August 2021, period with pandemic.

Table 2. Changeability of mean values of PM2.5 and PM10 at three points of Tbilisi city in three periods of time, mcg/m³

Location	KZBG	KZBG	TSRT	TSRT	VRKT	VRKT
Parameter	PM2.5	PM10	PM2.5	PM10	PM2.5	PM10
I. Mean (Mar 2017-Aug 2018)	15.8	39.0	23.0	54.3	17.5	35.9
II. Mean (Mar 2018 - Aug 2019)	15.5	39.2	21.5	49.0	16.9	36.1
III. Mean (Mar 2020 - Aug 2021)	10.9	29.0	12.8	30.9	11.2	26.5
Differ. (II-I)	No sign					
Differ. (III-II), α≤0.01	-4.6	-10.2	-8.7	-18.1	-5.7	-9.6
Differ. (III-I), α≤0.01	-4.8	-10.0	-10.2	-23.3	-6.3	-9.4

As it follows from table 2, in the second period of time, as compared with the first, the average values of PM2.5 and PM10 did not change at any of the measurement points. In the third time period (the period of the pandemic), as compared to the first and the second, a decrease in the mean values of PM2.5 and PM10 at the all measurement points are noted.

In particular, it comprises this decrease: PM2.5 - from 4.6÷4.6 mcg/m³ (KZBG) to 8.7÷10.2 mcg/m³ (TSRT); PM10 - from 9.4÷9.6 mcg/m³ (VRKT) to 18.1÷23.3 mcg/m³ (TSRT).

Conclusion

Over the long term is planned the more detailed study of the aerosol pollution of the atmosphere, in particular, conducting the statistical analysis of monthly, daily, day and night variations in the values of PM2.5 and PM10 for Tbilisi and other cities of Georgia.

References

1. Kirkitadze D., Nikiforov G., Chankvetadze A., Chkhaidze G. Some Results of Studies of Atmospheric Aerosols in M. Nodia Institute of Geophysics in the Recent Three Decades. // Trans. of Mikheil Nodia Institute of Geophysics, ISSN 1512-1135, vol. 66, Tbilisi, 2016, pp. 178-185, (in Russian).
2. Amiranashvili A., Bliadze T., Chikhladze V. Photochemical smog in Tbilisi. // Monograph, Trans. of Mikheil Nodia institute of Geophysics, ISSN 1512-1135, vol. 63, Tbilisi, 2012, 160 p., (in Georgian).
3. Amiranashvili A., Chargazia Kh. Intra-Annual and Seasonal Variations of Sub-Micron Aerosols Concentration and their Connection with Radon Content in Surface Boundary Layer of Tbilisi City. // Bulletin of the Georgian National Academy of Sciences, vol. 10, N 2, 2016, p. 72-78.
4. Bliadze T.G., Kirkitadze D.D., Tchankvetadze A. Sh., Chikhladze V.A. Comparative Analysis of Air Pollution in Tbilisi and Kutaisi. // Int. Sc. Conf. „Modern Problems of Ecology", Proceedings, ISSN 1512-1976, v. 6, Kutaisi, Georgia, 21-22 September, 2018, pp. 157-160.
5. Stankevich A.S., Titarenko O.V., Amiranashvili A.G., Chargazia Kh. Z. Determination of Distribution of Ozone Content in Lower Troposphere and Atmospheric Aerosol Optical Thickness over Territory of Georgia Using Satellite Data and Ground Truth Measurements. // Journal of the Georgian Geophysical Society, Issue (B). Physics of Atmosphere, Ocean, and Space Plasma, ISSN: 1512-1127, v.17b, 2014, pp. 26-37.
6. Stankevich S., Titarenko O., Amiranashvili A., Chargazia Kh. Determination of Atmospheric Aerosol Optical Depth over Territory of Georgia during Different Regimes of Cloudiness Using the Satellite and Ground-Based Measurements Data. // Bulletin of the Georgian National Academy of sciences, v. 9, No. 3, 2015, pp. 91-95.
7. Amiranashvili A.G., Chikhladze V.A., Mitin M.N. Preliminary Results of the Analysis of Radar and Ground-Based Monitoring of Dust Formation in Atmosphere Above the Territory of Eastern Georgia on 27 July 2018. // Journal of the Georgian Geophysical Society, ISSN: 1512-1127, Physics of Solid Earth, Atmosphere, Ocean and Space Plasma, v. 21(2), Tbilisi, 2018, pp. 61-69.
8. Kirkitadze D.D. Statistical Characteristics of Aerosol Pollution of Atmosphere in Three Points of Tbilisi in 2017-2018. // Journal of the Georgian Geophysical Society, ISSN: 1512-1127, Physics of Solid Earth, Atmosphere, Ocean and Space Plasma, v. 22(2), 2019, pp. 55 – 62.
9. Lagidze L., Matchavariani L., Svanadze D., Khomasuridze G. Influence of Meteorological Factors on Ecological Conditions of the Atmosphere in Tbilisi, Georgia. // J. Environ. Biol., 41, 2020, pp. 391-395.
10. Amiranashvili A.G., Kirkitadze D.D., Kekenadze E.N. Pandemic of Coronavirus COVID-19 and Air Pollution in Tbilisi in Spring 2020. // Journal of the Georgian Geophysical Society, ISSN: 1512-1127, Physics of Solid Earth, Atmosphere, Ocean and Space Plasma, v. 23(1), 2020, pp. 57-72.
11. Kirkitadze D. Variability of Monthly Mean Values of PM2.5 and PM10 in Three Points of Tbilisi from January 2017 to May 2020. Pandemic of Coronavirus Covid-19 and PM2.5/10 in Spring 2020 in Tbilisi. // International Scientific Conference „Modern Problems of Ecology", Proceedings, ISSN 1512-1976, v. 7, Tbilisi-Telavi, Georgia, 26-28 September, 2020, pp. 268-272.
12. WHO Air quality guidelines for particulate matter, ozone, nitrogen dioxide and sulfur dioxide. Global update 2005 Summary of risk assessment. // World Health Organization, 2006, 22 p., http://apps.who.int/iris/bitstream/handle/10665/69477/WHO_SDE_PHE_OEH_06.02_eng.pdf;jsessionid=48F380E7090ADBB4A166AC7A8610624A?sequence=1

ECOLOGICAL ASSESSMENT OF TCHITCHAKHVI KHEVI RIVER

Margalitashvili D., Davitashvili M., Berdzenishvili N., Aleksidze M.

Iakob Gogebashvili Telavi State University, 1, Kartuli Universiteti str., Telavi, 2200, Georgia
nanaka.berdzenishvili@yahoo.com

Summary: *The article discusses the assessment of the ecological condition of the Tchitchakhvi Khevi River and its surroundings. Chemical and microbiological research of river water has been carried out. Water samples were taken for analysis in compliance with the requirements of normative documents. The results of the study showed that the degree of pollution of the river is affected by settlements, agricultural lands, faulty sewage system. The microbiological contamination at the site we have studied as a whole can be assessed as, so far, epidemiologically safe, i.e. moderately contaminated, which can be explained at the expense of river self-cleaning.*

Key Words: *Pollution, river self-cleaning, microbiological contamination, anthropogenic, ecosystem.*

Introduction: Water is one of the most important factors in the formation of the physical and chemical environment, climate, weather, as well as the maintenance of life on Earth. Water pollution is a significant environmental problem. As a result of anthropogenic impacts, various biogenic or toxic compounds discharged into reservoirs disrupt the balance in the ecosystem, resulting in a decline or complete loss of its self-cleaning ability [1, 2].

Water shortage is not felt in Georgia yet, the main problem in Georgia is that water is polluted from more than 4/5 of industrial enterprises (metallurgy, oil refining, coal mining, chemistry, energy production). Utility companies also emit a significant amount of toxic substances. The main cause of pollution is often the malfunction of water filters and cleaning products [3, 4, 5].

The aim of our research was to study the ecochemical and microbiological condition of one of the rivers of Eastern Georgia, Tchitchakhvi Khevi and the influence of anthropogenic factors on it.

The subject of research is the left tributary of the Stori River - Tchitchakhvi Khevi. The Stori River originates on the south slope of Mount Didgverdi, at 2,950 m above sea level and merges with the Alazani River at Saniore village. The main tributaries of the River are the Usakhelo River (total length: 14 km) and the Tchitchakhvi Khevi (20 km, basin area – 92 km2 , width of flow – 5-10 m, flow depth – 0.4-0.7 m, flow rate – 1.3-1.6 m/sec, average height of the basin – 2,136 m, overall drop – 2,175 m). We have selected the river Chichakhvi khevi valley as the object of research in the sense that agriculture, livestock and viticulture are well developed in the surrounding villages (Sanyore, Pshaveli, Jughaani, Artana) [6, 9].

Research methods: We conducted the research in accordance with the normative documents (general requirements for water sampling LHG, №26.2014.01.03)We took surface samples at a depth of 10-15 cm from the water surface. If it was necessary to take the sample at the bottom, we would take it at a height of 30-50 cm from the bottom. We took water samples superficially in the bathing areas. In those reservoirs with a depth of not less than 0.5 m, samples were taken with a sterile batometer and sterile vessels. When taking several samples with one batometer. Before taking each sample, we sterilized it using flambio. We opened the container just before taking the sample (we opened the paper lid or the bottle from the vials with the stopper so as not to touch the throat of the container and the stopper by hand). After filling, we closed the container with a sterile stopper. When examining indicator microorganisms, we received - 500 ml. In the study of indicator and pathogenic microorganisms in water - 2500 ml [7, 8, 10].

We studied the chemical and microbiological pollution of the Chichakhvi khevi River. The river Chichakhvi khevi is used for swimming, irrigation and drinking of cattle. It is polluted by domestic sewage, industrial

water. The ecological condition of the river is also affected by pesticides and fertilizers used in agriculture. We conducted chemical studies on organoleptic properties, pH, precipitated substances and other typical contaminants. See also BOD and COD. The survey data are presented in table 1.

Table 1. 2019 data of chemical analysis of Chichakhvi khevi river water

Physico-chemical parameters of water	Location – village Saniore	
	Spring	Summer
Smell	0	0
Color	12	19
Transparency	7,6	8
Ph	8,2	7,8
BOD mg/l	2,3	1,3
COD mg/l	2,1	1,9
Dissolved oxygen mg/l	8,4	8,6
Compressed partikles mg/l	61	58

Our further experiments were directed at studying the effects of pesticides on the water system. Due to the fact that the river Chichakhvi khevi flows into areas rich in gardens and vineyards, it is possible to contaminate it with pesticides and fertilizers. Since Chichakhvi khevi is used by the population for irrigation of agricultural lands, we considered it important to determine the change of pesticides in the river water.

Table 2. Microbiological contamination and pesticides of Chichakhvi khevi
water content analysis 2019 data

place of sampling	Name of microorganisms					
	Total number of microbes		Coli index E. coli		Pathogenic microorganisms Solmonella	
	spring	summer	spring	summer	spring	summer
village Artana	$4,5 \times 10^3$	$6,7 \times 10^3$	22×10^3	30×10^3	Did not turn out	Did not turn out
	Name and content of pesticides					
	Karate		Icon		Samurai	
	spring	summer	spring	summer	spring	summer
	0,0031	0,0041	0,0029	0,0031	0,0031	0,0037

Based on the results obtained, we can conclude that the microbiological contamination at the site we studied can be assessed as generally epidemiologically safe, ie moderately contaminated, which can be explained at the expense of self-cleaning. The village of Saniore has an open copper quarry, so the number of karate and

icons has increased. Added to this is the excessive consumption of pesticides by the population, so their amount in river water is also increased.

Conclusion: Thus, the population of the village of Saniore near the gorge of the river Chichakhvi khevi (where mainly viticulture and horticulture is developed) mainly uses pesticides and fertilizers to fight pests and increase yields, without adhering to any norms, which leads to the accumulation of pesticides in the water. Therefore, we believe that it is necessary not only to monitor water, but also to raise public awareness about the issues that pesticides accumulate in the soil and at the bottom of the river with some violation of their regulation, leading to their involvement in the food chain of living systems. In addition, pesticides and fertilizers accumulate in the vegetative parts and fruits of the plant. As for the pesticides we have chosen - karate, icon and samurai, they cause gastrointestinal pathologies and poisoning in humans. It is therefore of great importance to adhere strictly to the norms when using these pesticides.

References

1. Supatashvili G. Ecochemistry of the environment. // TSU Publishing House, Tbilisi, 2011, p. 187.

2. Kereselidze Z. Biology of seas and freshwaters. // TSU Publisher, Tbilisi, 2003, pp. 202.

3. Jikia G., Museliani T., Petriashvili E. Study of the action of pesticides on a living organism on the example of the river Lopota. // Experimental and Clinical Medicine, Vol. 4, Tbilisi, 2015, pp. 82-86.

4. Jikia, G. Study of the influence of microbiological and anthropogenic stressors on the Alazani River on the example of the fish urchin and its ecotoxicological assessment. // Dissertation for the degree of Doctor of Biology, 2017.

5. Брагинский А. П., Сидоренко Л. А. Всесторонний анализ токсикологической опасности поверхностно-активных веществ для гидробионитов. // Гидробиологический журнал, 23(39), 2003, стр.115-1174.

6. Киричук Г. Е. Особенности накопления ионов тяжелых металлов в организме двустворчатых моллюсков. // Гидробиологический журнал, 3(39), 2003, стр. 45-55.

7. Моисеенко Т. И. Концепция биологической оценки качества вод. Экотоксикологический подход. // Вода: экология и технология, Экватек, М., 2002, стр. 80.

8. Никаноров А.М., Хоружая Т. А., Бражникова Л. В., Жулидов А. В. Мониторинг качества поверхностных вод: оценка токсичности. // Серия «Качество вод», Гидрометеоиздат, Санкт-петербург, 2000.

9. Романенко В. Д., Вернадский В. И. Учение о природных водах и его роль в развитии современной гидроэкологии. // Гидробиологический журнал, 3 (39), 2003, стр. 3-10.

10. Guler C., Thyne G. D., McCray J. E., Turner A. K. Evaluation of graphical and multivariate statistical methods for classification of water chemistry data. // Hydrogeology Journal, 10, 2002, pp. 455-474.

FOR THE METHODOLOGY OF ENVIRONMENTAL MONITORING AND EXPERTISE IN ENVIRONMENTAL POLLUTION

Matsaberidze M., Janelidze I.

Georgian Technical University, Tbilisi, Georgia
i.janelidze@gtu.ge

Summary: *Environmental pollution is called the appearance in it of new, uncharacteristic agents that have a negative impact on its processes and on the vital activity of organisms associated with it. Air pollution is one of the most dangerous in the biosphere, since the atmospheric air, due to its low density, is capable of dispersing toxic substances over long distances. The growth of atmospheric pollution in the last century is the result of a complex of environmental factors. First of all, these are factors of natural origin. Among them, the leading role is played by volcanic activity, vital activity of organisms, wind erosion, precipitation and fires. The factors of technogenic origin include the development of energy and metallurgy, transport, burning of fossil fuels, production and use of fertilizers, extraction and processing of oil and gas, chemical synthesis, radioactive emissions, as well as industrial accidents and disasters. The presented data are related to the methodologies of monitoring and disaster risk reduction and is the main purpose of the article.*

Key Words: *Sendai Framework; chemical, physical, mechanical and biological pollutants; vibration; light pollution; thermal pollution; electromagnetic pollution; Nuclear pollution; mechanical air pollutants; aerosols; biological air pollutants;*

Introduction. The consistency of the Sendai Framework and the Sustainable Development Goals targets creates conditions for the development of minimum standards and metadata for the collection of disaster-related data for disaster risk reduction. As is known, on 2 February 2017, by adopting resolution A / RES / 71/276, the United Nations General Assembly approved the report of the Open-ended Intergovernmental Working Group of Experts on Indicators and Vocabulary for Disaster Risk Reduction (IEWG) (A / 71/644). This work is presented to facilitate the development of a methodology for quantifying indicators and processing statistics for the Sendai Framework [1].

About methodologies. The term "pollutant" means any material agent of chemical, physical or biological nature that enters the environment as a result of natural or man-made processes and has a negative impact on it. In the monitoring system, it is accepted to divide all environmental pollutants, depending on their nature, into 4 groups: chemical, physical, mechanical and biological. Chemical pollutants in the air are various elements and substances that have a negative effect on atmospheric processes and on the vital activity of organisms associated with it. For example, toxic gases - NH_3, CO, SO_2, H_2S, etc.

Physical air pollutants mean various energetic phenomena and processes that change the basic physical constant atmospheres and have a negative impact on the vital activity of organisms. For example, noise, vibration, electromagnetic radiation, etc.

Biological air pollutants are pathogenic (pathogenic) organisms that can be transmitted through the atmospheric air to humans, animals and plants and cause their mass diseases. For example, pathogens of influenza, acute respiratory infections, tuberculosis, etc. The most important chemical pollutants of the atmosphere include various gases: Carbon dioxide CO_2, Carbon monoxide CO, Methane CH_4, hydrocarbons C_xH_x, Sulfur oxide IV SO_2, Hydrogen sulfide H_2S, Nitric oxide II NO, Nitric oxide IV NO_2, Ozone O_3, Chlorine Cl_2, Hydrogen fluoride and other hydrogen halides HF, HCl, HBr, HI. The group of chemical air pollutants also includes some metals: Mercury, Lead, Manganese, Copper, Zinc, Nickel, Cadmium - particles of which are capable of dispersing through the air. The most important forms of physical pollution of the atmosphere include: Noise pollution - excess of the natural and established noise level, i.e. the pressure of

the sound wave. Living organisms have physiological limits for their sensitivity to noise. At a high level of noise in a person, the function of the auditory analyzer is disrupted, irritability occurs, sleep disturbances, nervous diseases develop, and the biochemical composition of the blood changes. Prolonged exposure to noise levels of 90-100 dB can lead to complete loss of hearing. Noise pollution has many natural and man-made sources. For example, road transport increases the natural noise level by up to 85 dB; railway transport up to 100 dB; air transport up to 110 dB; heavy industry enterprises 120 dB; gas turbine units 140 dB, etc. Vibration is a complex oscillatory process resulting from the transfer of alternating pressure (energy fluctuations) from any mechanical source. Vibration, like noise, is measured in decibels (dB).

Numerous natural and man-made processes can be a source of vibration - earthquakes, volcanic eruptions, transport, industrial activities, etc. Long-term exposure to vibration on the human or animal organism causes vibration disease. At the same time, irritability, sleep disturbance, memory disturbance, arrhythmia develop.

Vibration is also extremely dangerous for buildings and various mechanisms. Light pollution is a violation of natural illumination of the area as a result of exposure to artificial light sources. Light pollution is most typical for large settlements, as well as for areas with a developed industrial and transport network (road and railways, airports, etc.). Long-term light pollution can lead to serious disruption of the vital processes of plants and animals - behavior, sleep, photosynthesis, etc. Ultraviolet radiation is a type of light pollution that occurs due to an increase in the level of ultraviolet rays in the environment. UV rays have a wavelength in the range of 400 to 10nm.

The sun is a natural source of ultraviolet radiation in the atmosphere, and various installations used in industry, medicine, and everyday life are man-made. Compared to infrared and visible rays, UV rays have the greatest amount of energy, which makes them dangerous for living organisms. Particularly dangerous is short-wave (hard) ultraviolet light, which, with short-term exposure, causes burns of the surface integuments, and with longer exposure, serious tissue damage, destruction of the genetic material of cells and the death of organisms. Hard ultraviolet light is almost completely absorbed by the ozone screen of the atmosphere. In addition to ozone, water and any mechanical shelter are natural protection against UV rays.

Thermal pollution is a violation of the natural temperature regime of the area due to the influx of streams of heated or cooled air. Thermal pollution of the atmosphere can be primary when heat flows from various natural or man-made processes directly change the air temperature. The negative consequences of thermal pollution include a change in the migration flows of elements in the air, a violation of the physiological rhythms of plants and animals, damage to mechanisms, etc.

Electromagnetic pollution is a violation of the electromagnetic properties of the environment. The electromagnetic background of the environment can change due to natural processes (for example, with a change in solar activity), as well as technogenic reasons. Any electrical appliance, from household equipment to powerful industrial installations, can become a source of electromagnetic rays. High-voltage power lines, television and radio towers, high-voltage generators, and military installations make a special contribution to the violation of the electromagnetic background.

The norms of the electromagnetic flux, determined through the power of its field, are: for power lines up to 30mW/cm2, military facilities up to 10mW / cm2, airport communication lines up to 1mW / cm2, for residential premises less than 1mW/cm2. With prolonged exposure to electromagnetic fields, a person develops chronic fatigue, headaches, memory impairment, and drowsiness. Electromagnetic rays lead to changes in the fine cellular and molecular structures of the body, which can cause various diseases. Electromagnetic pollution is associated with a malfunction of electronic systems, interference in the transmission of information.

Radioactive contamination - excess of the natural level of radioactive substances in the natural environment. The radioactive substance is represented by unstable isotopes of individual elements, which act as a source of hard ionizing radiation. The most common radioisotopes include Strontium-90, Cesium-137, Cerium-141, Iodine-131, Ruthenium-106, Plutonium-239, and a number of others. The source of radioisotopes entering the air is man-made processes - the development and enrichment of radioactive ores, testing of nuclear weapons, accidents at nuclear power plants, leaks from burial sites of radio waste, etc.

The group of mechanical atmospheric pollutants includes dust and aerosols. There are the following types of dust: 1.Fine dust - particle size is less than 0.001 microns. Able to stay in the air for a long time.

2.Semi-fine dust - particle size is from 0.001 to 2.5 microns. Has a higher rate of settling on substrates compared to fine dust. 3. Coarse dust - represented by heavy, inactive particles with a diameter of more than 2.5 microns. It quickly settles and becomes the cause of secondary pollution of the environment. Aerosols are represented by water particles suspended in the air. The average size of atmospheric aerosols is from 0.001 to 10 microns. Numerous natural and man-made processes act as a source of dust and aerosols entering the atmosphere. These are dust storms, volcanic eruptions, sea spray, fires, mining, agricultural and industrial activities, transport, household waste, etc. Dust and aerosols can seriously disrupt a number of important atmospheric processes. These include an increase in the albedo (ie, reflectivity) of the atmosphere, resulting in less solar radiation reaching the surface of the earth and ocean; reduced visibility of the atmosphere; secondary pollution due to subsidence of surface substrates; violation of the processes of photosynthesis and respiration of organisms; damage to mechanisms; reduction of aesthetic parameters of the environment, etc.

The group of biological air pollutants includes various pathogenic organisms. By etiology, they are divided into: causative agents of viral diseases - influenza, smallpox; causative agents of diseases of a bacterial nature - tonsillitis, acute respiratory infections, tuberculosis; pathogens and vectors of diseases of a eukaryotic nature - mosquitoes, horseflies, midges, biting midges, gadflies, allergenic plant pollen (ragweed), etc.

Modern methods for assessing the ecological state of the air environment are subdivided into remote (aerospace) and ground-based. According to the scope of research, global (biospheric), national, regional and local monitoring of the atmosphere are distinguished.

Local monitoring of the air environment can be divided into the following areas: monitoring of the most important climatic elements and phenomena; monitoring of the state of the surface air layer, carried out by bioindication methods; monitoring of the state of the surface air layer, carried out by physicochemical methods; mathematical modeling and forecasting of the state of the most important components of the air environment. Monitoring of soil and land pollution. Monitoring of soils and lands is aimed at assessing their condition as the most important resource of the environment and identifying their qualitative and quantitative pollution.

All the most important soil pollutants, depending on their nature, can be divided into chemical, physical, mechanical and biological. Chemical elements according to the degree of danger to soils are divided into three classes: 1. Highly hazardous - As, Cd, Hg, Se, Pb, Zn, F; 2. Moderately hazardous - B, Co, Ni, Mo, Cu, Sb, Cr; 3.Low hazardous - Ba, V, W, Be, Mn, Sr. In soils, gross and mobile forms of chemical elements and their compounds are distinguished. Gross forms are in the composition of chemical compounds and the organic part of the soil, are inactive.

The mobile forms include acid-soluble chemical elements, which make up 50% of the total, and acetate-ammonium soluble elements. These are, first of all, Ni, Cr, Mn, Co, Pb, Cu, Zn, Cd, etc. Assessment of the degree of soil contamination is carried out by the multiplicity of the excess of the content of elements in comparison with the clarkes[1] of substances or with their maximum permissible concentrations (MPC).

The main difficulties arise at the stage of interpreting the actual data on the content of elements and comparing them with a criterion (clarke or MPC). One of the generally accepted classifications of soil contamination looks like this: slightly contaminated soils have a 2–10-fold excess of the clarke; moderately contaminated - 10-30 excess; heavily contaminated - exceeding more than 30 clarkes.

In official documents, the level of soil contamination with gross forms of chemical elements is recommended to be calculated by exceeding the clarke in different multiplicity: copper by 3 times, nickel - 3 times, manganese - 2 times, cobalt - 50 times, zinc - up to 500 times. Physical pollutants of soils and lands. Among the most important physical soil pollutants are noise, vibration and radioactive radiation. Noise pollution - excess of the natural and established noise level, i.e. the pressure of the sound wave. Long-term noise pollution negatively affects the soil biota, which ultimately can become one of the reasons for the degradation of the soil layer. Noise pollution has many natural and man-made sources.

The most important are railway and road transport, production processes and household noise. Vibration is a complex oscillatory process resulting from the transfer of alternating pressure (energy

---

[1] numbers expressing the average content of chemical elements in the earth's crust, hydrosphere, Earth, space bodies, geochemical or cosmochemical systems in relation to the total mass of this system.

fluctuations) from any mechanical source. Numerous natural and man-made processes can be a source of vibration - earthquakes, volcanic eruptions, transport, industrial activity, etc. Long-term exposure to vibration on the soil cover and underlying rocks adversely affects their condition.

Radioactive contamination - excess of the natural level of radioactive substances in the natural environment. The most dangerous radionuclides entering the soil include strontium-90, cesium-137, cerium-144, yttrium-91, ruthenium-106, niobium-95, plutonium-239 and others. The source of radionuclides entering the soil cover is mainly technogenic processes - the development and enrichment of radioactive ores, nuclear weapons tests, accidents at nuclear power plants, leaks from radio waste burial sites, etc.

Mechanical pollutants of soils and lands. Soils are characterized by the widest range of mechanical pollutants in comparison with other geological environments. The surface of soils and lands is subject to constant pollution with coarse dust. The soil cover is able to accumulate the remains of metal, plastic, glass, rubber, building materials, etc. The main sources of mechanical pollutants are waste from large industrial enterprises, household and industrial waste, agricultural waste.

Biological pollutants of soils and lands. This group of pollutants is also very diverse. By etiology, they are divided into: causative agents of viral diseases - smallpox, HFRS; pathogens of bacterial diseases - tetanus, diphtheria, whooping cough, tuberculosis, anthrax, hepatitis, pathogenic forms of E. coli, etc. pathogens and carriers of diseases of a eukaryotic nature - eggs and larvae of many helminths - echinococcus, hepatic fluke, etc.

Monitoring the state of the aquatic environment. Water plays an extremely important role in all major natural processes. With its high mobility, water penetrates into the most diverse parts of the biosphere. It is in the form of clouds and vapor in the lower layers of the atmosphere, forms seas, oceans and fresh water bodies, forms high-mountain glaciers and powerful ice sheets in the polar zones of the planet. In the process of moisture circulation, atmospheric precipitation penetrates into the sedimentary rocks and forms groundwater. Pollution of natural water bodies can be divided into four types: chemical, physical, mechanical and biological.

Mechanical pollutants include various industrial, agricultural and household waste, partially or completely insoluble in water and not decomposing in soil - plastics, artificial polymers, rubber products, insoluble copper, lead, zinc, etc.

Chemical pollutants include substances of inorganic and organic nature that are widely used in energy, industry, agriculture, medicine and during the operation of military facilities, used as transport fuel. These include metals and their compounds, petroleum products, pesticides, hydrocarbons and others. To date, chemical pollution is the largest and most dangerous type of pollution in the hydrosphere. Physical contaminants include, first of all, sources of radioactive isotopes (^{137}Cs, ^{90}Sr, ^{91}It, ^{95}Nb, ^{131}I, ^{106}Ru, ^{239}Pu etc.), as well as thermal pollution, man-made noise, etc.

The oceans act as an environment that accumulates radioactive waste entering the atmosphere and soil. Water cenoses have the ability to accumulate radioactive isotopes and transfer them in food chains. Thermal pollution is a change in the natural temperature regime of a reservoir due to the release of heat into the environment. Thermal pollution is a type of physical pollution of the hydrosphere and can be caused by natural processes or man-made causes.

References

1. Sendai Framework for Disaster Risk Reduction 2015-2030. UNISDR / GE / 2015 - ICLUX EN5000 1st edition. https://www.preventionweb.net/files/43291_sendaiframeworkfordrren.pdf

ON THE DEVELOPMENT OF A DICTIONARY-REFERENCE BOOK OF TERMS AND DEFINITIONS OF THE FUNDAMENTALS OF ECOLOGY

Gunia G.

Institute of Hydrometeorology of Georgian Technical University, Tbilisi, Georgia
garrygunia@yahoo.com

Summary: *The modern process of development of ecology as a science dictates the need for a comprehensive study of the laws of interaction between the natural environment and human society, as well as the Ecologization of teaching a number of scientific disciplines. This will largely be facilitated by the development of a Georgian-language dictionary of unified terms and definitions of the fundamentals of Ecology, which will be useful for improving the process of teaching and learning the fundamentals of Ecology. With this aim, the first attempt to develop such kind dictionary-reference book is in progress and close to finalization at the Institute of Hydrometeorology of the GTU.*

Key words: *ecological education, dictionary-reference book.*

Introduction.

Recently, a number of academic disciplines have appeared in higher educational institutions, such as, for example, "Chemical Ecology", "Engineering Ecology", "Construction Ecology", etc. Analysis of the content of these new disciplines shows that they often only touch on certain aspects of the environment protection and nature management, while the whole content is far from the discipline of Ecology. Therefore, we believe that we should be more careful when applying the term "Ecology" and its derivatives. Otherwise, there is a conditional terminological substitution, which generally prevents the formation of Ecology as an educational discipline. In our view, any terminological substitution leads to chaos in the study of the most complex process of interaction between society and nature. Therefore, we consider inadmissible the incorrect use of the term "Ecology" and its derivatives. The elaboration of the "Dictionary-Reference Book of the Terms and Definitions of the Fundamentals of Ecology" will significantly help to eliminate these shortcomings.

Term "Ecology"

Nowadays, the term "Ecology" has many meanings [1], and is used to denote the science that studies:

- The organization and functioning of various levels of superorganisms, including: systems, populations, species, biogeocenoses, ecosystems and the biosphere as a whole;
- Joint development of people, human families as a whole and the natural environment;
- Ways to overcome the global environmental crisis.

Basic theoretical conceptions of ecology - ecosystem, population, ecological niche, relationships of organisms within population, family, ecosystems - were developed in the first half of the XX century. The studies of human impact on populations and ecosystems were developed in the second half of the XX century. During this period, people's attitudes towards the dangers of the ecological crisis have been significantly increased due to the following reasons: unregulated population growth, progressive environmental pollution, depletion of mineral and fossil energy resources, reduction of biodiversity, soil degradation and development of global biosphere processes, strengthening of greenhouse effects and ozone depletion. Thus, ecology - the science of the life of nature - experiences the second life.

Formulated more than 100 years ago as the doctrine of the relationship between the organism and the environment, we have witnessed the transformation of ecology into a science about the structure of nature, science of how the biosphere the earth as a whole work. Individual properties of the environment or

its elements are called factors, while environmental factors that act on living organisms are called ecological factors. Their diversity is divided into two major groups - abiotic and biotic (Table 1) [2].

Table 1. Classification of ecological factors.

Ecological factors	
Abiotic	Biotic
Light, temperature, humidity, wind, air,	Influence of plants on other members of
Mechanical composition of soil, its penetration,	Influence of animals on other members of the
Content of nutrients in soil or water, gaseous	Anthropogenic factors caused by human activity

Since the development of the living world is increasingly driven by human activity, highly progressive scientists see the future of ecology in the theory of the creation of a transformed world. Nowadaus,Ecology takes the form of a theoretical basis of behavior of a human, who is a representative of industrial society, in the natural environment.

Ecological Load of the Environment.

One of the most important problems of modernity is the protection of the natural environment from the results of the ecological load caused by anthropogenic influences. According to many estimates, this negative impact is assuming dangerous proportions; therefore, it is necessary to develop programs for the effective management of the ecological state of the environment. The development of these programs requires a lot of information about the research, assessment and forecasting of a given situation. At the same time, we consider the Earth as a global system of life activity and we study all possible options for managing this system. The solution to modern ecological problems is related to: processes of economic development, population growth, and the fight against poverty.

The problems of preventing an ecological catastrophe and achieving sustainable development in their scale outweigh all the problems that humanity has faced in the process of its development. Never before has there been such a huge gap between the scale of the problem and our ability to solve it.

It is known that the atmosphere and hydrosphere are the main routes for the circulation of substances in the natural environment, while the transfer of harmful substances into the environment is conditioned by hydrometeorological processes. Therefore, it is necessary to perform the monitoring, forecasting and management of the environmental load caused by anthropogenic impacts by considering the principles of hydrometeorological processes [1].

At present, it is difficult to imagine a large industrial area or city that does not take measures to protect the environment. Already nobody doubts anymore, that ecological monitoring of the natural environment - regular, long-term observations in time and space of the state of the natural environment and the phenomena occurring in it, as well as assessment and forecast of the state of the natural environment - is one of the main integral parts of an organized human life. At the same time, in the monitoring process, it is of great importance to register meteorological conditions, which have a significant impact on the speed and direction of air mass transfer. Because of this, the concentration, nature and behavior of impurities do not remain the same. Their integral characteristics in the atmospheric column and their geographical distribution in the environment also change significantly.

As it is stated in the monographs [1, 2], ecological monitoring is carried out in a complex way. It is carried out through the elaboration of scientific-research and practical issues in various fields.

In addition, it should be noted, that the solution of issues related to the ecological problems of global climate change, including desertification requires the attention of a wide range of environmental scientists. The latter process under extreme conditions can lead to a complete disruption of a biosphere and desertification, as a result of fluctuations in the restorative properties of the ecosystem.

In the beginning of the XXI century, the area of anthropogenic deserts ranges from 10 to 13 million km^2, and not less than 30 million km^2 of lands are at risk of desertification. As a result, the mass productivity of the planet has decreased by 1/3 compared to the previous period.

Table 2 shows the coefficients of anthropogenic load and the share of surviving natural areas, calculated for various countries [4].

Table 2. The coefficient of anthropogenic load and share of surviving natural areas in %

Country	Coefficient of anthropogenic	Share of natural areas,%
Netherlands	42	0
Germany	19	0
Japan	16	0
USA	3.4	4
The Republic of Korea	4	0
Mexico	1.2	2
China	1.1	20
India	1	1
Russia	0.7	45
Canada	0.4	65
Brasil	0.2	28
Algeria	0.2	64
Australia	0.2	33
The whole earth	1	39

Anthropogenic load ratios are obtained as a ratio of the energy capacity coming per unit area of the country to the average global energy capacity coming per unit area. As the table shows, on average, the territory of Europe is experiencing the greatest anthropogenic load, while the share of protected natural areas in the world is only 39%. If we take into account the process of uncontrolled human population growth - we are not far from the catastrophic decline of natural areas. Despite the fact that humans as a biological species, in terms of its biomass, make up one thousandth of a percent of the living matter of the planet, they produce several thousand times more waste than the entire biosphere of our planet. At the same time, they double every 15 years. As a result of the impact of these exponentially growing flows of household and industrial waste, historically established natural cycles and evolutionarily formed biogenic flows of various substances are seriously disturbed.

In addition to global effects, a number of negative effects of regional factors are often observed. For example, the environmental consequences of the construction and operation of power plants are primarily related to: the adverse impact of reservoirs on the microclimate of the surrounding area, hydrological regime, exclusion of large areas and flooding of fertile lands and forests, deterioration of the state of flora and fauna, etc. As a result, the loss of lowland biotopes in the plains is partially compensated, while in the mountains this loss remains largely irreplaceable. Because of this, the destructive impact of mountain reservoirs on the ecosystems of adjacent territories is extremely pronounced.

According to the performed assessments, this problem is multifaceted and severe in Georgia. Therefore, when assessing the energy efficiency of energy systems (in particular, hydroelectric power plants) required for the country's development, it is crucial to consider the consequences of the environmental impact of these systems on the natural and social environments [2]. Due to the obvious direct manifestations of their negative effects on the state of the natural environment, such elements constituting an environmental hazard as smog and acid rain come to the attention of the public. Attention to these factors of environmental strain is growing in the world. Acid rainfall monitoring programs have been developed in many countries. Nowadays, the problems of climate change and technogenic load on the environment represent not only a scientific, but also an economic and political problem. Any mistakes made in dynamics of the specified phenomena are carriers of the serious economic failures. Vivid example of this are the mistakes made in 50-60-s' years of the XX century in forecasting the decrease of the level of Caspian Sea by 2000. This mistake has resulted in a social and economic tragedy for this big region. Now, the price of

mistakes is much higher. For a number of countries expected climatic change is not only a geopolitical question, but represents an issue of rescuing humanity.

Ways to Successfully Solve the Problem.

Successful solution of the problem under consideration requires a complex approach, which is possible in the presence of a wide range of appropriately trained specialists. For this, first of all, it is necessary to indicate the availability of methodological manuals of uniform environmental terms and definitions corresponding to local conditions. It should be noted that in Georgia the full extent of this situation, its immediate and distant consequences are not fully realized. Moreover, this issue is still completely not studied and requires serious processing. In recent decades, there are broad changes in the content of education. The Ecology as a science is expanding and deepened. The awareness about the need to tackle the problems of human survival in the technosphere is increased. At the same time, the Ecologization of academic disciplines, the laws of the relationship between nature and society, natural - scientific, humanitarian, technical and technological areas dictate the need for comprehensive study. The future specialists should be familiar with issues such as: assessment of the condition, sustainability and development of territorial - natural and agricultural - natural complexes, ecological monitoring, management in the system of nature protection and consumption of natural resources, development of recommendations for the preservation of the natural environment, etc. Thus, solving the above issues, including: the transfer of harmful impurities in the natural environment, monitoring, forecasting, management of these processes, as well as obtaining adequate education in the required volume is difficult without a dictionary - reference book of unified terms and definitions adopted in Meteorology and Ecology. Nowadays, some traditional terms are often given new meanings, while definitions of a number of other terms and concepts can only be found in scientific literature, which often remains inaccessible to a wide range of population. The dictionary - reference book should contain: basic uniform terms adopted in Ecology; definitions of concepts and important reference material for different areas of fundamental and applied ecology, including geophysics and hydrometeorology. The dictionary-reference book should be intended as a manual for students of any specialty, whose education is related to various areas of ecology.

Conclusion.

The elaboration of a Georgian-language dictionary - reference book of the main unified terms adopted in Ecology will make a significant contribution to the sustainable and safe development of the country's economy and thereby it acquires the character of a state importance. Its elaboration and dissemination by print and electronic means will be useful for improving the processes of teaching and learning the basics of Ecology in Georgian higher educational institutions. The dictionary - reference book will also contribute to the successful implementation of the laws of Georgia in the field of Environmental protection and tackling the ecological issues of the country. The dictionary - reference book will also contribute to the successful implementation of the laws of Georgia in the field of Environmental protection and tackling the ecological issues of the country.

References

1. Gunia G.S. Questions of monitoring of atmospheric air pollution on the territory of Georgia. // L.: Gidrometeoizdat, 1985, 85 p.
2. Gunia G. Meteorological aspects of ecological monitoring of the atmosphere. // Tbilisi, Georgian Academy of Sciences, Institute of Gydrometeorology, 2005, 265 p.
3. United Nations Convention to Combat Desertification. // UNCCD, 1996.
4. Kotlyakov V.M., Losev K.S., Suetova I.A. Energy investment in a territory as an environmental indicator. // Izv. RAN Ser. Geogr., 1995. No. 3, pp.70-75.

IMPACT OF EXTREME NATURAL AND ANTHROPOGENIC FACTORS ON THE PHYTOCENOSES SUSTAINABILITY

*Gogebashvili M., *Ivanishvili N., **Salukvadze E., *Kontselidze A.

* *Laboratory of Radiation Safety Problems, I.Beritashvili Center of Experimental Biomedicine*
radiobiologia2020@gmail.com
** *Vakhushti Bagrationi Institute of Geography of Georgia State University of Ivane Javakhishvili*

Summary: *It was studied that defensive effects of an increasing number of radiated plants under high temperature conditions. The research revealed economical ground water consumption by radiated plants. However, the reduced transpiration rate at extreme temperatures does not provide effective surface protection in plant population and causes degradation of individual phytocenotic components. The article also discusses changes in stability parameters in various types of phytocoenosis and examines long-term forecast opportunities for successive processes.*

Keywords – *radiation, high temperature, phytocoenosis*

Introduction.

Phytocenoses of Georgia are featured by the structural characteristics. This, alongside the other factors, is conditioned by the vertical zonality of terrain, which, in turn, creates biodiversity in the composition of phytocenoses, even over small distances. The sustainability of any system, including the ecological system, is a significantly important parameter. The ability of the system to maintain stability during changes in environmental conditions is shaped by sustainability. In the aforementioned provision context, steadiness can be considered as a synonym of vitality. The numerous scientific articles report theoretical foundations of qualitative and quantitative evaluation of complex ecosystems sustainability [1,2,3,4]. Generally, it is shown that the vitality of the system is determined by the three groups of parameters – by volume (weight of system substances), productivity (the self-regeneration speed of system substances), and structural harmony. The parameters of the first two groups, in terms of ecological systems, are well-processed in classical biogeography, while the structural harmony of ecosystems and, in particular, the peculiarities of anthropogenic impact on it, are relatively less studied. The high-temperature potential of endemic ecosystems provides their maintenance of the initial state during the impact of extreme environmental conditions. Even if a significant portion of their area is lost, sustainable ecosystems continue to ensure that the natural cycle regime remains unchanged. This feature is related to the sustainability parameters that preserve many of the initial properties of ecosystems even after the anthropogenic transformation of their areas. The study of ecosystem stability parameters is important in order to predict the consequences of anthropogenic impact on phytocenosis sustainability, for the development of adequate methods. To solve this task, it is advisable to conduct model studies at the level of individual plant organisms, as well as to conduct monitoring observations on the whole landscape.

Research Object and Methods.

The study object was presented by the phytocenoses of the quarry area of Madneuli (Kazreti, Georgia). The choice was made considering the fact that, for obvious reasons, the phytocenoses present there are characterized by a pronounced anthropogenic load. The surface temperature of plants in phytocenosis was determined by remote laser scanning. Experimental plants grown in vegetation vessels were irradiated

with gamma radiation doses of 5, 10 and 20 Gy (irradiation source - ^{137}Cs). Temperature resistance of irradiated plants was determined by a standard method obtained in plant physiology [5].

Results and Discussion.

In our experiments, high temperature and ionizing radiation were used as extreme factors to determine the plant response parameters. The study aimed, on the one hand, to determine the radioresistance of specific plants and, on the other hand, to study the formation of radiobiological reactions under conditions of high temperature regime. Naturally, the focus was on the protective effects of plant organisms that contribute to the plant's resistance to high temperatures. The radioresistance of plant tissues directly to extreme conditions and their transpiration ability as a means of regulating the surface temperature of intact tissues were investigated. From the first picture it can be seen that plant tissues are characterized by a fairly high viability in relation to high temperatures.
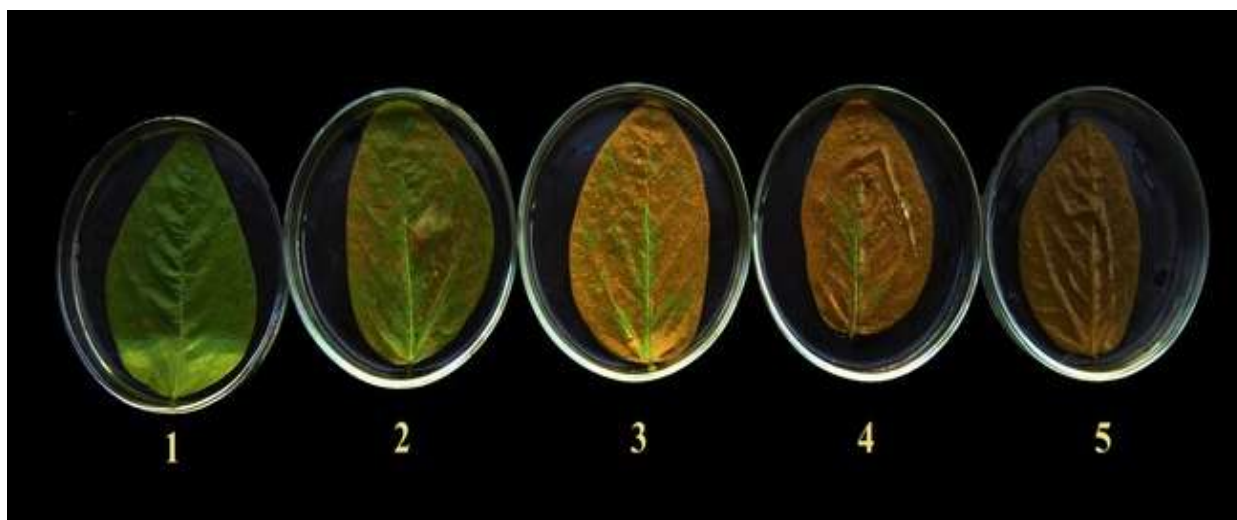
Fig. 1. Influence of high extreme temperatures
On the viability of leaf tissues
Up to: 1 - 30 °C; 2 - 40 °C; 3 - 50 °C; 4 - 60 °C; 5 - 70 °C

In these experiments, the study of the dependence of plant tissues on the temperature regime was carried out without water deficiency [5]; Subsequently the same experiments were performed on intact plants and as shown in Figure 2, changes in tissue transpiration intensity rates were observed.

In order to determine how the above effects are realized in the natural environment, we made observations in specific landscape conditions. The following pattern was observed here: the surface temperature of the leaves of the study plants increased due to the increase of the radiation dose (up to 20 Gy).

At the same time, experiments were carried out in vegetation vessels. Based on the obtained data, it was established that irradiated plants are characterized by economical consumption of soil water resources; However, reducing the level of transpiration under the influence of extreme temperatures does not provide an effective protection of the plant organism's surface. A special danger of the latter effect occurs when the temperature threshold exceeds 40 °C. In the cultivation of irradiated plants under such extreme temperature conditions, irreversible processes take place and, in the case of prolonged exposure, end in lethal effects.
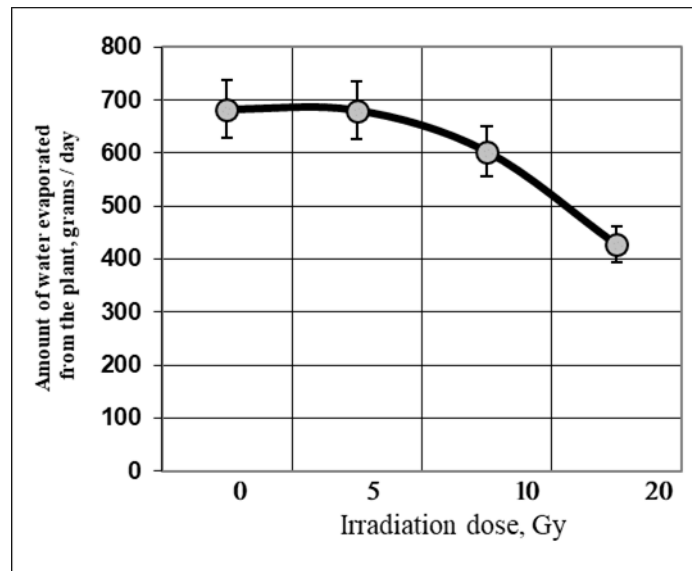
Fig. 2. Influence of gamma radiation on plant tissue transpiration intensity.

Experiments were performed at the landscape level to determine the sustainability parameters of phytocenoses under anthropogenic and climatogenic load conditions. The area adjacent to the Madneuli (Kazreti, Bolnisi district) quarry was selected as the study landscape. The choice was made due to the fact that the phytocenoses present in this area are distinctly different in anthropogenic load (Fig. 3).

Fig. 3. Location of study phytocenoses zones
(Camera height 14.21 km)

1-Minimum load zone; 2 - Highway and active cultivation
zone of agricultural crops; 3 - Adjacent area of the ore quarry

According to the latter characteristic, phytocenoses were conventionally divided into three zones: the first zone was considered to be the minimum load zone (Fig.3-1); The second zone was the roadway and areas of active cultivation of agricultural crops (Fig. 3-2); And the third zone was considered to be the area directly adjacent to the ore quarry (Fig. 3-3). A comparative analysis of phytocenoses stability parameters

was performed in relation to the above zones. The criterion was to determine the surface temperature parameters of plant leaves united in phytocenoses, which was determined by the method of remote laser scanning. It was found that under the conditions of optimal temperature regime (up to 30 °C), this parameter had uniform character in all three study zones; During the extreme temperature regime (above 40 °C), the surface temperature varied according to the zones, namely: the surface temperature of plant leaves in the phytocenoses of the second and third zones was 3-6 °C higher than the same rate of plant leaves in the phytocenoses of the first zone, which indicates a decrease in the sustainability of phytocenoses in these zones.

Conclusion.

Based on the conducted experiment, it was established that any change, which is reflected in the stability parameters of phytocenoses, during long-term or permanent exposure is manifested in the form of changes in both quantitative and qualitative characteristics of successive processes. The effect we have described clearly indicates that during anthropogenic and global climate tension, the anthropogenic factor can be crucial to the viability of a particular ecosystem.

References

1. Chen Sh., Chen B., Brian D. Ecological risks assessment on the system scale: A review of state-of-the-art models and future perspectives. // Ecological Modelling,Volume 250,10b, 2013, pp. 25-33.
2. Perrodin Y,, Boillot C,, Angerville R,, Donguy G,, Emmanuel E. Ecological risk assessment of urban and industrial system: A review // Science of The Total Environment, Volume 409, Issue 24, 15, 2011,pp. 5162-5176.
3. Critto A., Torresan S., Semenzin E., Giove S., Mesman M., Schouten A.J., Rutgers M., Marcomini A. Development of a site-specific Ecological risk assessment for contaminated sites: Part I. A multi-criteria based system for the selection of ecotoxicological tests and Ecological observations.//Science of The Total Environment, Volume 379, Issue 1, 15,2007,pp. 16-33
4. Bruce K., Hope. An examination of Ecological risk assessment and management practices. // Environment International, Volume 32, Issue 8, 2006, pp. 983-995.
5. Третьяков Н.И. Практикум по физиологии растений. // Агропромиздат, М., 1990, 272с.

NEW WAYS OF RADIATION MIGRATION INTO NATURAL ENVIRONMENT BY MEANS OF CESIUM-RICH CONDENSED MICRO-PARTICLES (CsMPs).

Chelidze L.

Georgian Technical University, Tbilisi, Georgia
liachelidze@gmail.com

Summary: *Cesium-rich micro-particles - CsMPs - generated at the Fukushima nuclear power plant were first detected in atmospheric particles 170 km southwest of the plant. Particle formation took place during melting inside the reactor. These particles provide important information about the physical and chemical properties of radioactive materials inside the reactor. A high-resolution transmission electron microscope as well as conventional radio-analytical techniques were used for their study.*

Key words: *Cesium-rich micro-particles, radioactive materials.*

Each disaster is an unique event. The second most significant nuclear disaster in the world history occurred in 2011 in Japan. It was preceded by an earthquake and tsunami. The accident posed a serious environmental threat: in the Fukushima prefecture 5.2×10^{17} Bq radionuclides were released from a nuclear power plant into the environment [1].

As a result of the processes, developed at the Fukushima Daiichi nuclear power plant, the catastrophe destroyed the complex and interdependent security systems. Clearly, the study of contamination process will help to increase security of power generation facilities in Japan and around the world. The most serious environmental consequences of the accident, including surface pollution by radioactive cesium, have not yet been explored. The big challenge of modern technologies is to control cesium nanoparticles in nature. Besides, the processes, currently going on inside the reactors, are not known, as it is impossible to get there due to the high radiation field. To prepare for the worst-case scenario and increase the sustainability of the space "at risk", the scientists considered the catastrophe from different angles.

To date, conclusions about reactions, developed in the Fukushima reactors, have been based on indirect studies. It is believed that after the shutdown of the cooling system, the temperature in the reactor rise to 2,200 K and from the irradiated fuel the radioactive Cs was released. All CsMPs (2.0-3.4 μm in size) contain SiO_2 glass and Zn-Fe-oxide nanoparticles associated with a wide range of Cs concentrations. Uranium U traces are also associated with Zn-Fe-oxides. Cesium-rich micro-particles of CsMPs generated at the Fukushima Nuclear Power Plant were first discovered in the atmosphere 170 km southwest of the plant[2]. These particles are solid body objects. Their formation took place during melting inside the reactor and they carry important information about the physical and chemical properties of the radioactive materials inside the reactor. CsMPs formation process studies use a high resolution electron microscope combined with conventional radio-analytical techniques and chemical and structural properties on an atomic scale.
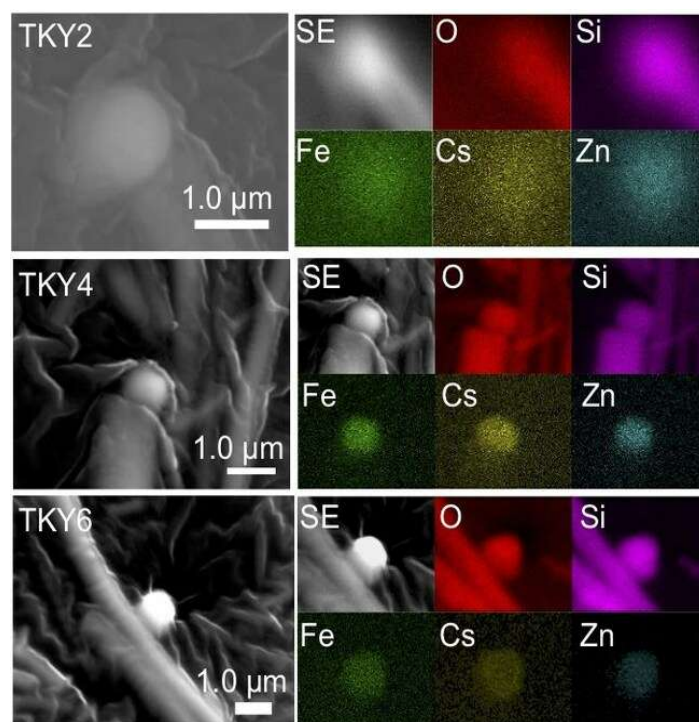
Image above: Secondary electron images from Utsunomiya et al. 2019, of CsMPs discovered in atmospheric particles trapped on a Tokyo air filter from March 15, 2011, with major constituent elements displayed.

Photo from internet source   https://safecast.org/2019/08/fukushima-cesium-enriched-microparticle-csmp-update/

The nanoscale texture of CsMPs reveals the process of their formation in the melting area of the active part of the reactor.

Interestingly, the process of formation of CsMPs at Fukushima is markedly different from the presented above process of microparticle formation. It take place as a result of interaction of the melted active zone of the reactor in experiments [3,4,5] with concrete particles (a process known as molten core concrete interaction - MCCI).

The atmosphere inside the reactor housing was to be filled with Cs-related aerosols, gaseous Cs particles, water vapor, and gaseous hydrogen. The interaction between the metal structures and the melting active zone of the reactor, when the reactor housing failed, resulted in the formation of large amounts of Zn-Fe nanoparticles.

Due to the extremely high radioactivity per unit mass, $\sim 10^{11}$ Bq / g, CsMPs particles can be an important source of radiation dose in the Fukushima environment. In addition, CsMPs are important carriers, through which volatile radionuclides, such as uranium (U), reach the environment [2].

It is very important to determine, whether artificial nanoparticles and specifically CsMPs retain their properties (size, original structure, reaction properties) in water, air, soil or sediment. Accidentally produced man-made CsMPs pose a significant environmental challenge in terms of both discovery and modeling of further migration pathway.

Conclusions

There are two mechanisms – natural and man-made - of environment contamination by nano-particles. The natural processes, such as forest fires, sand storms, dust and aerosols, bio-objects (viruses) are the sources of nano-particles' contamination by the last millenniums. In the case of man-made CsMPs, the

produced nano-particles are radiation sources, but it is impossible to monitor their concentration by usual radiation detectors. The CsMPs detection is not the only technical problem: besides expensive specific equipment and highly technical qualification of the staff, one need to know the particles complex migration path in the media. The investigation of CsMPs infiltration into environment and its further migration is one of main ecological and eco-toxicological challenges of modern science.

References

1. Steinhauser G., Brandl A., Johnson T. E. // Sci. Total Environ, 470, 2014, pp. 800–817.
2. Genki Furuki Junpei Imoto, Asumi Ochiai, Shinya Yamasaki, Kenji Nanba, Toshihiko Ohnuki, Bernd Grambow, Rodney C. Ewing, Satoshi Utsunomiya. Caesium-rich micro-particles: A window into the meltdown events at the Fukushima Daiichi Nuclear Power Plant. // Scientific Reports, 2017, www.nature.com/scientificreports
3. Sehgal B. R. Ed. Nuclear safety in light water reactors. Severe accident phenomenology. // Academic Press, Amsterdam, TheNetherlands. 2012, 714 pp, and references therein
4. Beattie I. R., Nichols, A. L. J. // Aerosol Sci., 23, 1992, pp. 847–852.
5. Kissane M. P. // Nucl. Eng. Design, 238, 2008, pp. 2792–2800
6. Klaine D.J., Alvarez P.J.J., Batley G.E. Nanomaterials in the environment: behavior, fate, bioactivity, and effects. //Environ. Toxicol. and Chem., Vol.27, № 9, 2008.

https://safecast.org/2019/08/fukushima-cesium-enriched-microparticle-csmp-update/

RADIOECOLOGICAL ASSESSMENT OF GARDABANI AREA

*Matiashvili S., **Chankseliani Z.

*Iv. Javakhishvili Tbilisi State University, M. Nodia Institute of Geophysics,1, Alexidze Str., 0160, Tbilisi, Georgia
sophiko79@mail.ru
**Soil Fertility Research Service of LEPL Agricultural Scientific Research Center, Tbilisi, Georgia

Summary: The aim of our research is to study the radiologically relevant areas of Georgia in terms of ecological pollution. This time the study area was the area adjacent to the Gardabani district power plant. Determination of radionuclide content in soils. The study was conducted at several points in the district. The criteria were the content of specific contaminants in the soil and their assessment of whether the concentration exceeded the maximum allowable norms. The monitoring revealed that the content of heavy metals in the soils is different. In the mentioned points of the Gardabani district, the soils are severely affected, which is reflected in the increase of heavy metals in the soils. As for radionuclides, radionuclide K40 and its high content were found in the analysis of the samples taken. In addition Cs137 is found; It is noteworthy that their content decreases with increasing depth. Based on the obtained digital material, we can say that the peak reaches Pb, but its content also decreases with increasing depth.

Keywords: Radiological research, radioactive contamination, radionuclides

Any country is valuable if the people of that country take care of the environment and its natural resources. If the environment is not taken care of and protected, then the value of this country will be drastically reduced, because such a country is unsuitable, first of all, for life and then for economic activity.

The rapid economic development of the country and the production and supply of competitive products and services should not be at the expense of environmental pollution. There are successful experiences in many countries around the world on how to produce a competitive product with minimal negative impact on the environment [1].

Industry and transport account for the largest share of environmental pollution. It is known that 2.4 billion tons of coal is consumed on the planet, as a result of which 280 thousand tons of arsenic and 224 thousand tons of uranium are scattered on the earth every day. At this time, the world produces 40 thousand tons of arsenic and 30 thousand tons of uranium. From this it is clear how much pollution of the environment with these substances prevails. Coal pollution and its recycling as well as its use are real and accountable.

This problem is really serious in Georgia. According to a study by the World Health Organization, Georgia ranks second in the world in terms of death rate due to air pollution per 100,000 inhabitants, and is only ahead of North Korea. Atmospheric precipitation, wind direction and others are known to be one of the main factors in the distribution of radionuclides. Waste management in parallel with polluted air is the most problematic issue in the country [2]. In most cases the waste is concentrated in the open air. During the wind, this waste is scattered over long distances in the hills and hills. Burial of waste damages and poisons the soil and, most importantly, pollutes one of our greatest treasures groundwater. For the second time, our target is soil research and its assessment in terms of radionuclide contamination. Also, with the content of heavy metals, since there is a thermal power plant in the territory of Gardabani.

The construction of a powerful thermal power plant "Tbilsres" in Gardabani started in the 60s of the 20th century. Today, Gardabani Municipality is one of the strongest agricultural, social and cultural regions for Georgia, Large enterprises are gathered here, including agricultural enterprises, educational and scientific institutions. Radiation background was measured a few years ago and samples were taken for analysis. The content of radionuclides and heavy metals was determined. The area around the Gardabani district thermal power plant was studied in terms of ecological pollution [3].

A similar study is conducted by our monitoring. Several soil samples were taken, including mixed-type, from agricultural areas. GPS coordinates were mapped and the sample taken from the corresponding detail was evaluated. Radionuclide contamination levels were determined. Cs137, Sr 90 and K40 were identified. The increase in pollution levels after the Chernobyl nuclear power plant accident is mainly due to the release of excess amounts of radioactive cesium. As it is known, one of the main factors in the distribution of radionuclides is atmospheric precipitation, wind direction and others. Influence.It is known that the content of radionuclides in the soil is directly related to the precipitated atmospheric precipitation [4].

A peculiar regularity of wind and precipitation distribution in the zone is manifested. A similar pattern was found in terms of radiation background Sampling took place in villages a few kilometers from the Gardabani thermal power plant as shown in the table, natural radionuclides of 40K were observed in the soils of the Gardabani district in all samples [5]. The presence of natural radionuclide 40K in soils is due to the composition of soil soils and also the use of phosphorus fertilizers. Sampling took place in villages a few kilometers from the Gardabani thermal power plant as shown in the table, natural radionuclides of 40K were observed in the soils of the Gardabani district in all samples. Measured doses of radionuclides as well as maximum allowable norms are given in the cells (Table 1-5).

Table 1. GPS coordinates 41.494063; 45.115063 (mixed)

	Radionuclide	Activity Bq/kg	St.err. %	Uncertainty Bq/kg	MPN Beck /kg
1	CS-137	2.12	92.1	2.03	50
2	SR-90	0.00	>100	21.0	20
3	K-40	403	4.7	108	370

Table 2. GPS coordinates 41.4963377; 45.109227

	Radionuclide	Activity Bq/kg	St.err. %	Uncertainty Bq/kg	MPN Beck/kg
1	CS-137	21.0	12.4	6.14	50
2	SR-90	0	>100	20.2	20
3	K-40	309	5.9	83.8	370

Table 3. GPS coordinates 41.471043; 45,102703

	Radionuclide	Activity Bq/kg	St.err. %	Uncertainty Bq/kg	MPN Beck/kg
1	CS-137	6.78	28.6	2.64	50
2	SR-90	18.4	>100	19.9	20
3	K-40	395	4.6	106	370

Table 4. GPS coordinates 41.477860; 45.074894

	Radionuclide	Activity Bq/kg	St.err. %	Uncertainty Bq/kg	MPN Beck /kg
1	CS-137	12.6	17.8	4.00	50
2	SR-90	10.1	>100	20.4	20
3	K-40	421	4.4	113	370

Table 5. GPS coordinates 41.516432; 45.065796

	Radionuclide	Activity Bq/kg	St.err. %	Uncertainty Bq/kg	MPN Beck / kg
1	CS-137	15.4	15.8	4.73	50
2	SR-90	0	>100	20.3	20
3	K-40	312	5.9	84.4	370

We also determined the content of heavy metals in the soil at 7 points [6]. The corresponding coordinates were taken and indicated in the table, we also have the maximum allowable norms of heavy metals, which we expressed graphically (Diagram 1,2).
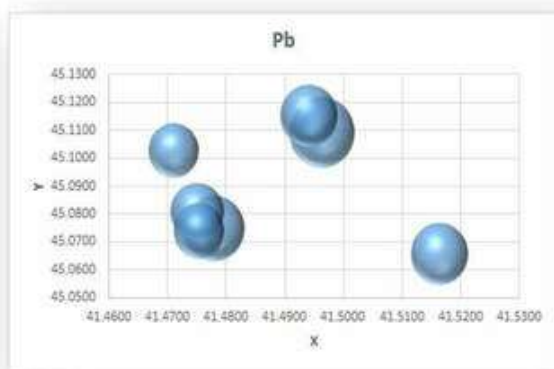
Diagram 1. Distribution of lead in the soil.
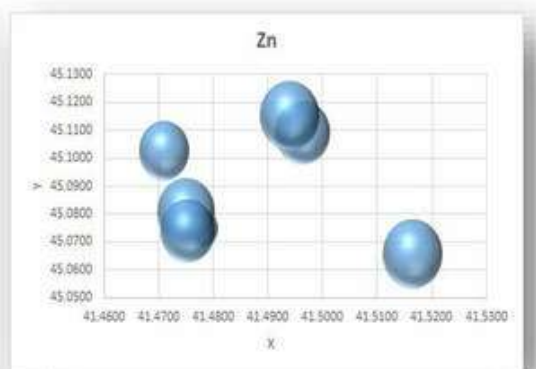
Diagram 2. Distribution of zinc in the soil.

Conclusion.

As a result of the research we can conclude: the soils of the area adjacent to the Gardabani district thermal power plant are exposed to it (heavy metals), which is reflected in the increase of the permissible level of heavy metals in the soils.

From the results obtained we focused on 137Cs, based on the obtained digital materials the radionuclide 137Cs, decreasing with respect to depth. We can say that there is no alarming situation regarding this radionuclide in the mentioned area of Gardabani. We have studied the content of heavy metals in the soils of the Gardabani district thermal power plant, namely Zn, Pb, and Fe.

As it turns out, the content of heavy metals in soils is different. As the depth of soil sampling increases, the content of heavy elements decreases. The following research can be concluded: Soils in the vicinity of the Gardabani district thermal power plant are exposed to it (heavy metals), which is reflected in the increase in the permissible level of heavy metals in the soils.

References

1. Chkhitunidze M. Matiashvili. S. Kereselidze Z. Diffuse model of change in soil contamination over time. // Int. Sc. Conf. "Modern Problems of Ecology", Kutaisi ,Georgia, September 21-22, 2018.
2. Palstzky A; Bergmann W. Ein beitrag zur reduzierung von zinkuberschus–Schaden auf einem mit zink kontaminierten Boden. // Arch. Phytop. Pflanzenschutz, Bd. 15, N2, 1979, .S.131.
3. Chankseliani Z., Zardalishvili O. Ecological Principles of Agro-chemistry. // (a Book). Tbilisi, 1992, 107 p. (in Georgian).
4. Gelashvili K. Radiation safety norms. // "Education", Tbilisi, 2000, p. 221
5. Amiranashvili A., Chargazia Kh. Intra-Annual and Seasonal Variations of Sub-Micron Aerosols Concentration and their Connection with Radon Content in Surface Boundary Layer of Tbilisi City. // Bulletin of the Georgian National Academy of Sciences, vol. 10, N 2, 2016, p. 72-78.
6. Standarts for the content of heavy metals and metalloids in soil. Soil science, №3, 2012, pp. 368-375.

RADON CONCENTRATION IN WATER ON THE SEVERAL REGIONS OF GEORGIA

*Melikadze G., **Vaupotič J., *Kapanadze N., *Tchankvetadze A., ***Chelidze L., *Todadze M., ****Gogichaishvili Sh., *Jimsheladze T.

*Mikheil Nodia Institute of Geophysics, 1, M. Alexidze Str., 0193, Tbilisi, Georgia, melikadze@gmail.com
*Jožef Stefan Institute, Jamova cesta 39, SI-1000 Ljubljana, Slovenia janja.vaupotic@ijs.si
***Georgian Technical University. 77 Kostava av., Tbilisi-0160, Georgia, lia.chelidze@gmail.com
****E. Andronikashvili Institute of Physics of the Iv .Javakhishvili Tbilisi State University

Summary: *A quantitative assessment of radon (^{222}Rn) distribution in the surface, shallow and deep layer waters in several regions of Georgia has been carried out. In total, about 600 samples were measured by a portable AlphaGUARD radon monitor. The radon concentration ranged from 0.1 to 222 Bq/l.*

Key words: Rn mapping, out-door radon.

Introduction

The works [1-3] present the results of our early studies of radon content in soil and water in various regions of Western Georgia.

According to GNSF project FN-19-22022, "Radon mapping and radon risk assessment in Georgia", during 2020–2021, the authors carried out fieldwork to quantify the radon distribution, ascertain geological factors influencing the radon concentrations in water in some geographical areas in Georgia.

Method

The field study was conducted by the mobile group of researchers who measured ^{222}Rn concentration in various water sources (boreholes, wells and springs) in several regions of Georgia. In total, about 600 water samples were analyzed by a portable radon monitor AlphaGUARD (Bertin Instruments). All observation sites were marked by GPS position.

The key method for fulfilling the project requirement is radon mapping based on the application of geochemical methods. Results of analyses on radon concentration were marked on topographic and geological maps. After that, the field data were digitized and transferred into the GIS system. The connection of radon anomalies to geological and hydro-geological structures is analyzed using GIS technology.

Data

From the tectonic point of view, the Northern of the tested territory belong to the Grate Caucasus folded system, Southern Adjara-Trialeti folded system and the territory between them to the Georgian plate. Lithology and geological structures of the region, presence of many tectonic faults, radioactive elements in rocks, various hydrogeological, geomorphological structures and soil characteristics determine the complexity of the territory. Based on all the above parameters, the map of ^{222}Rn concentration in waters was compiled using the GIS technique. Sampling points are shown in Fig. 1.
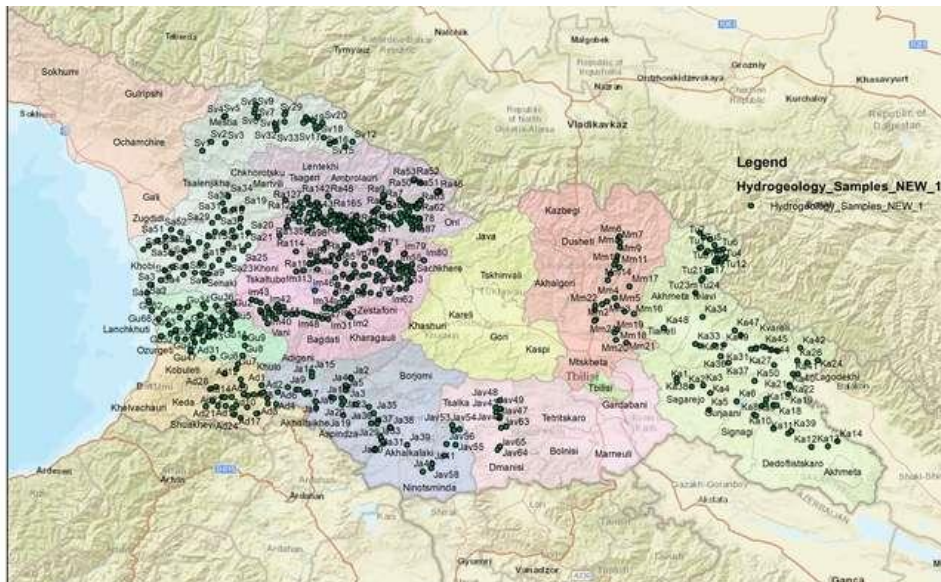
Fig. 1. Sampling points location on the territory.

Testing was carried out at selected areas in almost all tectonic regions. "Svaneti" and "Tusheti" regions were tested on the territory of the Central part Great Caucasus system. The distribution of radon concentrations in waters is presented in Fig. 2.
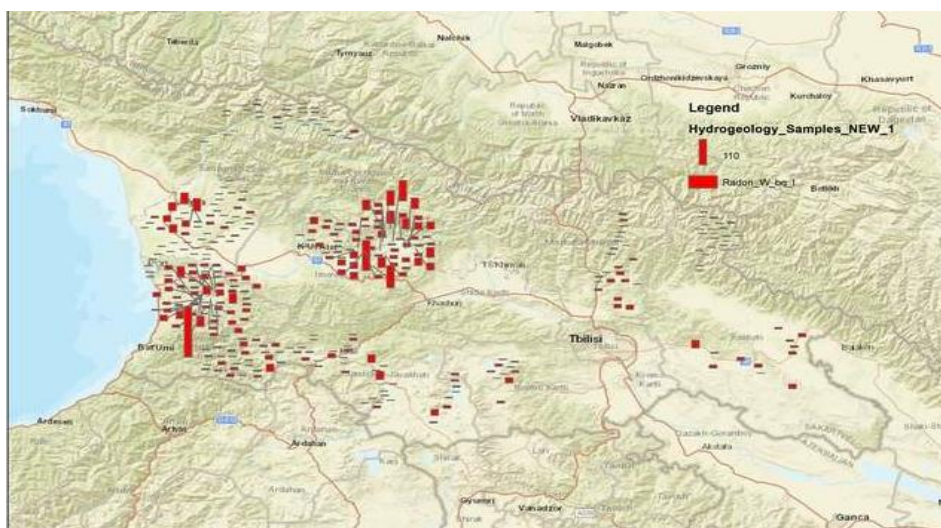
Fig. 2. Distribution of radon concentrations in waters on the territory.

In these areas, there are mainly developed spring waters that have been analyzed in almost all areas. In these surface waters, radon background levels are low. For example, in the "Svaneti" region, the radon concentration in springs varies between 0.8−2.2 Bq/l. In the mineral springs of deeper genesis, radon concentration grows up to 7−10 Bq/l (mineral springs "Shavghele", "Becho", etc.). In the "Tusheri" region, the background radon concentration in springs is lower, between 0.5−3.4 Bq/l.

Sampling was conducted on the territory of the West part of Georgian Plate on the territory of Western Georgia, in particular in the "Samegrelo", "Guria", and "Imereti" region. In the territory of "Samegrelo", were mainly tested the boreholes, both types of waters, shallow and deep thermal. Radon concentrations, observed in surface water of shallow wells, vary between 0.2−6.7 Bq/l. In deep thermal wells, their values reach 25−34 Bq/l ("Tsaishi" and "Zugdidi").

On the territory of the "Guria" region, the background radon concentration in shallow water reaches 2.9–10 Bq/l. In deep groundwater and mineral waters, radon concentrations are higher, such as in the village "Meria" with 24.4 Bq/l in a borehole and the village "Shemoqmedi spring" with 222 Bq/l.

The territory of the "Imereti" region is characterized by high levels of radon in waters. The background value in the shallow groundwater varies between 1.9–6.2 Bq/l. In the deep groundwater layer, the values increase. For example, on the North territory, there are Lower Cretaceous age rocks, which contain fissure and fissure-karstic type of pressurized groundwater (regions of "Tskaltubo" and "Kutaisi"); the characteristic example is the low-radioactive thermal water of "Tskaltubo Resort" (50–70 Bq/l). Here the springs have a large debit (200–220 l/s).

On the East part of the Georgian plate was tested territory of the "Tianeti" region, where a low concentration of radon in water, about 0.1–5.3 Bq/l, was found. Only in two springs (mm N19-20) it does increase till 13.8–18.5 Bq/l.

In South Georgia, the territory of Adjara-Trialeti folded system, and Javakheti Plate were sampled. In general, both parts dominate by the spring type of shallow groundwater. There is a law background radon concentration in water 0.6–7.2 Bq/l for the "Adjara" region and 0.87–6.7 Bq/l for the "Javakheti" region found. In the several mineral springs, radon value increases till 11.9–13.1 Bq/l for "Adjara" and 22.4–36.1 Bq/l for "Javakheti".

Conclusions

Peculiarities of distribution of radon concentration in selected surface, shallow and deep layer waters on some territory of Georgia were studied, such background and anomalous areas were outlined. The elevated radon concentration is related to the tectonic faults and hydrogeological "windows".

Acknowledgement

References

1. Amiranashvili A., Chelidze T., Melikadze G, Trekov I., Todadze M. Quantification of the radon distribution in various geographical areas of West Georgia". // Journal of Georgian Geophysical Association, №12, 2008. http://openjournals.gela.org.ge/index.php/GGS/article/view/652

2. Amiranashvili A., Chelidze L., Gvinianidze K., Melikadze G., Todadze M., Trekov I., Tsereteli D. Radon Distribution and Prevalence of Lung Cancer in Several Areas of West Georgia // Papers of the Int. Conference International Year of the Planet Earth "Climate, Natural Resources, Disasters in tne South Caucasus", Trans. of the Institute of Hydrometeorology, vol. No 115, ISSN 1512-0902, Tbilisi, 18 – 19 November, 2008, pp. 349 – 353 (in Russian). http://217.147.230.60/handle/123456789/742

3. Amiranashvili A., Chelidze T., Melikadze G, Trekov I., Todadze M., Chankvetadze A., Chelidze L. Preliminary results of the analysis of radon content in the soil and water in different regions of west Georgia". // Institute of Geophysics ISSN 1512-1135, vol. 60, Tbilisi, 2008, pp. 213 – 218 (in Russian). http://217.147.230.60/handle/123456789/315

MONITORING AND ASSESSMENT OF ANOMALIES OF 2020 MAGNETIC FIELD VARIATIONS AT DUSHETI GEOMAGNETIC OBSERVATORY

Kiria T., Nikolaishvili M., Mebaghishvili N.

M. Nodia Institute of Geophysics of Iv. Javakhishvili Tbilisi State University, 1 M Alexsidze Str 0160, Tbilisi, Georgia
kiria8@gmail.com

Summary: *The paper touches the study of the magnetic field variations (minute values) during 2020 by Dusheti Geomagnetic Observatory. We found out different category anomalies, for revealing of which we used some statistical methods and special Python library developed for observation on different components of magnetic field. As a result of the study we determined criteria for revealing low, moderate and high category perturbations in regards with 2020 data.*
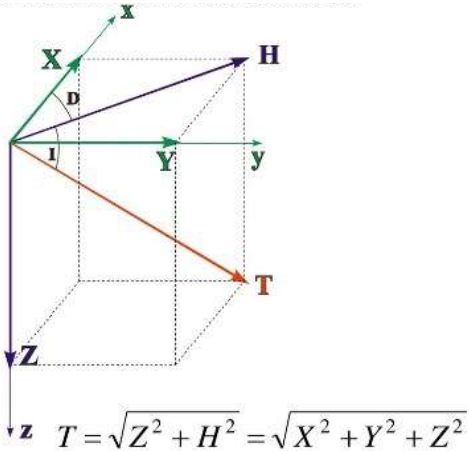
Key words: *Magnetic field variations*

Preface

Development of mathematical methods for the observation, assessment and forecast of the magnetic field of the Earth is the most essential task of this field of Geophysics. Our study touches processing the data obtained by the Observatory and mechanical processing of rare phenomena revealed in the data and issues of further forecast. In order to solve this task it became necessary to preprocess the data, highlight statistical hypotheses and prove them with high reliability. Obviously, forecasting issue includes so called revealing the preparation period of anomaly in the magnetic field variations and verifying them for every next period.

Let us mathematically formulate our work. Let us admit that $t' \in [t_0, t]$, where is t_0 January 1, 2020 and t is December 31,2020. Each $x_{t'}$, $y_{t'}$, $z_{t'}$ is (t' runs $[t_0, t]$ with minute discretization), where the three components of the magnetic field are determined for t'.

We will observe the graph of the magnetic field tension, T vector of the magnetic induction in a homogenous isotropic space.

$$T = \sqrt{Z^2 + H^2} = \sqrt{X^2 + Y^2 + Z^2} \qquad (1)$$

We receive time series for 2020 in the form of the values of tension of T magnetic field (minute discretization), which includes 508905 recordings.

Table 1. The structure of the data base.

	Time	X	Y	Z	T
0	2020-01-11 14:00:00	20.523	-3.206	23.7236	31.532224
1	2020-01-11 14:01:00	20.063	-3.136	23.7099	31.217268
2	2020-01-11 14:02:00	19.654	-3.405	23.7298	30.999631
3	2020-01-11 14:03:00	20.006	-3.364	23.7030	31.199179
4	2020-01-11 14:04:00	19.521	-3.986	23.7528	31.002470
...	...	...	...	...	...
508901	2020-12-31 23:55:00	1.267	57.572	39.6300	69.904774
508902	2020-12-31 23:56:00	-0.100	57.467	39.6870	69.839273
508903	2020-12-31 23:57:00	0.071	57.280	39.6764	69.679410
508904	2020-12-31 23:58:00	0.007	57.747	39.6677	70.058850
508905	2020-12-31 23:59:00	-0.001	57.561	39.6891	69.917762

On the basis of table 1 we will study T and the anomalies associated with it in time and distinguish different interesting statistical structures. The mechanism of solving this task is given mainly in so called task of detrending [1-2], when it is essential to construct such statistical function for transformed signal that will enable us to evaluate the useful (a regular value included in the process) part and distinguish it from the whole process as a regular one at any point of time.

Before discovering the random component (white noise) in our process we carried out a certain preliminary work and studied the statistical properties for our time series by months, days and hours. Below we present interesting statistics for the values of T magnetic field tensions.

mean	55.000161
std	17.181470
min	21.895756
25%	40.281857
50%	54.010227
75%	68.721086
max	150.000000
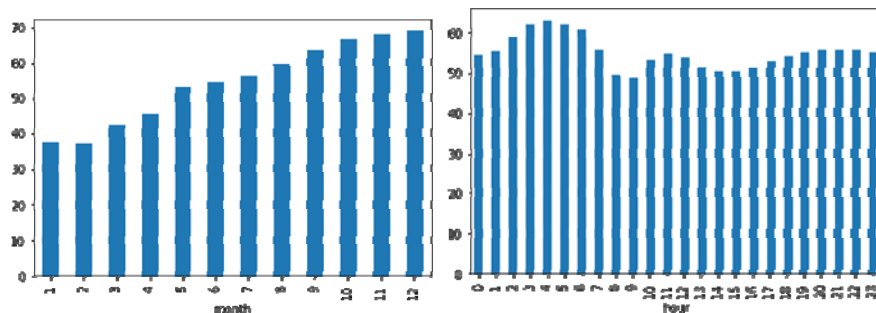
Fig.1. The values of monthly and hourly averages for T magnetic field tensions.

As a result of observing on these schemes we concluded that the process must not be homogenous in time, though intuitively we may say that it is stationary. At the same time, we verified the zero hypothesis on the stationarity of our process with value p<=0,05.

ADF Statistic: -31.261735
p-value: 0.000000
Critical Values:
    1%: -3.430
    5%: -2.862
    10%: -2.567

As shown above the process is characterized with stationarity depended on the time structure [3]. The autocratic function shows that there is a relationship between the previous and next values, though it decreases over time. It means that in the first half of 2020 the data of our study had interacting physical load in a narrow sense. However we cannot say the same on the last months of the year. Obviously it has an impact on the forecast quality. Consequently, the seconds half of 2020 is of higher entropy [4-5] and the values of T magnetic field tension are distinguished with higher dynamics that in its turn indicates to episodic stationarity of the process and strengthening the regular part in it.
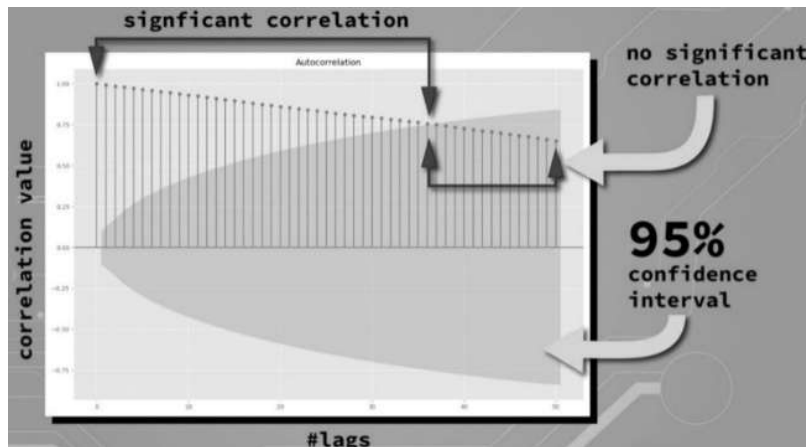
Fig. 2. The scheme of autocorrelation function of T magnetic field tension and confidence intervals with 50 lags.

The next stage for our data is their stationarization. It can be done by the first order derivative that will detrend the series. Further, we will observe the scheme with the first remainder and see whether the convergence of the average and dispersion can be reached near some constant numbers. Significant decrease of P value shows that the process was detrended.
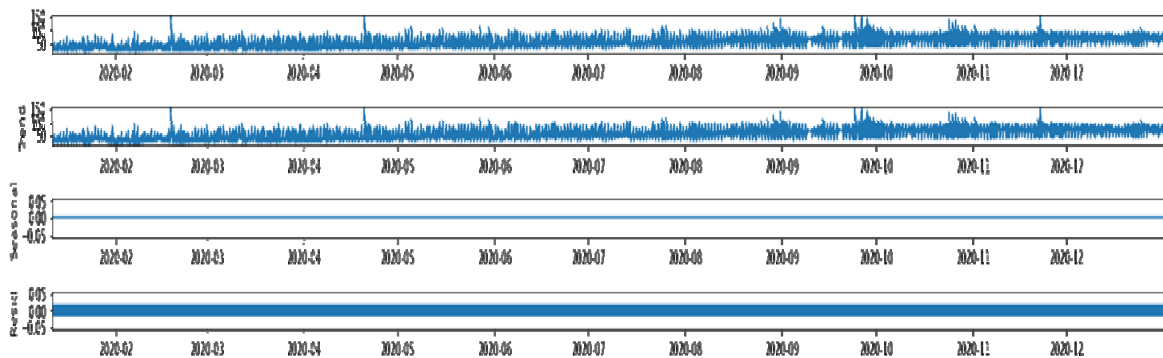
Fig. 3. The scheme of seasonality received by adaptive and multiplicate methods of decomposition and distinguished white noise.

132

Resume

Classification of magnetic field tension data as regular and singular parts by adaptive and mulitiplicate methods obviously shows seasonality and the role of white noise in all the data, on the basis of which it became much easier to find anomalies in the magnetic field data. In future on the basis of historical data, use of some machine learning technology of forecasting models in the imbalance anomaly missives will become more appropriate. The result of the study of forecasting models is a certain preliminary work, on the basis of which we will receive magnetic anomaly expectations in time and their probable assessments.

References

1. Emmanuel B. , Enegesele D., Arimie C. Additive Decomposition with Arima Model Forecasts When the Trend Component // Is Quadratic. Open Access Library Journal, 7, 2020, pp. 1-20. doi: 10.4236/oalib.1106435.
2. Marszalek Z., Duda K. Multifrequency Vector Measurement System for Reliable Vehicle Magnetic Profile Assessment. // Published: 31 August 2020
3. Bandaraa K., Hyndmanb R.J., Bergmeirc Ch. MSTL: A Seasonal-Trend Decomposition Algorithm for Time Series with Multiple Seasonal Patterns. // A School of Computing and Information Systems, Melbourne Centre for Data Science, University of Melbourne.
4. Bandara K., Bergmeir C., Campbell S., Scott D., Lubman D. Towards Accurate Predictions and Causal 'What-If' Analyses for Planning and Policy-Making: A Case Study in Emergency Medical Services Demand. // in: 2020 International Joint Conference on Neural Networks (IJCNN), pp. 1–10.
5. Bandara K., Bergmeir C., Hewamalage H. LSTM-MSNet: Leveraging Forecasts on Sets of Related Time Series with Multiple Seasonal Patterns. // IEEE Transactions on Neural Networks and Learning Systems 32, 2021a, pp. 1586–1598.

THE MAGNETIC FIELD AND MAGNETISM OF THE SAND IN THE BLACK SEA COASTLINE

Gogua R., Kiria J., Ghlonti N., Gvantseladze T., Tavartkiladze Sh.

M. Nodia Institute of Geophysics at Iv. Javakhishvili Tbilisi State University, Tbilisi, Georgia
kiria51@yahoo.com

Summary: *As a result of the geomagnetic studies in the Black Sea coastline (the river Natanebi, the boundary of the municipalities of Lanchkhuti and Poti) we determined the boundaries of the magnetic field and the limits of magnetic absorbability variation of the sand distributed on the territory. In the sand samples we defined the percent composition of ferromagnetic minerals. The results of the studies prove the assumption of the magnetic genesis of the Black Sea.*
Key words: *Geomagnetic, magnetic anomaly, magnetic absorbability*.

In the 2015-2019 the group of the presenters of the report carries out detailed geomagnetic studies of the above described territory, Fig. 1.
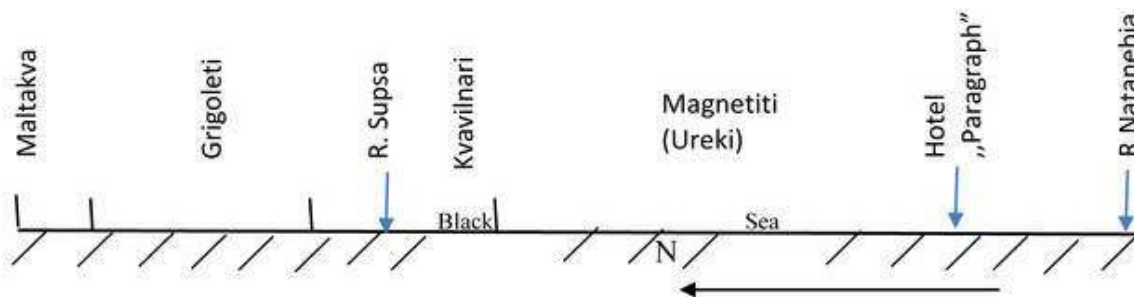
Fig. 1.

The magnetic field of the territory was investigated by means of a modern high definition digital proton magnetometer G856-Ax. The magnetic absorbability of the sand was determined by digital susceptimeter KM-7. Besides, the mineralogical composition of sand samples was studied in a laboratory.

The geomagnetic field investigations

We started planning of the study territory from the south, at the junction of the river Natanebi and the Black Sea. Fig. 2 shows the schemes of the variations of the anomalous magnetic field (a) and the magnetic absorbability of the sand (b) in the area of the river Natanebi – hotel "Paragraph".

As seen in the schemes, the anomalous magnetic field of the area varies in the limits of 200-600 nT, though its mean rate is 350 nT. The same can be said about the magnetic absorbability of the sand, the mean values of which are $200 \cdot 10^{-4}$, and variation limits are $(800-600) \cdot 10^{-5}$.

The results of the investigations conducted in another area (Magnetiti) of the territory are shown in Fig. 3 a, b.

As seen in the schemes, in this area, like in Fig. 2, the anomalous magnetic field varies significantly between (200-650) nT. The mean value of the magnetic field is 400 nT. The magnetic absorbability of the sand is also high in the area. Its mean values are $10000 \cdot 10^{-5}$, whereas the variation limits is $(4000 - 20000) \cdot 10^{-5}$ - SI.

From the boundary of the municipalities of Ozurgeti and Lanchkhuti to the river Supsa (Kvavilnari) the limits of the magnetic field variation is $200 – 650$ nT, whereas the mean value is 400 nT. The scope of the

magnetic absorbability of the sand is also wide and is equal to $(150-800) \cdot 10^{-3}$ - SI and the mean values are of $400 \cdot 10^{-3}$- SI order.
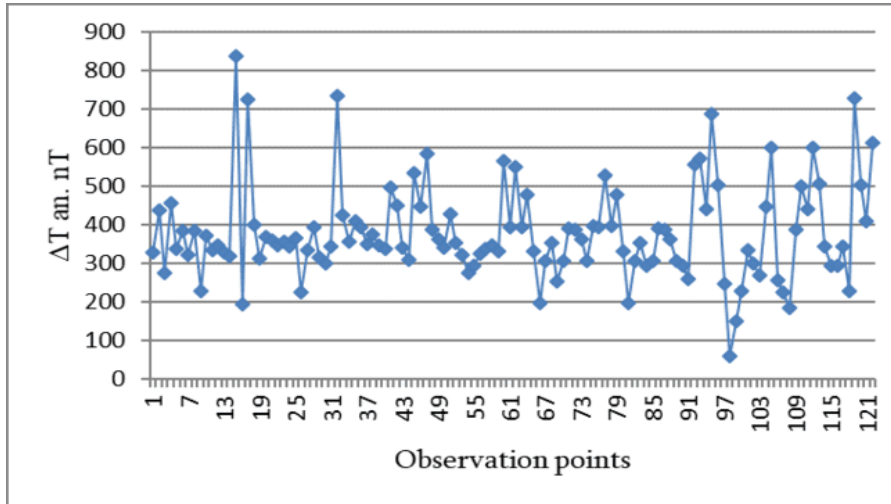
Fig. 2a. Anomalous magnet at the site river Natanebi - Paragraph hotel.
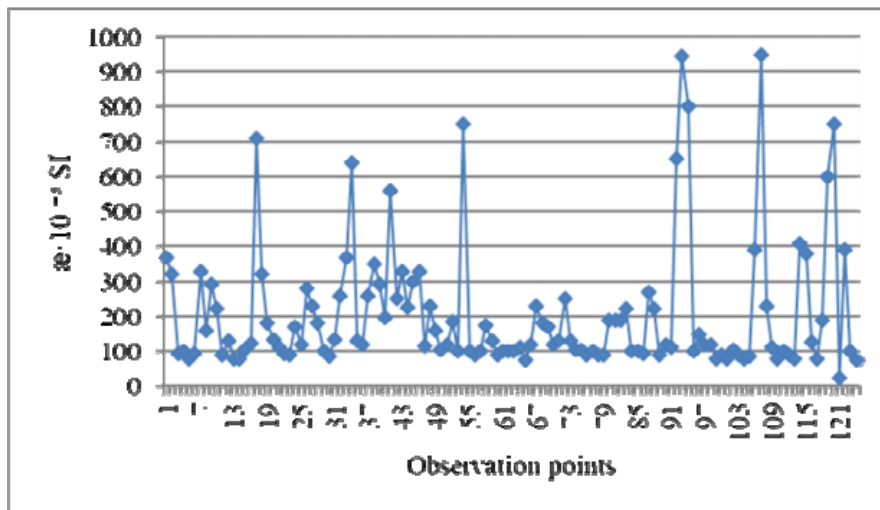
Fig. 2b. The magnetic absorbability variation limits at the site river Natanebi - Paragraph hotel.
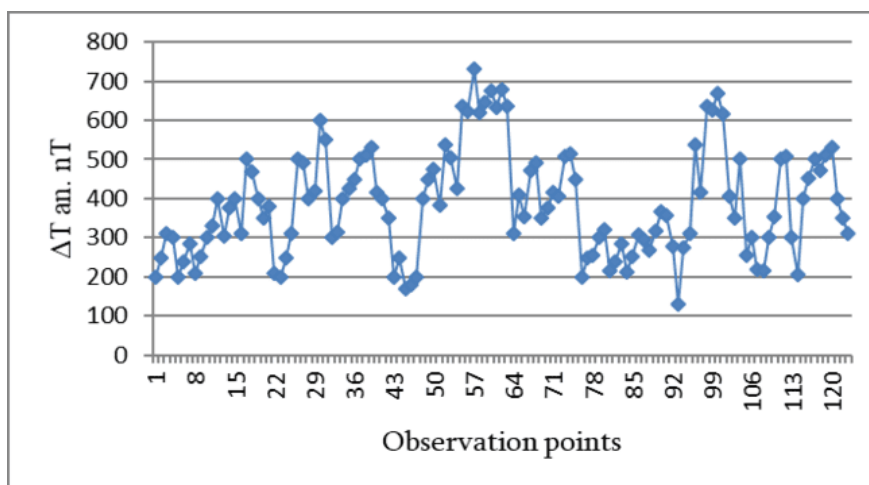
Fig. 3a. Anomalous magnet at the site Paragraph hotel- Magnetiti.
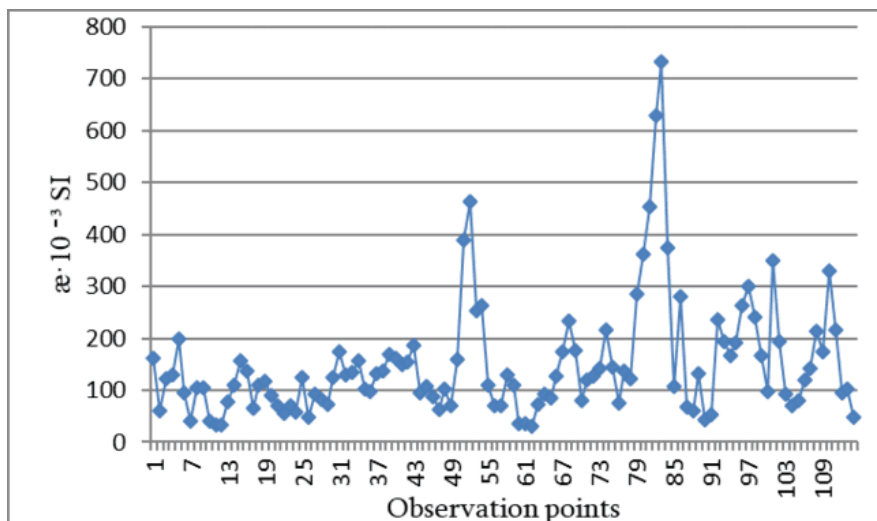
Fig. 3b. The magnetic absorbability variation limits at the site Paragraph hotel - Magnetiti.

From the right bank of the river Supsa to village Grigoleti, along 400-500 m distance, the territory is littered with iron items that makes it very difficult to determine the real magnetic parameters of the territory. Further to the north the mean values of the magnetic field anomalies are of 600 nT order. The magnetic absorbability of the sand is also high. It varies between $(2000-13000) \cdot 10^{-5}$- SI, whereas the average absorbability is $6000 \cdot 10^{-5}$ - SI.

At the north of the study territory to the boundary of the municipalities of Lanchkhuti and Poti (the area of Maltakva) the magnetic field of the territory usually varies between 500-550 nT, and the mean anomaly is 500 nT. The magnetic absorbability of the sand in this area varies between $(2000 - 12000) \cdot 10^{-5}$ - SI, whereas its mean value is $8000 \cdot 10^{-5}$- SI.

The results of the laboratory studies of the sand samples of the Black Sea coastline

We took six sand samples from the study territory. Among them two were taken from the area of Maltakva, one – from the right bank and another one from the left bank of the river Supsa and two samples were taken from the Magnetiti area. The samples were studied at the complex laboratory of the Geologic Studies of Ivane Javakhishvili Institute of Geology.

We determined that the main ferromagnetic minerals of the sand are magnetite and titanomagnetite.

In the sand samples taken from the territory of Maltakva the magnetic content in one of them is 10% and in the other – 12%. The content of titanomagnetite in one of the samples is 3% and 4% - in another correspondingly. In the sample taken on the right bank of the river Supsa the content of magnetite is 4% and titanomagnetite is 2%, whereas the sample taken on the left bank contains 12% magnetite and 6% titanomagnetite, that is the highest content of magnetic minerals.

In one of the sand samples taken near sanatorium "Megobroba" the magnetite content is 6% and the titanomagnetite content is 4%, whereas these values in the other sample are correspondingly 8% and 5%.

The results of the study

As a result of the studies of the magnetic field, the magnetic absorbability of the sand and mineral composition of the coastline of the Black Sea we determined that the territory is significantly anomalous. According to the studied areas (the intensity of the magnetic field, magnetic absorbability and ferromagnetic mineral content) the image is given in the table:

136

Studied territories	Variation scope of the anomalous magnetic field ΔT an. nT.	Average intensity of the magnetic anomaly ΔT an. nT.	Magnetic absorbability (æ) variation scope of the sand 10^{-5} -SI	Mean value of the magnetic absorbability of the sand 10^{-5} - SI	Total content of ferromagnetic minerals %
1.R. Natanebi – hotel "Paragraph"	200 – 600	350	800 – 6000	2000	
2. Magnetite	200 – 650	400	4000 – 20000	10000	10
3. Kvavilnari	200 – 650	400	15000 – 80000	40000	13.18
4. Grigoleti	500 – 700	600	2000 – 10000	6000	6
5. Maltakva	500 - 550	530	2000 - 12000	8000	13.16

Conclusion.

As a result of the geomagnetic studies carried out in the Black Sea coastline (the territory of the river Natanebi, the boundary of the municipalities of Lanchkhuti and Poti) we determined that the magnetic anomalies recorded on this territory, compared to other anomalies recorded on the territory of Georgia, are of moderate intensity [2]. The anomaly intensity increases towards the river Supsa from the south as well as from the north. The magnetic absorbability of the sand and percent contents of ferromagnetic minerals in the samples increase similarly. It strengthens the assumption that the source of the magnetic sands distributed on the territory is the river Supsa (together with other short rivers), which washes away the outcropped, distinguished with high magnetism, the middle Eocene volcanogenic rocks from the river gorges and takes them down to the sea [2].

References

1. Nodia M. The magnetic anomaly in Guria and some of its characteristics. // Bulletin of the Academy of Sciences of Georgian SSR, vol. 11, N5, 1941.
2. Gogua R. The magnetic field and magnetism of magmatic rocks. // M. Nodia Institute of Geophysics of Iv. Javakhishvili Tbilisi State University, Tbilisi, 2017.

GEORGIA, GURIA REGION, FRAGMENTARY GEORADAR SURVEY OF THE FORMER TERRITORY OF THE SOVIET UNION RESEARCH INSTITUTE OF RADIATION PLANT AGRONOM

Odilavadze D., Ghlonti N., Yavolovskaya O.

Ivane Javakhishvili Tbilisi State University, Mikheil Nodia Institute of Geophysics
davit.odilavadze@tsu.ge

Summary: *In Georgia, in the Guria region, the territory with signs of radioactive contamination was surveyed by the GPR method. Interpretation of crossed GPR profiles for possible subsurface underground objects revealed the existence of simple and mixed burial grounds.*

Key words: *georadar survey, Zond 12-e, GPR method, Prism-2.5 software*

Introduction. The Research Institute of Radiation Agronomy of Plants was located and operated on the territory of Georgia, in the Guria region since the 1960s, at present, the remains of the institute building, the remains of the perimeter of the foundation, the remains of a number of demolished buildings have survived. Inside the ruins of the site of the institute and around it there were signs of radiation pollution, the sources of which could be located under the day's surface in more or less protected conditions.

Purpose. The purpose of the study by the GPR method [1, 2, 3, 4] was to determine the radio images of objects, their location, shape and location of possible underground objects [5,6,7] in pre-designated places.

Instrumental part. Georadar works were carried out by the Georadar "Zond 12-e" with its standard antennas at frequencies of 150 MHz and 75 MHz, the data were collected and processed using the "Prism-2.5" software.

Working environment. The work was carried out on the territory, the soil of which consists of red soil, it is located in the southwestern part of the humid subtropical zone (Adjara, Guria) at an altitude of about 100-300 m above sea level and occupies a hilly area. Red soil is characterized by heavy clay, clay texture and heavy clay. The red color is due to the content of ferric iron.

Fig. 1. Photo shows zone-2 of the study area. White lines mark the directions for conducting GPR profiles.

Results and discussion. Fig. 1 is a photograph of the surface of one of the sites in the study area, radiograms of transverse GPR profiles and the results of their interpretation.

The location of the boundaries of the cavity environment is indicated in the center of the profile-2a (Fig. 2) at depths of 1-4.5 m from the surface and at distances from 2 to 7 m. Some probable cavities are marked with white lines. The depth of their placement is 0.5-1.5 m, the distance is 5.5 m.

Clearly distinguishable from the environment, walls, floor, base. The radio image is obtained as a result of reflection and refraction of electromagnetic waves from the surfaces that form the cavity of the desired object.
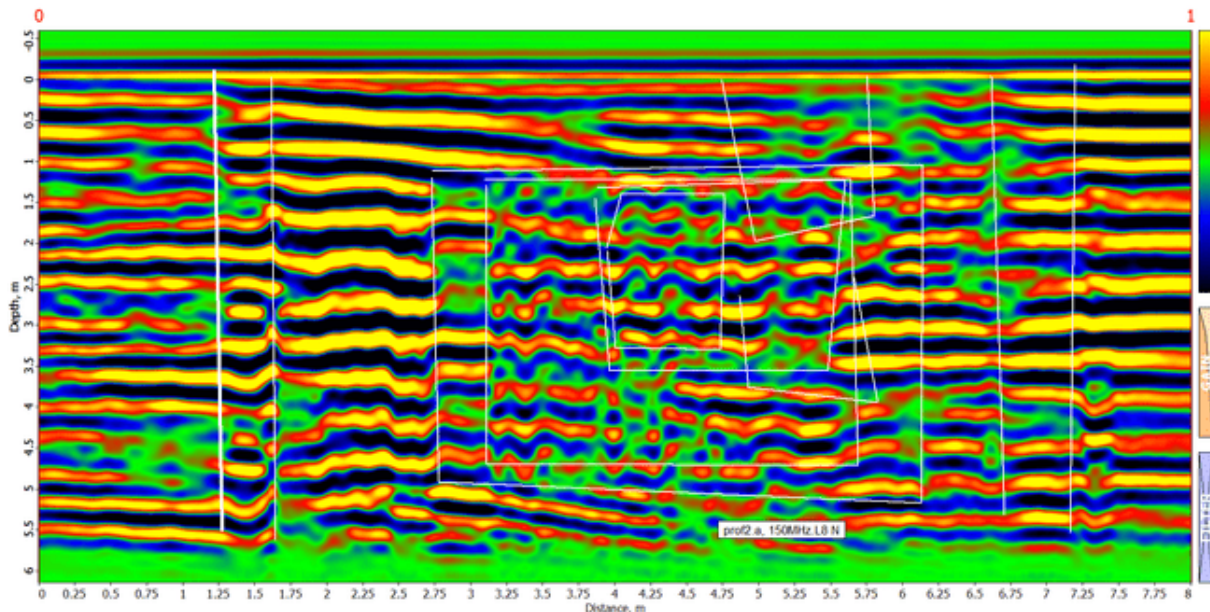
Fig. 2. The radarogram shows a GPR section (profile-2a) 6 m deep and 8 m long, made by the Zond 12e GPR with its standard 150 MHz dipole antenna.
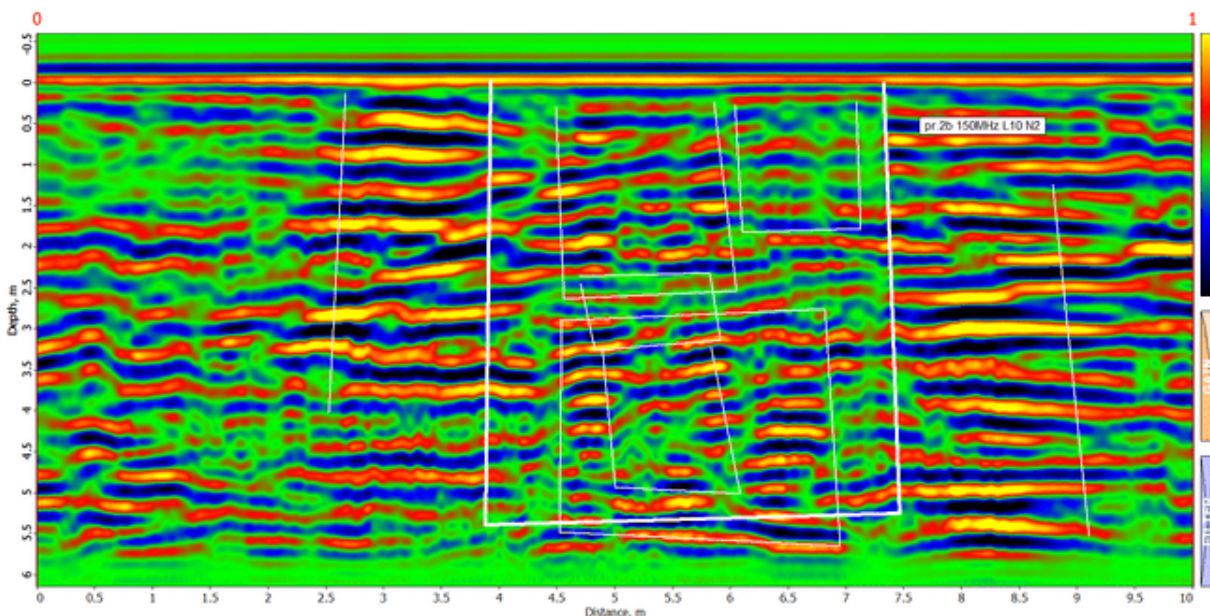
Fig. 3. Shows a GPR section (profile-2b) 6 m deep and 10 m long, made by the "Zone 12" GPR with its standard 150 MHz dipole antenna.

A probable cavity is indicated in the center of profile-2b (Fig.3), an approximate depth at a distance of 4.5-5 m from the surface and at a distance of 4-7 m, possible cavities are marked with white lines in the center of the radarogram. The walls of the cavity are at distances of 3-4 m and 8-9 m.

Profiles 2a and 2b are in good agreement with each other and clearly distinguish the marked cavity.

Conclusion. Fragmentary GPR studies [8, 9] in the marked areas of the former territory of the Research Institute of Radiation Agronomy of Plants revealed a variety of radioactive images, indicating the existence of various types of burial grounds and underground structures for the protection of radioactive waste. The location, shape and, in some cases, identification of possible underground targets have been determined.

References

1. Odilavadze D., Ghlonti N., Tarkhan-Mouravi A. Subsurface Monitoring of Near-Surface Burial Sites Storages in Seismically Active Territories. // International Scientific Conference „Natural Disasters in Georgia: Monitoring, Prevention, Mitigation", Proceedings, Tbilisi, Georgia, December 12-14, 2019, pp. 50-53.
2. Odilavadze D.T., Chelidze, T.L. Physical Modeling of Lava Tubes in the GPR. // Mikheil Nodia Institute of Geophisics, Transactions, vol. LXVII, ISSN 1512-1135, Publishing house of the Tbilisi State University, Tbilisi, 2017, pp. 129-142.
3. Odilavadze D., Chelidze T., Tskhvediashvili G. Georadiolocation Physical Modeling for Disk-Shaped Voids. // Journal of the Georgian Geophysical Society, Physics of Solid Earth, vol. 18, 2015.
4. Одилавадзе Д.Т., Челидзе Т.Л., Глонти Н.Я., Кирия Д.К., Тархнишвили А.Г. Физическое моделирование модели типа "слоистый клин" в прямых и обратных задачах георадиолокации, 2018.
5. Neal A. Ground-Penetrating Radar and its Use in Sedimentology: Principles, Problems and Progress. // Earth-Sci. Rev., 66, 2004, pp. 261—330.
6. Negi J. G., Gupta C. P. Models in Applied Geoelectromagnetics. // Earth Sci. Rev., 4, 1968, pp. 219-241.
7. О Одилавадзе Д. Т., Челидзе Т. Л. Физическое моделирование георадиолокационного поля в прямой и обратной задачах электродинамики. // Geophysical Journal, v.35, №4, 2013 (in Russian).
8. Sena D'Anna A. R. Modeling and Imaging of Ground Penetrating Radar Data. // Texas: The University of exas at Austin, 2004, 251 p. (repositories. Lib.Utexas. edu).
9. Sharma P.V. Environmental and Engineering Geophysics. // Cambridge: Cambridge University Press, 1997.

VERTICAL ELECTRICAL SOUNDING AND GEORADIOLOCATION TO ASSESS LANDSLIDE AREA WATER SATURATION

Varamashvili N., Odilavadze D., Kiria J., Ghlonti N., Tarkhan-Mouravi A., Amilakhvari D.

Ivane Javakhishvili Tbilisi State University, Mikheil Nodia Institute of Geophysics, Tbilisi, Georgia
ldvarama@gmail.com

Summary: *The vertical electrical sensing method is effectively used by studying landslides. The georadiolocation method is also a powerful tool for studying structure and watering at shallow depths. The paper presents a brief analysis of the landslide works carried out in 2021 on Machavariani Street in Tbilisi. For the landslide study the methods of vertical electrical sounding and ground penetrating radar were used. Together, these two methods yielded reliable results at different search depths, which was additionally confirmed during the drilling process.*

Key words: *Vertical electrical sounding (VES), georadiolocation, Landslide*

Introduction

In the spring of 2021, a landslide activated on Machavariani Street in Tbilisi, endangering the surrounding road and territory. Along with other research works, geophysical surveys were conducted in the landslide area, including methods of vertical electrical sensing and georadiolocation. The study was conducted with modern equipment (Fig. 1a), by the method of vertical electrical sounding. The measurements were performed with modern Italian (PASI GL-15N) equipment (Fig. 1 a).Ground-penetrating radar work was carried out using the Zond-12e GPR (Fig.1b).

Fig.1. a) Earth Resistivity Meter PASI 16GL-N, b) ground penetrating radar ZOND 12

Electroprospecting

In electroprospecting (resistance method) electric currents are injected into the ground and the resulting potential differences are measured at the surface, yielding information about the distribution of electrical resistivity below the surface. Finaly this gives an indication of the lithological and structural variation of the subsoil (since resistivity depends on sediment porosity and pore water).

On March 29, 2021, electrical prospecting works were carried out on the landslide on Machavariani Street by the method of vertical electrical sounding. The measurement was performed at two points (Fig. 2). The paper presents the results of measurements performed in the language of landslides in the first point (Vashlijvari1).

N	ρ	h	d	Alt
1	62.6	22.1	22.1	-22.07
2	32.9	46	68	-68.04
3	18			

a.   b.
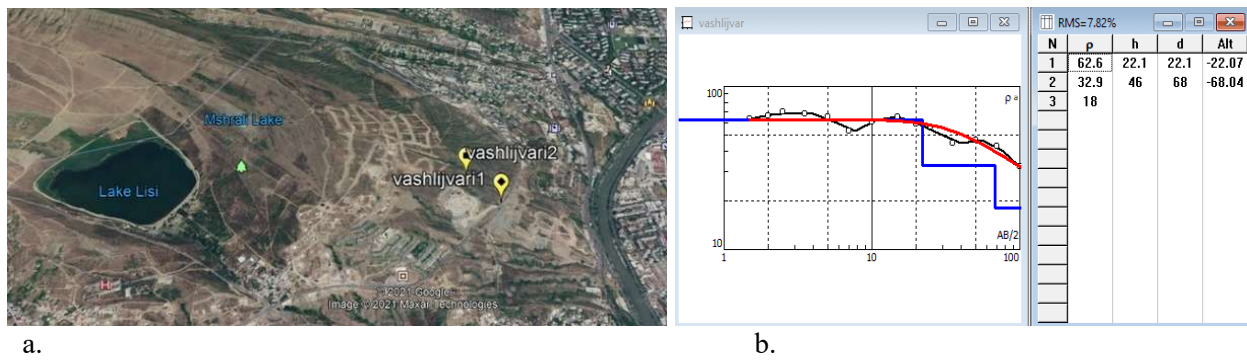
Fig.2. a) Location of vertical electrical sounding points on the landslide body. b) Vertical electrical sounding curve obtained by measurement near the landslide toe.

The first measurement was performed near the landslide toe, on Machavariani Street (Fig. 2a). The measurement was performed by the vertical electrical sounding method, with the Schlumberger spread. The maximum spread of the power electrodes was 100 meters. The corresponding vertical electrical sounding curve is shown in Fig.2 b.

The analysis of the vertical electrical sounding curve shown in Fig. 2b allows us to assume that a clay-enriched layer starts from a depth of about 25-30 m. The clay-enriched layer, under certain conditions, can play the role of a sliding surface. This result is quite consistent with the results obtained by drilling wells in the vicinity of the vertical electrical sounding point.

Georadiolocation prospecting

What is GPR? The GPR emits ultra-wideband pulses in the meter and decimeter range of electromagnetic waves and receives signals reflected from irregularities, objects or other inclusions in the soil that have a dielectric conductivity different from the medium. In order to obtain data from different depths, antenna units are used that operate at different frequencies. It is necessary to take into account the general rule: the lower the operating frequency of the antenna, the higher the signal penetration depth, but the lower the antenna resolution. GPR allows the operator to "see" through water, soil and stone.

In our case, we use the GPR Zond 12- e with our standard receiving and transmitting antenna using a frequency of 75 MHz (Fig.1). To receive and process georadar data, we use the PRIZM 2.5 software.

Four 50-meter profiles were selected on the section of Machavariani Street near the Vashlijvari landslide and georadiolocation works were carried out (Fig.4). For our work, we selected the results obtained by measuring with a 75 MHz dipole antenna, for the second precinct, located near the vertical electrical sensing point (vashlijvari1, Fig.1a). We were interested in how the results of vertical electrical sensing and georadolocation work correlated with each other.

Fig.3. Georadar work area along the concrete wall
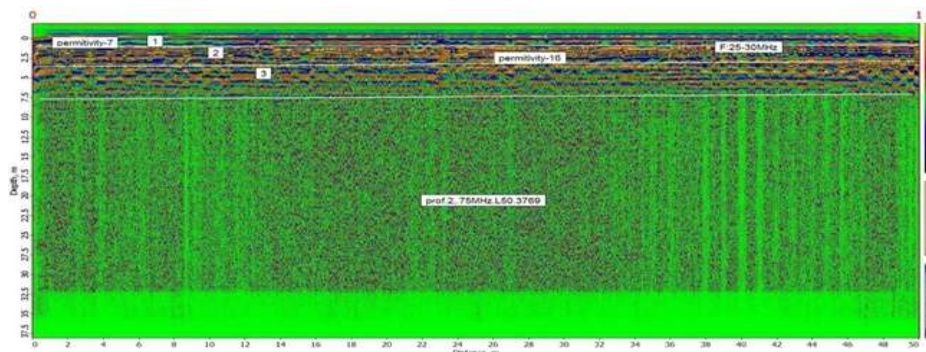
Fig.4. Prof.2, radarogram performed by Georadar Zond-12e, software Prizm 2.5, staff dipole antenna 75 MHz, distance -50 m.

On the 75 MHz radarogram of Prof.2 (Fig. 5) a georadiolocation layer -1 with electromagnetic wave synchronization axes about 1 m thickness, was distinguished, the texture being different from the second layer-2, whose relative dielectric permeability corresponds to that of mixed clay. Layer-2 is about 7.5 meters thick. Next, the texture layer is distinguished by a vertical layering, homogeneous clays, and crumbling limestone. Layer-2, for depths of 3-4 m, is characterized by a high level of hydration, and from a distance of about 26-30 m, to the end of the profile contains signs of watering.Therefore, with the activation of geodynamic processes, this section of the road can play the role of a sliding surface and contribute to the intensification of landslide.

Conclusion

1.Georadiolocation and electrometric search methods are effective in determining groundwater levels, lithology of subsurface and estimating moisture of the subsurface rock. Also, to evaluate the thickness of moistened areas.

2.Each of these methods has its limitations. In the complex they complement each other and can be used without geological restrictions.

3. The results of vertical electrical sounding and georadiolocation measurements, based on the available materials, correlate with each other to determine the possible location of the sliding surface.

4. However, it should be noted that the work done is not sufficient to study the issue in depth. Further studies are needed.

References

1. Varamashvili N., Chelidze T., Devidze M., Chikhladze V. Laboratory and mathematical modeling of landslides triggered by external factors. Field research. // Transactions of Mikheil Nodia Institute of Geophysics of Ivane Javakhishvili Tbilisi State University, vol. LXVIII, Monography, Tbilisi, 2017, (in Georgian).

2. Chelidze T., Varamashvili N., Chelidze Z., Kiria T., Ghlonti N., Kiria J., Tsamalashvili T. Costeffective telemetric monitoring and early warning systems for signaling landslide initiation. // Mikheil Nodia Institute of Geophysics of Ivane Javakhishvili Tbilisi State University. Monography. Tbilisi, 2018, (in Georgian).

3. Varamashvili N., Tefnadze D., Amilaxvari D., Dvali L., Chikadze T., Qajaia G. Vertical electric sounding in water search tasks and for landslide hazards assessment. // International Scientific Conference „Modern Problems of Ecology", Kutaisi, Georgia, 21-22 September, 2018.

4. Odilavadze D., Tarkhan-Mouravi A.,Varamashvili N., Arziani Z. Prevention of the Danger Triggered by an Earthquake of Exogenous and Endogenous Processes, using a Combination of Geophysical-Geoelectric Methods In Geotechnics. // International Scientific Conference Natural Disasters in Georgia: Monitoring, Prevention, Mitigation, Tbilisi, 2019.

5. Varamashvili N.D., Tefnadze D.V., Amilaxvari D.Z., Dvali L.B., Chikadze T.G., Qajaia G.T., Varamashvili D.N.. Water search and landslides study using electroprospecting. // Journal of the Georgian Geophysical Society, 22(1), 2019.

6. Odilavadze D.T., Varamashvili N.D. Vertical electrical sounding and georadiolocation to assess groundwater level during orchard cultivation. // Journal of the Georgian Geophysical Society, 23(2), 2020.

RADAR STUDIES OF FORMATION AND DEVELOPMENT OF HAIL CLOUDS

*Liev K.B., *Kushchev S.A., **Anischenko E.A.
.
*High-Mountain Geophysical Institute, Nalchik, Russia
** Kabardino-Balkarian State University named after H. M. Berbekov, Nalchik, Russia
Stasuk6@mail.ru

Summary: The results of analysis of long-term radar observations of hailstorms are presented. The dynamic characteristics of formation and development of hail cores in severe convective clouds are studied. The statistical sample of radar data included 764 hail cells; for each cell the temporal distributions of measured and computed major radar parameters were constructed using the automated system of acquisition, processing, and presentation of radar data. The most informative time characteristics of hail cores development and the interrelation between them were identified. The natural variability of hail core volume is demonstrated.

Key Words: First hail storm echo, hail core, hail core volume, radar reflectivity, dual-wavelength hail detection method.

Introduction. The researching of the processes of hail initiation and growth by radar methods has become more popular during last years because of the development and improvement of automated systems of collecting and processing of radar data on hailstorms. With the help of these programs researchers can calculate parameters of hailstorms and track their change. The radar studies of the dynamic characteristics of the formation and development of hail sources in powerful convective clouds in the area of Kabardino-Balkarian Republik are the purpose of this work.

Methods. The authors has collected the results of complex radar studies of hailstorm processes which were made on scientific proving ground of High-Mountain Geophysical Institute from 2003 to 2018. The statistical sample included 801 cases of registration of hail cells. The researching were made with the help of two-wave meteorological radar MRL-5, automated systems of collecting of radar data MeteoX and the database of radar characteristics of hail clouds [1]. The radar observations were carried out continuously from the moment the first radio echo appeared to the complete dissipation of the cloud. The period between the observations was about 3 minutes. For the researching were built temporal allocations of the main radar parameters (fig.1) both measured and calculated within the framework of the used automated system for collecting and processing information. Further analysis included the construction of distributions of four parameters which characterizing the process of formation and development of hail sources in powerful convective clouds [2]:
     — dT^1 — the period from the registration of the first radio echo of the hail cloud to the indication of hail in the cloud;
     — dT^2 — the period from the indication of hail to the maximum volume of the hail focus is reached in the cloud;
     — dT^3 — the total time of the existence of the hail hearth;
     — dT^4 — the period from the reaching the maximum volume of the hail source in the cloud until the indication of hail in the cloud stops;
     — V — the maximum value of the volume of a hail chamber in a cloud for the entire time of its existence.
     As we can see on Fig.1 the hail in the cloud appeared at 17:41 and its volume was 0.5 km^3; the period from the registration of the first radio echo of the hail cloud to the indication of hail in the cloud (dT^1) was 11 minutes. At 18:50, the maximum value of the volume of the hail source in the cloud (V) 84 km^3 was

reached; the period from the indication of hail to the achievement of the maximum volume of the hail source in the cloud (dT2) was 80 minutes. At 19:17, the volume of hail in the cloud became equal to 0, and the total lifetime of the hail focus was 96 minutes.
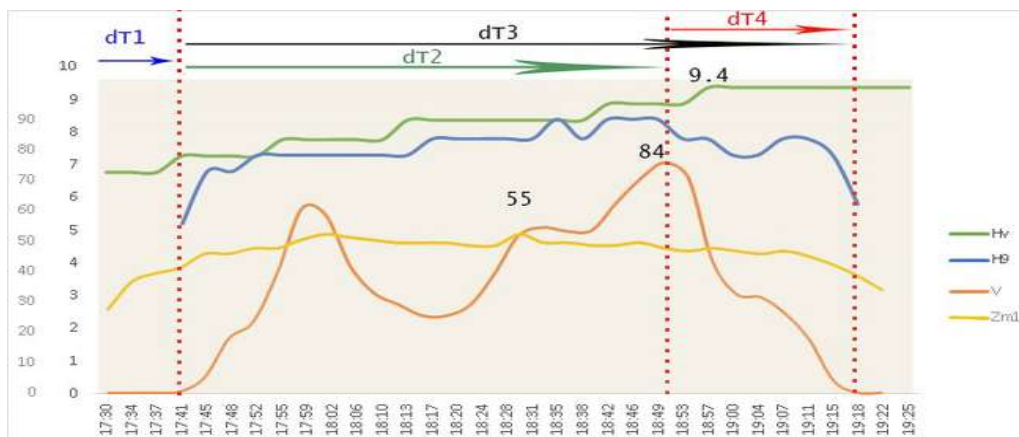

Fig.1. Time distributions of the main radar parameters.

With the help of method, 764 hail cells were analyzed. For each of the above time parameters dT_1, dT^2, dT^3, dT^4 characterizing the process of formation and development of hail sources, distributions were constructed showing the range of variation of each parameter.

Results and discussion. Both of the parameters on Fig.2 depends on the nature of the course of certain different microphysical processes at different stages of the development of the hail cloud.

a)

b)

c)

d)
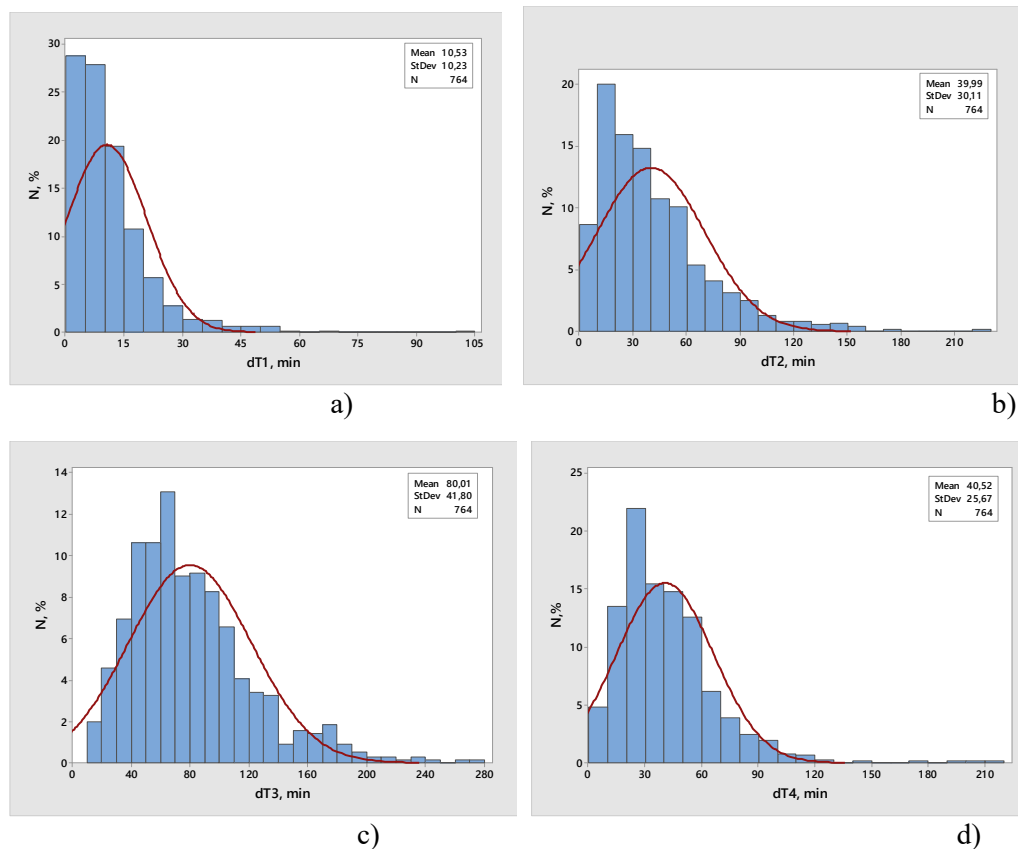
Fig.2. Distribution of temporal characteristics of the formation and development of hail foci dT^1 (a), dT^2 (b), dT^3 (c), dT^4 (d) for 764 hail cells that developed on the territory of the Kabardino-Balkarian Republic from 2003 to 2018.

As we can see on Fig.2 the average time of registration of a hail focus from the moment the first radio echo appears (dT^1) is 10 minutes, the minimum time before the appearance of a hail in the cloud is 3 minutes, and the maximum time is 102 minutes, but this is an isolated case. This stage is preceded by a long time of cloud development before the appearance of the first radio echo.

The time from the moment of the hail indication to the time of registration of the maximum volume of the hail hearth (dT^2).

This parameter is significantly influenced by the rate of the ascending flow and the water content in the hail growth zone, as well as their optimal ratio [3]. As seen in Fig. 2b, the average time of development of the maximum value of the hail focus is 39 minutes, the minimum time is 3 minutes and maximum 229 minutes.

The lifetime of a hail source (dT^3) often depends on the ratio of the energy storage of the atmospheric instability and wind shear. With a low energy of instability, the lifetime of a hail source in most cases is less than 30 minutes. At low wind shear, the cells are also short-lived, due to the suppression of ascending flows by precipitation [4]. As can be seen from Figure 2c, about 7% of such cells are investigated. The maximum time of the existence of a hail focus of 280 min was shown by a supercell hail cloud on July 10, 2003. In total, the average time of existence of a hail focus in a cloud is 80 minutes.

Time from the moment of registration of the maximum volume of the hail focus to its disappearance (dT^4). As we can see in Fig. 2d, the average time of this parameter is 40 minutes, the maximum is 220 minutes.

Conclusion. The analysis of the data gives us an understanding of how rapidly the hail cloud is developing. This information can be especially useful in case of active influence on hail cells, it gives information on how quickly a hail focus can develop. Unfortunately, the dependence of the time of the existence of a hail source dT^3 on the time of the appearance of the first radio echo until the time of the appearance of a hail source in the cloud dT^1 was not found. This regularity would make it possible to estimate the lifespan of a hail cloud based on the first measurements of the cloud parameters. But the correlation between the total time of existence of a hail focus (dT^3) and the time from the indication of hail to reaching the maximum volume of a hail source in the cloud (dT^2) is 0.79.

References

1. Inyukhin V. S., Kushchev S. A., Liev K. B. Radar studies of the distribution of the formation zones of the first radar echoof hail clouds. // Izvestiya. Atmospheric and Oceanic Physics. B. 52, No. 6, 2016, pp. 615–621.
2. Inyukhin V.S., Makitov V.S., Kushchev S.A. Radar studies of formation and development of hail cores in severe convective clouds. // Russian Meteorology and Hydrology. T. 42, № 7, 2017, pp. 471–476.
3. Liev K.B., Kushchev S.A., Inuhin V.S., Anischenko E.A. Movements of hail cells on the territory of the Kabardino-Balkarian Republic in 2017. // IOP Conference Series: Earth and Environmental Sciencethis link is disabled, 840(1), 2021, pp. 12-20.
4. Makitov V. Radar measurements of integral parameters of hailstorms used on hail suppression projects. // Atmos. Res., vol. 83, 2007, pp. 380—388.

MODERN METEOROLOGICAL RADAR "WRM200" IN KUTAISI (GEORGIA)

Gvasalia G., Loladze D.

National Environmental Agency of Georgia, Tbilisi, Georgia
gvantsigvasalia@gmail.com

Summary: *The description and technical characteristics of the new meteorological radar "WRM200", installed in Kutaisi (Georgia) in 2021, in order to monitor the weather in Western Georgia, are provided. The technical characteristics of this radar were compared with the "Meteor 735CDP 10" radar installed earlier in 2015 in the village Chotori (Kakheti) for the needs of anti-hail service.*

Key Words: *meteorological radar, radar observation.*

Introduction

At present, meteorological radars are widely used all over the world. They have a wide range of capabilities and are tailored to the needs of a particular country. In addition to storm warning and meteorological support, these radars are also an effective means of obtaining information about the state of cloud cover after physical and chemical impact on its in order to prevent showers and hail, or increase precipitation in arid regions. In particular, in the sixties-eighties of the last century in Georgia, a large number of meteorological radars were used when carrying out anti-hail work [1,2]. These works continued until 1989 and were renewed using newest technologies in Kakheti region of Georgia in 2015 [3-5]. Accordingly, radar observations were also discontinued.

The anti-hail service is equipped with a modern meteorological radar "METEOR 735 CDP 10" [6,7], which in the future, in addition to anti-hail activities, is planned to be used for operational monitoring of different dangerous hydro-meteorological processes in eastern Georgia and adjacent territories [8].

In parallel with this, the National Environmental Agency of Georgia also began to be equipped with modern meteorological radars. In 2021, the Vaisala Weather Radar "WRM200" made in Finland was launched in Kutaisi (Western Georgia) [9,10]. It is a dual polarization Doppler weather radar with real-time hydrometeor classification software. Its location allows you to monitor changes in weather and precipitation within a radius of up to 200 km. The distance to the Black Sea coast (Poti) does not exceed 95 km, and the distance to Anaklia and Batumi is 115 and 125 km, respectively. This is already the second modern weather radar in Georgia (if we do not take into account specialized aviation weather radars).

The brief technical characteristics of the "WRM200" meteorological radar are presented below [9,10]. Comparison of the technical characteristics of the radars "WRM200" and "Meteor 735CDP10" is also given.

Results

Results in fig. 1-2 and table 1 are presented.

With new solutions and innovative designs, Finnish Vaisala has become a leading supplier of C meteorological radars. A high quality, high performance antenna with the world's best "

Sigmet" signal processor and IRIS software guarantee high quality radar data that meets even the most stringent dual polarization requirements for the most demanding clients. The state-of-the-art design and high quality fabrication of the antenna and rack also contribute to low maintenance costs throughout the life of the system [9,10]. Appearance of the radar "WRM200" in Kutaisi in fig. 1 is presented.
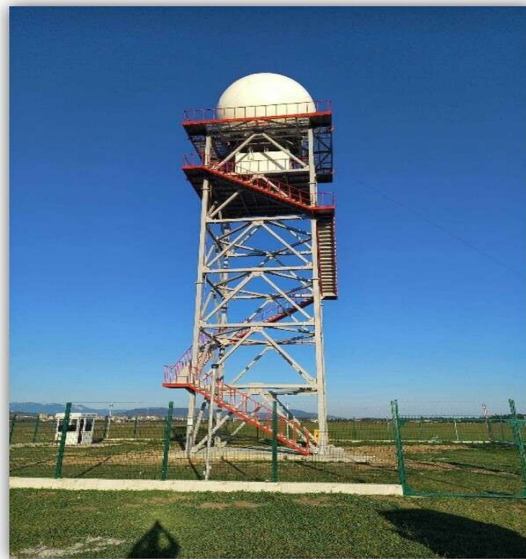

Fig. 1. Appearance of the radar "WRM200" in Kutaisi.

The radar data are telemetrically sent to Tbilisi, where they are continuously analyzed in the National Environmental Agency of Georgia. In fig. 2 shows one of the images from the monitor of this radar as an example.
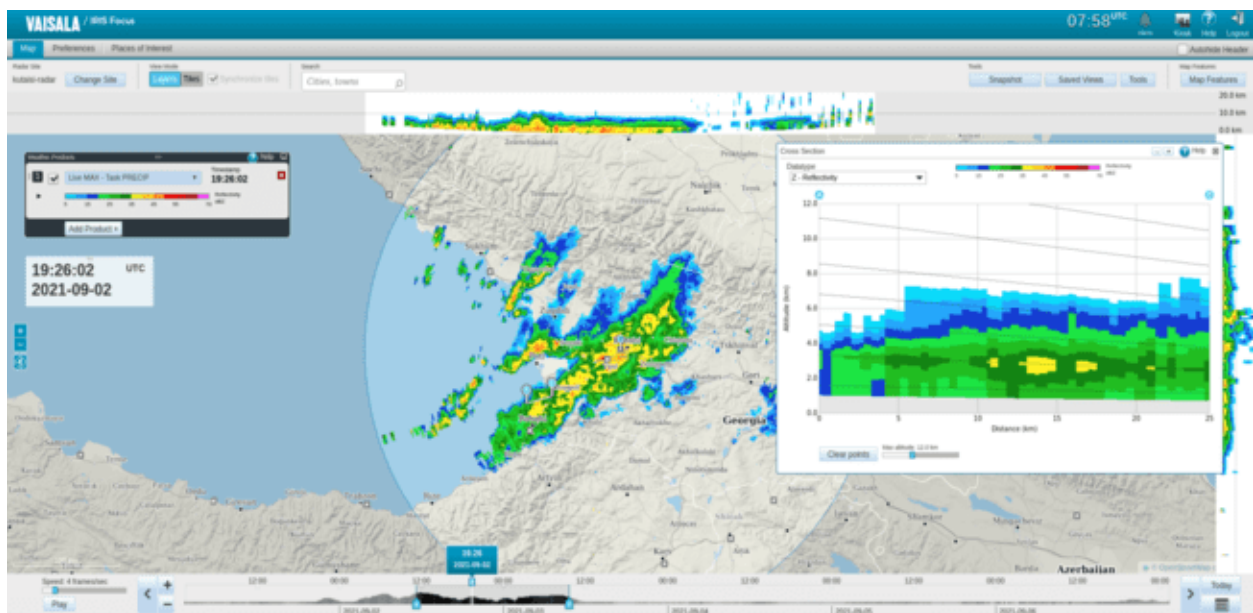
Fig. 2. Screenshot of the monitor of the "WRM200" radar in the National Environmental Agency of Georgia in Tbilisi.

Dual Polarization Adds New Dimension The WRM200 [9] is Vaisala's new dual polarization C-band magnetron Doppler Weather Radar. The radar operates in either STAR mode (simultaneous transmit and receive of H and V) or LDR mode (linear depolarization mode, during which H alone is transmitted and

both are received). STAR mode enables use of the high sensitivity power estimator increasing detectability by up to 10 dB versus the competition. The polarization variables, depending on the mode, are ZDR, RHOHV, PHIDP, KDP and LDR. However, the goal of a polarization radar is not only to produce and display these outputs; rather it is to expand the capabilities of the radar for the operational forecaster. The WRM200 provides the following benefits: Hydrometeor identification; Attenuation correction; Data quality improvement; Improved rainfall estimates HydroClass™ - Seeing much More HydroClass™ software uses polarization measurements in a proven fuzzy logic algorithm to classify targets into categories. i.e. hail, graupel, rain, snow, wet snow or non-meteorological targets (such as sea clutter, birds, insects, wind turbines, interference, or military chaff). While traditional Doppler clutter filtering can remove stationary targets, HydroClass™ can also remove moving non-meteorological targets like sea clutter. The benefit is improved data quality and more accurate warnings for hazardous weather such as hail.

Attenuation by intervening heavy precipitation has been a long-standing problem with C-band weather radars, making S-band radars preferable, especially in tropical environments where heavy rain is common. However, with dual polarization, a radar performs accurate, real-time attenuation corrections. The benefit is that you can obtain the same precipitation measurement accuracy using the WRM200 as with an S-band system that typically costs two or three times more. Experience, Innovation and Dependability Vaisala Sigmet Product line has three decades of experience in providing signal and data processing systems for dual polarization applications, and delivers more dual polarization processing systems than any other manufacturer. Vaisala and Sigmet, as a part of Vaisala, continue developing the dual polarization applications with respected consultants in the research community [9].

In table 1 information about comparison of the technical characteristics of "WRM200" (Kutaisi) and "Meteor 735CDP10" (Chotori, Kakheti) radars are presented.

Table 1. Comparison of the technical characteristics of "WRM200" and "Meteor 735CDP10" radars.

Technical characteristics	WRM200 (Kutisi)	Meteor 735CDP10 (Chotori)
Working frequency range	5.5-5.7 GHz	5.43 – 5.80 GHz
Peak power	250 kw	400 kw
Pulse width	0.5; 0.8; 1.0; 2.0 μs	0.5 – 3.3 μs
Pulse repetition rate	200 - 2000 Hz	250 – 2000 Hz
Working range	200 km	100 - 300 km
Resolution	15 m	15 m
Resolution elements	3096	20000
Antenna diameter	4.5 m	4.3 m
Beam width	<1 degree	<1 degree
Elevation range	from -3 to 110 degrees	from -2 to 182 degrees
Max. scanning speed	40 deg/sec	36 deg/sec
Acceleration	20 deg/sec²	20 deg/sec²
Positioning accuracy	0.1 deg	0.1 deg
Antenna gain	45 dB	44.5 dB
Cap diameter	6.7 m	6.5 m
Cap material	Fiberglass + polyurethane	Fiberglass + polyurethane
Losses in the cap	Less than 2 dB	Less than 0.3 dB
Receiver dynamic range	95 dB	105 dB

As follows from Table 1, many technical characteristics of these radars are close to each other (working frequency range, pulse repetition rate, resolution etc.). There are some differences though. For example, peak power, working range, elevation range etc.

Below are the distinctive features of the WRM200 meteorological radar [10]:
- 250 KW magnetron transmitter with low-maintenance solidstate modulator
- High sensitivity mode processing to recover sensitivity loss in STAR mode. - Vaisala's lightweight, semi-yoke style pedestal
- 1 degree beamwidth low side lobe antenna
- >35 dB integrated crosspolarization isolation
- Precision horizontal and vertical beam matching

- Modular single cabinet design containing transmitter, receiver, controller, processor, dehydrator, polarization waveguide assembly
- Built around Sigmet RVP900, RCP8, IRIS software
- Dual channel digital IF receiver
- Built-in automatic dual channel calibration
- Image rejection >80 dB (>100dB with Vaisala WG filters)
- Dynamic range >99 dB (2μs pulse)
- Integral flat screen display for local maintenance
- Remote control/monitoring
- HydroClass™ for real-time target identification (hail, graupel, rain, snow, wet snow, non-met)
- Accurate attenuation correction
- Rainfall estimation based on KDP
- Option: Low-loss, random

Conclusion
The commissioning of the meteorological radar "WRM200" in Kutaisi will provide the ability to timely detect, observe and predict in real time adverse atmospheric phenomena, such as severe hurricanes, hail, rainstorms and floods in Western Georgia.

References

1. Amiranashvili A.G. History of Active Effects on Atmospheric Processes in Georgia. // In the book: Essays of the History of Weather Modification in the USSR and the Post-Soviet Territory, ISBN 978-5-86813-450-0, St. Petersburg, RSHMU, 2017, 352 pp., ill., pp. 234-254, (in Russian), http://mig-journal.ru/toauthor?id=4644.
2. Abaiadze O., Avlokhashvili Kh., Amiranashvili A., Dzodzuashvili U., Kiria J., Lomtadze J., Osepashvili A., Sauri I., Telia Sh., Khetashvili A., Tskhvediashvili G., Chikhladze V. // Radar Providing of Anti-Hail Service in Kakheti. Trans. of Mikheil Nodia Institute of Geophysics, ISSN 1512-1135, vol. 66, Tbilisi, 2016, pp. 28-38, (in Russian).
3. Amiranashvili A., Ghlonti N., Dzodzuashvili U., Lomtadze J., Chikhladze V. On the renewal of anti-hail works in Georgia. // Int. Conf. "Advanced Problems in Geophysics". // Reports, presented on the Scientific Conference "80 years of the M. Nodia Institute of Geophysics". Tb., 2014, pp. 208-212, (in Russian).
4. Amiranashvili A.G., Chikhladze V.A., Dzodzuashvili U.V., Ghlonti N.Ya., Sauri I.P. Reconstruction of Anti-Hail System in Kakheti (Georgia). // Journal of the Georgian Geophysical Society, ISSN: 1512-1127, Issue B. Physics of Atmosphere, Ocean and Space Plasma, vol. 18B, Tb., 2015, pp. 92-106.
5. Amiranashvili A., Burnadze A., Dvalishvili K., Gelovani G., Ghlonti N., Dzodzuashvili U., Kaishauri M., Kveselava N., Lomtadze J., Osepashvili A., Sauri I., Telia Sh., Chargazia Kh., Chikhladze V. // Renewal works of anti-hail service in Kakheti. Trans. of Mikheil Nodia institute of Geophysics, ISSN 1512-1135, vol. 66, Tb., 2016, pp. 14 – 27, (in Russian).
6. Selex ES GmbH · Gematronik Weather Radar Systems. // Rainbow®5 User Guide, 2015, 464 p., www.gematronik.com
7. Avlokhashvili Kh., Banetashvili V., Gelovani G., Javakhishvili N., Kaishauri M., Mitin M., Samkharadze I., Tskhvediashvili G., Chargazia Kh., Khurtsidze G. / Products of Meteorological Radar «METEOR 735CDP10». Trans. of Mikheil Nodia Institute of Geophysics, ISSN 1512-1135, vol. 66, Tb., 2016, pp. 60-65, (in Russian).
8. Amiranashvili A., Chikhladze V., Dzodzuashvili U., Ghlonti N., Sauri I., Telia Sh., Tsintsadze T. Weather Modification in Georgia: Past, Present, Prospects for Development. // International Scientific Conference „Natural Disasters in Georgia: Monitoring, Prevention, Mitigation", Proceedings, Tbilisi, Georgia, December 12-14, 2019, pp. 213-219.
9. http://www.vaisala.ru/ru/meteorology/products/weatherradars/Pages/default.asp
10.   WEA-MET-WRM-200-Datasheet-B210698EN-E-LOW

SOME EXAMPLES OF THE CLOUDINESS MONITORING WITH MODERN METEOROLOGICAL RADAR "WRM200" IN WESTERN GEORGIA

Gvasalia G.

National Environmental Agency of Georgia, Tbilisi, Georgia
gvantsigvasalia@gmail.com

Summary: *Some examples of the cloudiness monitoring with modern meteorological radar "WRM200" in Western Georgia are presented. In particular, the radar data for September 2-3, 2021, when intense precipitation and tornado were observed on the Black Sea coast of Georgia (the city Kobuleti) are given.*

Key Words: *meteorological radar, radar observation, cloudiness.*

Introduction

As is known, since 2015, the anti-hail service working has been resumed in Eastern Georgia (Kakheti). This service is equipped with a modern radar station "Meteor 735CDP 10" [1]. In recent years, a number of works have presented the results of studies of some atmospheric phenomena in Eastern Georgia and neighboring countries (Azerbaijan, Armenia) using this radar: hail processes [2-5], precipitation [6-8], dust migration [9] and others [10].

Since 2021 in Kutaisi (Western Georgia) to monitor atmospheric processes in this region, National Environmental Agency of Georgia installed a modern radar "WRM200" [11].

Some examples of the cloudiness monitoring with this radar in Western Georgia are presented below.

Study area, data description

Study area: Western Georgia. Data on radar reflectivity (dBz) of clouds of radar "WRM200" installed in Kutaisi are used (product – Live Max). A description of the technical characteristics of this radar is presented in [11,12]. Data from an VAISALA automatic weather station for September 2-3, 2021 installed in Kobuleti were also used.

Results and discussion

Results in fig. 1-5 are presented.

On September 1, 2021, the National Environmental Agency of Georgia issued a warning about deteriorating weather in Western Georgia. In particular, it said that heavy rainfall with a thunderstorm, as well as a strong westerly wind, were expected on September 2-3. According to the synoptic description, the weather in Western Georgia was caused by the interaction of masses of cold and humid air coming from the north-west of the Black Sea and masses of warm air acting from the south. Further, based on the data received from the "WRM200" meteorological radar, a short-term warning was issued about the deterioration of the weather in this region of Georgia.

These data are clearly visible in the images taken from the radar screen (fig. 1, 2). Areas of heavy precipitation are clearly visible, the reflectivity of clouds is about 40-45 dBz, which is also clearly visible on the vertical sections of the clouds. Simultaneously with the noted intensity of the development of processes, the height of the clouds also grows. So, for example, on September 2, the height of the clouds was about 8 km (fig. 1), and on September 3, it exceeded 9 km (fig. 2).
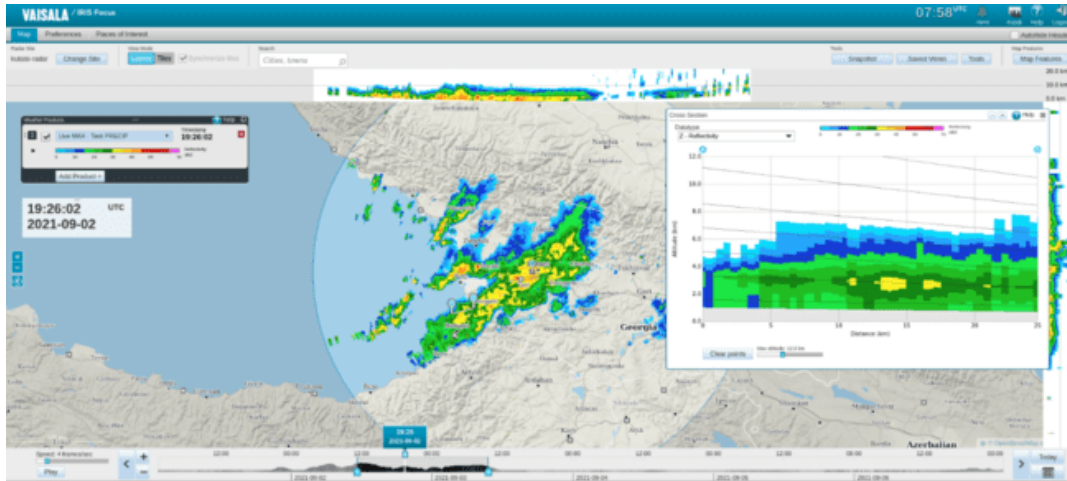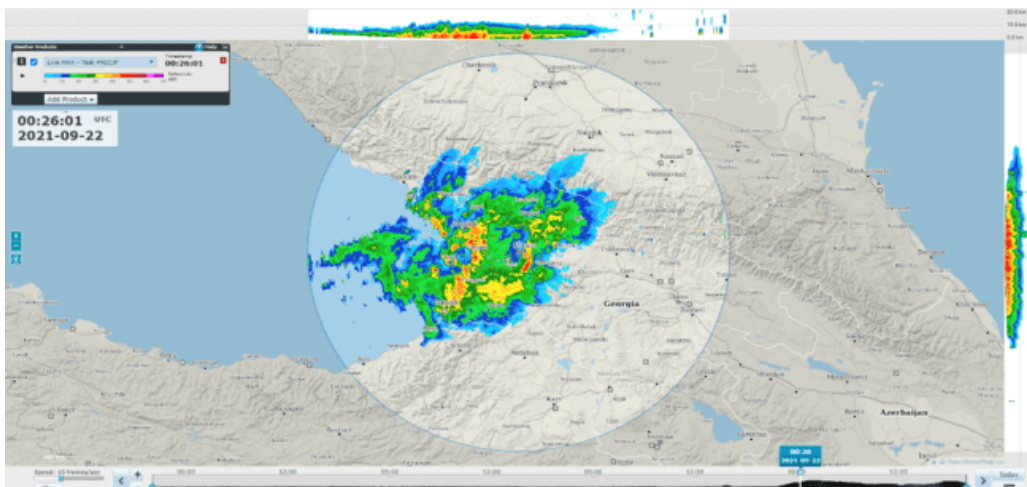
Fig. 1. The picture of radar reflectivity of clouds on September 02, 2021 in 19:26:02 UTC.
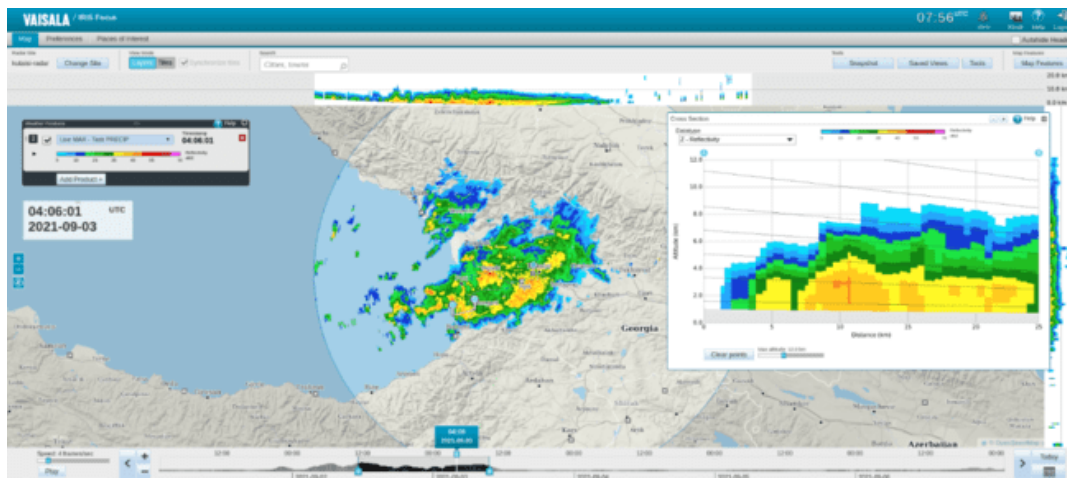
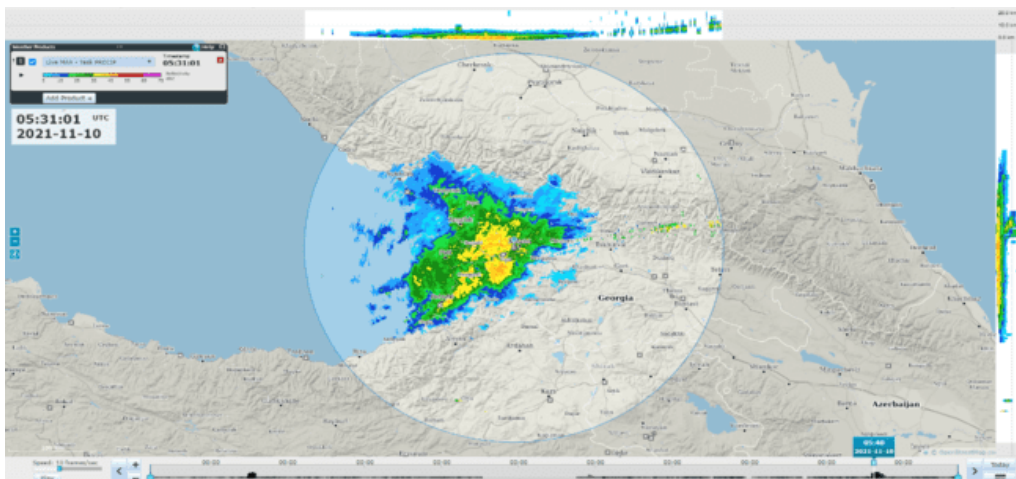Fig. 2. The picture of radar reflectivity of clouds on September 03, 2021 in 04:06:01 UTC.

The active process in Kobuleti began on the night of September 2. The automatic weather station VAISALA recorded the following data on the amount of precipitation over the past time: on September 2, 46 mm of precipitation fell at night, rain was also noted on September 3. During the day, 76 mm of precipitation fell, and at night - 25 mm, for a total of 101 mm. In the afternoon of September 4, 175 mm of precipitation fell, after which a significant decrease in their intensity began. The maximum wind speed for the specified period is 16 m/s.

The aforementioned heavy rainfall caused the paralysis of the central streets of Kobuleti, which was also facilitated by the flood on the Avchala River. The disaster also caused flooding of residential buildings and courtyards. It is noteworthy that along with the heavy rainfall, there was also a tornado, which originated over the sea and came ashore. As a result, several roofs were ripped from houses and several trees were uprooted. The village of Chakva was also badly damaged.

In fig. 3-5 show three other examples of cloudiness distribution over the territory of Western Georgia.

In particular, as follows from these figures, the radar reflectivity of clouds on September 11, 2021 reached up to 45-50 dBz, maximum cloud height - above 10 km (fig. 3), on September 22 - up to 50-55 dBz, maximum cloud height - above 10 km (fig. 4), and on November 10 - up to 40-45 dBz, maximum cloud height – up to 8 km (fig 5). In all cases, cloud cover spread significant areas over the territory of Western Georgia.

Fig. 3. The picture of radar reflectivity of clouds on September 11, 2021 in 20:36:01 UTC.

Fig. 4. The picture of radar reflectivity of clouds on September 22, 2021 in 00:26:01 UTC.

Fig. 5. The picture of radar reflectivity of clouds on November 10, 2021 in 05:31:01 UTC.

Conclusion

This is the first work on the preliminary scientific analysis of data from the meteorological radar "WRM200". In the future, we will continue similar studies, in particular, in the aspect of studying of hydrometeorological disasters in Western Georgia.

153

References

1. Amiranashvili A., Chikhladze V., Dzodzuashvili U., Ghlonti N., Sauri I., Telia Sh., Tsintsadze T. Weather Modification in Georgia: Past, Present, Prospects for Development. // International Scientific Conference „Natural Disasters in Georgia: Monitoring, Prevention, Mitigation", Proceedings, Tbilisi, Georgia, December 12-14, 2019, pp. 213-219.
2. Banetashvili V., Grebentsova A., Javakhishvili N., Jamrishvili N., Kaishauri M., Mitin M., Saginashvili N., Khurtsidze G., Tsereteli A., Chargazia Kh., Chkhaidze B. Some Examples of Hail Processes in Kakheti According to the Data of Radar Surveillance in 2015. // Trans. of Mikheil Nodia Institute of Geophysics, ISSN 1512-1135, vol. 66, Tb., 2016, pp. 66-74, (in Russian).
3. Amiranashvili A., Bliadze T., Jamrishvili N., Kekenadze E., Tavidashvili Kh., Mitin M. Some Characteristics of Hail Process in Georgia and Azerbaijan on May 28, 2019. // Journal of the Georgian Geophysical Society, ISSN: 1512-1127, Physics of Solid Earth, Atmosphere, Ocean and Space Plasma, v. 22(2), 2019, pp. 40–54.
4. Jamrishvili N. K., Javakhishvili N.R., Sauri I. P., Tavidashvili Kh.Z., Telia Sh. O. Comparison of the Radar and Ground-Level Characteristics of the Hail Process On 10 June 2017 In Tbilisi. // Int. Sc. Conf. „Modern Problems of Ecology" Proc., ISSN 1512-1976, vol. 6, Kutaisi, Georgia, 21-22 September, 2018, pp. 134-137.
5. Gvasalia G., Kekenadze E., Mekoshkishvili N., Mitin M. Radar Monitoring of Hail Processes in Eastern Georgia And its Neighboring Countries (Azerbaijan, Armenia). // International Scientific Conference „Natural Disasters in Georgia: Monitoring, Prevention, Mitigation", Proceedings, Tbilisi, Georgia, December 12-14, 2019, pp. 170-174.
6. Banetashvili V., Gelovani G., Grebentsova A., Javakhishvili N., Iobadze K., Mitin M., Saginashvili N., Samkharadze I., Khurtsidze G., Tsereteli A., Tskhvediashvili G., Chkhaidze B. Some Examples of Strong Precipitation in Eastern Georgia According to the Data of Radar Surveillance of 2015. // Trans.of Mikheil Nodia Institute of Geophysics, ISSN 1512-1135, vol. 66, Tb., 2016, pp. 75-83, (in Russian).
7. Amiranashvili A., Kereselidze Z., Mitin M., Khvedelidze I., Chikhladze V. Alarming Factors of the Microclimate of the Vere River Valley and their Influence on the Floods Intensity. // Trans. of Mikheil Nodia Institute of Geophysics, ISSN 1512-1135, vol. 69, Tbilisi, 2018, pp. 204-218, (in Georgian).
8. Javakhishvili N., Janelidze I. On the Prediction of Floods Caused by Rainfall in the Area of Action of the Meteorological Radar "Meteor 735CDP10". // International Scientific Conference „Natural Disasters in Georgia: Monitoring, Prevention, Mitigation", Proceedings, Tbilisi, Georgia, December 12-14, 2019, pp. 175– 179.
9. Amiranashvili A.G., Berianidze N.T., Chikhladze V.A., Mitin M.N., Mtchedlishvili A.A. Preliminary Results of the Analysis of Radar and Ground-Based Monitoring of Dust Formation in Atmosphere Above the Territory of Eastern Georgia on 27 July 2018. // Journal of the Georgian Geophysical Society, ISSN: 1512-1127, Physics of Solid Earth, Atmosphere, Ocean and Space Plasma, vol. 21(2), 2018, pp. 61 – 69.
10. Avlokhashvili Kh., Banetashvili V., Gelovani G., Javakhishvili N., Kaishauri M., Mitin M., Samkharadze I., Tskhvediashvili G., Chargazia Kh., Khurtsidze G. Products of Meteorological Radar «METEOR 735CDP10». // Trans. of Mikheil Nodia Institute of Geophysics, ISSN 1512-1135, vol. 66, Tb., 2016, pp. 60-65, (in Russian).
11. Gvasalia G., Loladze D. Modern Meteorological Radar "WRM200" In Kutaisi (Georgia). // International Scientific Conference „Natural Disasters in the 21st Century: Monitoring, Prevention, Mitigation".Proceedings, Tbilisi, Georgia, December 20-22, 2021.
12. http://www.vaisala.ru/ru/meteorology/products/weatherradars/Pages/default.asp

THE STATISTICAL ANALYSIS OF TOTAL NUMBER OF FIRE ALERT IN GEORGIA IN 2012-2020

Bliadze T.
Mikheil Nodia Institute of Geophysics of Ivane Javakhishvili Tbilisi State University, Tbilisi, Georgia
teimuraz.bliadze@gmail.com

Summary: *The results of a statistical analysis of the daily and monthly values of total number of fire alert in Georgia in 2012-2020 are presented. In the study period number of days with fire alert was 2525, and total number of fire alert – 27631. The monthly number of fire alerts changes from 2 (January) to 1164 (November). The mean monthly number of fire alerts changes from 89 (May) to 493 (March).*

Key Words: *Fire, fire alert.*

Introduction

The problem of fires is actual for many countries of world, including Georgia [1, https://firms.modaps.eosdis.nasa.gov/download/create.php]. In Georgia the works regarding the forests fire index hazard were continued for Tbilisi and Telavi cities [2,3]. In this work results of a statistical analysis of the daily and monthly values of total number of fire alert in Georgia in 2012-2020 are presented.

Study area, material and methods

Study area is Georgia. Data of the about the daily values of number of fire alert (NFA) in period 2012-2020 are used [https://firms.modaps.eosdis.nasa.gov/download/create.php].

The standard statistical methods are used. The following designations will be used below: Min – minimal values; Max - maximal values; St Dev - standard deviation; C_v - coefficient of variation (%); year – period from January to December; cold – period from October to March; warm - period from April to September.

Results and discussion

Results in table 1-2 and fig. 1-4 are presented.
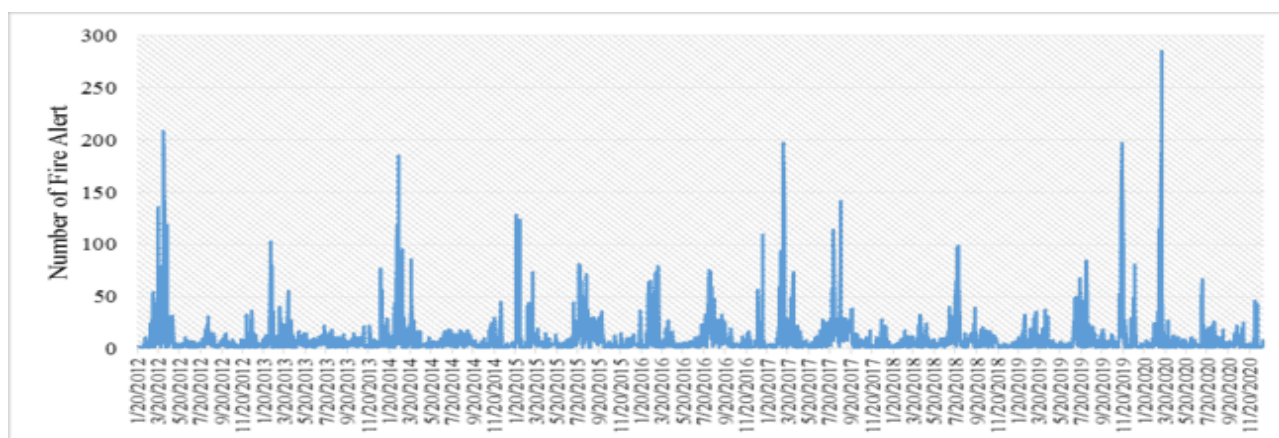
Fig. 1. Daily number of fire alerts in Georgia in 2012-2020.

Table 1. Statistical characteristics of daily number of fire alerts in Georgia in 2012-2020.

Min	Max	Mean	St Dev	Cv, %	Number of days with fire alert	Total number of fire alert	Number of days without fire alert
1	285	11	19.5	177.8	2525	27631	763

In fig. 1 data about daily number of fire alerts in Georgia in 2012-2020 is presented and in table 1 - the statistical characteristics of these data. As follows from fig. 1 and table 1 in the study period number of days with fire alert was 2525 and total number of fire alert – 27631. The max daily number of fire alerts = 285 and on March 10, 2020 was observed. Mean value of NFI = 11. Number of days without fire alert comprise 763.
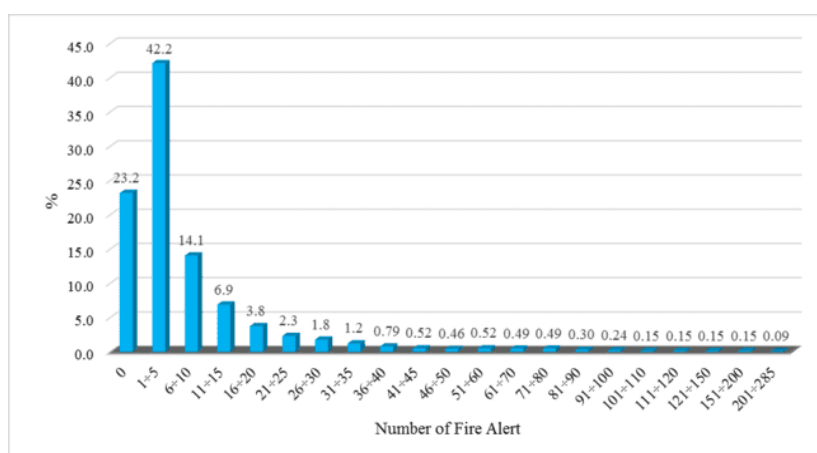
Fig. 2. Repetition of daily number of fire alert in Georgia in 2012-2020.

In fig. 2 data about repetition of daily number of fire alert in Georgia in 2012-2020 is presented. As follows from this fig. the max repetition of daily number of fire alert rate falls on the NFI range from 1 to 5 (42.2%). Repetition of daily number of without fire alert comprise 23.2 %.
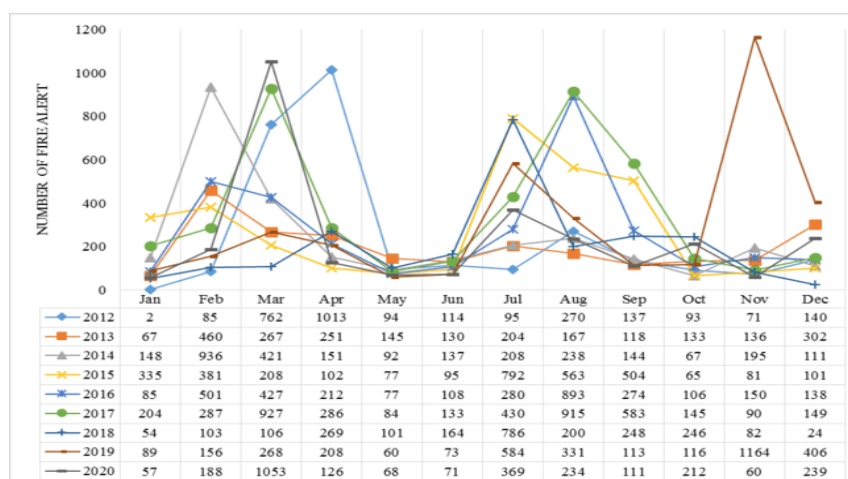
Fig. 3. Monthly number of fire alert in Georgia in 2012-2020.

In fig. 3 data about montly number of fire alerts in Georgia in 2012-2020 is presented and in table 2 and fig. 4 - the statistical characteristics of these data.

Table 2. Statistical characteristics of monthly number of fire alerts in Georgia in 2012-2020.

Parameter	Min	Max	Mean	St Dev	Cv, %
Jan	2	335	116	101	87.1
Feb	85	936	344	269	78.1
Mar	106	1053	493	338	68.6
Apr	102	1013	291	278	95.6
May	60	145	89	25	27.9
Jun	71	164	114	31	27.0
Jul	95	792	416	255	61.1
Aug	167	915	423	296	69.8
Sep	111	583	248	179	72.1
Oct	65	246	131	62	47.2
Nov	60	1164	225	355	157.3
Dec	24	406	179	117	65.3
Year	198	353	256	49	19.3
Cold	103	367	248	80	32.4
Warm	162	405	264	88	33.6
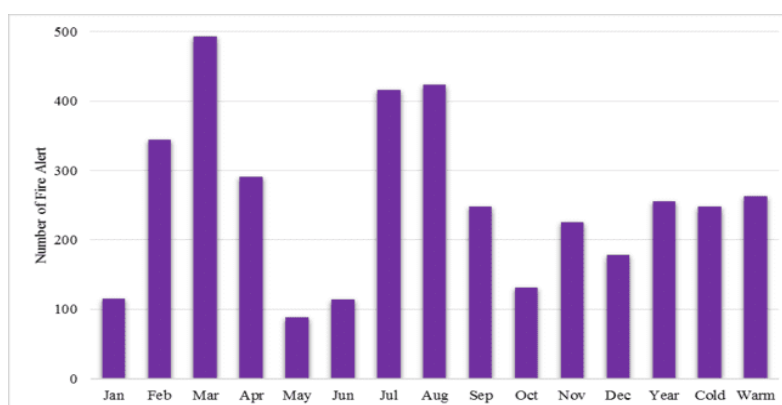
Fig. 4. Intraannual distribution of mean monthly and seasonal number of fire alert in Georgia in 2012-2020.

As follows from these table and fig. the monthly number of fire alerts changes from 2 (January) to 1164 (November). The mean monthly number of fire alerts changes from 89 (May) to 493 (March). The mean annual and seasonal number of fire alert in Georgia differ little from each other (respectively: year – 256, cold period – 248, warm period - 264).

References

1. Amiranashvili A.G. Increasing Public Awareness of Different Types of Geophysical Catastrophes, Possibilities of Their Initiation as a Result of Terrorist Activity, Methods of Protection and Fight with Their Negative Consequences. Engaging the Public to Fight Consequences of Terrorism and Disasters. // NATO Science for Peace and Security Series E: Human and Societal Dynamics, vol. 120. IOS Press, Amsterdam•Berlin•Tokyo•Washington, DC, ISSN 1874-6276, 2015, pp.155-164.
2. Bliadze T., Kirkitadze D., Samkharadze I., Tsiklauri Kh. Statistical Characteristics of Angstrom Fire Index for Tbilisi. // Int. Sc. Conf. "Natural Disasters in Georgia: Monitoring, Prevention, Mitigation". Proc., ISBN 978-9941-13-899-7, Publish House of Iv. Javakhishvili Tbilisi State University, December 12-14, Tbilisi, 2019, pp.86-90.
3. Bliadze T., Kirkitadze D., Samkharadze I., Tsiklauri Kh. Statistical Characteristics of Angstrom Fire Index for Telavi (Georgia). // International Scientific Conference „Modern Problems of Ecology",Proceedings, ISSN 1512-1976, v. 7, Tbilisi-Telavi, Georgia, 26-28 September, 2020, pp.64-67.

COMPARISON OF ANGSTROM FIRE INDEX FOR TBILISI (GEORGIA) AND KISLOVODSK (RUSSIA)

[*]Bliadze T., [**]Povolotskaya N., [***]Senik I.

[*]*Mikheil Nodia Institute of Geophysics of Ivane Javakhishvili Tbilisi State University, Tbilisi, Georgia*
teimuraz.bliadze@gmail.com
[**]*Pyatigorsk Research Institute of Resort Study of the Federal Medico-Biological Agency, Russia*
[***]*A.M. Obukhov Institute of Atmospheric Physics of Russian Academy of Sciences*

Summary: *The results of a statistical analysis of the daily and mean monthly values of Angstrom Fire Index (AFI) for Tbilisi (Georgia) and Kislovodsk (Russian Federation) in the period 2011-2020 are presented. AFI = (R/20) + (27-T)/10, where R is the minimum relative humidity, T is the maximum air temperature. The gradations of the values of I are as follows*: *I. AFI ≥ 4.1 – Low, II. AFI = 4.0 ÷ 3.0 - Moderate, III. AFI = 2.9 ÷ 2.5 - High, IY. AFI = 2.4 ÷ 2.0 - Very High, Y. AFI = <2.0 - Extreme. In particular, it was found that a extreme fire hazard in Tbilisi is observed on average within 70 days a year and in Kislovodsk - within 42 days a year. Between the daily and monthly mean values of AFI in Tbilisi and Kislovodsk direct linear correlation is observed.*

Key Words: *Angstrom Fire Index, temperature, fire.*

Introduction

As you know, the problem of fires, including forest fires, is relevant for many countries of the world. [http://www.sasquatchstation.com/Fire_Weather.php; http://www.forestservice.gr/meteo/fwi1.html]. This problem is also important for Russia and Georgia, where forest fires are frequent [1-4].

In the last few decades, this problem has become even more urgent in connection with global and local climate warming [5,6], which affects the increase in fire hazard [7].

In different countries of the world, different indicators of forest fire hazard are used [1-4, 7-10]. These indices are mathematical formulas that formalize the influence of air temperature and humidity, atmospheric precipitation, forest fuel moisture, thunderstorm activity, etc. Along with climatological and operational information on the levels of forest fire hazard, their short-term and long-term forecast is carried out [1-4, 11].

In Georgia the works regarding the forests fire index hazard based on the example to Tbilisi began in 2019 year [2]. Analogous studies were continued for Telavi and Nalchik cities [3,4]. In these cases was used simple Swedish Angstrom Index [8,9] with four-range scale [http://www.forestservice.gr/meteo/fwi1.html].

This work is a continuation of previous research. The results of a statistical analysis of the daily values of Angstrom Fire Index (AFI) for Tbilisi (the capital of Georgia, large city with a population of over a million people) and Kislovodsk (Russian Federation, resort town with a population around 130 thousand people) with used of five-range scale [http://www.sasquatchstation.com/Fire_Weather.php] in the period 2011-2020 are presented below.

Study area, material and methods

Study area is Tbilisi and Kislovodsk cities. Data of the about daily maximum of air temperature T and minimum relative humidity R in the period 2011-2020 are used [http://www.pogodaiklimat.ru/archive.php?id=ru&region=07]. The Swedish Angstrom Index calculated from the formula: AFI = (R/20) + (27-T)/10 [8,9]. The gradations of the values of AFI are as follows [http://www.sasquatchstation.com/Fire_Weather.php]: I. AFI ≥ 4.1 – Low, II. AFI = 4.0 ÷ 3.0 - Moderate, III. AFI = 2.9 ÷ 2.5 - High, IY. AFI = 2.4 ÷ 2.0 - Very High, Y. AFI = <2.0 - Extreme.

The standard statistical methods are used. The following designations will be used below: Min – minimal values; Max - maximal values; St Dev - standard deviation; C_v - coefficient of variation (%); σ_m – standard error; 99%(+/-) - 99% upper and lower levels of the confidence interval of average; R – coefficient of linear correlation; α - the level of significance; a and b – linear regression equation coefficients.

Results and discussion

Results in table 1, 2 and fig. 1-4 are presented.

Table 1. Statistical characteristics of daily values of Angstrom Fire Index in Tbilisi and Kislovodsk for different months in 2011-2020.

Month Param	Jan	Feb	Mar	Apr	May	Jun	Jul	Aug	Sep	Oct	Nov	Dec
						Tbilisi						
Min	2.9	1.5	1.0	1.0	0.9	0.1	-0.2	-0.2	0.3	1.0	1.4	1.6
Max	7.2	7.1	7.3	6.1	6.2	4.8	4.4	4.4	5.3	6.9	7.1	7.3
Mean	4.8	4.7	3.9	3.4	2.8	2.1	1.8	1.8	2.5	3.5	4.4	5.0
St Dev	0.91	1.06	1.00	1.09	0.94	0.86	0.83	0.87	0.89	1.07	1.05	0.85
Cv,%	18.7	22.7	25.5	32.3	33.3	41.4	45.8	49.5	36.1	30.6	23.5	17.1
σ_m	0.05	0.06	0.06	0.06	0.05	0.05	0.05	0.05	0.05	0.06	0.06	0.05
99%(+/-)	0.13	0.16	0.15	0.16	0.14	0.13	0.12	0.13	0.13	0.16	0.15	0.12
						Kislovodsk						
Min	2.1	1.4	0.8	0.4	0.6	0.8	0.2	0.4	0.5	0.3	1.1	1.6
Max	7.4	7.2	7.3	6.7	5.8	5.9	5.6	5.7	6.0	7.0	7.5	7.3
Mean	5.0	4.5	4.1	3.4	3.4	3.1	2.9	2.6	3.0	3.5	4.2	4.5
St Dev	1.30	1.46	1.54	1.42	1.07	0.87	0.86	0.92	1.16	1.51	1.53	1.41
Cv,%	26.1	32.5	37.2	42.2	31.2	28.7	30.1	35.8	38.9	43.5	36.4	31.0
σ_m	0.07	0.09	0.09	0.08	0.06	0.05	0.05	0.05	0.07	0.09	0.09	0.08
99%(+/-)	0.19	0.22	0.22	0.21	0.16	0.13	0.13	0.13	0.17	0.22	0.23	0.21
	The values of the correlation coefficient (**R**) and the coefficients of the linear regression equation between the AFI values in Tbilisi and Kislovodsk. (**AIF_Kisl=a·AFI_Tb + b**)											
R	0.40	0.47	0.44	0.56	0.54	0.53	0.51	0.43	0.41	0.60	0.50	0.37
a	0.5675	0.6503	0.6793	0.7364	0.6109	0.5381	0.5357	0.4589	0.5294	0.8417	0.733	0.614
b	2.2272	1.4643	1.4611	0.8892	1.6996	1.9341	1.8917	1.7744	1.6751	0.5212	0.949	1.4757
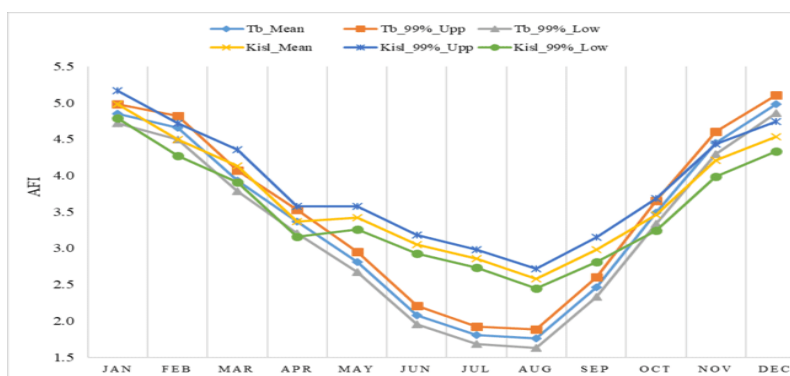
Fig. 1. The intraannual diatributions of mean monthly values of AFI in Tbilisi and Kislovodsk in 2011-2020.

In table 1 and fig. 1 the statistical characteristics of daily and mean monthly values of Angstrom Fire Index in Tbilisi and Kislovodsk for different months in 2011-2020 is presented. In particular, as follows from table 1 in Tbilisi values of AFI changes from -0.2 (July and August, fire occurrence is extreme) to 7.3 (March and December, fire occurrence is low). The greatest variations in the values of AFI are observed during August (C_v = 49.5%), smallest - in December (C_v = 17.1%). The mean monthly values of Angstrom Fire Index (table 1, fig. 1) changes from 1.8 (July and August, fire occurrence is extreme) to 5.0 (December, fire occurrence is low).

In Kislovodsk daily values of AFI changes from 0.2 (July, fire occurrence is extreme) to 7.5 (November, fire occurrence is low). The greatest variations in the values of AFI are observed during October (C_v = 43.5 %), smallest - in January (C_v = 26.1%). The mean monthly values of Angstrom Fire Index changes from 2.6 (August, fire occurrence very is high) to 5.0 (January, fire occurrence is low).

Coefficient of linear correlation between daily values of AIF in Tbilisi and Kislovodsk (table 1) changes from 0.37 (December) to 0.60 (October) – α < 0.05. In table 1 the coefficients of the linear regression equation between the daily AFI values in Tbilisi and Kislovodsk (AIF_Kisl=a·AFI_Tb + b) are presented also.
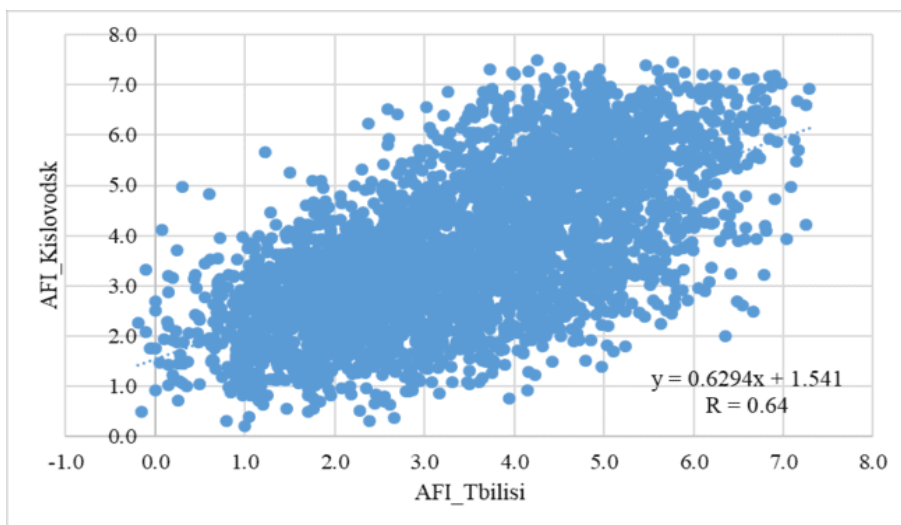
Fig. 2. Linear correlation and regression between daily values of AIF in Tbilisi and Kislovodsk (full data).
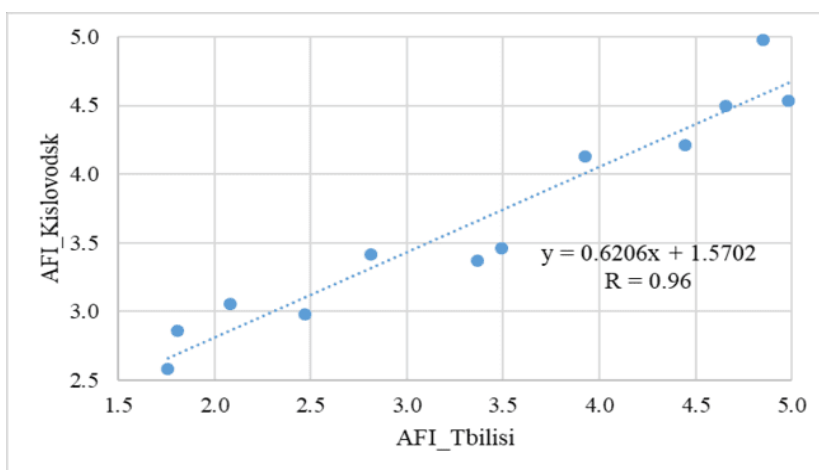
Fig.3. Linear correlation and regression between mean monthly values of AFI in Tbilisi and Kislovodsk.

In fig. 2 and 3 for examples of linear correlation and regression between daily and mean monthly values of AIF in Tbilisi and Kislovodsk are presented.

Table 2. Repetition of AFI in Tbilisi and Kislovodsk in different months for five gradations in 2011-2020.

Location	Tbilisi					Kislovodsk				
AFI	≥ 4.1	4.0 – 3.0	2.9 – 2.5	2.4 – 2.0	< 2.0	≥ 4.1	4.0 – 3.0	2.9 – 2.5	2.4 – 2.0	< 2.0
Jan	80.3	19.0	0.6	0.0	0.0	71.3	22.3	5.8	0.6	0.0
Feb	70.7	25.1	2.8	1.1	0.4	61.5	20.1	9.9	5.3	3.2
Mar	44.5	40.3	8.7	4.8	1.6	52.6	22.3	9.0	6.8	9.4
Apr	25.3	36.3	16.7	14.0	7.7	30.3	21.7	16.3	15.7	16.0
May	11.0	29.0	22.9	18.4	18.7	27.4	41.9	10.0	10.6	10.0
Jun	2.3	13.7	16.3	24.0	43.7	13.0	42.0	20.0	14.0	11.0
Jul	1.3	7.1	11.6	20.6	59.4	8.4	38.7	23.2	16.5	13.2
Aug	1.6	8.1	10.0	18.1	62.3	7.4	24.5	20.6	20.0	27.4
Sep	5.7	18.7	23.3	22.7	29.7	17.3	32.7	17.3	13.0	19.7
Oct	27.7	36.5	21.9	10.0	3.9	36.5	21.9	12.6	10.6	18.4
Nov	62.0	32.3	3.3	1.7	0.7	54.7	21.0	6.7	9.7	8.0
Dec	89.4	9.4	0.3	0.6	0.3	59.7	24.5	9.7	3.9	2.3

In table 2 data about repetition of AFI in Tbilisi and Kislovodsk in different months for five gradations is presented. As follows from table 2 on average in Tbilisi in the majority of the cases extreme fire hazard from June to September is observed (repetition are 43.7, 59.4, 62.3% and 29.7 % respectively). In January the values of AFI<2.0 is not observed. From November through March in the majority of the cases fire hazard is low (repetition of AFI> 4.1 changes from 44.5% for March to 89.4% for December).

In Kislovodsk (table 2) on average in the majority of the cases extreme fire hazard in August is observed (repetition is 27.4%. In January, as in Tbilisi, the values of AFI<2.0 is not observed. From October through April in the majority of the cases fire hazard is low (repetition of AFI> 4.1 changes from 30.3 % for April to 71.3% for January).
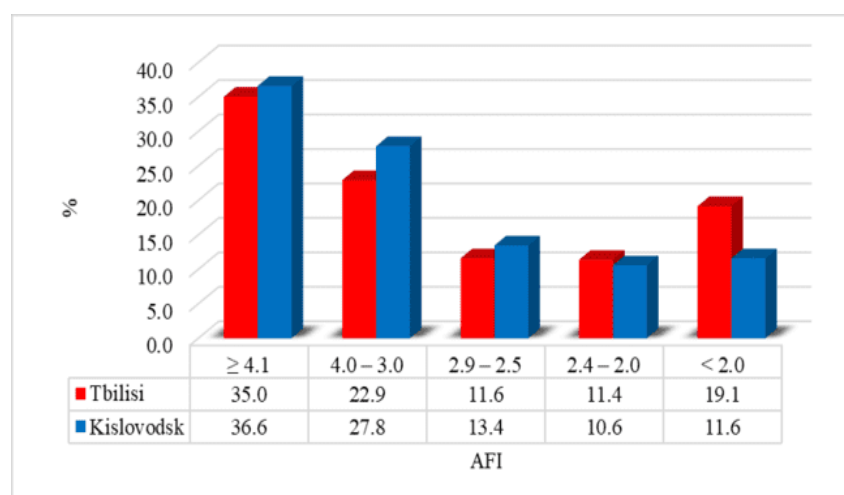
Fig. 4. Repetition of AFI in Tbilisi and Kislovodsk (full data).

An extreme fire hazard in Tbilisi (fig. 4) is observed on average within 70 days a year (repetition – 19.1 %), and very high - within 42 days a year (repetition – 11.4 %). In Kislovodsk an extreme fire hazard is observed on average within 42 days a year (repetition – 11.6 %), and very high - within 39 days a year (repetition – 10.6 %).

Thus, the level of the extreme and very high forests fire hazard under the conditions of Tbilisi is higher than under the conditions of Kislovodsk.

Conclusion

Further, it is planned to expand work on this issue (using other more complex fire hazard indices, studying their trends in connection with climate change, etc.).

<div align="center">

References

</div>

1. Gubenko I. M., Rubinshteyn K. G. Sravnitel'nyy analiz metodov rascheta indeksov pozharnoy opasnosti. // Trudy Gidrometeorologicheskogo nauchno-issledovatel'skogo tsentra Rossiyskoy Federatsii, № 347, 2012, s. 207–222.
2. Bliadze T., Kirkitadze D., Samkharadze I., Tsiklauri Kh. Statistical Characteristics of Angstrom Fire Index for Tbilisi. // Int. Sc. Conf. "Natural Disasters in Georgia: Monitoring, Prevention, Mitigation". Proc., ISBN 978-9941-13-899-7, Publish House of Iv. Javakhishvili Tbilisi State University, December 12-14, Tbilisi, 2019, pp.86-90.
3. Bliadze T., Kirkitadze D., Samkharadze I., Tsiklauri Kh. Statistical Characteristics of Angstrom Fire Index for Telavi (Georgia). // International Scientific Conference „Modern Problems of Ecology",Proceedings, ISSN 1512-1976, v. 7, Tbilisi-Telavi, Georgia, 26-28 September, 2020, pp.64-67.
4. Bliadze T., Gekkieva S., Kirkitadze D. Comparison of Angstrom Fire Index for Nalchik (Kabardino-Balkaria, Russian Federation) and Telavi (Georgia). // International Scientific Conference „Modern Problems of Ecology",Proceedings, ISSN 1512-1976, v. 7, Tbilisi-Telavi, Georgia, 26-28 September, 2020, pp.68-72.
5. Amiranashvili A.G., Kartvelishvili L.G., Trofimenko L.T., Khurodze T.V. The Statistical Evaluation of the Expected Changes of Air Temperature in Tbilisi and St.-Petersburg up to 2056 Years. Trans. of the Institute of Hydrometeorology, Georgian Technical University, ISSN 1512-0902, 2013, vol. 119, pp.58-622, (in Russian).
6. Amiranashvili A. Changeability of Air Temperature and Atmospheric Precipitations in Tbilisi for 175 Years. // Int. Sc. Conf. "Natural Disasters in Georgia: Monitoring, Prevention, Mitigation". Proc., ISBN 978-9941-13-899-7, Publish House of Iv. Javakhishvili Tbilisi State University, December 12-14, Tbilisi, 2019, pp.189-192.
7. Ullah M.R., Liu X.D., Al-Amin M. Spatial-Temporal Distribution of Forest Fires and Fire Weather Index Calculation from 2000 to 2009 in China. // Journal of Forest Science, *59*, 2013 (7), pp. 279–287.
8. Skvarenina J., Mindas J., Holecy J., Tucek J. Analysis of the Natural and Meteorological Conditions During Two Largest Forest Fire Events in the Slovak Paradise National Park. // Forest fire in the wildland-urban interface and rural areas in Europe: an integral planning and management challenge. Athens. 2003.
9. Lukić T., Marić P., Hrnjak I., Gavrilov M.B., Mladjan D., Zorn M., Komac B., Milošević Z., Marković S.B., Sakulski D., Jordaan A., Đorđević J., Pavić D., Stojsavljević R. Forest Fire Analysis and Classification Based on a Serbian Case Study. // Acta Geographica Slovenica, 57-1, 2017, pp. 51–63.
10. Klassifikatsiya prirodnoy pozharnoy opasnosti lesov. // Prikaz Rosleskhoza ot 5 iyulya 2011 g. № 287, 6 s., dokument s sayta aviales.ru
11. Kats A.L., Gusev V.L., Shabunina T.A. Metodicheskiye ukazaniya po prognozirovaniyu pozharnoy opasnosti v lesakh po usloviyam pogody. // M., Gidrometeoizdat, 1975, 16 s.

INFLUENCE OF VARIATIONS OF THE ANNUAL INTENSITY OF GALACTIC COSMIC RAYS ON THE MORTALITY OF THE POPULATION OF GEORGIA

[*]Amiranashvili A., [*]Bakradze T., [*]Ghlonti N., [**],[***]Khazaradze K.,
[***],[****]Japaridze N., [**]Revishvili A.

[*]*M. Nodia Institute of Geophysics of Iv. Javakhishvili Tbilisi State University, 1 M Alexsidze Str 0160, Tbilisi, Georgia, avtandilamiranashvili@gmail.com*
[**]*Georgian State Teaching University of Physical Education and Sport, Tbilisi, Georgia*
[***]*Ministry of Internally Displaced Persons from Occupied Territories, Labour, Health and Social Affair of Georgia, Tbilisi, Georgia*
[****]*Tbilisi State Medical University, Tbilisi, Georgia*

Summary: *Results of study of influence of variations of the annual intensity of neutron component of galactic cosmic rays on the mortality of the population of Georgia in 1995-2014 are presented. In particular, the previously obtained results on a direct correlation between the intensity of cosmic rays and total mortality of the population have been confirmed. However, as it turned out, an increase in the intensity of cosmic rays mainly increases the mortality rate of the male part of the population of Georgia. The mortality rate of women is very weakly dependent to the galactic cosmic rays influence.*

Key words: *galactic cosmic rays, mortality, ecology, bioclimatology, medical meteorology.*

Introduction

Research into the effect of cosmic rays on human health is being carried out in various countries [1-4], including Georgia [5-7]. In this work are presented the results of a study of the effect of the annual changeability of neutron component of galactic cosmic rays intensity on the mortality of the population of Georgia in 1995-2015.

Material and methods

In the work are used the data of National Statistics Office of Georgia about the total, male and female annual mortalities of the population of Georgia normalized to 1000 inhabitants [https://www.geostat.ge/en]. Information about mean annual values of intensity of neutron component of galactic cosmic rays (CR, impulse/min) is obtained at the Cosmic Rays Observatory of M. Nodia Institute of Geophysics [http://cr0.izmiran.ru/tbls/main.htm]. The observation period is 1995-2014.

In the proposed work the analysis of data is carried out with the use of the standard statistical analysis methods of random events and mathematical statistic methods for the non accidental time-series of observations [8].

The following designations will be used below: Min – minimal values, Max - maximal values, St Dev- standard deviation, R - coefficient of linear correlation, R^2 –coefficient of determination, K_{DW} – Durbin-Watson statistic, α - the level of significance (for significant correlation and regression ratios, the α value is not worse than 0.15). Res – residual component, Real - measured data.

The curve of trend is equation of the regression of the connection of the investigated parameter with the time at the significant value of the determination coefficient and such values of KDW, where the residual values are accidental. Background component is usually entered into the curve of trend. The value of

background component is most frequently unknown. From the physical considerations, random component can be represented in the form: Rand = Res + absolute value of the min value of Res. In this case random components have positive values with the minimum value = 0 (if there would be known the value of background component, that min Rand will be = Back). Accordingly, Trend + Back (sum of the trend and background components of time series) will be curve of equation of the regression of the connection of the investigated parameter with the time minus absolute value of the min value of Res. So, Real = (Trend + Back) + Res.

M_Total, M_Male and M_Female – total, male and female annual mortalities in Georgia normalized to 1000 inhabitants. ΔM_Total, ΔM_Male - growth of the annual total and male mortality with a change of the intensity of cosmic rays within the variation scope (max - min). The dimensions of the investigation parameters are omitted below.

Results

Results in table 1 and fig. 1-7 are presented.

Table 1. Statistical characteristics and trends types of CR, M_Total, M_Male and M_Female in Georgia in 1995-2014.

Variable	CR	M_Total	M_Male	M_Female
Max	9100	13.49	7.14	6.52
Min	8396	10.57	5.28	5.28
Mean	8763	12.33	6.27	6.06
St Dev	201	0.94	0.64	0.36
Cv, %	2.3	7.7	10.2	5.9
Trend type	Fifth order polynomial	Fourth order polynomial	Fifth order polynomial	Fifth order polynomial
R²	0.78	0.98	0.97	0.92
K$_{dw}$	2.13	2.02	1.71	1.77

In table 1 the data about statistical characteristics and trends types of cosmic rays intensity and mortality (M_Total, M_Male and M_Female) in Georgia in 1995-2014 are presented. As follows from this table, the values of CR varied from 8396 up to 9100 (average = 8763), values of M_Total – from 10.57 up to 13.49 (average = 12.33), values of M_Male – from 5.28 up to 7.14 (average = 6.27) and M_Female - from 5.28 up to 6.52 (average = 6.06). Trends of CR, M_Male, and M_Female take the form of fifth power polynomials, trend of M_Total - fourth power polynomial (corresponding values of R^2 - α < 0.005, and KDW - α = 0.05).
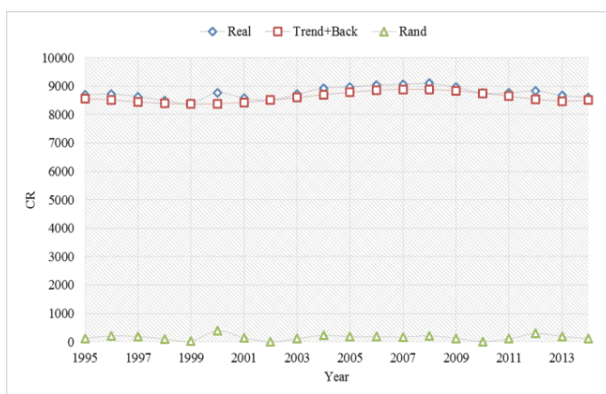
Fig. 1. Trend of the mean annual intensity of galactic cosmic rays in Tbilisi in 1995-2014.
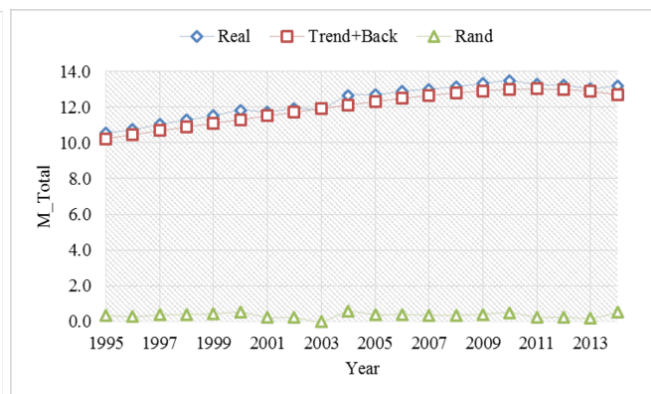
Fig. 2. Trend of the annual total population mortality in Georgia in 1995-2014.
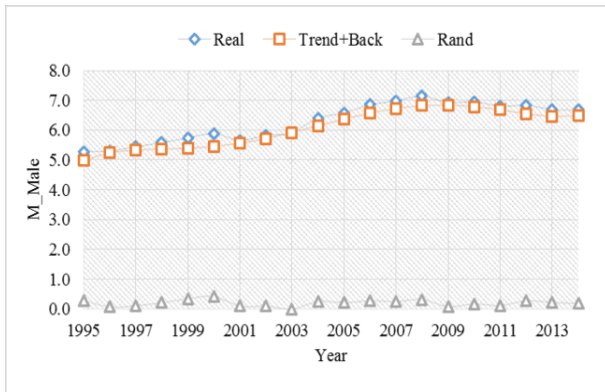
Fig. 3. Trend of the annual male mortality in Georgia in 1995-2014.
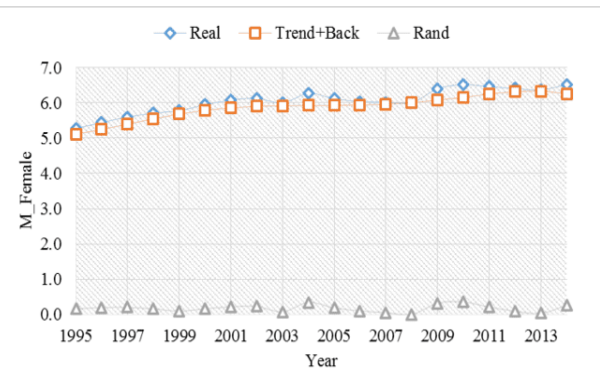
Fig. 4. Trend of the annual female mortality in Georgia in 1995-2014.

For the clarity in fig. 1-4 are presented the curves of real data, (trend+ background) and random components of time-series of mean annual intensity of galactic cosmic rays, annual total population mortality, as well as male and female annual mortalities in Georgia in 1995-2014.
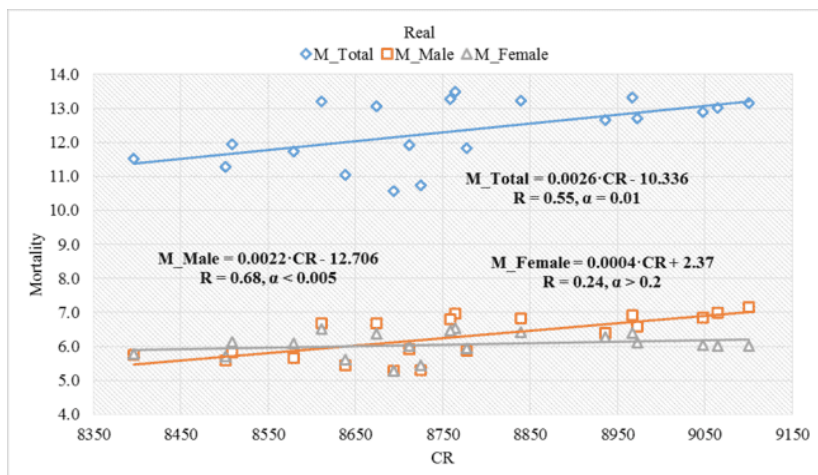

Fig. 5. Linear correlation and regression between annual cosmic ray intensity and total, male and female mortalities in Georgia (real data).
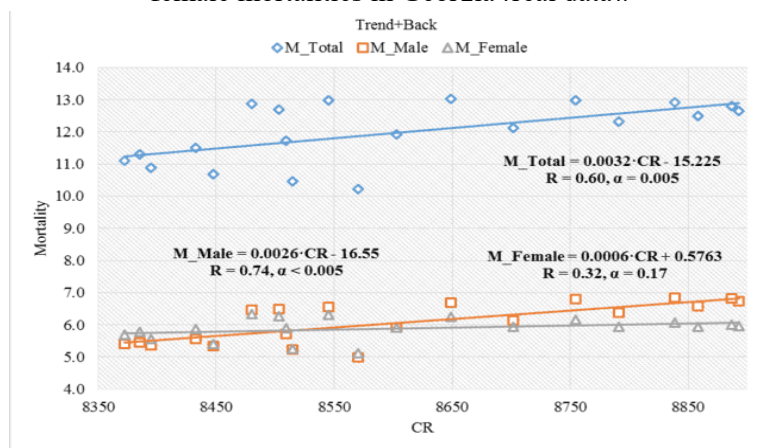
Fig. 6. Linear correlation and regression between annual cosmic ray intensity and total, male and female mortalities in Georgia (trend+ background components).
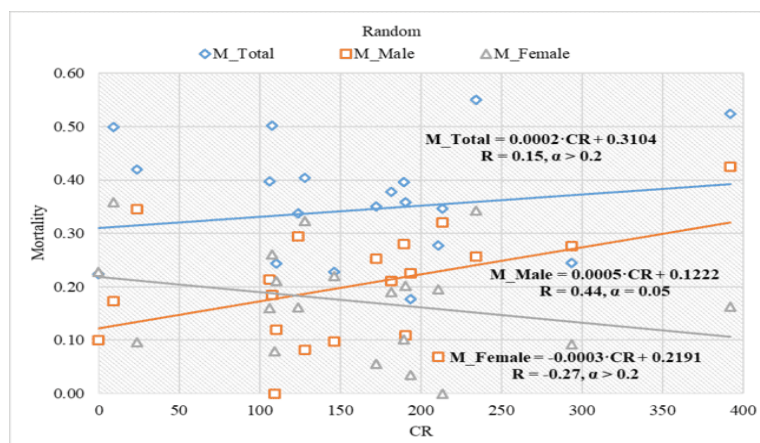
Fig. 7. Linear correlation and regression between annual cosmic ray intensity and total, male and female mortalities in Georgia (random components).

In fig. 5-7 data about linear correlation and regression between annual cosmic ray intensity and total, male and female mortalities in Georgia are presented: fig. 5 – for real data, fig. 6 - for trend+ background components, fig. 7 – for random components. As follows from fig. 5 and 6 a significant positive linear correlation and regression is observed between the CR and M_Total for real data and for trend + background components (R = 0.55, ΔM_Total = 1.83 and R = 0.60, ΔM_Total = 1.76, respectively; $\alpha \leq 0.01$). In all cases, a significant positive linear correlation and regression is observed between the intensity of galactic cosmic rays and the male mortality of the population of Georgia (fig. 5-7. R = 0.68, ΔM_Male = 1.55; R = 0.74, ΔM_Male = 1.43; R =0.44, ΔM_Male = 0.28, respectively; $\alpha < 0.05$). Simultaneously the mortality rate of women is very weakly dependent to the galactic cosmic rays influence (fig. 5-7, R = 0.24, 0.32 and -0.27 respectively; $\alpha \geq 0.17$, few significant correlation).

Conclusion. In the future, we plan to carry out these studies, taking into account the age of the population of Georgia.

References

1. Singh A.K., Siingh D., Singh R.P. Impact of Galactic Cosmic Rays on Earth's Atmosphere and Human Health. // Atmospheric Environment, 45, 2011, pp. 3806-3818.
2. Vieira C. L. Z., Janot-Pacheco E., Lage C., Pacini A., Koutrakis P., Cury P. R., Shaodan H., Pereira L. A., Saldiva P. H. N. Long-Term Association Between the Intensity of Cosmic Rays and Mortality Rates in the City of Sao Paulo. // Environ. Res. Lett. 13, 2018, 024009, 8p., https://iopscience.iop.org/article/10.1088/1748-9326/aaa27a
3. Reteyum A.YU. Deystviye galakticheskikh kosmicheskikh luchey na populyatsii cheloveka. // Tezisy doklada na konferentsii «A.L. Chizhevskiy. vklad v nauku i kul'turu», Kaluga, Rossiya, 20–21 noyabrya 2019 g., s. 89-91, (in Russian).
4. Stoupel E., et al. Cosmic Ray and Human Health. // EC Pharmacology and Toxicology 8.4, 2020, pp. 167-176.
5. Amiranashvili A.G., Gogua R.A., Matiashvili T.G., Kirkitadze D.D., Nodia A.G., Khazaradze K.R., Kharchilava J.F., Khurodze T.V., Chikhladze V.A. The Estimation of the Risk of Some Astro-MeteoGeophysical Factors for the Health of the Population of the City of Tbilisi. // Int. Conference "Near-Earth Astronomy 2007" Abstract, Terskol, Russia, 3-7 September 2007, p. 86
6. Amiranashvili A., Bliadze T., Chikhladze V. Photochemical smog in Tbilisi. // Monograph, Trans. Of Mikheil Nodia institute of Geophysics, ISSN 1512-1135, v. 63, Tb., 2012, 160 p., (in Georgian).
7. Amiranashvili A.G., Bakradze T.S., Berianidze N.T., Japaridze N.D., Khazaradze K.R. Effect of Mean Annual Changeability of Air Temperature, Surface Ozone Concentration and Galactic Cosmic Rays Intensity on the Mortality of Tbilisi City Population. // Journal of the Georgian Geophysical Society, Issue B. Physics of Atmosphere, Ocean and Space Plasma, v.19B, 2016, pp.135-143.
8. Kendall M.G. Time-series. // Moscow, 1981, 200 p., (in Russian).

ANALYSIS OF THE SHORT-TERM FORECAST OF COVID-19 RELATED CONFIRMED CASES, DEATHS CASES AND INFECTION RATES IN GEORGIA FROM SEPTEMBER 2020 TO OCTOBER 2021

[*]Amiranashvili A., [**],[***]Khazaradze K., [***],[****]Japaridze N., [**]Revishvili A.

[*]*Mikheil Nodia Institute of Geophysics of Ivane Javakhishvili Tbilisi State University, Tbilisi, Georgia*
avtandilamiranashvili@gmail.com
[**]*Georgian State Teaching University of Physical Education and Sport, Tbilisi, Georgia*
[***]*Ministry of Internally Displaced Persons from Occupied Territories, Labour, Health and Social Affair of Georgia, Tbilisi, Georgia*
[****]*Tbilisi State Medical University, Tbilisi, Georgia*

Summary: *Results of analysis of averaging ten day, two week and monthly interval prediction of daily data associated with such parameters of the new coronavirus covid-19 pandemic in Georgia, as infection cases (C), deaths cases (D) and infection rate (I) from September 2020 to October 2021 are presented. Comparison of real and calculated predictions data of C, D and I are carried out. It was found that in the study period the mean ten day, two-week and monthly real values of C, D and I practically fall into the 67% - 99.99% confidence interval of these predicted values.*

Key Words: *New Coronavirus COVID-19, statistical analysis, short-term prediction.*

Introduction

Almost two years have passed since the outbreak of the new coronavirus (COVID-19) in China, which was declared a pandemic on March 11, 2020 due to its rapid spread in the world [1]. During this period, despite the measures taken (including vaccination), the overall level of morbidity and mortality in many countries of the world, including Georgia, remains very high [https://www.soothsawyer.com/john-hopkins-time-series-data-with-us-state-and-county-city-detail-historical/; https://data.humdata.org/dataset/total-covid-19-tests-performed-by-country; https://stopcov.ge].

In our previous works, we present the results of a statistical analysis of daily data related to infection with the new coronavirus COVID-19 of confirmed (C), recovered, deaths (D) and infection rate (I) of the population of Georgia in the period from March 14, 2020 to August 31, 2021 [2-6]. The results of the analysis of a regular ten-day and two-week forecast of C, D and I values are also presented [3-6]. From September 2021, a regular monthly forecast of C, D and I values began. Information was regularly sent to the National Center for Disease Control and Public Health of Georgia and posted on the Facebook page https: // www.facebook.com/Avtandil1948/

In this work results of analysis of averaging ten day, two week and monthly interval prediction of daily values of confirmed, deaths and infection rate coronavirus-related cases from September 2020 to October 2021 are presented.

Study area, material and methods

The study area: Georgia. Data of John Hopkins COVID-19 Time Series Historical Data (with US State and County data) [https://www.soothsawyer.com/john-hopkins-time-series-data-with-us-state-and-county-city-detail-historical/; https://data.humdata.org/dataset/total-covid-19-tests-performed-by-country] and https://stopcov.ge about daily values of confirmed, deaths and infection rate coronavirus-related cases are used.

The calculation of the interval prognostic values of C, D and I taking into account the periodicity in the time-series of observations was carried out using Excel 16 (the calculate methodology was description in [3]). R^2 - coefficient of determination, α – the level of significance.

The regular ten day prediction values of C from September 23, 2020 to December 31, 2020 was carried out (10 cases); two week prediction – from January 1, 2021 to August 31, 2021 (16 cases); monthly prediction – from September 1, 2021 to October 31, 2021 (2 cases). In total - 28 cases of prediction.

The regular two week prediction values of D from January 1, 2021 to August 31, 2021 was carried out (16 cases); monthly prediction – from September 1, 2021 to October 31, 2021 (2 cases). In total - 18 cases of prediction.

The regular two week prediction values of I from February 1, 2021 to August 31, 2021 was carried out (14 cases); monthly prediction – from September 1, 2021 to October 31, 2021 (2 cases). In total - 16 cases of prediction.

67%...99.99%_Low - 67%...99.99% lower level of confidence interval of prediction values of C, D and I; 67%...99.99%_Upp - 67%...99.99% upper level of confidence interval of prediction values of C, D and I.

In the Table 1 [7] the scale of comparing real data with the predicted ones and assessing the stability of the time series of observations in the forecast period in relation to the pre-predicted one (period for prediction calculating) is presented.

Results and discussion

The results in fig. 1- 3 and tables 1 - 3 are presented.
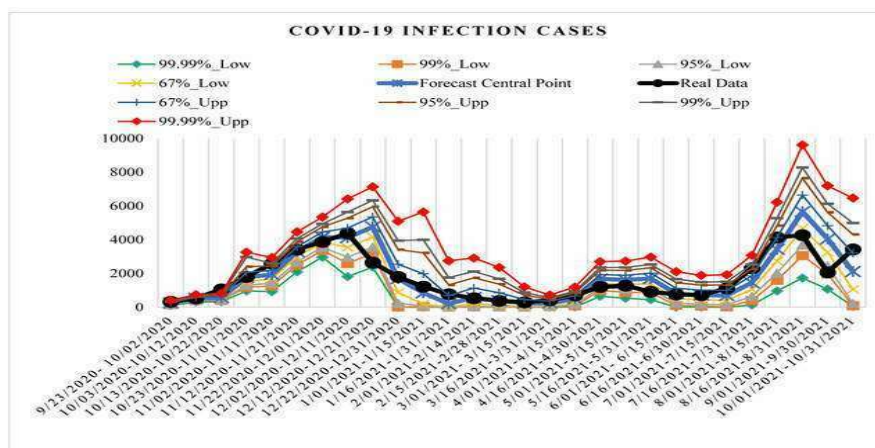
Fig. 1. Verification of the time-averaged forecast of interval prediction of Covid-19 infection cases in Georgia from 23.09.2020 to 31.10.2021.
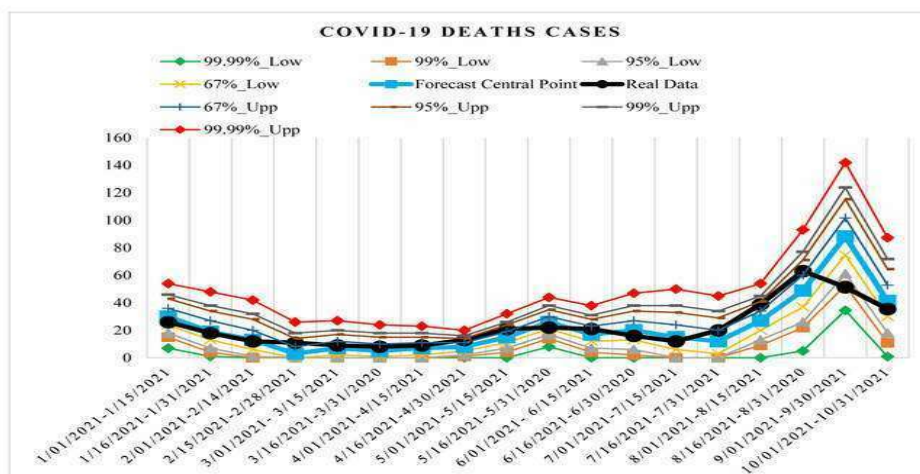
Fig. 2. Verification of the time-averaged forecast of interval prediction of Covid-19 deaths cases in Georgia from 01.01.2021 to 31.10.2021.
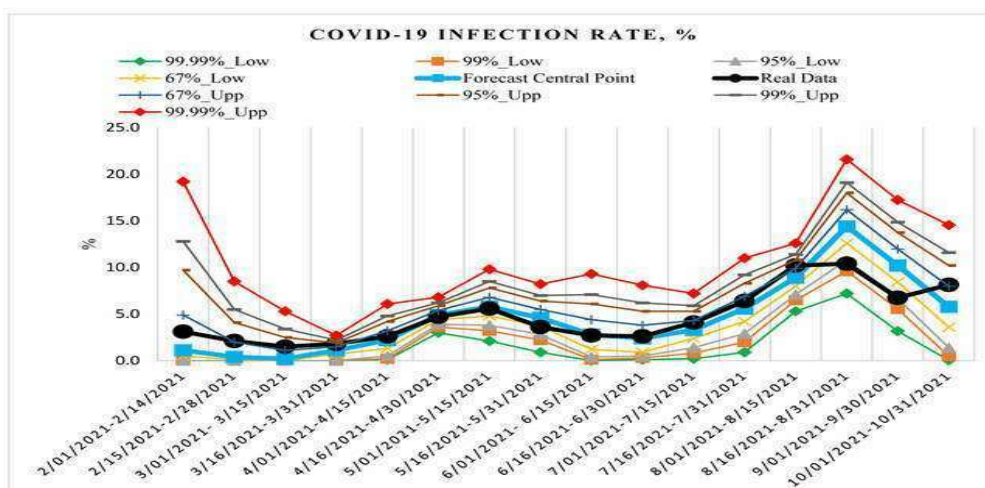
Fig. 3. Verification of the time-averaged forecast of interval prediction of Covid-19 infection rate in Georgia from 01.02.2021 to 31.10.2021.

In fig. 1-3 for clarity graphical information about of the time-averaged forecast of interval prediction of Covid-19 infection cases, deaths cases and infection rate in Georgia for investigation period are presented. In tables 1-3 data about comparing of mean real data of C, D and I with the predicted ones and assessing the stability of the time series of observations in the forecast period in relation to the pre-predicted one are presented.

Table 1. Comparing of mean real data of C with the predicted ones and assessing the stability of the time series of observations in the forecast period in relation to the pre-predicted one.

Change in the forecast state in relation to the pre-predicted one	Date (period for averaging)	Range of Forecast Level
COVID-19 Infection Cases		
Alarming deterioration, violation of the stability of a time-series of observations (1 case)	10/13/2020-10/22/2020	Real Data > 99.99% Upp
Significant deterioration, stability of a time-series of observations (2 cases)	11/02/2020-11/11/2020; 7/16/2021-7/31/2021	95% Upp <Real Data ≤99%Upp
Noticeable deterioration, stability of a time-series of observations (7 cases)	9/23/2020- 10/02/2020; 1/16/2021-1/31/2021; 3/16/2021-3/31/2021; 4/01/2021-4/15/2021; 7/01/2021-7/15/2021; 8/01/2021-8/15/2021; 10/01/2021-10/31/2021	67% Upp <Real Data ≤95% Upp
Preservation, stability of a time-series of observations (12 cases)	10/03/2020-10/12/2020; 10/23/2020-11/01/2020; 11/12/2020-11/21/2020; 11/22/2020-12/01/2020; 12/02/2020-12/11/2020; 12/22/2020-12/31/2020; 1/01/2021-1/15/2021; 2/01/2021-2/14/2021; 2/15/2021-2/28/2021; 3/01/2021- 3/15/2021; 6/01/2021- 6/15/2021; 6/16/2021-6/30/2021	67% Low ≤ Real Data ≤ 67% Upp
Noticeable improvement, stability of a time-series of observations (3 cases)	4/16/2021-4/30/2021; 5/01/2021-5/15/2021; 8/16/2021-8/31/2021	95% Low ≤Real Data < 67% Low
Significant improvement, stability of a time-series of observations (2 cases)	5/16/2021-5/31/2021; 9/01/2021-9/30/2021	99% Low ≤Real Data < 95% Low
Sharp improvement, stability of a time-series of observations (1 case)	12/12/2020-12/21/2020	99.99% Low ≤Real Data < 99% Low

Table 2. Comparing of mean real data of D with the predicted ones and assessing the stability of the time series of observations in the forecast period in relation to the pre-predicted one.

Change in the forecast state in relation to the pre-predicted one	Date (period for averaging)	Range of Forecast Level
COVID-19 Death Cases		
Noticeable deterioration, stability of a time-series of observations (5 cases)	2/15/2021-2/28/2021; 4/16/2021-4/30/2021; 5/01/2021-5/15/2021; 8/01/2021-8/15/2021; 8/16/2021-8/31/2021	67% Upp <Real Data ≤95% Upp
Preservation, stability of a time-series of observations (12 cases)	1/01/2021-1/15/2021; 1/16/2021-1/31/2021; 2/01/2021-2/14/2021; 3/01/2021- 3/15/2021; 3/16/2021-3/31/2021; 4/01/2021-4/15/2021; 5/16/2021-5/31/2021; 6/01/2021- 6/15/2021; 6/16/2021-6/30/2021; 7/01/2021-7/15/2021; 7/16/2021-7/31/2021; 10/01/2021-10/31/2021	67% Low ≤ Real Data ≤ 67% Upp
Sharp improvement, stability of a time-series of observations (1 case)	9/01/2021-9/30/2021	99.99% Low ≤Real Data < 99% Low

Table 3. Comparing of mean real data of I with the predicted ones and assessing the stability of the time series of observations in the forecast period in relation to the pre-predicted one.

Change in the forecast state in relation to the pre-predicted one	Date (period for averaging)	Range of Forecast Level
COVID-19 Infection Rate		
Noticeable deterioration, stability of a time-series of observations (5 cases)	2/15/2021-2/28/2021; 3/01/2021- 3/15/2021; 3/16/2021-3/31/2021; 8/01/2021-8/15/2021; 10/01/2021-10/31/2021;	67% Upp <Real Data ≤95% Upp
Preservation, stability of a time-series of observations (8 cases)	2/01/2021-2/14/2021; 4/01/2021-4/15/2021; 4/16/2021-4/30/2021; 5/01/2021-5/15/2021; 6/16/2021-6/30/2021; 7/01/2021-7/15/2021; 7/16/2021-7/31/2021; 6/01/2021- 6/15/2021	67% Low ≤ Real Data ≤ 67% Upp
Noticeable improvement, stability of a time-series of observations (2 cases)	5/16/2021-5/31/2021; 9/01/2021-9/30/2021	95% Low ≤Real Data < 67% Low
Significant improvement, stability of a time-series of observations (1 case)	8/16/2021-8/31/2020	99% Low ≤Real Data < 95% Low

As follows from Fig. 1 and table 1, except for the period from October 13 to October 22, 2020, all averaged real data of C coincide with their averaged predicted data within 67-99.99% of the forecast confidence interval. All averaged real data of D and I coincide with their averaged predicted data within indicated forecast confidence interval (fig. 2,3 and tables 2,3). Except the period from October 13 to October 22, 2020 the stability of all pre-forecast and forecast time-series of observations are observed.

Depending on the range of forecast level the following correspondence of real data with predicted is observed (tables 1-3).

67% Low ≤ Real Data ≤ 67% Upp, practically accurate forecast (preservation of the real situation in comparison with the pre-forecast): C - 42.9 %, D - 66.7 % and I – 50 % of all cases of corresponding predictions.

67% Upp <Real Data ≤95% Upp and 95% Low ≤Real Data < 67% Low, noticeable deterioration or improvement of real situation in comparison with the pre-prediction: C – 35.7 %, D – 27.8 % and I – 43.8 % of all cases of corresponding predictions.

95% Upp <Real Data ≤99%Upp and 99% Low ≤Real Data < 95% Low, significant deterioration or improvement of real situation in comparison with the pre-prediction: C – 14.3 %, D – 0 % and I – 6.3 % of all cases of corresponding predictions.

99.99% Low ≤Real Data < 99% Low, Sharp improvement of real situation in comparison with the pre-prediction: C – 3.6 %, D – 5.6 % and I – 0 % of all cases of corresponding predictions.

Real Data > 99.99% Upp, deterioration of real situation in comparison with the pre-prediction: C – 3.6 %, D – 0 % and I – 0 % of all cases of corresponding predictions.

Thus, taking into account the extreme instability of the initial time series of observations, the results of short-term forecasting of the values of C, D and I, in our opinion, can be considered quite satisfactory.

Conclusion

In the future, we will continue to carry out regular monthly forecasting of C, D and I values in Georgia. We will also consider the prospects for increasing to more than one month the time to predict Covid-19-related infection cases, deaths cases and infection rates.

References

1. World Health Organization. Coronavirus Disease 2019 (COVID-19). // Situation report, 67, 2020.
2. Amiranashvili A.G, Khazaradze K.R, Japaridze N.D. Twenty weeks of the pandemic of coronavirus Covid-19 in Georgia and neighboring countries (Armenia, Azerbaijan, Turkey, Russia). Preliminary comparative statistical data analysis. // Int. Sc. Conf. „Modern Problems of Ecology", Proc., ISSN 1512-1976, v. 7, Tbilisi-Telavi, Georgia, 26-28 September, 2020, pp. 364-370.
3. Amiranashvili A.G., Khazaradze K.R., Japaridze N.D. Analysis of twenty-week time-series of confirmed cases of New Coronavirus COVID-19 and their simple short-term prediction for Georgia and neighboring countries (Armenia, Azerbaijan, Turkey, Russia) in amid of a global pandemic.// medRxiv preprint, 2020, doi: https://doi.org/10.1101/2020.09.09.20191494, 13 p.
Europe PMC, https://europepmc.org/article/ppr/ppr213467
4. Amiranashvili A.G., Khazaradze K.R., Japaridze N.D. The Statistical Analysis of Daily Data Associated with Different Parameters of the New Coronavirus COVID-19 Pandemic in Georgia and their Short-Term Interval Prediction from September 2020 to February 2021. // medRxiv preprint, 2021, doi: https://doi.org/10.1101/2021.04.01.21254448, 18 p.
5. Amiranashvili A.G., Khazaradze K.R., Japaridze N.D. The Statistical Analysis of Daily Data Associated with Different Parameters of the New Coronavirus COVID-19 Pandemic in Georgia and their Short-Term Interval Prediction in Spring 2021. // medRxiv preprint, 2021, doi: https://doi.org/10.1101/2021.06.16.21259038
6. Amiranashvili A.G., Khazaradze K.R., Japaridze N.D. The Statistical Analysis of Daily Data Associated with Different Parameters of the New Coronavirus COVID-19 Pandemic In Georgia and their Two-Week Interval Prediction in Summer 2021. // medRxiv preprint,2021, doi: https://doi.org/10.1101/2021.09.08.21263265, 20 p.

ASSESSMENT OF CLIMATIC RISKS FROM HAZARDOUS WEATHER PHENOMENA

* Elizbarashvili E.Sh., ** Elizbarashvili M.E., * Elizbarashvili Sh.E., ** Elizbarashvili I.Sh.

* *Institute of Hydrometeorology of Georgian Technical University, Tbilisi, Georgia*
** *Ivane Javakhishvili Tbilisi State University, Tbilisi, Georgia*
eelizbar@hotmail.com

Summary: *Droughts, strong winds, hurricanes, torrential rains, hail, floods, floods, blizzards, extreme temperatures, and other similar disasters cause more severe economic losses than volcanic eruptions, tsunamis, and earthquakes, and these hazards pose climate risks. The main factors of the process of occurrence of climatic risk of dangerous meteorological phenomena are considered. The article describes a methodology for assessing the vulnerability of objects (risk recipients) exposed to hazardous phenomena. On the example of two points located in different geographical conditions - Tbilisi and Dmanisi, possible social and economic risks associated with these phenomena are identified. The greatest climatic danger is represented by fog and strong winds, and in summer, Tbilisi is very hot with concomitant soil, atmospheric drought, and extreme fire hazards. To a lesser extent, the area is damaged by heavy rainfall and hail.*

.

Key Words: *hazardous phenomenon, probability, vulnerability, social and economic risk.*

Introduction

According to the United Nations, more than a million people have died due to natural disasters over the past five decades. At the same time, about 90% of the most severe economic losses are accounted for not by such natural phenomena as volcanic eruptions, tsunamis, and earthquakes but by hydrometeorological phenomena. Droughts, strong winds, hurricanes, heavy rains, hail, floods, floods, blizzards, extreme temperatures, and other similar disasters result from climate change and become more powerful. Thus, we can discuss climatic risk if dangerous or unfavorable meteorological phenomena are observed in a given territory and a particular object (risk recipient) is under their probable influence.

In order to mitigate the expected negative consequences of hazardous phenomena and unfavorable weather conditions, the associated potential risks should be assessed and compared with the value of the acceptable risk, and then adaptation decisions should be made.

Materials and methods

Climate risk is a combination of the likelihood and consequences of a hazardous or adverse event occurring. Risk is defined as the product of the probability of a specific meteorological hazard by the conditional probability of the vulnerability of the recipient who may be exposed to this hazard [1]:

$$R = pU \qquad (1)$$

where: **p**- is the probability of an event; **U**- is the consequences of an event or the vulnerability of an object exposed to a hazardous phenomenon, which is determined by the formula:

$$U = (s/S) \cdot m \cdot t \cdot K \qquad (2)$$

s — average area of impact of this phenomenon (sq. km),
S — area of the region (sq. km),
m — population of the administrative region (people),
t — time of action of a dangerous meteorological phenomenon or unfavorable weather conditions (day);
K — coefficient of aggressiveness of the phenomenon.

Climate risk is usually called social risk, i.e., the risk of social damage to the territory under consideration since it determines the size of the population affected by this phenomenon. The general formula of social risk or the likelihood of injury to a particular recipient is as follows [1,2]:

$$Rc=p(s/S) \ (si/S)·m·t·K \qquad (3)$$

where **si** - recipient area, sq. km.

The basis of the economic risk management mechanism is the definition of economic damage caused by a hazardous event. The cumulative damage in a given area is called economic risk. Economic risk is the product of the probability of a meteorological hazard by the amount of damage; expressed in monetary units [1,2]:

$$Re= ARc=p(s/S) \ (si/S)·m·t·K·A \qquad (4)$$

Where **A**- is the share of gross domestic product per day per inhabitant of a given administrative unit. In the conditions of Georgia, emergencies mainly create the following weather phenomena:
• Hot days (**SU25** when the maximum air temperature exceeds 250).
 • Strong wind (**W**, when the wind speed is not less than 15m / s).
• Heavy precipitation (**R30**, when the daily precipitation is at least 30 mm).
 • Mist (**F**).
• Hail (**Ha**).
 • Blizzard (**B**).

In the calculations, the coefficients of aggressiveness of the phenomena were taken in accordance with [1], and the areas of influence of this phenomenon were taken from our previous studies [3-9] (Table 1).

Table 1. The coefficient of aggressiveness (K) and the average area of influence (s) of the phenomenon.

Characteristics	Meteorological phenomena					
	SU25	**R30**	**Ha**	**F**	**W**	**B**
K	0.02	0.03	3	0.5	1.0	0.8
s кв. км	10000	3000	7	6000	4000	5

The discussion of the results. Table 2 provides some information on hazardous weather damage taken from a catalog compiled by us at the Institute of Hydrometeorology of Georgia.

Table 2. Damage from some hazardous weather phenomena.

Phenomenon	Year	Month	Day	Damage million US dollars	District (center highest intensity)
Shower	1972	June	7	Human casualties	Tbilisi
Strong wind	1961	November	16-17	2	Tbilisi
Strong wind	1962	October	26	0.5	Tetri-Tskaro
Hurricane	1973	March	4	5	Tbilisi-Bolnisi
Intense heat and drought	1997	April-May	-	20	Tbilisi
Intense heat and drought	2000	April-May	-	150	Tbilisi
Hail	1978	M	28	22	Kakheti (Sighnaghi)
Hail	1987	M	9	26	Kakheti (Udabno, Nukriani)
Hail and hurricane	2012	July	19	30	Kakheti (Telavi)
Fog	1966	March	5	0.1	Kvemo-Kartli (Tetri-Tskaro)

Noteworthy is the catastrophic downpour observed on June 7, 1972 in Tbilisi, when over a short time (245 minutes), more than 100 mm of precipitation fell. The downpour caused significant material damage to industrial enterprises, communications, transport, utilities and municipal

services, and the city's population. More than 200 individual houses were destroyed, in which more than 1000 families lived, factories were stopped, there were human casualties. According to Table 2, material damage from strong winds on November 16-17, 1961, amounted to USD 2 million, and on March 4, 1973, damage from a hurricane wind in the Tbilisi-Bolnisi region amounted to USD 5 million. The intense heat and drought in the city of Tbilisi and its environs in April-May 1997 caused losses of 20 million, and in June 2001 - 10 million US dollars, on March 5, 1966, heavy fog caused damage to the Kvemo-Kartli region of 10,000 US dollars, etc.

Tables 3 and 4 present data on social and economic risks from hazardous weather phenomena in two different geographic conditions - in Tbilisi and Dmanisi, calculated according to formulas (3) and (4). When calculating the economic risk, the gross domestic product (GDP) was assumed to be $ 26 (in 2015 prices).

Table 3. Social (Rs people) and economic (Re US dollars in 2019 prices) risks from a single phenomenon in Tbilisi.

Weather phenomenon	Season							
	Winter		spring		Summer		Autumn	
	Rc	Re	Rc	Re	Rc	Re	Rc	Re
SU25	0	0	5347	160410	18492	554760	8466	253980
W	66840	2005200	89120	2673600	44560	1336800	44560	1336800
R30	0	0	668	20040	668	20040	334	10020
F	122540	3676200	11140	334200	0	0	77980	2339400
Ha	0	0	322	9660	322	9660	0	0
B	1.2	36	0	0	0	0	0	0

Table 4. Social (Rc people) and economic (Re USD in prices of 2019) risks from one phenomenon in Dmanisi.

Weather phenomenon	Season							
	Winter		spring		Summer		Autumn	
	Rc	Re	Rc	Re	Rc	Re	Rc	Re
W	725	18850	4359	113334	1453	37778	2421	62946
R30	0	0	6	156	12	312	5	130
F	8035	208910	8035	208910	2556	66436	8035	208910
Ha	0	0	4	104	5	130	1	26
B	2	52	1	26	0	0	0	0

Social risk indicates the number of people affected at a certain level, and it characterizes the severity of the consequences (catastrophic) of the implementation of hazards.
Table 3 shows that the distribution of social risks is seasonal. Fog and strong winds pose the most significant risk. In particular, the greatest risk from fog is expected mainly in the autumn-winter period; in summer, it is absent. The social risk from strong winds is most remarkable in spring, although the risk is also significant for other seasons.

The economic risk is also most significant from fog and strong winds. For example, in Tbilisi in winter, the economic risk from the fog in one case may amount to more than USD 3.6 million, in autumn - more than USD 2.3 million. The economic risk from strong winds in spring exceeds $ 2.6 million and exceeds $ 2 million in winter.

Conclusion

The main factors of the process of occurrence of climatic risk of dangerous meteorological phenomena are considered. The article describes a methodology for assessing the vulnerability of objects

(risk recipients) exposed to hazardous phenomena. On the example of two points in different geographic conditions - Tbilisi and Dmanisi - the possible social and economic risks associated with these phenomena have been identified. The greatest climatic danger is represented by fog and strong winds, and in summer, Tbilisi is very hot with concomitant soil, atmospheric drought, and extreme fire hazards. To a lesser extent, the area is damaged by heavy rainfall and hail.

References

1. Kobysheva N.V, Akentieva E. M, Galyuk L.P. Climate risks and adaptation to climate change and variability in the technical sphere. // St. Petersburg, 2015, 144 p., (in Russian).
2. Kobysheva N.V, Galyuk LP, Panfutova Yu. A. Methodology for calculating social and economic risks created by dangerous weather phenomena.// Proceedings of the MGO, vol. 558, 2008, pp. 162-172, (in Russian)
3. Elizbarashvili E.Sh., Varazanashvili O.Sh., Tsereteli NS, Elizbarashvili M.E. Hurricane winds in the territory of Georgia. // Meteorology and Hydrology, No. 3, 2013, pp. 43-46, (in Russian)
4. Elizbarashvili E.Sh., Varazanashvili O.Sh., Tsereteli NS, Elizbarashvili M.E., Elizbarashvili Sh.E . Dangerous fogs on the territory of Georgia. // Meteorology and Hydrogy, No. 2, 2012, p. 52-59, (in Russian)
5. Elizbarashvili E.Sh., Elizbarashvili M.E. Natural meteorological phenomena on the territory of Georgia. // Zeon. Tbilisi, 2012, 104 p., (in Russian)
6. Elizbarashvili E. Sh., Elizbarashvili M.E., Elizbarashvili Sh.E. Investigation of the frequency of occurrence of the most dangerous meteorological phenomena for Georgia. // Meteorology and Hydrology, No. 10, 2020, p. 82-89, (in Russian)
7. Elizbarashvili E. Sh., Elizbarashvili M.E., Elizbarashvili Sh.E., Pipia M.G., Kartvelishvili L.G. Snowstorms in the mountainous regions of Georgia. // Meteorology and Hydrology, No. 1, 2020, p. 58-62, (in Russian).
8. Elizbarashvili E. Sh., Elizbarashvili M.E., Elizbarashvili Sh.E., Pipia M.G., Chelidze N.Z. Catastrophic Precipitation in Georgia. // European Geographical Studies, 6(1), 2019, pp. 50-60.
9. Varazanashvili O, Tsereteli N, Amiranashvili A, Tsereteli E, Elizbarashvili E, Dolidze J, Qaldani L, Saluqvadze M, Adamia S, Arevadze N, Gventcadze A. Vulnerability, hazards and multiple risk assessment for Georgia. // Natural Hazards, vol.64, 2012, pp. 2021-2056.

IDENTIFICATION OF BUILDING CLIMATIC GUIDELINES OF GEORGIA BASED ON THE REGIONAL CLIMATE CHANGE

Kartvelishvili L., Megrelidze L.

National Environmenta Agency of Georgia, Tbilisi, Georgia
lianakartvelishvili@yahoo.com

Summary: *Identification of building-climatic norms and rules may be estimated as the project of important social-economical and financial effects. The problem urgency is preconditioned by the fact that the renewal of legal guidelines base has been taken place in Georgia. By joined action of Georgian government, UNDP (United Nations Development Program), also national and international funds the revision and adjustment with existed legislation of current technical norms and rules is conducting. According existing legislation the above mentioned standards and norms that acted in former USSR have no legal power, and the Georgian analogs don't exist in many cases. Hence the vacuum has been formed and the preparation of science based acts is necessary - for the creation of new guidelines base and provision of its adaptation with national legislation.*
Thus in Georgia the elaboration of new building climatic norms and rules is necessary because in real situation practically the building-climatic norms established according building norms and rules elaborated in Soviet period have been used, that is the reason of unbiased decisions and is connected with significant negative economic effect.

Key Words: *Climate change, climatic norms, climatic-building parameters, mathematical modeling.*

The building-climatic norms established according building norms and rules elaborated in Soviet period are defined on the base of those monitoring materials that reflect the climatic observation data of explored region including 1966 year. In this guidelines document (practically in acting climatic building norms and rules) Georgia is placed in forth climatic zone together with Armenia and Azerbaijan. It is unacceptable because the climate of South Caucasus and especially of Georgia for its geographic location, large hypsometric factors and other climate generating factors is characterized by important peculiarities. Reasoning from above said the assumption of the territory homogeneity of South Caucasus and particularly Georgian territory is wholly unjustified from the point of view of identification of building norms. Correspondingly it is necessary to detailed consider climatic conditions of separate regions in national building norms. This gives possibility to protect building objects from the negative impact of local climatic conditions what in future will make great economical profit (this differ from the current situation when all planned and started construction is realized without any consideration of risks connected with local climatic factors).

For the purpose of perfection of building-climatic zoning of Georgia at first it is needed to specify values of existing climatic parameters, based on the use of regular climatic monitoring data starting from 1966 year period, especially because of the global and regional climatic variations of last decades. The existing norms because of the limited period of its information base can't imply the modern climate change dynamics, what is the essential for the right planning and constructive decisions for building.

Implying climatic parameters is especially important for current situation when the shifting on the light construction has been taken place that is more sensible against change of climatic conditions. The sharp changes of air humidity and temperature influence of heavy showers and winds damages building objects that caused the decreasing of its exploitation level. For the correct projecting the different combinations of climatic parameters and their calculated values have to be considered – according different values from identified climatic norms.

The urgency and novelty of problem is preconditioned by the fact that by the project results complex approach of scientific research will be achieved, identification of building –climatic guidelines implying climatic variations, where the important role is given to the following:

- Specification of significances of existed climatic parameters (because climatic norms are defined up to 1966 year and don't consider climate change dynamics connected with the increasing of intensity of modern anthropogenic impact on environment);

-Complex influence of two and multidimensional climatic factors on building objects;

- New building-climatic zoning of Georgia (implying regional peculiarities of the state territory);

- Elaboration of safety norms against climate negative impact on the building objects and existing constructions.

The main goal of the project is the identification of building-climatic guidelines for separate regions of Georgia using methodical base determined according international standards and based on the corresponding calculations considering regular observation data of local climatic monitoring for the last periods.

In building climatology that is one of the branches of applied climatology, the great significance has the identification of special climatic parameters that are directly used while projecting some objects. Hence the science based identification method of one and multidimensional climatic complexes and its further development are essential.

The increasing rate of civil constructions building using new building materials caused the specification of climatic parameters considered by building guidelines requirements and the necessity to process corresponding special materials that determines the rapid development of building climatology.

To study climate impact on some object the negative as well as positive climatic factors have to be identified. In last years the experimental and theoretical investigations have been widely used to identify corresponding climatic factors. It has to be mentioned that the characters of many climatic factors used in building are identified according values determined from general climatic investigations. Particularly it mainly are the mean and extreme values of some climatic elements.

Using of existed climatic characters simplifies and accelerates their implementation in practice, but the consideration of climate by mean values of separate climatic parameters can't be taken reliable, because means are observed seldom and the provision of significance more than mean value is 50%. The use of extreme data isn't robust while solving practical issues.

For the identification of special climatic parameters it is necessary to ascertain:

-      Peculiarities of climatic observations;
-      Assessment of current meteorological and general climatic information from application point of view;
-      Data processing methods;
-   Relation between climatic elements.

The identification of those factors is necessary, to account atmospheric processes for given concrete issues.

The special climatic parameters determined in the presented project, that will be entered in building norms and rules.

Among them:

1. Solar radiation quantity on surfaces of different orientation and sloping including data of last ten year period

2. To realize thermal-technique report it is necessary to determine so called calculated temperature (internal air temperature for the most cold period of year). While determined this factor the following situation is important – rather than the wall is less massive, the short period averaging is needed to identify calculated temperature value. It is preconditioned by the fact that less massive wall rapidly reacts on the change of internal air temperature and became cold in short period. According calculated temperature value identified by location climatic parameter it is possible to determine required thermal resistivity and its thickness.

3. While studying thermal regime of building it is necessary to determine – is there any need in artificial regulation of microclimate inside the building. Thermal effect of internal air negative temperature in building is originated mainly from thermal-technical features and equipments (heating, ventilation) of supporting construction.

4. With the aim of regulation of building heating system it is necessary to calculate degree-day number and their distribution by months. Table data represent comfort (basic) temperature, that would be maintained between building and internal air temperature. This character is especially important while heating period

For degree-days calculation the following equation is applied

$$\overline{Q} = (T_i - \overline{T})n.$$

where: $\overline{Q}$-is mean degree-days number of heating period, T- air temperature in building is equal 18^0C, $\overline{T}$ - monthly mean multiyear temperature, n-number of days per year

5. Wind influence on buildings is revealed as the loading and presents the main source of building vibration. Excluding wind influence while constructing causes destruction of bridges, high buildings, breaking of wires. Main reason of accidents is incorrect assessment of wind loading, its character an distribution, neglecting of aerodynamical characters, construction vibration. While projecting high building the most important is the including of wind loading. For determination of building durability and dimensional instability it is desirable to obtain detailed information on wind in guidelines.

For the assessment of wind influence on buildings its calculating velocity and strength, profile by height, wind probability of different velocities and direction are determined.

In surface air layers wind direction and velocity is sharply changed due to different factors. It can act during relatively short time as shocks and also change directions. Air flows experience pulsation due to shocks and it is known as wind strength. It is explained using disorder motion or turbulence. In the case of small velocities may happen homogeneity or laminar flows.

On the base of observations in different climatic regions is determined the irregular character of wind strength, that excludes building possible resonance.

Wind loading on buildings is determined by the following equation:

$$Q = n\Sigma C_X \beta q$$

where: n- is overloading factor which is obtained according building height, q-wind velocity loading, β-dynamical factor that includes building reaction against wind strength.

While determine of wind loading great significance has the specification of wind velocity, because it is in second degree and thus the deviation may be too big.

Wind of high speed is rare event, but they produce too great wind loadings, the consideration of those ones is required.

Wind velocity load is determined by equation

$$q = \frac{v^2}{16} kg/m^2$$

6. It has to be emphasize the great significance of practical use of two and multidimensional climate complex. The matching is important of such elements as are the following:
-    Temperature – water vapor partial pressure
-    Temperature- relative humidity
-    Temperature-cloudiness
-    Temperature-wind velocity
-    Wind-rain (especially indirect rain)

Wind and air temperature are important determent factors of building thermal regime. The whole thermo transfer will be greatest when low temperature contemporizes with very strong winds, thus to determine wind velocity and temperature (effective temperature) complex is required.

The effective temperature is the temperature when building thermal passing will be same as in case of internal temperature (T) and wind velocity (V)

The equation for calculating effective temperature has the following expression:

$$T_{ef} = T - CV^2(T_{in} - T)$$

where: T – internal temperature (while ordinary calculations it is equal to18 °C), C- factor characterizing infiltration characters of support constructions (ordinarily C=0.005), T –external air temperature, V-wind velocity m/sec.

7. The coincidence of greatest values of air temperature and humidity, sharp changes of temperature, heavy showers and influence of strong winds damages constructing. High humidity reduces service ability of constructions, negatively influences into the internal microclimate and may caused its destruction. To create normal humidity level all sources of moisturize have to be considered. Exploring humidity regime is impossible except study of thermal regime. Air temperature and humidity are main factors characterizing climate and influence on the humidity regime of supporting construction. To investigate temperature-humidity complex as ranged as well as hour observations will be used. The selection of temperature initial data is conducted after each 5 degree, and of relative humidity after every 5%.

To choose humidity zones, humidity complex parameter k is presented by project implementers

$$K = \frac{H\varphi}{Q_s \sqrt{A_t}}$$

where: H- is precipitation amount in warm period on vertical surface, mm, φ-relative humidity of he most warm month at 13h,%, Q_s- yearly mean radiation on horizontal surface, kj/m, Ai-annual amplitude of air mean temperature (January and July). %.

8. The identification of precipitation amount on the surfaces of different orientation and slopes is the important research issue of project. In observation net, precipitation measuring methods are equally distributed, as in plain also in mountain places. At plains precipitation measure shows real amount of precipitations, in mountain regions it is mentioned the inconsistency between slope moisturize and measured precipitations.

Precipitation amount on surface of different orientation and slope is mainly depended on wind velocity and direction. To determine precipitation amount for surface of any orientation and sloping the following equation is used:

$$H_{Hn} = H_g \quad \frac{\cos\alpha\sin\beta + \sin\alpha\cos\beta(\theta - \theta_0)}{\cos\alpha}$$

where: H_{Hn} – rain amount on ramp mm, H_g -rain amount on horizontal surface, mm, α- rain incident, β-surface incident, θ-rain orientation (is obtained according wind orientation), θ_0- ramp orientation.

Precipitation amount on vertical surface is determined by the equation:

$$H_\Delta = H_j K \frac{V_w}{V_0} \cos(\theta - \theta_0)$$

where: H_Δ-is the precipitation amount on vertical surface (mm), H_j-precipitation amount on horizontal surface(mm), K-factor, considers distance from Earth, $V_0 = 4.5.I^{0.107}$ -rain drop velocity, with depending on intensity.

The characters of precipitations on the vertical surface will be the basis for elaboration of building protection measures against atmosphere impact, to protect building from moisturizing

9. On the service level of buildings the influence of precipitation mineralization is too great. The important role in atmosphere washing out from aerosol admixtures has precipitations. The assessment of amount of mineral matters washing down has significant interest, for this matter the realization of special researches has been determined considering peculiarities of different climatic conditions.

Expected results of the project are:

1.Identification of distribution peculiarities in space-time of special parameters:
-       calculating temperature;
-    degree days;
-    wind strength;
-     wind velocity loading

1. mathematical modeling of radiation on surface of any orientation and slope;

2. Investigations of distribution peculiarities of two and multidimensional complex climatic-building parameters (temperature-wind, temperature-humidity, indirect rain);

3. new building-climatic zoning and elaboration of relevant recommendations for the building protection from climate negative impact based on the revealed regularities of complex climate parameters;

4. Elaboration of safety recommendations of urbanization conditions, building infrastructure development strategy and investment medium for separate regions of Georgia

Scientific and commercial significances are:

From scientific and commercial point of view the project is most important because the identification of perfect climatic building norms may be estimated as important scientific, social-economical and financial project, that will be revealed in strengthening of scientific potential Georgian urban developing, particularly – the possibility to use specificated building-climatic norms at any step of projecting. It is most important that this specification will be realized considering modern climate change tendencies. For Georgia as for independent state it will be firstly constructed science based building-climatic guidelines considering climate change.

The project significance is determined by the following:

-   Specified building-climatic norms based on climatic monitoring observation data over Georgian territory;
-   Based on the specified building-climatic norms perfection of building-climatic zoning and elaboration of relevant recommendations;
-   Elaboration of building mitigation and protecting recommendations against precipitation influence;

References

1. Wijingaard J.B., Klein Tank A.M.G., Konnen G.P. Homogeneity of 20th century European daily temperature and precipitation series. // Int. J. Climatol.,vol.23, 2003, pp. 679-692.
2.   Gilleland E., Katz R.W. Analyzing seasonal to interannual extreme weather and climate variability with theExtremes Toolkit (extRemes). // Preprints: 18th Conference on Climate Variability and Change, 86th American Meteorological Society(AMS) Annual Meeting, 29 January – 2 February 2006, Atlanta, Georgia, P2.15.

PASSIVE AND ACTIVE LIGHTING PROTECTION

Mkurnalidze I., Kapanadze N.

Institute of Hydrometeorology at the Georgian Technical University, 150-a D.Agmashenebeli Ave, 0112
i.mkurnalidze@gmail.com

Summary: *The article discusses various types of lightning protection, from a Franklin lightning rod to a heavy-duty laser lightning protection device. Description of passive (protects only one object) and active (protects several objects at once) lightning protection systems.*

***Key words*:** *Lighting, lightning rods, protection.*

Lightning is a formidable natural phenomenon with tremendous destructive power. The danger of a lightning strike arises due to high voltage (hundreds of millions of volts), high amperage (tens of thousands of amperes) and tremendous temperature (25000-30000ºC).

Lightning discharges pose a significant danger not only to human life, but also to many of his activities. Such as air and sea transport, gas and oil pipelines, power lines, building, agriculture and forestry, communication services, etc. [1,2]. According to some sources deaths caused by thunderstorms claim 6,000-24,000 lives annually. Material damage is estimated at hundreds of millions of dollars [3].

According to WMO and UN reports, the number of natural disasters has especially increased in recent decades. Most of them are thunderstorms. For example: in the United States in 2021, 44 thousand were recorded. forest fires, of which 80% are caused by the so-called dry thunderstorms. The damage amounted to about 75 ml. dollars.

Since the Russian scientist Lomonosov suggested the electrical nature of lightning, and the American scientist Franklin (18th century) established that lightning is a dangerous manifestation of atmospheric electricity, mankind has been looking for a means of protection against this phenomenon. In 1752, Franklin installed a 9-foot-high metal rod on the roof of his house and wired it to a well. The wire ran through the house and connected to an electric bell. Lightning struck the rod and triggered the bell. This invention became the forerunner of modern grounded lightning rods. It should be noted that, despite the many technologies and devices, the principle laid down in 1752 is fundamental and effective. Currently, there are two types of lightning protection: passive and active [4].

Fig.1. Passive and active lightning rods.

The passive construction includes the following elements:
• Lightning rod (catches atmospheric electrical discharge)
• Down conductors (redirect the received energy to the ground)
• Earthing switches (prevent further current propagation)

Lightning rods can be in the form of a metal rod, a cable on two roof supports or a special mesh. For each object, the number of such devices is calculated individually. Down conductors are steel conductors. The grounding electrode system is formed by several electrodes connected to each other. The active type of protection is very similar in design to the passive one, the main difference is the lightning rod device. This is not just a steel rod, but a special electronic device that, when a thundercloud approaches, begins to create high-voltage pulses around itself. Reverse ionization of air flows occurs, and lightning is literally itself attracted and redirected through a safe channel. Such a receiver is installed one meter higher from the most protruding part of the building. It is believed that active lightning protection extends to an area that is four to five times larger in area at the same placement height.

For a passive lightning rod, you will need at least two conductors (according to the number of down conductors and ground electrodes), for an active system, one is enough. Custom-built houses usually have roofs with large differences in height. Therefore, the calculation and installation of a passive system is a laborious process and requires the consumption of a large number of parts. With an active structure, installation is much easier with a minimum of elements. There are many different options for devices in both passive and active systems. Structural elements are made of different materials; the electronic elements used have different characteristics, depending on the type of protected objects.

It should be noted. That over the past decades, due to climate change on Earth, the data on the characteristics of thunderstorms has also changed. Therefore, when installing various types of lightning protection, this circumstance must be taken into account [5].
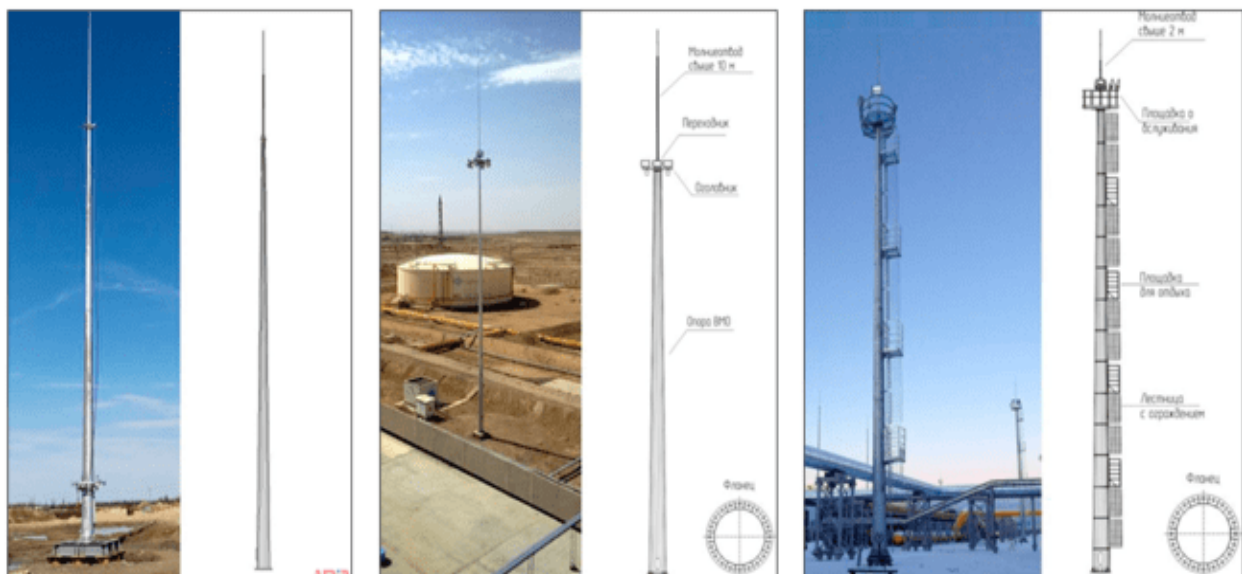
Fig.2. Examples of lightning rods of various designs

In connection with the rapid development of laser technologies in recent years, the idea arose of developing a new type of lightning protection based on high-power femtosecond lasers. Such a laser was developed as part of the Laser Lighting Rod (LLR) project in Switzerland. On Mount Sentis (2502 m) in the Alps (there is a 124-meter antenna on the mountain, to which more than 100 lightning discharges are attracted annually), a one-of-a-kind terawatt laser lightning rod is installed. Every second, the laser sends 100short pulses into the atmosphere.

Fig.3. Laser lightning rod on Mount Sentis (Switzerland).

In the course of its operation, a long ionized channel is created through which the lightning deflects from the protected places. The range of the laser is sufficient to protect large areas with forests and infrastructure [6]. This is a big breakthrough in lightning protection.

The problem of lightning protection is topical for Georgia as well, since the region is considered to be a thunderstorm. The average annual number of thunderstorm days in Georgia, according to the weather station, is about 40 [7]. This fact is confirmed by the map of the global distribution of thunderstorms obtained by NASA from satellite data [8].
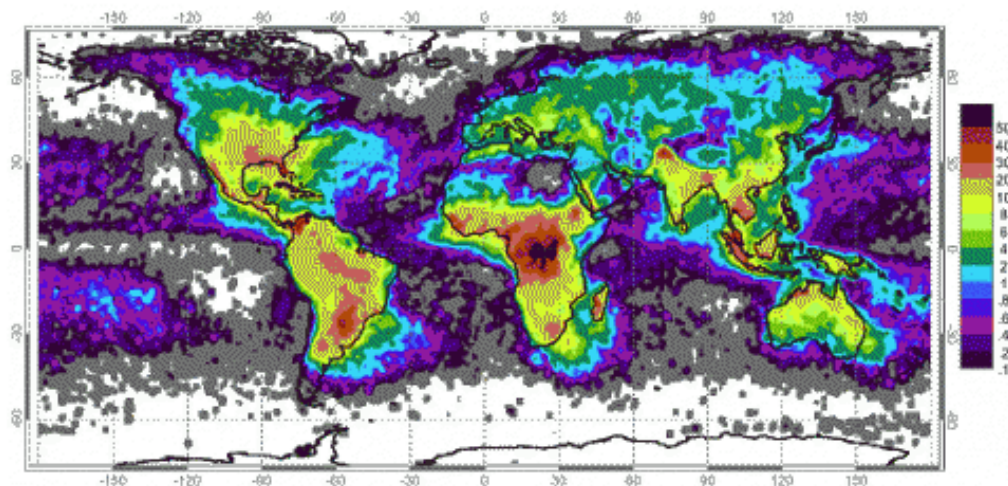
Fig.4. Global frequency of lightning strikes per year per square kilometer.

References

1. Govorushko C.M.   Risk for human activity associated with thunderstorms. // Problems of risk Analysis, volume 8, №4, 2011, (Rus)
2. "Lightning Facts and Information". // National Geographic., October 9, 2009.
3. Holle R.L. Annual rates of lightning fatalities by country. // (PDF). 0th International Lightning Detection Conference, 21–23 April 2008, Tucson, Arizona, USA, Retrieved on 2011-11-08.
4. Features of passive and active lightning protection in comparison. // (voltstream.ru), (Rus)
5. Lightning rods - purpose, types, advantages. // (www.amira.ru), (Rus)
6. Laser lightning rod at the top of Sentis. // (www.swissafisha.ch), (Rus)
7. Tatishvili M., Kartvelishvili L., Mkurnalidze I., Meskhia R. Dynamics and Statistical Distribution of Hail and Thunderstorms in Georgia Against the Background of Global Climate Change. // ”Mtsignobari” Publishing House, Tbilisi, 2018, (Geo).
8. Where Lightning Strikes. // (science.nasa.gov).

WATER DEFICIENCY IN EAST GEORGIA AND RECOMMENDATIONS FOR ADAPTATION

Basilashvili Ts.

Institute of Hydrometeorology of Georgian Technical University, Tbilisi, Georgia
jarjinio@mail.ru

Summary: *The objectives of the study are the assessment of water deficiency and desertification processes risks in East Georgia, planning of measures to reduce the losses and elaboration of adaptation recommendations. The specification of river runoff long-range parameters and features of their anticipated change has serious practical importance for water management calculations in scientific, design and commercial organizations to obtain reliable technical and economic grounding for water management constructions. They will greatly assist both the agrarian experts and designers, ecologists, etc. The implementation of recommended adaptation measures on the basis of river runoff projection will allow to slow down or stop desertification processes and avert the ecological peril. They are highly important and significant for the prevention of hazardous events at the background of progressing climate warming. Their application in practice will assist regional administration and land owners to timely implement corresponding preventive measures for neutralizing expected negative processes, reduction of losses and provision of environmental safety.*

Key Words: *Hazardous events, river runoff, water management.*

Introduction

Water consumption, as a key factor of country's environmental and economic development, has significantly increased in line with the growth of population, expansion of industry and agriculture, resulting in the decline of water resources. This process is substantiated by the global warming which has initiated acute water shortage in a number of regions of the world, causing the hampering of the development in many branches of economy. According to the UN experts` forecast, water consumption to 2025 will increase by 40% and 2/3 of the population may experience water deficiency that will provoke epidemics and mass mortality in underdeveloped countries.

The process of desertification at present is running rather fast than ever in history. The UN has declared desertification as a global problem being related with poverty and environmental changes. About 250 million people are in direct contact with problems of desertification and 1 billion are under its potential threat. More than 100 nations have signed the treaty according to which a global model to combat desertification should be worked out, along with regional models. Therefore, problems of water resources, their projection and rational strategy of water consumption are extremely urgent for today.

Study area and method

Georgia is reach in water resources, but they are distributed very unevenly at the territory. In this respect highly problematic is East Georgia where under the arid climate conditions the productivity of large areas of fertile soils is low without artificial irrigation. Here the 85% of Georgia's irrigated lands are disposed, while 77% of water recourses are concentrated in West Georgia and only 23% - in its Eastern part. At the same time, in contrary to the Western part, the rise in temperature and decrease of atmospheric precipitation is projected in XXI century in East Georgia that eventually will cause the decline of river runoff. This will very negatively affect the water provision of irrigation systems and related productivity of vegetation, efficiency of enterprises and hydropower plants (HPPs) [1].

Besides, as a result of intense droughts and anthropogenic loading the land erosion has been amplified in East Georgia. An area of more than 200 thousand ha is already damaged and 3000 ha are decertified. In this respect most vulnerable regions are: Outer Kakheti, Lower Kartli, Inner Kartli and partly South Georgia. If

the necessary measures would not timely be taken here, the slow-down of desertification process in these regions will become more complicated and expensive in the future [2].

Ensuing from this, the assessment of risks to processes of water shortage and desertification at the territory of East Georgia, study of their development conditions regarding the upcoming climate change and anthropogenic impact is extremely topical. Thus, the objectives of the study are the assessment of water deficiency and desertification processes risks in East Georgia, creation of their projection models, planning of measures to reduce the losses and elaboration of adaptation recommendations. For reaching these goals the solving of following problems is necessary:

Provision, systematization and analysis of information sources and observation materials related with processes to be examined, anthropogenic, hydrological and meteorological factors causing them; description of phenomena connected to the studied processes in East Georgia, selection of characteristic region (river basin and section of the river) for the assessment of their development; specification of main features and calculation parameters of events to be studied and factors causing them for the selected region; examination of multi-year dynamics of events and factors to be studied, definition of their expected variability and development scales. Creation of river runoff long-range forecast model for different time intervals aimed at the provision of selected regions irrigation systems and HPPs with necessary data; working out of recommendations for the reduction of losses in case of the development of water shortage and desertification processes.

Under the conditions of limited hydrometeorological information on river runoff and its forming factors, for the projection of river discharge the multi-factor statistical model will be applied, in which from the existing complex of factors the predictors will be selected and the model will be adjusted using mathematical criteria and multi-stage sifting method. For the determination of numerical quality of optimal projection model the expansion of equation system with the gradual inclusion of factors, when the forecast information is reduced, prediction period is increased and accuracy is grown will be used [3, 4].

As e result the projection formulae are obtained containing different information on the river runoff in vegetation period (IV-IX), its separate quarters (IV-VI, VII-IX) and months, based on which the operational forecasts are issued annually both in single and several case regime, when additional information is included specifying the data. The provision of all kinds of mathematical calculations will be realized based upon unified computation principle using special computer program [5, 6].

Discussion

In the current conditions of global economic crisis and unemployment, Georgia's rural population is keeping its livelihood only by harvesting agricultural produce grown on its plots. Hence, it is highly important to guarantee systematic provision of these plots with water for irrigation. In East Georgia the vegetation, water-demand phases do not correlate with rainfall intervals. Therefore to secure harvesting a wide network of irrigation systems was operating here, destroyed since 1992, wind belts were logged out along with elements and registration of runoff at the rivers has been suspended [7].

Currently the revitalization of agriculture has started in Georgia accompanied with the restoration of irrigation systems, new hydropower plants are built. To provide the filling of their reservoirs it is necessary to define more exactly the discharge of rivers, determine their interannual distribution and variability, that has altered in connection with global warming [8].

In terms of agricultural production volume Kakheti is the leading region. However the plant productivity here is highly vulnerable to weather and climate changes. According to computations performed with the modern climate models it has been established that compared to 2010, the mean annual temperature at the territory of Kakheti will increase by 1.1 °C to 2050 and by 3,5 °C to 2100, while the atmospheric precipitation would change slightly (by ± 5%) to 2050, but decrease by 10-20% to 2100. In such conditions the demand on irrigation water will grow [9].

In Kakheti the irrigation water is provided from the river Alazani. Hence, up to now it is highly urgent to assess its irrigation potential. Ensuing from this, the main problem in the project is the specification of r. Alazani's runoff parameters and definition of its expected variations, that will allow to work out concrete recommendations for the correct determination of water consumption regime. The norms of mean annual, vegetation period quarter and separate months runoff are specified.

Kakheti vast fertile valleys are irrigated from river Alazani water with the biggest irrigation system constructed on it (in Georgia) and composed of two – upper and lower Alazani magistral channels. The upper magistral canal takes start from the upper part of the river, near hydrological post in village Birkiani,

where natural river runoff used to be measured earlier. 76 thousand hectares of land are attached to it for irrigation. The lower magistral canal begins at presently operating post near village Shaqriani and it irrigates 262 thousand hectares of arable. There bas been ascertained the vegetation period of river according to individual months, quarters, maximum and minimal water discharge, extremes, alteration and other statistical qualities – Table 1.

In order to evaluate the impact of climate warming and man-made factors, dynamics of multi-year fluctuation of maximal and minimal runoff, also different intervals of annual and vegetation period of river Alazani water have been studied. Relevant trends have been developed and equations made reflecting their rectilinear approximation, parameters of which are provided in table 2. Their analysis show that tendencies of the change in river Alazani water runoff vary at different periods. This can be explained by diversity of watery tributaries (flowing into the river before these cross-sections) and their regimes, conditioned by natural conditions in these basins.

Table 1. Features of under discharges (Qm^3/s) of the Alazani river

Estimated Period	IV- IX	IV	V	VI	VII	VIII	IX	IV-VI	VII-IX
r. Alazani – Birkiani F = 282 km^2, H = 2200 m, Q_0 = 13.9 m^3/s									
Average	20.4	16.7	26.8	27.7	22.3	15.4	12.	23.7	16.8
Part, % Q_0	73.0	10.1	16.4	16.4	13.6	9.0	7.5	43.1	30.2
Greatest	32.0	27.6	42.7	57.2	51.1	31.0	26.	39.4	27.1
Least	13.4	8.16	17.8	13.5	12.4	7.98	5.9	15.7	9.48
r. Alazani – Shaqriani F = 2190 km^2, H = 1260 m, Q_0 = 45.7 m^3/s									
Average	62.0	70.3	94.0	80.2	52.4	37.0	37.	81.5	42.3
Part, % Q_0	69.4	12.9	17.3	15.1	9.9	6.9	7.0	45.4	24.0
Greatest	128	120	246	223	112	109	117	176	91.3
Least	36.5	25.0	32.4	31.3	15.8	5.72	9.2	40.4	14.4

Trend equation of descending (drop) tendency of natural runoff (Q m^3/wm) of river Alazani vegetation period is presented as follows:

$$T_Q = - 0,0084 \, N + 20,642, \qquad (1)$$

Along with such water deficit in the vegetation period, river Alazani runoff in fall-winter and spring flooding periods is left unused, as water consumption is minimal in this period. This remained water volume is big enough and its accumulation in specific water reservoirs makes it possible to avoid deficit of irrigation water in the vegetation period [10, 11]. In order to economically and rationally manage utilization of the existing water resources of river Alazani in the vegetation period, their forecast is required for different time intervals. River runoff is a complex dynamic process conditioned by multiple factors. But, for forecasting purpose can be used only those that are subject to standard observations and provide operative information.

Table 2. Parameters (a and b) of trends' equations ($T_Q = aN + b$) of river Alazani water discharge periods

Periods of the water discharges	Months	Village Birkiani 1950 – 1996		Village Shaqriani 1933 – 2010	
		a	b	a	b
Annual	I-XII	− 0.002	13.98	0.050	43.79
Maximum	max	− 1.079	98.42	− 1.184	347.8
Minimum	min	0.019	3.731	− 0.126	20.44
Vegetation	IV-IX	− 0.008	20.642	0.031	60.80
April	IV	0.004	16.64	0.337	57.29
May	V	− 0.058	28.23	0.060	90.44
June	VI	− 0.009	27.90	− 0.015	80.79
July	VII	− 0.041	23.30	− 0.014	53.00
August	VIII	0.094	13.13	− 0.005	37.20
September	IX	0.005	12.60	− 0.036	39.01

In our case, existing information on atmospheric precipitations (R mm), air temperature (θ, $^{\circ}$C) and water-consistency of snow (W mm) have been used for forecasting of river water runoff (Q m^3/sec) in river Alazani basin and an enlarged forecast model has been developed, in which separate previous period factors are broken down into different period indicators, thus, impact of their dynamics is envisaged for future runoff. For example, precipitations at fall, winter and spring have diverse impact on the vegetation period runoff. So, it is not expedient to imagine their total sum in this forecast model [3, 4].

Based on the available data and correlation analysis, we revealed the most effectively operating previous period factors and developed a multi-factor forecast model by using them. But, many variables in the forecast model reduce sustainability of the equation, that's why, by specific mathematical criteria and multi-pitched screening method, we corrected the model based on the principle: maximal accuracy with minimal factors [5]. Thus, we developed optimal forecast models by taking into account up to 3-4 factors.

In the process of determination of numerical quality of forecast dependencies, two equation systems are discussed by gradual adding of separate factors, when direct and reversed break down of multi-factor equation is done [6]. In order to plan the rational use of existing water resources for the irrigated agriculture, water discharge forecasts of the whole vegetation period (IV - IX) as well as of its separate quarters (IV - VI and VII - IX) is required (table 3).

Table 3. Forecast equations of river Alazani water average discharge (Q, m^3/sec) of the vegetation period (April-September) and its separate quarter; their assessment criteria

Forecast Equations	Assessment criteria			
	s / σ	P %	r	Э %
r. Alazani – Birkiani F = 282 km^2, H = 2200 m, Q_0 = 20.4 m^3/s				
$Q_{IV\text{-}IX}$ = 0.04 R_I + 0.60 Q_{III} – 0.75 θ_{IV} + 10,52	0.72	61	0.72	61
$Q_{IV\text{-}VI}$ = 0.03 R_I + 1.1 Q_{III} + 0.10 R_{II} + 11,1	0.65	73	76	68
$Q_{VII\text{-}IX}$ = 0.21 Q_{VI} – 1.05 θ_{VI} + 25.3	0.79	60	0.63	65
r. Alazani – Shaqriani F = 2190 km^2, H = 1260 m, Q_0 = 62.0 m^3/s				
$Q_{IV\text{-}IX}$ = 0.48 Q_{II} + 0.27 R_{II} – 0.53 Q_{III} + 0,09 R_{IV} + 44.5	0.84	68	0.63	67
$Q_{IV\text{-}VI}$ = 0.34 R_{III} – 3.36 θ_{III} + 0.12 W_{III} – 58,4	0.73	71	0.74	63
$Q_{VII\text{-}IX}$ = 0.13 Q_V + 0.12 θ_{VI} – 0.34 Q_{VI} + 0.19 R_{VII} + 22.4	0.73	75	0.71	69

Comment: s / σ – correlation between the forecasts' error and average square deviation of the runoff; P % – forecast prediction reliability; r – correlation between the actual and forecast meanings; Э % – economic effectiveness of forecasts. Forecasts are permissible, when: (s / σ) < 0.80; P > 60; r > 0.60; Э > 50.

Forecasts of II quarter (IV - VI) are exceptional by their accuracy, which is very important as this is the quarter when biggest spring floods occur in this river and often create danger to the environment and the population. That's why, these forecasts have two-fold designation. The economic effect received using the developed forecasts exceeds by 10-35% the effect received using the forecast discharge norm. Now, we may say that their application in practice with the purpose to serve irrigation systems and channels, gives possibility to rationally use and appropriately plan the existing water resources of river Alazani – this will increase productiveness of agricultural crop.

Conclusion

Based on the forecast calculations, by the end of the 21st century, due to significant temperature growth (up to 5 °C) as well as increased evaporation from the surface of river Alazani basin, river runoff will decrease by 8,5% compared to the second half of the 20th century [9]. Similar conditions are favorable to frequent drought processes in Kakheti region and the desertification process. For mitigation of negative results of the expected droughts, it is required to use river Alazani runoff in an optimal regime without losses. This requires specific measures:

  • Rehabilitation and expansion of water systems, cleaning, restoration and reconstruction of irrigation channels;

• Putting the pumping stations in operation for additional supply of channels with water;

•   Development and introduction of optimal water distribution/utilization time-tables for water consumers;

•   Accumulation of unused water (of fall-winter and spring floods) in small reservoirs for further utilization during the irrigation water deficit in summer [11];

• Creation of a drip irrigation network; this will increase yield and use less water compared to surface irrigation [12];

• Introduction of a pivot irrigation with those equipment that can be used in huge inclinations and complex relief [13];

• Restoration of windbreak lines in agricultural fields and introduction of drought-resistant varieties;

• Planting of trees on slopes of river ravines;

• Introduction of an active impact on clouds, during which, atmospheric precipitations increase and plants get protected from hail [14];

• Raising awareness of population and farmers to moderately and economically use water resources;

• Annual long-term forecast of river Alazani water discharge for separate intervals of vegetation period (quarters, months and decades). As a result of the planned water consumption regime (and taking into account the water prognosis), the right time for river water irrigation will be determined, as well as timeline for putting the pumping stations in operation, using pivot irrigation systems or increasing precipitations by impact on the clouds [15].

Implementation of the mentioned measures will slow down and suspend desertification process, fight against drought, increase crop productivity and improve economic condition of the population.

References

1. Basilashvili Ts. Changes of Georgia mountainous rivers water flows, problems and recommendations. // American Journal of Environmental Protection, vol. 4, № 3-1, 2015, pp. 38-43.
2. Basilashvili Ts., Machavariani L., Lagidze L. Desertification risk in Kakheti region (East Georgia).   // Journal Environmental Biology, vol. 36, 2013, pp. 33-36.
3. Basilashvili Ts. Multifactorial statistical methodology for forecasting floods-high water flows. // Monograph. Technical University, 2013, p. 180, (in Georgian).
4. Basilashvili Ts. Forecast of mountain river flow with a rare observation network. // Meteorology and Hydrology, № 6, 2014, pp. 61-66, (in Russian).
5. Basilashvili Ts. Statistical analysis of variables and selection of predictors for forecasting dependencies. // Annotation index of Algorithms and Programs, 1971, pp. 43-44, (Russian).
6. Basilashvili Ts., Plotkina I. Determination of multifactor dependencies in equations, estimates of their features and determination of probablity forecasts. // Annotation list of new arrivals in OFAP of GosComHydromet. 4th edition, 1985, pp. 21-22, (in Russin).
7. Basilashvili Ts. Current problems of fresh water and trends in the flow of water in the rivers of the South Caucasus in Georgia. // European Geographical Studies, vol. 7, isssue 1, 2020, pp. 57-67.
8. Basilashvili Ts. Means to mitigate water supply problems in low-water rivers. // Modern problems of ecology, vol. VII, 2018, pp. 33-37, (in Georgian).
9. Georgia's second national communication to the UNFCCC. // Ministry of Environmental Protection and Researcher UNPP, 2009, p. 237, (in Georgian).
10. Svanidze G., Chikvaidze G. On the deficit of irrigation water in river basins of Eastern Georgia.   // Transactions of the Institute of Hydrometeorology, v. 106, 2001, pp. 31-39, (in Georgian).
11. Basilashvili Ts. Reservoirs on the mountain rivers and their safety. // Annals of Agrarian Science, vol. 14, issue 2, 2016, pp. 61-63.
12. Chikvaidze G., Shvelidze O., Geladze I., Devdariani N., Arkielidze N. Introduction of drip irrigation system in arid areas as a tool for rational use of water resources and combating droughts. // Proceedings of Hydrometeorology Institute, v.107, 2002, pp. 218-221, (in Georgian).
13. Nanitashvili O. New generation equipment for the drought-afflicted areas. // Proceedings of Hydrometeorology Institute, v.107, 2002, pp. 223-229, (in Georgian).
14. Begalishvili N., Kapanadze N., Robitashvili N., Rukhadze I. Statistical analysis of cloud resources in East Georgia Territory. // Proceedings of Hydrometeorology Institute, v.107, 2002, pp. 241-253, (in Georgian).
15. Basilashvili Ts. Challenges of expected low water levels on the rivers of East Georgia and the ways of overoming them. // Natural disasters in Georgia: Monitoring, prevention, mitigation, 2019, pp. 70-73, (in Georgian).

FOREST COVER – MAIN PROTECT FROM OF VARIOUS DISASTERS IN MOUNTAINOUS AREAS

Basilashvili Ts.

Institute of Hydrometeorology of Georgian Technical University, Tbilisi, Georgia
jarjinio@mail.ru

Summary: *Today for Biosphere and environmental protection in mountain regions the maintenance particular importance has the forest cover. The mountain forest is the main factor that facilitates the transfer of atmospheric precipitations to the depth of the soil, thus regulating the liquid surface runoff improving the water balance and protecting the river from the drying. The main thing is that forests protect the inhabited areas and populations, roads, fields and soils from dangerous disasters such as floods, mudflows, landslides, avalanches, erosion, etc.*
But, humans are not caring for it and resulting from unsystematic feeling forest are becoming sparse, are losing their protective functions. Therefore, for the present time the environment protection and rational use of forest resources is the global problem of paramount importance.

Key Words: *Avalanches. erosion, floods, mudflows.*

Introduction

Today one of the main concerns of the world society is the anomaly cataclysmic processes caused by global warming on our planet, which resulted in increasing catastrophic disastrous events that led to large destruction and casualties. With the increase of the population of the planet. The capture of forest areas and the irrational cutting of trees causes the reduction of photosynthesis process and the resulting increased heat beams of the sun is the reason that causes global warming, oxygen reducing, new viral, bacterial and chronic diseases [1].

In the XXI century it is expected to increase the temperature on the Earth, which will lead to the melting of Antarctic and Greenland ice, the sharp rise of the world ocean level and flooding the coastline, loss of crops, deficit of drinking water, floods, storms, and coastal erosion will increase as well [2]. Nowadays, for the purpose of Biosphere and environmental protection, for the climate regulation, stabilization of oxygen balance and the maintenance of biodiversity particular importance has the forest cover.

Study area and method

The forest is a vital component of the biosphere and represents a complex combination of trees, bushes, and herbs, animals, birds, and microorganisms that are interconnected affect both the environment and each other. The forest has a substantial impact on the processes that are occurring in the atmosphere, on the surface of the Earth and below its depths. The forest cover participates in the emergence of natural resources such as soil, water, animals, minerals, energy, recreations, and resorts. The forest also plays an important role in economic activity. It is a source of raw material, which is widely used in different industries. The timber is used as building materials and still as a fuel. The forest also provides food and medicinal products. Paper, cardboard, furniture, parquet are made of it. 15 thousand types of a piece of work are made from trees, so the increase in population in the world and technical progress is the reason for an incredible increase in demand for forest resources [3].

The historical, informational and literary sources regarding forest have been studied.

Discussion

The biosphere is the layer of the earth where the life exists and develops. It covers the whole hydrosphere, lithosphere and atmospheric parts. The atmosphere holds part of the space beams and the majority of meteorites. Only 48% of solar radiation reaches the Earth. If there was no atmosphere, the average temperature of the air on the surface of the earth would be 23 ° C, not 15 ° C [4].

In the past, the atmosphere did not contain much oxygen. Then it was rich with carbon dioxide, methane and nitrogen compounds. Nearly 3 billion years ago, the first living organisms on the earth were created at the bottom of the non-deep parts of the hydrosphere, where with the carbon dioxide absorbed by the plant's chlorophyll and from the weather with help of solar energy, free oxygen is released. This process is called photosynthesis. Over a year there are more than 10 billion kcal of solar radiation per 1 Ha on Earth, which is used by the plant for photosynthesis. Every year, with the solar effect, by the green plants, about 83 billion tons of organic substance is formed on Earth. Because of these, 53 billion tons are created on land and the rest in the seas and oceans. Because of photosynthesis, the quantity of carbon dioxide in the atmosphere was reduced to 0,03%, and the number of free oxygen increased to 21% or 1000 times [5].

The development of plants containing chlorophyll on the ground along with the increase of oxygen contributed to the formation of soils. As a result of photosynthesis intensity atmospheric ozone was created, which stopped the adverse effect of ultraviolet beams of the sun. This contributed to the development of the organic world first in the upper layers of water, then on land. Millions of years later, various species of plants were developed that were the primary products for animal and human nutrition [6]. Later, thanks to the increased amount of oxygen, a variety of flora and fauna, including humans have developed on earth.

At present, there are about 2 million species of plants and animals, including animals up to 1.5 million.

The vegetation of the earth annually assimilates around 5×10^{10} tone carbon, or absorbs $1,8 \times 10^{11}$ tone carbon dioxide, decomposes 1.3×10^{11} tone water, separates $1,2 \times 10^{11}$ tone molecular oxygen and gathers 4×10^{17} Kcal solar energy [7].

It is estimated that all 50-60% of oxygen is released by land vegetation and the rest by the phytoplankton. 1 ha forest in 1 hour absorbs so much carbon dioxide as 200 people breath out in 1 hour. During one year, 1 ha of mixed forest absorbs 15 t. Carbon dioxide and releases 13 t. Oxygen. The use of oxygen by humans depends on the physiological condition of his body, age, weight, and sex. In medicine, it is known that the person in a waiting period in one minute spends 0,35-0,40 liters Oxygen and 5 l / min during work. A person needs 500-600 liters Oxygen in a day, therefore a forest area per person should consist of at least 0.3 ha [6]. So the vegetation cover is the source of oxygen, food, and energy, and therefore the existence of humans and animals depends on the condition of the forest cover. But the forest is ruined unmercifully by people [8]. The oldest vegetable cover is found in Australia, which is 395 million years old. About 370 million years ago, vegetation was a form of a bush. Primary forests were low. 345 million years ago, the Stone Age began, when dense, wide forests have been spread with 30 meters high trees. Over the last 800 thousand years, humans have been able to get rid of around 50% of the forest area. Several hundred years ago the forest areas were 7.2 billion hectares, covering 48% of the land. At present, the area covered by vegetation is 12.2 billion hectares 4,1 billion of which are covered with forests [4].

Table. Areas of the World Forest and Their Dynamics

| Region | Common area, Mln ha | Forests of local species, Mln ha | Forest, % from the total area | Forest areas, Mln ha | | Forest Plant Area |
| | | | | Change of forest area 2010 – 2015 | | |
				Total	Annual	2015
World	3999	1277	31	- 17	- 3,0	290
Africa	624	135	23	- 14,2	- 2,4	16
Asia	593	117	19	- 3,4	0,8	129
Europe	1015	277	34	1,9	0,3	82
North America	751	320	33	0,4	0	43
South America	842	400	49	- 10,1	- 2	15
Oceania	174	27	23	1,5	0,3	4

According to FAO estimates (Table 1) in 2015 forests were covering 4000 million ha of land or 31% of its total area. In the early twentieth century, the forest area was about 2 ha per capita. In 2015, per capita comes only 0.6 ha of forests. With regular inventory manufactured by FAO, forestry is decreasing with high rates: from 1990 to 2000 annual decrease was 16 million hectares, and in 2000-2010, 13 million hectares, in 2010-2015 the forest area decreased with 16.5 mln ha or yearly forests were decreased by 3,3 mln ha. In 2016, the destroyed forest area was 29.7 million hectares.

Destroying the forest increases with geometric progress every year. The reason for this, besides the tree cutting, is that the forest area goes into land use categories (arable, towns, roads, etc.). Forests are also destroyed because of natural disasters (landslides, avalanches, etc.) after which the trees will not be restored. According to National Geographic, 80,000 m^2 green cover is damaged annually, causing not only material loss but also victims. For instance, fires resulted in 100,000 deaths in Indonesia. In 2017, about 100 people were killed in California, Portugal, and Spain because of fire. The fires were hugely destructive in California in November 2018 when more than 70 people were killed, 1400 people were lost, and up to 100 ha forest were burnt and about 80 thousand houses were destroyed. It is important to note that during the fires besides people, a lot of live beings, living in the woods die.

With the destruction of forest from the beginning of XXI century, forest cover will be increased by artificial forest or naturally restored forest. From 2000 to 2010, forest area in Asia grew by 2,2 million ha, mainly due to the intensive cultivation of forest in China. Forest areas in Europe have grown annually by 700 thousand ha. Mountain slopes in Georgia were covered with frequent forests, where many varieties of fruits were produced, and many species of animals and birds lived there. That's why the Georgian peasants were kept, defended and fed by the forest. Therefore, in the past, the forest industry has been created here.

Forests in Georgia
(National Atlas of Georgia, 2018)

The forest cover starts from the seashore and extends to 2100-2200 m, and in some cases up to 2500 m. The total forest fund of Georgia amounted to 3007.6 thousand hectares in 2010, which is 43.2% of the country's territory, but it is spread unequally: 58% in west and 42% in the east. 73% of the forests are located at the height of 1000 m above 80% of which are spread over the slopes of over 20°. Forests cover 2770 thousand ha of the state forest fund of Georgia, with 86 protected areas covering 600 thousand ha [9].

In the valleys of high mountains and hard to reach gorges the untouched forests (566 thousand ha) are still remaining. According to World Bank experts, in Europe, we can hardly find a country where the natural landscapes of unique beauty are so exquisitely replaced by old cultural landscapes. It is noteworthy that the forests of Georgia, is the shelter of pre-ice age flora and fauna, or Relics, that connect us with ancient geologic epochs and their area will be a huge loss not only for Georgia but for all mankind.

Along with timber, more than 150 species of plants in the forests give fruits, berries, walnuts, and other resources, using of which can make significant contributions to economic development. More than 110 species of plants are used in medicine. 2/3 out of 48 medicinal and 200 recreational resorts of Georgia are located or surrounded by forest. Their existence in the forest is justified by an aesthetic viewpoint. Therefore, ecotourism and resort-recreational farming are developed in Georgia. The potential of hunting tourism is also great in Georgian forests [10, 11].

The forest is factor of climate formation. Its importance of the forest is first revealed in the regulation of the air elements (air temperature, humidity, motion speed, etc.) that affects human health. In the forest, where almost all the tree-plant emissions of gliding aromatic essential substances Fitoncides, which can disappear many microbes and viruses, that cleans and makes the air healthier. 1 m^3 air contains up to 500 pathogenic bacteria, while the in the 1 m^3 air of the city there are 36,000 bacteria. The forest is the strong filter of the air from dust. It is estimated that 1 ha forest during the year filters 50-70 tons of dust. In this regard, beech copse,1 ha area of which filters about 68 tonnes of dust. Forest to absorb various kinds of noise. In the case of a forest cover, the yield increases by 20-25% [10]. The impact of the forest stripes is particularly pronounced in the months leading up to drought. It is said: "The forest produces water, the water produces a harvest, and the harvest produces the life".

In particular note water management and soil protection skills of the forest. Part of the atmospheric precipitation on the land surface is slept down in the soil that feeds the river all year round. The higher is the seepage in the river the less is the flood and erosion of the soil. Therefore, forests also perform watershed and protective functions. In this regard, the importance of forest is huge in mountainous areas where there are many other defensive features added to the multilateral purposes of the forest, described above. The forest in the mountains regulates the flow of rivers. According to statistical observations, the high frequency (> 0,8) mountain forest is the main factor that facilitates the transfer of atmospheric precipitations to the depths of the soil, thus regulating the liquid surface runoff, improving the water balance and protecting the river from the drying. The main thing is that forests protect the inhabited areas and populations, roads, fields and soils from dangerous disasters such as floods, mudflows, landslides, avalanches, erosion, etc. [12].

No one argues about the great importance of the green forest cover, but as for the proper attention to it, it is not yet visible. The reason for this is the enormous increase in demand for forest resources as a result of population growth and technical progress. In addition, tree-plants are usually cut into forest copse as well as in the towns and planting strips, which, in addition to the lack of oxygen, resulting in the reduction of water keeping and catchment function, which causes drying of some springs, rivers, and lakes.

Conclusion

Forest is a complex ecosystem of trees, plants and living organisms, which is the guarantee of preservation of the cosmic-ecological - economic- sustainable environment of the biosphere on Earth, along with water, air, and soil. The forest absorbs carbon dioxide and releases large amounts of oxygen, regulates microclimate (humidity, temperature, and wind). The forest is a powerful filter for cleaning air and water from harmful impurities. By doing so, it makes the environment healthy and friendly affects human and other living organisms. The forest also provides many types of food and medicinal products.

Forests protect agriculture and populated areas from strong wind. Forest is also the main factor for regulating water resources. It improves groundwater quality, increases their debate. In the mountains, forests protect communities, roads, and fields from floods and mudflows, erosive processes, landslides, and avalanches. The forest promotes an increase in yield.
The forest has great importance in agricultural activities, as a source of raw timber, which is used in various industries. With the increase of population and farming, demand on the timber is increasing as well. Because of this, forests are cut and the forest area is reduced to 0.3% annually in the world.
In addition to plant cutting and disease, the forest is also damaged by fires, which have become more frequent in areas of different countries due to the negligence of adolescents in terms of climate warming.

Because of this the number of oxygen decreases and the amount of carbon dioxide increases in the atmosphere and climate heats intensively.

It is noteworthy that the use of forest areas has helped not only the plant but also the reduction of unique representatives of animals and birds. Particularly negative consequences are to eliminate forests in mountainous areas where the river water regime changes, catastrophic floods and torrents increases, erosive and landslide phenomena develop, soil erosion, stone erosion, snow-glacier evolution, etc. occurs. The areas that aren't covered by the forest began to become a desert that was accompanied by the reduction of food production.

According to expert conclusions, the global warming in the XXI century will continue and the temperature of the Earth may increase by 2 - 4 °C, which will seriously damage the ecosystems and most of the world's countries' economies. So technical progress, on the one hand, improves the conditions of human well-being, but on the other hand, threatens their future. Today, the protection of nature and the rational use of its resources is the primary problem of human significance. It is a necessary precondition for biosphere existence. Therefore, in all countries of the world, special attention should be paid to the protection and expansion of forest cover. In agricultural fields, the protective lines of the forests should be planted, which will help to increase yield. In order to ensure rational use of forest resources, its manufacturing and processing processes must be undertaken with complex non-waste technologies.

In order to protect the biodiversity of forests in the perspective, the system of biomonitoring should be created and timely restoration of forests and their management should be carried out; It is necessary to develop long-term programs for the rational use of forest resources in order to improve forest productivity and its qualitative composition; Complex production of timber raw materials - introduction of techniques of progressive methods of processing and non-waste technologies and finally creating protected areas for the purpose of maintaining biological and landscape diversity.

It is also necessary to raise the knowledge of the broad parts of society on nature and its rational use. Proper bring up of the youth and their love of nature can save the biosphere and our natural environment from destroying and bring us economic prosperity.

References

1. Basilashvili Ts. The importance of forest and results of anthropogenic impact on the mountainous areas. // Actual problems of Geography, 2019, pp. 123-125.
2. Basilashvili Ts. Modern challenges of biosphere safety. // Science and Technologies. Tb., No. 3, (721), 2016, pp. 36-46, (in Georgian).
3. Basilashvili Ts. The role of forests in the development of the biosphere in the context of global warming. // Science and Technologies. Tb. No.1 (721), 2016, pp. 15-23, (in Georgian).
4. Miqadze I. Ecology. 2016, (in Georgian).
5. Qajaia G. Ecological principles of environment protection. 2008, (in Georgian).
6. Dre F. Ecology. 1976, (in Russian).
7. Eliava I, Nakhutsrishvili G, Qajaia G. Foundations of Ecology. 1992, (in Georgian).
8. Basilashvili Ts. Forest and problems caused by global warming. // Global warming and agrobiodiversity, 2015, pp. 75-78, (in Georgian).
9. Geography Atlas of Georgia. 2018, (in Georgian).
10. Kharaishvili G. Water control and antierosion role of mountain forests of Georgia. // Erosion – debris flows phenomena and some adjacent problems, 2001, pp. 237-241, (Georgian).
11. Basilashvili Ts. Forest cover for the safety of biosphere and environment. // European Geographical Studies, vol. 7, issue 1, 2020, pp. 57-67.
12. Basilashvili Ts., Berdzenishvili N. Forest is a factor of environmental safety. // Modern Problems of Ecology, vol. VII, 2020, pp. 60-63, (in Georgian).

RECOMMENDATIONS OF MITIGATING DAMAGES CAUSED BY RIVER FLOODING IN GEORGIA

Basilashvili Ts.

Institute of Hydrometeorology of Georgian Technical University, Tbilisi, Georgia
jarjinio@mail.ru

Summary: *In the recent years, with respect to climate change, in the mountainous river gorges, floods become more frequent and they bear serious hazard and damage as well has casualties. The historical informational and literary sources regarding flooding have been studied. For the water management calculations in order to present the water-related disasters of main rivers of Georgia, the maximum discharge parameters are specified.*
To mitigate the hazards of floods a complex is proposed, in particular: purification and deepening of river beds, reinforcing and complete construction of river bank protecting edifices, laying spillway canals, terracing of slopes, enlargement of forest cover. The main way of water bodies safety is the forecasting of river runoff, which are necessary for the rational use of water resources, too. With the use of the multifactorial model, we obtained the forecast of floods and flooding in advance and accuracy level. The timely awareness about forthcoming high river runoff will give an opportunity to make respective preventive measures and safe human lives, as well as avoid damages.

Key Words: *Disaster, maximum water discharge, parameters, reservoir.*

Introduction. In connection with global climate change on the Earth the number of catastrophic floods has been enormously increased and caused great damages. This problem is especially urgent for Georgia where high waters and continuous floods are preconditioned by the landscape-climatic state. 60-80% of river annual discharge flows during floods. It is formed by simultaneous participation of the melting waters of seasonal snow, rain, eternal snow and glaciers in different ratio. In highland basins flood lasts 5-6 months (from March till August), and in lowland where eternal snow and glaciers are absent it covers March-June months [1].

Indeed floods are the reason of enormous damages but it is fact that on Georgian rivers there has been built 51 reservoirs, due to the hydro power stations, also irrigate and water supply systems are functioning [2]. The annual restore and operation of reservoirs depend especially on the river flood discharges. So floods are the reason as of damages as of great benefit, because at the expense of flood water storages electricity is generated, crop is growing and population and industrial objects water supply is secured.

Except of spring floods on Georgian rivers take place also high waters at any season of year that in rainy periods take catastrophic character. Besides because of the growth of anthropogenic impact (elimination of lakes and growth) the high water increases, that caused irreversible destruction to the separate regions, population, industry, nature and ecological state. Especially during last 20 years in Georgia there were repeated large-scaled catastrophes in several times, that damaged economy significantly (1.5 billion GEL), especially were damaged bridges, rail and high ways, communications, canals, seeding, animals and also humans have been lost.

Method. Within this research various information has been studied, as well stationary observation and expedition materials about phenomena itself also on caused damages were investigated. The formation of Georgian river discharge has been realized in different hydrometeorological and physical-geographical conditions. The water regime of each one is characterized by individuality and thus they aren't identical. For this reasons for each river the different forecasting methodic is needed.

The general physical base of modern hydrological forecasting models is the solution of water balance equation for forecasting period, including many different factors. But in our case under complex mountain relief conditions because of the lack of required information the identification of those regulations that are essential for applying mentioned model isn't available. So we elaborated multi factorial statistical

prognostic model [3] (Basilashvili Ts. 2006), that fully discuss those hydrometeorological factors on which the information exists during operational forecasting: atmospheric precipitation (R mm), air temperature (θ^0C), snow water-content (W mm) and river water discharge (Q m^3/sec). For this reason firstly using definite mathematical criteria less efficient and duplicated factors have been subtracted. From the rest using multi sieve method the optimal prognostic model has been deduced [4]. To calculate all possible variants of prognostic relationships the multi factor dependence was directly and indirectly expanded, when two equation systems have been calculated by gradual adding of separate predictors ($X_1, X_2, X_3 \dots, X_m$):

$$
\begin{aligned}
Y' &= a'_0 + a'_1 X_1; \\
Y'' &= a''_0 + a''_1 X_1 + a''_2 X_2; \\
Y''' &= a'''_0 + a'''_1 X_1 + a'''_2 X_2 + a'''_3 X_3;
\end{aligned}
\tag{1}
$$

$$
\dots\dots\dots\dots\dots\dots\dots\dots\dots\dots\dots\dots\dots\dots\dots\dots\dots
$$

$$
Y^{(m)} = a^{(m)}_0 + a^{(m)}_1 X_1 + a^{(m)}_2 X_2 + a^{(m)}_3 X_3 + \dots + a^{(m)}_m X_m
$$

$$
\begin{aligned}
Z' &= b'_0 + b'_1 X_m; \\
Z'' &= b''_0 + b''_1 X_m + b''_2 X_{m-1}; \\
Z''' &= b'''_0 + b'''_1 X_m + b'''_2 X_{m-1} + b'''_3 X_{m-2};
\end{aligned}
\tag{2}
$$

$$
\dots\dots\dots\dots\dots\dots\dots\dots\dots\dots\dots\dots\dots\dots\dots\dots\dots
$$

$$
Z^{(m)} = b^{(m)}_0 + b^{(m)}_1 X_m + b^{(m)}_2 X_{m-1} + b^{(m)}_3 X_{m-2} + \dots + b^{(m)}_m X_1
$$

Such method is realized by special soft [5], using them the prognostic methods have been elaborated for inflow water discharges in main reservoirs of Georgia for flooding, vegetation periods, quarters, months, decades, daily and flooding maximal discharges [6].

Discussion. To eliminate damages and increase safety it is essential to assess past flood- high waters. But unfortunately during Soviet period the information on great damages and human losses haven't been disseminated. It is remarkable that in the earliest record on floods in Georgia dated by VIII Century great number of losses is fixed. It happened on 735 when invader Murvan the Deaf's 3500 fighters with their horses were lost in river Tskhenistskali flood. Thus after this river was called Tskhenistskali (Horse Water). Catastrophic high waters are frequent on river Rioni within Kolkheti lowland, where high intensive precipitations are common. On October 25, 1922 on river Rioni passed greatest catastrophic flood, which's extreme water discharge (1470m^3/sec) in river basin upper part (vill. Alphana) was regarded as the greatest. In Rioni lower part on April 2 1982 there has been happened greatest flood with maximal discharge (6000 m^3/sec). River Rioni water discharge on February 1, 1987 while high water was 5000 m^3/sec, that was strengthened by 1600 m^3/sec water from Vartsikhe reservoir emptying that was resulted in break of right bank dike and surrounding settlements were flooded. Material losses amounted in 500mln GEL [7].

Catastrophic high waters are frequent especially in Black Sea rivers. Annual precipitations in Adjara reach 2000-3000mm. Two days precipitation sum is 200-350mm. In river Chorokhi near village Erge maximal water discharge (3840m^3/sec) was passed on May 8,1942. Adjara River levels rose up to 4-5m and water flow velocity was up to 5m/sec. Sudden flood on August 31,1979 broke buildings, bridges,roads,gardens [8].
The investigation of last year floods revealed the fact that they aren't decayed but strengthened. The 2005 flood was distinguished, were resulted in catastrophic floods that covered country's many regions. The damage was enormous (Basilashvili Ts. 2008). It is remarkable that in Georgia except snow and rain high waters are caused also by accumulated water discharges resulted from snow slides and ice encumbering. Besides on Georgian rivers it happen ice, stone-avalanches and landslide encumbers, resulted in formation of lakes [9].

Floods are observed every year but they aren't always destructive. They are catastrophic if intensive snow melting coincides with heavy rains, when river basin can't fit water from catchments area, flows over banks and floods surrounding territories. For example on river Mtkvari during observation 76 year period the flood passed only 30 times which's maximal discharge exceeds its mean value. The exceptional flood was on 1968 when in river Mtkvari bank protecting constructions, roads, bridges were destroyed, railroad and vehicle traffic were broken. Mtkvari highest water peak passed in city of Tbilisi with 2450 m^3/sec water discharge that exceeded river basin those capacity -1800 m^3/sec, calculated for last year maximum on 650 m^3/sec or by 36%. In result water overflowed and flooded surrounded territory.

To avoid such situations it is necessary to specify river features especially maximal runoff characteristics, considering new data. Thus firstly river runoffs and their maximal discharge norms, extreme and probable values with 10%, 5%, 1%, and 0.1% support and starting from 10 till 1000 year repeatability have been specified [10] (Table 1). This data are essential for projecting organizations in water industry calculations for building safety.

Table 1. Average Annual Water Discharge of the Rivers of Georgia and Maximum Discharge of Flooding Period (Q m^3/sec)

River-Point	Area of basin km^2	Annual Q m^3/sec	Q_{max} (m^3/sec)			Provision (%)			
			Ave-rage	Maxi-mum	Mini-mum	0.1	1	5	10
						Frequency, year			
						1000	100	20	10
Enguri-Khaishi	2780	118	534	1440	250	2220	1360	930	770
Rioni-Alpana	2830	103	467	825	276	1270	900	690	615
Kvirila-Zestaphoni	2490	60.7	395	1030	140	1700	1070	721	605
Khanistskali-Bagdati	655	15.9	86.6	209	27.1	484	277	178	146
Mtkvari-Tbilisi	21100	203	1152	2450	448	3500	2300	1760	1580
Didi Liakhvi-Kekhvi	924	27.0	136	330	42.2	1200	470	200	134
Ksani-Korinta	461	9.39	64.3	262	16.9	560	293	165	124
Aragvi-Jhinvali	1900	45.1	243	660	67.0	1000	700	500	420
P.Aragvi-Magaroskari	736	19.3	118	338	50.1	530	340	245	200
Tetri Aragvi-Pasanauri	335	12.1	61.1	173	24.8	324	200	130	80
Shavi Aragvi-Shesartavi	235	7.76	47.1	156	21.6	266	160	104	85
Alazani-Birkiani	282	13.9	75.4	365	30.0	1000	350	170	122
Alazani-Shaqriani	2190	43.4	318	1160	94.3	1730	1080	700	550

Multiyear change dynamics analysis of floods revealed maximal discharges growth tendency in Western Georgia on the Caucasus south slopes rivers (Bzipi, Kodori, Enguri, Rioni, Kvirila), and on south-western and eastern Georgian rivers they reduced. During last years the growth of flood maximal discharge is caused basically by global climate change, but also in past years forests were intensively felt down, they deter water surface runoff and reduce its maximal peaks. Besides river basins aren't cleaned that reduces its water discharge ability and causes environment flooding [11]. On fig. 1 is presented maximal discharges dynamics.

a)

b)
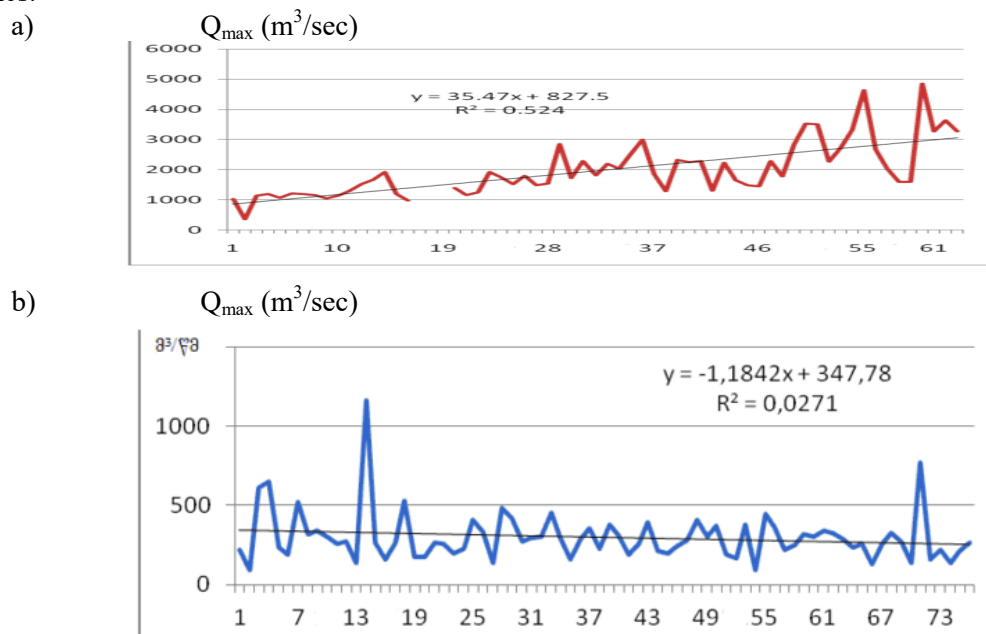
Fig. 1. The multiyear variation dynamics of river water maximal discharges in river
a) - Rioni – Saqochakidze (1928 – 1990) and b) - Alazani – Shaqriani (1933 – 2010).

For the passing flood smoothly the slopes have to be terraced, and woodland has to be renewed and widened. Also reservoirs significantly reduce flood hazard, which accumulate a great amount of flowing water and provide water resources conservation: for electricity generation, water supply and melioration. Reservoirs are also base for enlargement of sports and fitness and tourist- recreation zones. Using reservoirs energetic problems in mountain regions became possible to resolve, deforestation process will be decelerated, populations social-economical state will be improved. Thus in mountainous river conditions it will be useful to construct small size reservoirs, that will be the most safe and efficient facility [12].

Academician Givi Svanidze indicated on the necessity of reservoir construction in Georgia: "The reservoirs net have to be widening to renew water resources that are the most safety and efficient means" [13]. Together with construction of reservoir it is necessary to draw up its emergency emptying schedule based on the exact hydrological calculations in the way that in flood it emptied ahead of peak reaching step by step no simultaneously, that at its end, can caused flood strengthening. In future reservoir net would be enlarged. Their construction needs significant expenditures but mountainous small rivers upwelling may be the reason of more losses. Reservoirs water resources may multiply be used to improve state economy.

For present because new reservoirs are unconstructed in Georgia and also forest recover in short period of time is impossible, then for the mitigation of flooding hazard and safety of flood catastrophes the following activities are recommended: river basins to be cleaned and deepened after flooding, picked stones may be used to strengthen and rebuild bank protecting constructions; tunnel in the mountain bottom spillways; identify flooding margins, where settlements, building and industry would be prohibited.

For flooding safety most appropriate is to elaborate flood long-term and high water short-term forecasting methods that are essential also for water resources conservation and reservoir exploitation. The forecasting development can't avoid event but makes possible to mitigate its negative impact.

Long-term operative forecasts of flood maximal discharges are generated in March, when the observation data of passed winter period have been known, and maximal discharges will pass after 1-3 months (in April-June) in that extreme situation when snow intense melting coincides with rains. In this period the impact of existing factors on the formation of maximal peak is too significant, but its consideration in prognostic computation is really impossible, because of lack of corresponding numerical prognosis.

The forecasting methods were formed using statistical model [4], where the predictors selection was carried out using multistep exclusion rule, and the equation is worked out the multifactor equation system was directly (1) and indirectly (2) expanded by corresponding assessment criteria. Using such method it is possible to reduce prognostic information, increase operability and accuracy. In the result of research for 17 industrial hydro section of Georgia the prognostic equation of maximal discharges (Q m^3/sec) have been obtained considering following factors: atmospheric precipitations (H mm), air mean temperature (θ^0 C), water-content of snow cover (W mm) and river water discharge of last period (Q m^3/sec) [6]. Gradual adding of those factors makes possible to precise prognosis step by step. The forecasting results are presented in table 2.

Table 2. Examples of river maximal discharges (Q_{max} m^3/sec) long-term and high water (Q_m m^3/sec) short-term forecasts with their stepwise accuracy

Prognostic equation	Assessment criteria		
	S/σ	P%	r
River Mtkvari-city of Tbilisi			
$Q_{max}=6.16H_{XII-II}+551$	0.73	62	0.70
$Q_{max}=5.65H_{XII-II}-57.7\theta_{III}+745$	0.68	66	0.75
$Q_{max}=4.76H_{XII-II}-84.67\theta_{III}+2.21Q_{III}+538$	0.67	70	0.76
$Q_{max}=2.60H_{XII-II}-1177\theta_{III}+2.78Q_{III}0.63W_{III}+752$	0.64	72	0.80
River Rioni-village Namokhvani			
$Q_m=0.71Q_b+269$	0.65	75	0.76
$Q_m=0.73Q_b+0.87\theta_{n-1}+233$	0.63	77	0.77
$Q_m=0.72Q_b-9.1\bar{\theta}_{n-1}-5.72\ \theta_{n-1}+249$	0.62	79	0.78
$Q_m=.73Q_b+14.0\ \bar{\theta}_{n-1}13.8\ \theta_{n-1}+12.3H_b+296$	0.61	80	0.79
$Q_m=0.71Q_b+7.5\ \bar{\theta}_{n-1}-9.2\ \theta_{n-1}+13.9H_b+1.7H_{n-1}+283$	0.60	82	0.80

Marks: S/σ is the ratio of prognosis mean square deviation (S) with mean square deviation of prognostic element (σ); P% - prognosis justification; r-correlation factor between actual and prognostic values.

In this prognosis (1-3 month beforehand) winter precipitation sum ($H_{XII-II-mm}$) and March month data: air mean temperature (θ_{III} °C), river water expenditure (Q_{III} m³/sec) and snow water content (W_{III} mm) are used. For short-term forecast (24 hr. beforehand) high water pre-day (b) and passed maximal discharge pre-day (n-1) data; for air temperature as its mean daily ($\bar{\theta}$ °C) also its maximal (θ °C) values have been taken.

Conclusion. The received prognosis give possibilities to conduct all preventable measures in case of expected high peaks, to secure all objects and avoid damages and losses. River water high peak forecast urgently have to be passed to corresponding bodies and organizations, for timely alert population and carry out evacuation and safe tangible property. Besides reservoirs must be emptied to receive water flows in what follows.

In future for the elaboration of perfect prognostic methods except hydrometeorological net it is necessary to use satellite and vertical aerial photograph data. Also it is necessary to create radiolocation and remote sensing net. Scientific analysis of those data makes possible to create prognostic methods of anomaly hydrometeorological processes.

References

1. Basilashvili Ts., Saluqvadze M., Tsomaia V., Kherkheulidze G. Catastrophic of flooding, mudflow and avalanches in Georgia and their safety. // Monograph. Technical University, 2012, 243 p. (in Georgian).
2. Cadaster of Georgia's water reserves. // Tbilisi, 2018, 260 p. (in Russian).
3. Basilashvili Ts. The method of working out hydrological prognosis conditions of limited information. // Bulletin of the Georgian Academy of Sciences, vol. 162, Number 1., Georgian Academy of Sciences. 2000, pp. 110-112.
4. Basilashvili Ts. Multifactorial statistical methodology for forecasting floods-high water flows. // Monograph, Technical University, 2013, p. 180, (in Georgian).
5. Basilashvili Ts., Plotkina I. Determination of multifactor dependencies in equations, estimates of their features and determination of probablity forecasts. // Annotation list of new arrivals in OFAP of GosComHydromet. 4th edition, 1985, pp. 21-22. (in Russian).
6. Basilashvili Ts. Forecasting mountain river flow when having inadequate information. // Monograph, Technical University, 2013, 148 p. (Georgian).
7. Tsomaia V. Maximum water discharges of disastrous flows on the river Rioni. // Erosion – Debris flows phenomena and some adjacent problems, 2001, pp. 224-228. (in Georgian).
8. Svanidze G., Khmaladze G. Flash flood and floods. // Dangerous Hydrometeorological phenomena in the Caucasus. Gidrometeoizdat, 1989, pp. 194-210. (in Russian).
9. Tsomaia V., Gachechiladze G., Tsintsadze T., Gorgijanidze S., Pkhakadze M. Clogging floods and flows on Georgian territory, 2009, 134 p. (in Georgian).
10. Basilashvili Ts. Characteristics of the floods on the rivers of Georgia and ways of their prevention. // Transactions of the Georgian Institute of Hydrometeorology, vol. 115, 2018, pp. 313-321. (in Georgian).
11. Basilashvili Ts. Changes of Georgia mountainous rivers water flows, problems and recommendations. // American Journal of Environmental Protection. vol. 4, № 3-1, 2015, pp. 38-43.
12. Basilashvili Ts. Reservoirs on the mountain rivers and their safety. // Annals of Agrarian Science. vol. 14, issue 2, 2016, pp. 61-63.
13. Svanidze G., Tsomaia V., Meskhia R. Vulnerability and adaptation measures for water resources in Georgia. // Transactions of the Institute of Hydrometeorology, vol. 106, 2001, pp. 11-30 (in Georgian).

BASIC PRINCIPLES OF PLANNINGAND IMPLEMENTATION OF RAPID RESPONSE FORCES IN THE EVENT OF A DESTRUCTIVE EARTHQUAKE

*Nazaretyan S.N., *Nazaretyan S.S., **Mirzoyan L.B., ***Mughnetsyan E.A.

* *Territorial survey for seismic protection", Ministry of Emergency situations of Armenia. 3115 V. Sargsyan str. 5a, Gyumri, Armenia,*
** *Yerevan State University, 0025, A. Manukyan str. 1, Yerevan, Armenia*
*** *D2S Calibri quality assurance, Siemens electronic design automation. 0038 Halabyan str. 16, Yerevan, Armenia*
snaznssp@mail.ru

Summary: *In the aftermath of a destructive earthquake, in order to provide operative and effective assistance by the rapid response forces (rescue, police, traffic police, security facilities, medical, anti-epidemic, fire, water and sewerage, electricity, gas, telephone, etc.), to the minimizing victims, the possible material losses, it is necessary to apply the following principles, which are based on the 1988 Spitak earthquake lessons:1. Develop specific action plans based on seismic risk assessments and risk maps. 2. Plan to achieve high efficiency within 3-5 days of the earthquake, when there are great opportunities to save lives and prevent secondary consequences of the earthquake. 3. Make plans taking into account the conditions of extreme action (most unfavorable conditions of the year and day, lack or absence of means of livelihood, losses of rapid response forces, etc.) and the maximum possible consequences of the earthquake. 4. To ensure the coordinated actions of more than 10 rapid response forces, that is, to make complex plans. 5. Make complex plans simple and accessible so that they are feasible for outside forces.It is necessary to distinguish between the actions of the rapid response forces before the earthquake (preparatory phase) and immediately after the earthquake (rapid response phase).*

Keywords: *Destructive earthquake, rapid response forces, losses, operative and effective assistance.*

Introduction. The purpose of the rapid response is: provide prompt, effective assistance to victims and reduce potential losses, especially in the first 3-5 days [1-3]. These include forces for: life support (water supply and sewerage, electricity, gas supply, electronic communication -telephone, heat supply), providing non-emergency assistance to the population (rescue, medical, fire), establishing order (law and order, protecting important facilities, regulating vehicle traffic), bury of the dead, prevention of epidemics (anti-epidemic) [5]. To achieve this you need:

A. Before the earthquake.
1. Identify and assess vulnerable areas and objects [4],
2. Develop earthquake action plans,
3. Develop a crisis management system,
4. Create information systems,
5. Accumulate resources for task implementation,
6. Develop response mechanisms,
7. Educate the population, local self-government bodies and local authorities, conduct training exercises to minimize losses and to mitigate or localize the secondary effects of an earthquake.

B. After the earthquake [5, 6].
1. Receive operative information about the disaster situation,
2. Cooperation between rapid response forces,
3. Cooperation of actions with the local authorities,

4. Carrying out priority actions, including search and rescue; pre-medical and medical care; Disaster survival (food, water, temporary shelter; restoration of means of communication; infrastructure; providing information; provision of logistical means; order, security etc.) and prevention of quake secondary effects or localization.

The socio-economic and political situation of the disaster zone, the scale of the disaster, the level of readiness of the population and local authorities, rapid response forces, and local customs should be taken into account when planning and carrying out operations [5, 6].

Action plans should be included and corrected:
1. Gathering information,
2. Adjustment of plans,
3. Search and save,
4. Evacuation and Migration management,
5. Organization of emergency medical care,
6. Disaster life support,
7. Restoration of media,
8. Establishment of order,
9. Establishment of an information service,
10. Organization of material and technical supply.

When carrying out operations, it is necessary to take into account the forces, means, material and technical supply system (roads, railways, airport, etc.).

The structure of action plans. The final goal of the developed methodology is to draw up a comprehensive plan for the operational and effective actions of the rapid response forces in a devastating earthquake. A comprehensive plan means a plan of mutually agreed and joint actions of all rapid response forces (services).To achieve this goal, it is necessary first to draw up a plan for each service and according to a single structure using a unified approach, and then coordinate these plans from the standpoint of mutual actions. This way of drawing up a comprehensive plan is more effective and focused.A structure for drawing up plans for services is proposed, consisting of the following sections: general data about the service (address, means of communication, the same for its facilities), the potential of the service (number of specialists and basic equipment), seismic resistance of buildings, including its facilities and equipment, the possibility earthquake redeployments, emergency supplies (electricity, water, fuel, etc.), vehicles, priorities, actions after a devastating earthquake, data on coordination with other services, etc. Action plans of the services are drawn up by their specialists with the help of seismologists. The role of a seismologist is important in compiling a forecast map of the consequences of an earthquake, in determining the seismic resistance of buildings of service facilities and in predicting the situation that may develop after an earthquake. Of a certain complexity and importance is the compilation of the priority tasks that arose immediately after the earthquake and their implementation. It should be taken into account that all urgent actions should be aimed at saving lives, preventing or localizing the secondary consequences of an earthquake, life support and the establishment of law and order.

Special attention should be paid to the important factors that threaten the life support of the city. They can radically change the situation in the city. Therefore, when defining the operational objectives of the actions of the services, one must start with these factors.

When drawing up schedules for the implementation of specific tasks, it is advisable to start them simultaneously, because in all three areas of work are very important. For example, it is difficult to say which is more important in rescue work or fire prevention, etc.

In the plans, much attention should be paid to the issues of attracting the forces and capabilities of services that came to the rescue from outside. It should be borne in mind that the plan is drawn up for them as well, but they do not know the city, the current situation, the location of important objects, etc.

Whenever possible, plans should be drawn up both in the national language and in Russian and English.

Importance of international and interstate agreement on relief in severe earthquakes. Managing international and other rapid response forces is an important issue for seismic risk management. Many states

located in seismic active regions are not able to independently provide rescue operations and eliminate the consequences of a strong earthquake. Therefore, it is necessary to solve this problem with the involvement of the forces and means of other states and international organizations. For this, it is necessary to create a number of prerequisites, including: to become a member of international organizations to unite the national civil protection forces; conclude an agreement with neighboring states on mutual assistance in case of earthquakes, etc.

Some of the most common mistakes in compilation and implementation. An analysis of the results of a survey of specialists from the municipal services of Armenia and Georgia concerning their activities after the Spitak (1988) and Racha (1991) earthquakes, as well as world experience, showed that the main reasons for the low efficiency of the actions of the rapid response services are as follows: a) significant errors in predicting the possible consequences of a strong earthquake, including large-scale destruction;
 b) shortcomings and difficult implementation of action plans, especially comprehensive plans; c) failure (death or injury) of part of the service personnel; d) lack of the required amount of equipment, equipment and material resources; e) blockages of streets and traffic jams, leading to a change in the usual routes of action; f) forced separation of service employees from their duties; h) irrational distribution of external rapid reaction forces in the area of large destruction, etc.

Results and discussion: In the event of a devastating earthquake, rapid response forces need to have specific action plans aimed at reducing casualties, preventing or localizing secondary consequences, ensuring the livelihood of the population of the destruction zone and establishing order. In order to make these plans, it is necessary to follow certain principles: to be applied immediately after the earthquake and to be planned especially for the first 3-5 days; take into account the possible consequences of the earthquake and the emergency situation; rely on the potential of the rapid response force, taking into account the possible loss of manpower and equipment; plans should be mutually agreed upon by all forces - complex plans should be drawn up; plans should be agreed with local self-government and state bodies; be simple and workable, including for outside forces.

References

1. Captain Jason C. Mackay. The CSS Quick Reaction Force. // Archived from the original on August 2015. Internet archive „Wayback Machine,,. http://www.alu.army.mil/alog/issues/MarApr01/MS574.htm
2. Michael T. Chychota and Edwin L. Kennedy Jr. Who You Gonne Call? Deciphering the Difference Between Reserve, Quick Reaction, Striking and Tactical Combat Forces. // INFANTRY, pp. 16–19. Archived from the original on 2019. Retrieved 2021-01-06.
   https://www.benning.army.mil/infantry/magazine/issues/2014/Jul-Sep/Chychota.html
3. Nazaretyan S.N. Seismic hazard and risk of the city's of zone 1988 Spitak earthquake. // Publishing House "Gitutyun-Scienes" NAS RA. Yerevan, 2013, 212 p. (in Russian).
4. Nazaretyan S.N. Main features of the new methodology for seismic risk assessment of Armenian cities. // Seismic Instruments, 56, 2020, pp. 317-331. DOI: 10.3103/S0747923920030093
5. Nazaretyan S.N., Nazaretyan S.S., Mirzoyan L.B. Some Baseline data for a Effective Response of Emergency Servicis in a Seismic Disasters in Soutern Caucasus. // Proceedings of Inter. Scientific Conference „Natural Disasters in Georgia: Monitoring, Prevention, Mitigation". Publish House of Tbilisi State University, 2020, pp. 36-39. DOI:10.13140/RG.2.2.11733.78565
6. Nazaretyan S.N., Nazaretyan S.S. Assessment of the Need for Rescue Forces during Destructive Earthquakes (a Case Study of Armenia). // Seismic Instruments, vol. 57, N 2, 2021, pp. 150-162. Doi.org:10.3103/S0747923921020298
7. Nazaretyan Sergey, Nazaretyan Siranuish. The Public and Liquidation of Consequences of Seismic Catastrophe. // Engaging the Public to Fight the Consequences of Terrorism and Disasters. IOS Press, NATO Science for Peace and Security Series. Vol. 120. Netherlands, 2015, pp. 250-256.

RIVER TEREK GLACIAL BASIN DEGRADATION DYNAMICS ON THE BACKGROUND OF CURRENT CLIMATE CHANGE

*Kordzakhia G., *Shengelia L., **Tvauri G., ***Dzadzamia M.

* Institute of Hydrometeorology, Georgian Technical University
** Iv. Javakhishvili Tbilisi State University E. Andronikashvili Institute of Physics
***National Environmental Agency of the Ministry of Environmental Protection and Agriculture of Georgia,
Ahmashenebeli av. 380077, Tbilisi, Georgia,
giakordzakhia@gmail.com

Summary: *In Georgia, on the ridge of the Greater Caucasus, there are well-developed, rather high glaciers. The study of glaciers has gained more importance since the second half of the twentieth century due to the negative impact of current climate change, which has led to significant and rapid degradation of glaciers, exacerbating natural disasters of glacial origin. Due to the degradation of glaciers in the country, a change in the water balance and degradation of landscapes, an increase in the level of the Black Sea, and the growth of the natural disasters frequency and intensity of glacial origin are having a place. This poses a serious threat to the sustainable development of the country and, therefore, the study of glaciers has become a priority in the research program of Georgia. Using satellite remote sensing, GIS technologies, glacial catalogue, field ground observations and expert knowledge, the negative impact of modern climate change was revealed and, as a consequence, the dynamics of degradation of glaciers in the glacial basins of East Georgia was studied in detail. In this article, the dynamics of the degradation of glaciers in the glacial basins of River Terek is overviewed. For this purpose, a comparison is made of the state of glaciers (area and number) for three time periods. The initial state is taken to be the state of glaciers in this basin at the time of the finish of the glaciers researches (1960). The data gathered were published in several editions of the glacier catalogue. Subsequent states - middle (2015) and final (2020) are determined using high-resolution satellites. Technological and methodological research proved to be effective for studying the dynamics of glacier degradation based on innovative high-resolution satellite remote sensing since the best practices were used in conjunction with the methods developed by the authors. A comparison of these conditions showed that the area and number of glaciers are greatly decreasing due to climate change. It should be noted that the dynamics of glacier degradation is nonlinear, which makes the melting of glaciers in the second period more intense than in the first. This conclusion also confirms one of the main theses of the 6th IPCC report that the main problem is not climate change, but its speed.*

Keywords: climate change, satellite remote sensing, glacial basin, glaciers, degradation dynamics.

Introduction. Glaciers are important climatic and economic resources of Georgia. They contain large amounts of freshwater and play a decisive role in water regime and regional climate forming. Current climate change has a very negative impact on the cryosphere, in particular on the glaciers [1]. The study of glaciers has gained more importance since the second half of the twentieth century due to the negative impact of climate change. With high confidence this has led to significant and rapid degradation of glaciers, exacerbating natural disasters of glacial origin. Due to the degradation of glaciers, a change in the water balance and degradation of landscapes, an increase in the level of the Black Sea, and the growth of the natural disasters' frequency and intensity of glacial origin are having a place [2]. This poses a serious threat to the sustainable development of the country and, therefore, the study of glaciers has become a priority in the research program of Georgia.

Georgia's Second and Third National Communications to the UN Framework Convention on Climate Change analyze climate change influence on glaciers, particularly those found in Zemo Svaneti and Kvemo Svaneti regions of Georgia. The papers explain that available information is incomplete, because the complexity of glaciological research makes simultaneous monitoring of all glaciers impossible, and note that the research uses several assumptions.

The uncertainties found in the above communications can be significantly reduced if glaciological researches will be carried out with the help of satellite remote sensing (SRS).

Methodology and data. Following large-scale glaciological researches, conducted mainly by field works in 1860-1960 the data about glaciers characteristics were systematized and catalogued as part of the Caucasian glacier system. After these activities, the glacier catalogue (hereinafter – the catalogue) of the former Soviet Union [3] was issued.

At present to give a science-based response to glacier melting caused by climate change, it is necessary to use a high-resolution SRS because currently, it is impossible to carry out the costly ground observations at a necessary scale; and in resource- and time-constrained environment, SRS allows conducting simultaneous glacier monitoring on large territories with the necessary resolution and accuracy in conditions of limited resources and restricted time.

For the determination of the conditions of the glaciers, we have conducted works based on processing satellite data and determined the conditions and characteristics of Georgian glaciers [4]. For data accuracy along with SRS information, historical data and expert knowledge are used. The technological-methodological approaches of the research proved to be effective for the study of glaciers based on innovative high-resolution satellite remote sensing, as the best practices [5] were used together with the methods developed by the authors [6].

To ensure the effectiveness of the established surveys, high-resolution SRS images are used, namely: 1. Landsat satellite data (15–30 m resolution), 2. Satellite information free databases are stored in the archives of the National Aeronautics and Space Administration (NASA) and the Global Land Ice Measurements from Space (GLIMS) project. Various GIS applications are used to process satellite data. Effective software is Google Earth, which offers satellite images of high spatial resolution (0.5- 0.8 m), which allows determining the contours of glaciers with great accuracy.

The impact of current climate change on glacial basins can be researched in several ways. One of the effective ways is to study the degradation dynamics of the glaciers from the glaciation basins.

The study region is the glacial basin of the river Terek (East Georgia). This well-developed glacial basin is located in a high mountain region on the watershed ridge of the Caucasus, where mountain ranges are more than 3,500 m high. Our objective is to research r. Terek glacial basin degradation. This is possible by comparing information about glaciers areas and numbers existing in the past with the data currently available. As initial data, we are using the data from the catalogue about glaciers areas and their numbers. The second condition (medium data) is the information regarding glaciers areas and numbers from the Terek glacial basin received by processing satellite data for the period 2006−2015 (mainly the SRS images from 2015) [6]. Conventionally this data we call SRS 1. For having the data characterizing the dynamics of glaciers we added processed data (final data) derived from Landsat 8 satellite September 13, 2020 images. Conventionally this data we call SRS 2. The data received from the SRS (SRS1 and SRS2) were compared with each other and the initial data.

To complete the studies carried out in the basin, two problems needed to be clarified. Specifically, the issue of identification, mainly of small glaciers in the satellite images, and the issue of inaccuracies identified, mainly of the areas of small glaciers in the catalogue. For the identification i.e. determination of locations of the small glaciers on satellite images was used the special schemes (maps) of the glaciers existing in the catalogue. Regarding the second problem, the solution was found in the refinement of the data on glaciers areas using topographic maps from the 1960s [7].

Results and discussion. The river Terek glacial basin is interesting by the fact that all large glaciers spread in East Georgia are located in this basin. Fig. 1. presents: Part a. Small glaciers of the Terek Basin (№98 − 111) and corresponding contours determined based on the methodology of the processing of SRS data mentioned above and part b. same glaciers (№98 − 111) and their contours on the topographic map of 1960.

The colour of the pins in the satellite images conveys the following information: the glacier for the relevant period is marked in green, the glacier turned into a snowfield is marked in yellow, and the place where the glacier once existed i.e. fully melted is marked in red.
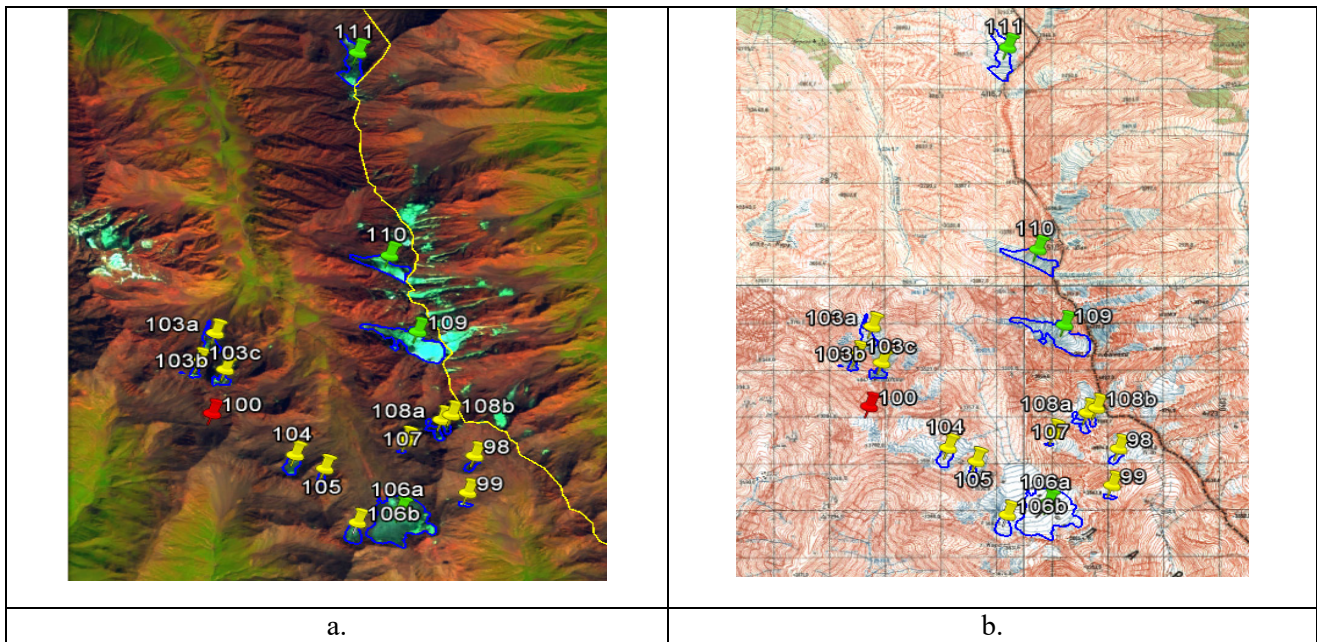
Fig.1. Small glaciers of the Tergi Basin (№98 − 111) and their contours in the satellite image (a) and 1960s. topographic map (b).

Table 1 is compiled for the river Terek glacial basin glaciers. It represents the glacier's area values and the numbers from the catalogue, SRS 1 and SRS 2 data.

Table 1. R. Terek Glaciation Basin Glaciers Number and Area according to Sizes determined   to Catalogue, SRS 1 and SRS 2 data

Glaciers № according to the catalogue	Size	Glaciers number			Glaciers area, km^2		
		Catalogue	SRS 1	SRS 2	Catalogue	SRS 1	SRS 2
44−111	Small	43	22	14	10.5	4.3	2.4
	Medium	16	7	7	14.1	6.9	5.7
	Large	9	7	6	42.9	29.2	26.2
	Total	**68**	**36**	**27**	**67.5**	**40.4**	**36.3**

According to the catalogue, there are 68 glaciers in the r. Terek glaciation basin. From this amount, small glaciers number was 43, medium glaciers amount – 16 and large glaciers number was 9. After 50 years small glaciers number decreased by 21(48.8 %) and was 22, correspondingly the medium glaciers amount decreased by 9 (56.2 %) and made 7 and the large glaciers amount decreased by 2 (22 %) and were equal to 7. After 5 more years, the number of small glaciers decreased by 8 (36.3 %) and large glaciers quantity decreased by one (14.3 %). The glaciers total amount for these two periods decreased by 32 (47 %) and 9 (25 %).

The area of small glaciers was 10.5 sq. km, correspondingly medium glaciers area – 14.1 sq. km and large glaciers – 42.9 sq. km. After 50 years small glaciers area decreased by 6.2 sq. km (59 %) and was equal to 4.3 sq. km, correspondingly the medium glaciers area decreased by 7.2 sq. km (51 %) and was equal to 6.9 sq. km and the large glaciers area decreased by 13.7 sq. km (31.9 %).

After 5 more years, the small glaciers area decreased by 1.9 sq. km (44.2 % for only 5 years) and was equal to 2.4 sq. km, correspondingly the medium glaciers area decreased by 1.2 sq. km (17.4 %) and was equal to 5.7 sq. km and large glaciers area decreased by 4.1 sq. km (31.9 %). The glaciers total area for these two periods decreased by 27.1 sq. km (40.1 %) and by 4.1 sq. km (10.1 %).

Conclusion. Studying the degradation of glaciers due to the impact of current climate change in Georgia is an important national economic task to obtain a scientifically sound answer on the present conditions of the glaciers. To determine the degradation dynamics of the glacial basin of the r. Terek under the impact

of the current climate change, it is necessary to use a high-resolution SRS because currently, it is impossible to carry out the costly ground observations at a necessary scale and in a resource- and time-constrained environment.

Processing of the satellite images gave the possibility to receive the dynamics of the degradation of river Terek glacial area for the periods of 50 years from the issue of the initial conditions and then for the latest 5 years. Calculations showed that the area and number of small glaciers decreased correspondingly by 59 and 49.8 % after 50 years and 44.2 and 36.4 % after 5 more years. Correspondingly, the same numbers for the medium glaciers are 51 and 56 % after 50 years and the medium glaciers area decrease was equal to 17.4% after 5 years and the total number of the medium glaciers did not change after 5 years. For the large glaciers, these numbers are consequently 40.1 and 22.2 after 50 years and 10.1 and 14.3% after 5 years.

The glaciers total area of the river Terek glacial basin for these two periods decreased by 27.1 sq. km (40.1 %) and by 4.1 sq. km (10.1 %). The glaciers total amount for these two periods decreased by 32 (47 %) and 9 (25 %).

The analysis of the given numbers clearly shows that climate change has a significant impact on the degradation of r. Terek glacial basin. Comparison of the speed of glaciers degradation in 50 and 5 years period show that glacier degradation speed is much more intense in the second period than in the first one i.e. glacial basin degradation is nonlinear.

This conclusion also proves the main thesis of the IPCC 6th report that the main problem is not climate change, but its speed.

References

1. Bates B.C., Kundzewicz Z.W., Wu S., Palutikof J.P., Eds. Climate Change and Water. // Technical Paper of the Intergovernmental Panel on Climate Change. IPCC Secretariat, Geneva, 2008, 210 pp.
2. Kordzakhia G., Shengelia L., Tvauri G., Dzadzamia M. Research of the Devdoraki Glacier Based on Satellite Remote Sensing Data and Devdoraki Glacier Falls in Historical Context. // American Journal of Environmental Protection, vol. 4, issue 3-1, 2015, pp. 14-21.
3. "Katalog of Lednikov SSSR" (USSR Glaciers Catalogue), vol. 8, part. 11 (1977), part 12 (1977); vol. 9, ed. 1, parts 2 – 6 (1975), ed. 3, part. 1 (1975), *L: Gidrometeoizdat* (in Russian).
4. Kordzakhia G., Shengelia L., Tvauri G., Dzadzamia M.:Impact of Modern Climate Change on Glaciers in East Georgia. // Bulletin of the Georgian National Academy of Sciences, vol. 10, issue 4, 2016, pp. 56-63.
5. Pellikka P., Gareth Rees W. Remote Sensing of Glaciers Techniques for Topographic, Spatial and Thematic Mapping of Glaciers, 2010, 330 p.
6. Kordzakhia G. I., Shengelia L. D., Tvauri G. A., Dzadzamia M. Sh. The climate change impact on the glaciers of Georgia. // In Journal-World science, vol. 1, № 4(44), Warsaw, Poland, 2019, pp. 29-34.
7. Shengelia L.D., Kordzakhia G.I., Tvauri G.A., Dzadzamia M.Sh. Results of the Research of Small Glaciers of Georgia against the Background of Modern Climate Change, Geography. // Development of Science and Education, a collective monograph on materials of Annual International Scientific and Practical Conference LXXI Hertsen Readings, St. Petersburg, A.I. Hertsen RSPU, April 18-21, 2018 St. Petersburg: A.I. Hertsen RSPU publishing house, vol. I, 2018, pp. 206-212 (in Russian).

PREVENTIVE JET FORCING AND THE ALAZANI VALLEY HAIL SUPPRESSION PROBLEM

Shekriladze I.

Georgian Technical University, Tbilisi, Georgia
i.shekriladze@gtu.ge

Summary: *The Alazani Valley hail problem is considered within the framework of the Preventive Jet Forcing concept based on the modification of energy flows forming convective clouds. The system with natural meteotron (Mount Tsivi) is considered. The regional wind through the orographic lift (together with solar thermal forcing) triggers a strong enough convective cloud and then delivers it to the valley. The concept provides for limiting the concentration of instability energy in the cloud by artificial time shift in its triggering and delivery using installed on Mount Tsivi decommissioned jet engine (meteotron). A comparison is made of the efficiency of using a jet engine in the arid zone, in the Alazani Valley, and on the Tsivi Mountain. The solar thermal forcing capacity of Tsivi mountain is estimated.*

Key words: preventive jet forcing, meteotron, orographic lift, solar thermal forcing.

Introduction. In [1], an attempt was made to draw attention to an alternative approach to the problem of severe convective storm by modifying the energy flows forming convective clouds. The preventive jet forcing concept (the PJF concept) is aimed at limiting the concentration of energy in a single cloud, leading to the most dangerous development, by artificially preventive forcing of convective clouds in those places and at those points of time that will allow a relatively safe discharge of the accumulated convective available potential energy (CAPE) using for forcing clouds of jet engines, also called meteotrons [2].

In [3], the problem was considered in the context of the role of the jet engine placement height in increasing the efficiency of a convective cloud forcing.

A terminological update of the research line was also carried out.

Starting from [1], the role of the main keyword was assigned to the term "restratification", which was used at that time in the Soviet scientific literature. In relation to the layers of the atmosphere in the modern English-language scientific literature, this term is usually not used (sometimes it is used in relation to the layers of the sea).As convective cloud forcing inevitably leads to the very "restratification", it becomes more appropriate to bring to the fore the keyword reflecting the principle of artificial forcing: "preventive jet forcing". Accordingly, "the anticipatory restratification" evolved into "the Preventive Jet Forcing".

Methods. The study includes consideration of the main features of the qualitative model of the hail in the Alazani Valley, the model of the system with a natural meteotron (the SNM model), taking into account the formation of a primary cloud on Mount Tsivi as a result of the orographic lift of the westerly wind and its further delivery to the valley by the same wind.

The PJF concept [1] is based on the well-known idea of the pre-cloud atmosphere as an unstable layer of humid air under the capping inversion, where the latter prevents the CAPE discharge. As soon as convective currents manage to break through the first channel through capping inversion, the latter begins to assist to the cloud in collecting the CAPE from the largest possible area, continuing to close the convection path in the rest of the territory. Since the maximum power of a convective cloud depends on the CAPE it has mastered, this is the right path to a strong convective storm, including hail

For the case of a large plain, the prevention of such a development is proposed by the preventive discharge of the accumulated CAPE by several convective clouds, artificially launched at various points of the protected area at distances safe for cloud merging using meteotrons (jet engines) [2].

Initially the meteotron was used without much success to make it rain in arid zones [2]. As shown below the task becomes much easier when implementing the PJF concept.

The SNM model refers to the implementation of the PJF concept in valleys with adjacent ridges. In particular, hail in the Alazani Valley is considered to be the result of a "lucky" correlation of the formation time of the primary cloud on Mount Tsivi with the build-up of CAPE in the valley. Finally, due to this correlation, the cloud arrives in the valley when a sufficiently large amount of CAPE has already accumulated to ensure the intensive development of the cloud, up to severe hail.

To break this "luck" is proposed to ensure the early arrival of cloud when the accumulated CAPE is still insufficient to amplify it to hail and the end result is rain. This task can be performed by a jet engine placed on the top of Tsivi, which in this case should only accelerate the forcing convective cloud formation by orographic lift and solar thermal forcing, which can be a low energy-consuming action.

As a result, the anticipatory appearance of the convective cloud in the valley is ensured, when the losses from its further development will be minimal.

In addition, since, compared to many of the studied mountains (eg, Mount Catalina, Arizona, USA [4]), Mount Tsivi has a very small area from where anabatic winds can deliver solar heat to the summit, it is also interesting to estimate its solar thermal forcing capacity and even compare it with the potential heat dissipation by the jet engine.

In general, one should also emphasize the universal nature of the principle of instability energy discharge distributed in time and space, applicable to prevent or mitigate almost all severe meteorological phenomena. The main difficulty, of course, lies in the effective implementation of the principle.

Results and discussion. In order to first clarify the level of the possible contribution of a jet engine in the thermal forcing in the specific conditions of Mount Tsivi, we begin with an assessment of its natural solar thermal forcing capacity. To avoid overestimating the role of the jet engine, when determining the required for the assessment parameters, approximations always are made in the direction of overestimating the natural solar forcing capacity,

The relief map and top view of Mount Tsivi are shown in Fig. 1.

a)   b)
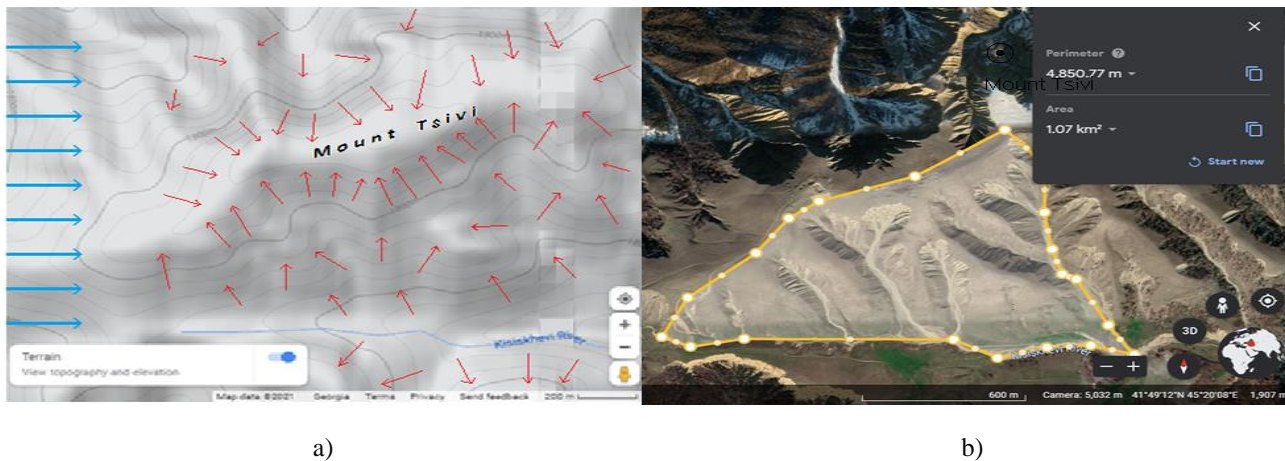
Fig .1. The zone of Mount Tsivi: a) relief map of the zone according to Google Map; b) top view of the zone via Google Earth showing the portion of the southern slope of the mountain involved in solar thermal forcing.

As follows from Fig. 1a, the summit of Tsivi is a narrow, almost rectangular strip about 100×800 m² from west to east, collecting anabatic winds (red arrows) from the southern and northern slopes.

The relief of the western slope is very convenient for the development of the orographic ascent of the westerly wind (blue arrows).

At the same time, in contrast to the southern and northern slopes, the western slope contributes very little to the lateral concentration of solar heat by anabatic winds at the summit (only a narrow part of the front of the anabatic wind will fall directly to the summit), which diminishes the significance of this slope in terms of building up the energy base for solar thermal forcing (our consideration covers only the period of maturation of the situation).

However, an indirect mechanism remains in force - the transfer of solar heat from the anabatic flows of the western slope by joining the anabatic flows of the southern and northern slopes.

As for the eastern slope, it is excluded from the focusing of the anabatic winds at the summit for the simple reason: the anabatic wind would have to overcome the much more powerful westerly wind.

We begin the assessment of the solar heat inflow at noon on a summer day from the southern slope, the three boundaries of which are clearly defined: the summit itself, the western watershed and the Kisiskhevi River. We slightly move the eastern border to the zone where the anabatic wind has to partially blow against the main wind, thereby somewhat overestimating the active area of the southern slope (Fig. 1b)

The projected area of the slope and its average incline are determined using Google Earth and the area of the slope itself is calculated (1.12 km^2). Further, we use the value of the maximum heat flow from the surface of the earth to the air at noon on a summer day according to the data for Mount Catalina [4] (200 W / m^2) located 10 degrees south of Mount Tsivi, again slightly overestimating the thermal power of the slope.

Next, the total heat flux from the slope to the air (224 MW), determined from these data, is considered to be completely supplied to the summit, although a significant part of it is carried away by the main wind, and this is not considered an overestimate: in this way we take into account the above heat brought by the anabatic flows from the western slope.

Having determined the contribution of the southern slope to solar thermal forcing on Mount Tsivi, we proceed to a comparative assessment of the thermal capacity of the northern slope, which, naturally, is inferior to the southern one in terms of heat flow from the surface into the air, but is practically not limited by the length of the slope.

However, as our analysis shows, despite its much greater extent, the capacity of the northern slope is clearly less than the capacity that we have already attributed to the southern slope. The fact is that due to the influence of the main wind, only slope section close to the summit can participate in the thermal forcing. At a distance from the summit, for example, more than 800 m, with the same velocities of the main and anabatic winds, the overheated particle will most likely be carried away by the main wind before reaching the summit. At that, in reality, the speed of the main wind is always much higher.

Thus, taking into account the exclusion of the eastern slope and the adaptation of solar heat received on the western slope by the anabatic flows of the southern and northern slopes, we can attribute the thermal capacity of the southern slope to the northern slope (overstating its value) and estimate the Mount Tsivi full solar thermal forcing capacity at 448 MW (roughly 500 MW).

At the same time, according to the reference data on the specific fuel consumption of various aircraft, heat dissipation by a passenger jet engine ranges from 1 to 30 MW. Thus, the meteotron cannot make a tangible contribution to thermal forcing even in the specific conditions of Mount Tsivi, with very little surface area for the development of anabatic flows.

Having decided on the thermal forcing, let's move on to a comparative consideration of the conditions of the primary, main function of the jet engine, dynamic forcing of convective cloud.
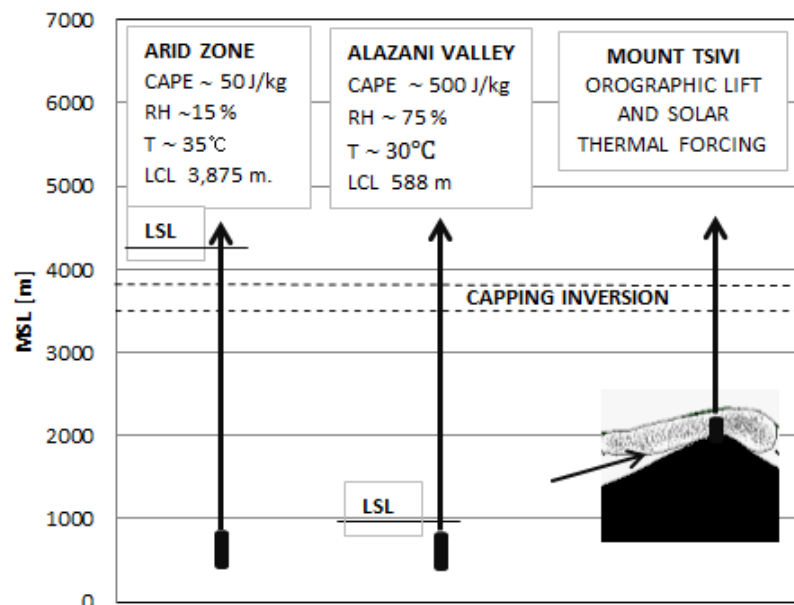
Fig. 2. The comparison of a jet engine functioning in arid area, in Alazani Valley, and on Mount Tsivi.

The comparison of a jet engine functioning features in arid area, in Alazani Valley and on Mount Tsivi (Fig. 2) allows us to draw some interesting conclusions.

The operating conditions of the first two jet engines (in arid zone and in Alazani Valley) coincide only by their location above sea level (400 MSL). Otherwise, strongly differing initial air parameters (shown in Fig. 2) lead to sharply different potential development patterns, which is reflected in the values of the Lifting Condensation Level (LCL). If in the Alazani Valley the jet produced by the engine almost instantly turns on powerful latent condensation heat release, then in the arid zone such a jet should rise and break through the capping inversion on its own, which, accordingly, will dramatically affect the required power of the jet engine.

The next sharp decrease in the required power of the jet engine looms at the transition from the valley to Mount Tsivi.

There, in the supposed operating time interval (10-00 - 17-00), the jet engine is not only close to capping inversion, but from the very beginning is in non-convective clouds and only has to assist the orographic lift and solar thermal in anticipatory forcing of a convective cloud.

The part of these conclusions is indirectly confirmed by the long-term statistics of hail in the valley [5], which records an absolute minority of the cases of hail due to the formation of intra-massive clouds. Another part also indirectly is confirmed by approximate analysis [3].

Not excluded, it will be possible to speak of a decrease in the required power of the jet engine relative to the arid zone by one or two orders of magnitude, which would open up the prospect of effective implementation of the concept.

Conclusion. The first important step towards the possible implementation of the looming optimistic perspective should be a detailed analytical and numerical modeling of the corresponding processes.

First of all, this concerns the system with natural meteotron, in particular, the Alazani Valley - Tsivi Mountain system.

Of particular interest is modeling of orographic lift and solar thermal forcing in combination with dynamic forcing by the jet engine, with the subsequent inclusion into unified model of the Alazani Valley - Tsivi Mountain system.

If preliminary expectations are confirmed, the next step should be a large-scale field experiment.

It is also necessary to start modeling the system of the centralized optimal control of the network of meteotrons covering a large region including a short-term forecast of the regional situation.

Finally, given that global warming only promises continuous increase in humidity, CAPE, and the strength of hail and tornadoes [6], we can set our doubts about PJF concept aside for a moment and look to the future with over-optimism.

Admitting instantly the ideal success of the concept (functional, economic, and ecological), one can imagine a vast region covered by a network of meteotrons (located, where possible, on hills and mountains), with a unified control system that allows redistributing (within certain limits) precipitation in space and time, to reduce the CAPE and humidity in places of expected hail, tornado, hurricane or cold front.

References

1. Shekriladze I. G. On the Concept of Preventing Hail by Artificial Anticipatory Restratification of Unstable Atmosphere. // Bull. Acad. Sci. Georgia. 146 (2), 1992, pp. 141-145.
2. Vul'fson N. I., Levin L. M. Meteotron as a Means of Influencing the Atmosphere. // Gidrometeoizdat, 1987, 129 p. (in Russian).
3. Shekriladze I. G. Preventing Severe Convective Storm: Anticipatory Restratification of Lower atmosphere. // Bull. Georg. Natl. Acad. Sci. 6 (2), 2012, pp. 73-82.
4. Geerts B., Miao Q., Demko C. J. Pressure Perturbations and Upslope Flow over a Heated, Isolated Mountain. // Monthly Weather Review, 136(11), 2008, pp. 4272-4288.
5. Pipia M. G. Climatology of Hail in East Georgia. // Doctoral Thesis, Telavi, 2016, 114 pages.
6. Raupach T.H., Martius O., Allen J.T. Kunz M., Lasher-Trapp S., Mohr S., Rasmussen K. L., Trapp R. J., Zhang Q. The Effects of Climate Change on Hailstorms. Review Article. // Nat Rev Earth Environ 2 (3)**,** 2021, pp. 213–226

Content

211

IVANE JAVAKHISHVILI TBILISI STATE UNIVERSITY
MIKHEIL NODIA INSTITUTE OF GEOPHYSICS
VAKHUSHTI BAGRATIONI INSTITUTE OF GEOGRAPHY
GEORGIAN TECHNICAL UNIVERSITY
INSTITUTE OF HYDROMETEOROLOGY

INTERNATIONAL SCIENTIFIC CONFERENCE

Natural Disasters in the 21st Century: Monitoring, Prevention, Mitigation

Tbilisi, December 20-22, 2021

Proceedings

Layout Designer **Lali Kurdghelashvili**

Cover Designer **Mariam Ebralidze**